Auditory Processing During Sleep: A Causal Approach to Manipulate Memory Consolidation Through Event-Locked Stimulation

Hugo R. Jourde

A Thesis in
The Department
of
Psychology

Presented in Partial Fulfillment of the
Requirements For the Degree of
Doctor of Philosophy

at Concordia University
Montreal, Quebec, Canada

April 2025

CONCORDIA UNIVERSITY
SCHOOL OF GRADUATE STUDIES

This is to certify that the thesis prepared

By: Hugo R. Jourde

Entitled: Auditory Processing During Sleep: A Causal Approach to Manipulate Memory Consolidation Through Event-Locked Stimulation

and submitted in partial fulfillment of the requirements for the degree of

Doctor of Philosophy (Psychology)

complies with the regulations of the University and meets the accepted standards with respect to originality and quality.

Signed by the final examining committee:

_____ Chair

Dr. Claudine Gauthier

_____ External Examiner

Dr. Stuart Fogel

_____ Examiner

Dr. Christopher Steele

_____ Examiner

Dr. Julien Doyon

_____ Examiner

Dr. Virginia Penhune

_____ Thesis Supervisor

Dr. Emily Coffey

Approved by

_____

Dr. Andrew Chapman, Graduate Program Director

May 26, 2025

_____

Dr. Pascale Sicotte, Dean of Faculty of Arts and Science

Abstract

Auditory Processing During Sleep: A Causal Approach to Manipulate Memory Consolidation Through Event-Locked Stimulation

Hugo R. Jourde, Ph.D.
Concordia University, 2025

Sleep represents a considerable part of our lives and its important roles in cognition and health are constantly being emphasized by emerging research. Investigations of sleep's role in human memory consolidation have primarily focused on correlative relationships with sleep architecture or characteristic patterns of electrical activity, such as brain oscillations. While non-invasive neuroimaging studies cannot provide direct causal evidence of oscillations' functional roles, emerging brain stimulation techniques fill this gap by allowing direct interaction with endogenous brain activity. Closed-loop auditory stimulation, which uses quiet sounds time-locked to neural events, shows promise in research and clinical applications, particularly for targeting neural events previously correlated with, and therefore hypothesized to be involved in learning and memory. The present thesis investigates the bidirectional relationship between auditory processing and sleep using a combination of electroencephalography, magnetoencephalography, and behavioural paradigms. This dissertation comprises six studies. In our first studies (Chapters 2 and 3), which used source-localized magnetoencephalography, we demonstrated that cortical sources of auditory evoked responses are affected by sleep depth, while subcortical regions remain unaffected. We also identified the source of sleep-specific evoked responses that are involved in closed-loop auditory stimulation effects. The next study (Chapter 4) challenges a widely held assumption in sleep science by showing that auditory input can still reach the cortex during spindles and their refractory period. This finding is key to our goal of manipulating sleep spindles with sound. In the next group of studies (Chapters 5 and 6), we validated a deep learning-based tool to modulate neurophysiology by stimulating spindles in real-time, and explored the optimal timing for its delivery. This work established the foundation for our behavioural study. Finally, the last study (Chapter 7) assessed the behavioural effects of slow oscillation and spindle stimulation on simple laboratory tasks and on a complex, music-based learning task. We evaluated relationships between stimulation-evoked responses and memory performance across tasks. Our findings provide mechanistic insights into how non-invasive brain stimulation affects neurophysiology and memory and offer a framework for linking brain activity with its function.

Acknowledgements

What you are about to read is the result of a long and, at times, challenging process that took more than five years to complete. From moving across an ocean to surviving a worldwide pandemic, these past years were undoubtedly defining, and the writing of this manuscript prompted me to reflect on that chapter of my life. While this manuscript bears my name as the primary author, its creation, like any meaningful achievement, was enriched by a multitude of collaborations—both professional and personal. In the following lines, I will briefly take a moment to acknowledge some of my collaborators while mindful of the many others whom I cannot individually name.

First, my most sincere thanks go to my supervisor. Dr. Emily Coffey, whose invaluable guidance and support were crucial in bringing this work to completion. I want to genuinely thank Emily for taking that bet six years ago and answering that impromptu email. Recruiting this French engineer with little academic experience and no prior publications was risky, and I hope I've proven her faith in me well-placed. Throughout this journey, Dr. Coffey consistently provided unexpected and compelling opportunities—from co-leading a workshop for the International Space Agency to exploring underground caves in Mexico, she ensured there were countless chances for growth, not only as a scientist but also as a human being. A guiding motto I tend to refer to states that: *"Between an adventure and no adventure, always choose the adventure"*. Working with Dr. Coffey brought me many occasions to live by this principle, none of which are regretted, and all of which have shaped my path as a researcher. Dr. Coffey once told me that a Ph.D. was like a marathon. Now, facing the starting line on race day, I would like to suggest an update. This was not a marathon, it was an ultra-trail, and for both of us. There were steep climbs and rocky descents (I might have even been responsible for involuntarily placing boulders on the path), but the challenges only made reaching the destination more meaningful—exhausted, but proud of the journey. Thanks for teaching me so much, I hope that we find many more occasions to cover whiteboards with exciting research ideas.

My gratitude is also due to my advisory committee (Dr. Christopher Steele, Dr. Julien

Doyon and Dr. Emily Coffey) for providing directions and structure to a young, enthusiastic aspiring researcher who was full of ideas yet uncertain about how to shape them into a coherent research project.

Next, I would like to acknowledge my academic adventure companions. First, soon-to-be Dr. Alex Albury: we started this journey together and although I'm taking an earlier train than you, I want to express my gratitude for navigating these uncertain roads with me. I'm excited to see where your path leads. Next, I want to express my thanks to my friend and colleague Keelin Greenlaw, you welcomed me into the laboratory and into your life and were and will forever be my first Canadian friend. Finally, I would like to offer a special thanks to my co-author and friend Dr. Anita Paas. Your friendship, guidance and support have been invaluable, and I feel I've learned so much from you (except when it comes to knitting, apparently...). I also want to extend my gratitude to all the other members of the CL:ASP who crossed my path and made this journey ten times better: Marie-Anick Savard, Mary Brooks, Gregory Rattray, Zseyvin Eyqvelle, Katerina Sita and so many more.

My thanks also go to the SpeleoQC association, and particularly to Jérôme Genairon, Guillaume Pelletier, and Samuel Bassetto. You gave me the opportunity of a lifetime to live a dream by being part of the scientific team on an exploratory expedition in a remote area.

I would also like to acknowledge the expert assistance of numerous researchers within the Canadian research community, such as Giovanni Beltrame (Polytechnique Montreal), Karine Lacourse (Université de Montréal) and Latifa Lazzouni (McGill University). From troubleshooting experiments to technical problem solving, engaging with you and learning from our exchanges has broadened my research interests and helped me develop new skills.

I extend my sincere thanks to Dr. Eden Debellemanière, Dr. Marion Létisse, and Dr. Christelle Peyron for their initial support in this project and their kind reference letters that helped secure my admission to the program.

I would also like to gratefully acknowledge the more than 180 participants, some strangers, some friends, who let me record their brain activity for the sake of science, some lying down in the MEG, others in a tent or the comfort of their own home. Credit is also due to the many students who helped me collect this massive amount of data over the years. Thanks for your time and efforts.

I also want to take a moment to thank the great province of Quebec. Running your trails, hiking your mountains and cycling your roads kept me sane during my Ph.D. and enriched

me in so many ways. Learning about your culture has been a highlight of my doctoral experience. Your artists made me dance and your singers made me cry. From roommates to running partners, your people offered me not just hospitality, but a sense of home and these words, timid as they are, are my deepest attempt to thank them. I finish this adventure with countless stories and friendships that I hope will last no matter where life brings me next. I cannot possibly name everyone individually, but please rest assured that my heart has grown from sharing this journey with all of you, leaving me with an indelible Quebecer feeling.

Profitant du bilinguisme du Québec, j'aimerais continuer (sans m'éterniser, car les mots ne sauraient exprimer toute la gratitude que je ressens à leur égard) dans ma langue maternelle pour remercier ceux qui m'accompagnent inlassablement et inconditionnellement depuis de longues années: à mes parents, pour l'amour, la confiance et la curiosité, à mon frère pour l'exemplarité, à mon grand-père pour l'espoir et à ma grand-mère pour la tendresse infinie. J'espère avoir réussi à vous rendre fiers. Et enfin, à Noémie, ma confidente et complice de chaque instant qui transforme nos expériences partagées en souvenirs précieux. Ton soutien inébranlable a été absolument déterminant à la réussite de ce projet et cet accomplissement est aussi le tien. Tu as été mon pilier chaque fois que le poids de cette épreuve semblait trop lourd pour mes épaules. J'ai hâte de te rendre la pareille dans la suite de notre chemin commun.

Suivant les conseils du grand Jacques, qui nous *"souhaite des rêves à n'en plus finir et l'envie furieuse d'en réaliser quelques-uns"*, je viens, grâce à vous tous, d'en réaliser un dont l'envie furieuse remonte à de nombreuses années. J'aimerais donc conclure avec cette fois les mots du grand Karl: *"pour cette bizarre épopée assise sur des amitiés, merci ben."*

Merci à tous,

Contributions of Authors

I am the primary author of the six manuscripts presented in this thesis (Chapters 2-7; all published or submitted for review). During my doctoral studies, I also made contributions to four additional published or submitted works, for reasons ranging from the necessity of contributing to development and validation of research tools used in my scientific work (Appendix A and B), to having played an active role in mentoring junior students (Appendix C), to having an interest and sufficient outdoor experience to participate in collecting sleep and human performance data in unusual environments (Appendix D; shared first authorship with my colleague Dr. Anita Paas). As these topics are secondary to this dissertation's main focus, a brief summary of their relationship to my doctoral work and their abstracts are presented outside the main body of the thesis, as Appendices. Specific contributions for each work are detailed below. Please see 'Acknowledgements' in each chapter for additional details concerning contributions.

Chapter 2

Jourde, H. R., & Coffey, E. B. (2025) Sleep state influences early sound encoding at cortical but not subcortical levels. Submitted for publication.

The research questions presented in Chapter 2 (Jourde et al., in review) about FFR in sleep were proposed by Emily Coffey (EC). Raphaelle Merlo (RM) and Keelin Greenlaw (KG) assisted me and EC for the data collection. Analysis was done jointly with EC. The manuscript was written in collaboration with EC, with inputs from RM.

Chapter 3

Jourde, H. R., Merlo, R., Brooks, M., Rowe, M., & Coffey, E. B. (2024). The neurophysiology of closed-loop auditory stimulation in sleep: A magnetoencephalography study. European Journal of Neuroscience, 59(4), 613-640.

The study design was conceived by EC and data were collected prior to my arrival in the lab, by RM, Meredith Rowe (MR), and EC, and assisted by several lab members. I was responsible for formal analysis, data visualization, and writing the paper, with contributions during the writing process from EC, RM, MR, and Mary Brooks (MB).

Chapter 4

Jourde, H. R., & Coffey, E. B. (2024). Auditory processing up to cortex is maintained during sleep spindles. PNAS nexus, 3(11), pgae479.

The work presented in Chapter 4 was conceptualized by EC and myself. It combined data from three different experiments to address a single research question from different perspectives. The data from the first experiment (work presented in Chapter 2) was collected by me and my colleagues: MR, RM, KG and EC. The data from the second experiment (work presented in Chapter 3) was collected by RM, MR, and EC and the data from the third experiment (work presented in Chapter 5) was collected by me with the help of undergraduate student Arina Ujevco (AU). I was responsible for formal analysis, data visualization, and writing the paper, with contributions during the writing process from EC.

Chapter 5

Jourde, H. R., Sobral, M., Beltrame, G., & Coffey, E. B. (2025). Neurophysiological effects of targeting sleep spindles with closed-loop auditory stimulation. Accepted for publication in Sleep Advances as part of the Special Issue Festschrift in Honor of Dr. Robert Stickgold.

I was responsible for the conception of the work presented in Chapter 5 which was developed through consultation with EC and Giovanni Beltrame (GB). The technical development of the required tool was made by master students Nicolas Valenchon (NV) and Milo Sobral (MS) under the supervision of GB. The piloting of the study and validation of the device was done with inputs from external collaborators from McGill University (Julien Doyon, Latifa Lazzouni, Prakriti Gupta and Vaishali Mutreja). I was responsible for monitoring at-home data collection by participants, data curation and formal analysis. Data visualization and writing the paper was done in collaboration with EC.

Chapter 6

Jourde, H. R., Ujevco, A., & Coffey, E. B. (2025) Thalamocortical spindle phase modulates

the effectiveness of auditory stimulation in sleep. Submitted for publication.

I conceived the study design in collaboration with EC. AU was responsible for recruiting and training participants, AU and I monitored the in-home data collection process from participants, and I mentored AU in her undergraduate research project which focused on a preliminary dataset. I was responsible for data curation, formal analysis, and data visualization. EC and I collaborated on writing the paper, with contributions from AU.

Chapter 7

Jourde, H. R., & Sita, K. Z., Eyqvelle, Z., Brooks, M., & Coffey, E. B. (2025) Modulating sleep: slow oscillation and spindle stimulation effects on physiology and memory. Submitted for review.

This study is the result of an intense collective data collection effort for which undergraduate students Katerina Sita, Zseyvfin Eyqvelle and MB helped me greatly collect more than a hundred and twenty participants, each requiring 5-6 hrs of experimental effort. The research questions regarding the effects of auditory stimulation to different brain events were created by EC and myself. The computerized tasks were adapted from previous work and implemented by Alexandre Morinvil. The piano learning paradigm was extensively piloted and validated by myself with inputs from EC and Robert Zatorre. The analysis was also done by me with their advice. The manuscript was written in collaboration with EC.

Appendix A

Valenchon, N., Bouteiller, Y., Jourde, H. R., L'Heureux, X., Sobral, M., Coffey, E. B., & Beltrame, G. (2022). The Portiloop: A deep learning-based open science tool for closed-loop brain stimulation. PloS one, 17(8), e0270696.

My contribution focused on conceptualization and sleep data analysis. This included sleep spindle detection for model training, extensive validation of online detection output from electroencephalography (EEG) data, and iterative improvements to the online detection algorithm. Additionally, I contributed to the joint development of the hardware tool used in this process.

Appendix B

Sobral, M., Jourde, H. R., Bajestani, S. E. M., Coffey, E. B., & Beltrame, G. (2025). Advancing Closed-Loop Brain Stimulation: Continual Learning for Subject- Specific Sleep Spindle Detection. Submitted for publication.

The work presented in Appendix B originated from MS's master thesis, an engineering student who continued the project after NV's graduation (detailed in Appendix A). I maintained my role as sleep consultant, testing both hardware and software components, and designing the user interfaces.

Appendix C

Rattray, G., Jourde, H. R., Baillet, S., & Coffey, E. B. (2025). Exploring deep magnetoencephalography via thalamocortical sleep spindles. Submitted for review.

The primary author of the work presented in Appendix C was Gregory Rattray (GR), an undergraduate student whom I have mentored over the past four years including during his undergraduate thesis. I contributed to collecting the dataset used in this work, pre-processing it, teaching GR to code, about sleep research, scientific writing, poster and presentation creation. I participated in regular meetings throughout the project's evolution, and writing and editing of the final paper.

Appendix D

Paas, A., Jourde, H. R., Brignol, A., Savard, M. A., Eyqvelle, Z., Bassetto, S., Beltrame, G., & Coffey, E. B. (2024). Beyond the lab: Feasibility of cognitive neuroscience data collection during a speleological expedition. Journal of Environmental Psychology, 99, 102443.

The work presented in Appendix D is a co-first author paper resulting from a research project conducted jointly with Anita Paas (AP) and EC. Building on EC's theoretical work and AP's technical expertise, I contributed to the project's conceptualization and participated in data collection with EC in a remote region of Mexico, allowing me to gain experience extending our work on measuring sleep outside of the lab to extreme conditions. The analysis was carried out in collaboration with AP, with input from AB, ZS, and MS, under the guidance of EC and GB. The manuscript was written collectively.

Contents

List of Figures

List of Abbreviations

AASM American Academy of Sleep Medicine

AC Auditory Cortex

ANOVA Analysis of Variance

ARAS Ascending Reticular Activating System

BF Bayes Factor

BOLD Blood-Oxygen-Level Dependent

CLAS Closed-Loop Auditory Stimulation

CN Cochlear Nucleus

CNN Convolutional Neural Network

ECG Electrocardiography

EEG Electroencephalography

EMG Electromyography

EOG Electrooculography

ERP Event-Related Potential

eCHT Endpoint Connected Hilbert Transformation

FDR False Discovery Rate

FFR Frequency-Following Response

FFT Fast Fourier Transform

FIR Finite Impulse Response

FOOOF Fitting Oscillations and 1/F

fMRI Functional Magnetic Resonance Imaging

FSA Fast Spindle Activity

GLT Grid Location Task

IC Inferior Colliculus

iCOH Imaginary Coherence

IQ Intelligence Quotient

LC Locus Coeruleus

LFP Local Field Potential

LME Linear Mixed Effects

MCTQ Munich Chronotype Questionnaire

MEG Magnetoencephalography

MGB Medial Geniculate Body

MMHQ Montreal Music History Questionnaire

MNE Minimum-Norm Estimate

MRI Magnetic Resonance Imaging

MSL Motor Sequence Learning

NA Noradrenaline

NREM Non-Rapid Eye Movement Sleep

OFC Orbitofrontal Cortex

PSQI Pittsburgh Sleep Quality Index

PVT Psychomotor Vigilance Task

REM Rapid Eye Movement Sleep

RMS Root Mean Square

rmANOVA Repeated Measures ANOVA

RNN Recurrent Neural Network

ROI Region of Interest

SD Standard Deviation

SE Standard Error

SEM Standard Error of the Mean

SNR Signal-to-Noise Ratio

SO Slow Oscillation

SOA Stimulus Onset Asynchrony

SPL Sound Pressure Level

SWA Slow Wave Activity

tACS Transcranial Alternating Current Stimulation

TC Thalamocortical

TE Echo Time

TI Inversion Time

TMS Transcranial Magnetic Stimulation

TR Repetition Time

TRN Thalamic Reticular Nucleus

TST Total Sleep Time

Chapter 1

Introduction

This dissertation concerns the roles of neural patterns that are unique to sleep and are thought to play particularly important roles in memory, and how we can better understand their functions using non-invasive causal manipulation techniques. In the following sections, I will first provide an overview of sleep architecture and the specific neural phenomena that constitute the foundation of this research, reviewing relevant background concerning sleep's role in memory consolidation. Subsequently, I will briefly present the auditory system's functional organization and introduce tools for measuring its responses to environmental stimuli, which will be our entry point for altering sleep processes. I will then review what is known concerning how sound can be used to manipulate sleep, before establishing the concept of closed-loop auditory stimulation. These foundational elements contextualize the experimental findings that motivate the projects of my doctoral work.

1.1 Sleep and cognition

Sleep is a homeostatically regulated process known to be essential for many cognitive functions in the brain extending beyond simple physical rest. From flushing toxic waste from the cerebrospinal fluid (Hauglund et al., 2020) to reorganizing synapses through selective strengthening and deletion (Blanco et al., 2015; Timofeev & Chauvette, 2017), sleep is indispensable for overall brain health. Studies on sleep-related brain dynamics reveal a fundamental reorganization of functional neural connectivity, characterized by enhanced long-range communication facilitated by global neuronal synchronization. The specialized neurophysiology of sleep is thought to subserve its functions, and is hypothesized to be incompatible with the cognitive processes required during the wake state. The effectiveness of these cognitive processes therefore relies on maintaining sleep continuity, as frequent disruptions can impair the restorative and consolidation functions of sleep (for a review see

McCoy & Strecker 2011). It also likely relies on the neural patterns that are unique to sleep, notable instances of which are 'sleep spindles' and 'slow oscillations'.

1.1.1 The electrophysiology of sleep

Sleep is a biological process regulated by two mechanisms: the circadian rhythm and sleep pressure. The former, controlled by an internal biological clock in the suprachiasmatic nucleus of the hypothalamus (Hastings et al., 2018; Evans & Silver, 2022) responds to various environmental cues—with light being one of the most powerful—and orchestrates many physiological functions, including sleep. Jet lag provides a relatable example of circadian rhythm disruption, wherein rapid travel across time zones temporarily desynchronizes the internal biological clock from local environmental cues. The latter refers to a homeostatic mechanism that builds up during wake and drives our need for sleep as we experience cumulative fatigue (Holst & Landolt, 2015). The balance between the two controls sleep onset, duration, and depth.

Sleep is thought to be homeostatically regulated because of its crucial role in neurological processes supporting brain function during wakefulness such as clearing metabolic waste products through the glymphatic system (Hauglund et al., 2020), regulating synaptic strength through homeostatic scaling (Tononi & Cirelli, 2006; Blanco et al., 2015; Timofeev & Chauvette, 2017), and of particular interest in this work, transforming newly acquired memories into long-term representations (Diekelmann & Born, 2010; Schabus et al., 2004; Antony et al., 2019; Klinzing et al., 2019). This process, known as memory consolidation, relies on effective communication between several distant brain structures, notably, the hippocampus, the thalamus and the neocortex (see Section 1.1.2). The nature and timing of neural activity, which is the basis of these interactions, differs considerably in sleep as compared to the wake state. Linking features of sleep neurophysiology to their functional roles has therefore been a prominent focus of research in recent decades to understand the underlying mechanisms of memory consolidation.

In humans, neural activity is most often studied using electroencephalography (EEG), a non-invasive neuroimaging technique that measures the summed activity of postsynaptic potentials from large groups of neurons via electrodes placed on the scalp. To study sleep, EEG is frequently supplemented with electrooculogram (EOG) and electromyogram (EMG) channels, which are helpful to categorize it into REM (rapid eye movement) and NREM (non-rapid eye movement) phases. NREM sleep is further subdivided into stages according to the presence and prevalence of neural oscillatory patterns in the EEG (from NREM1 representing light sleep to NREM3 representing deep sleep). Within NREM sleep, three types

of brain oscillations have been linked to memory consolidation processes: slow oscillations (including K-complexes), sleep spindles, and hippocampal ripples.

Slow oscillations are high-amplitude, low-frequency fluctuations in brain activity. The specific frequency thresholds used to identify them vary across studies, with upper limits ranging from 1.0 to 4.0 Hz (Carrier et al., 2011; Ngo et al., 2013b; Jaar et al., 2010; Vyazovskiy & Harris, 2013). They are thought to reflect synchronized transitions between periods of high and low excitability across cortical and subcortical networks during NREM sleep. These oscillations appear to play a role in all major sleep functions mentioned above, serving as a fundamental organizing element of sleep-dependent processes. K-complexes are a special type of slow oscillation that can occur either spontaneously or in response to sensory input during NREM2 and NREM3 sleep (Riedner et al., 2011; Latreille et al., 2020; Bellesi et al., 2014). When evoked by external stimuli, they manifest as an initial negative wave appearing about 550 ms after stimulus onset followed by a positive wave appearing at about 900 ms ('N550-P900 complexes'). Although spontaneous and evoked K-complexes may have slightly different characteristics, both appear to originate from the same neurobiological mechanisms (Amzica & Steriade 1997; see also Neske 2016, for a review). Slow oscillations originate in deep cortical layers, especially in the frontal cortex, and propagate as large-scale waves across the brain (often in an anterior to posterior direction; Massimini et al. 2004). They can occur independently in de-afferented cortical tissue, but can be instigated, modulated, and coordinated via thalamic input (see Sanchez-Vives 2020, for a recent review of the origin and dynamics of slow oscillations).

Sleep spindles are transient bursts of neural activity within the 11-16 Hz frequency band that reflect thalamocortical neuronal activity (see Fernandez & Lüthi 2020, for a comprehensive review of spindles' mechanisms and functions). Sleep spindles are posited to arise from intricate thalamocortical circuits involving reciprocal interactions between the thalamic reticular nucleus (TRN) and the neocortex. In brief, GABAergic neurons in the thalamic reticular nucleus generate rhythmic bursts via intrinsic oscillatory properties, which provide strong and synchronous inhibition of thalamocortical (TC) relay neurons. These TC cells subsequently produce a rebound burst discharge and send projections back to TRN cells close to those that initially inhibited them, creating a feedback loop that sustains spindle oscillations and enhances synchronization. TC cells also project to the cortex, which further promotes spindle synchrony through corticoreticular cells. This feedback leads to stronger inhibition from the TRN cells and stronger rebound responses from the TC neurons, also maintaining the spindle. However, repetitively bursting TC cells produce an 'after depolarization' that decays slowly over tens of seconds, eventually suppressing rebound burst generation in TC cells and ultimately leading to spindle termination. Cortical

desynchronization (i.e. following a slow oscillation) results in weaker corticothalamic inputs which can also contribute to spindle termination. After spindle offset, new spindles tend to not occur spontaneously for a refractory period of several seconds (Antony et al., 2018). Sleep spindles are temporally organized on an infraslow (i.e., 0.02 Hz) timescale that mirrors the fluctuating stability of NREM sleep and other physiological markers such as brain temperature (measured in murine sleep; Csernai et al. 2019). Their role in processes that might preserve sleep continuity has been subject to debate (see Section 1.1.3), with evidence for both a protective (Dang-Vu et al., 2011), meaning that they might attenuate sensory input; and a reactive role, meaning that they are stimulated by sensory input during sleep (Sela et al., 2016).

Hippocampal sharp-wave ripples are transient episodes of synchronized high-frequency neural activity (80-200 Hz; Axmacher et al. 2008). They are best recorded in local field potentials (LFP) and are not easily measured on scalp EEG, for which reason they do not feature prominently in our experimental work. However, they are proposed to serve as a critical mechanism for memory consolidation and spatial processing with their occurrence during periods of inactivity allowing the brain to replay and strengthen neural patterns formed during active experiences. For example, in rodent studies, selective suppression of hippocampal sharp-wave ripples led to deficits in spatial memory tasks suggesting that their integrity is essential for effective memory consolidation (Roux et al., 2017). In contrast to slow oscillations and sleep spindles, hippocampal ripples also occur in the wake state, in which they are engaged in replay and tasks such as rapid navigational planning (Roumis & Frank, 2015).

In NREM sleep, slow oscillations, spindles, and sharp-wave ripples frequently exhibit temporal relationships in which the higher frequency oscillations are nestled within a specific phase of the slower oscillations (see Figure 1.1B). Spindles occur frequently during the up-states of slow oscillations, and ripples occur in the down states of spindles (Staresina et al., 2015; Mölle et al., 2006). This 'phase-amplitude coupling' is believed to facilitate memory consolidation, a topic that will be explored in the next section. While the importance of nested oscillations in sleep-related neural processes explains many extent observations, it should be emphasized that there are numerous unexplained or unexplored aspects of how electrophysiological indices of sleep processes relate to one another, and their functional roles. For example, coupling rates are typically quite low, in the order of $\sim$10%; if nesting is critical to function, what are the 90% of uncoupled oscillations doing? Furthermore, sub-classes of these oscillations have been found to have different phase-amplitude relationships with one another. For example, while higher-frequency spindles (12–15 Hz) tend to cluster at SO peaks, slower frequency spindles (9-12 Hz) instead are more frequently found within the SO

troughs (Klinzing et al., 2016). Evidently, timing is important to neural communication, but its meaning with respect to the functional roles of sleep oscillations is largely unknown. As with most aspects of neurobiology, sleep is complex and nuanced; a more fine-grained understanding of sleep physiology is needed to develop better models of sleep's role in memory consolidation.

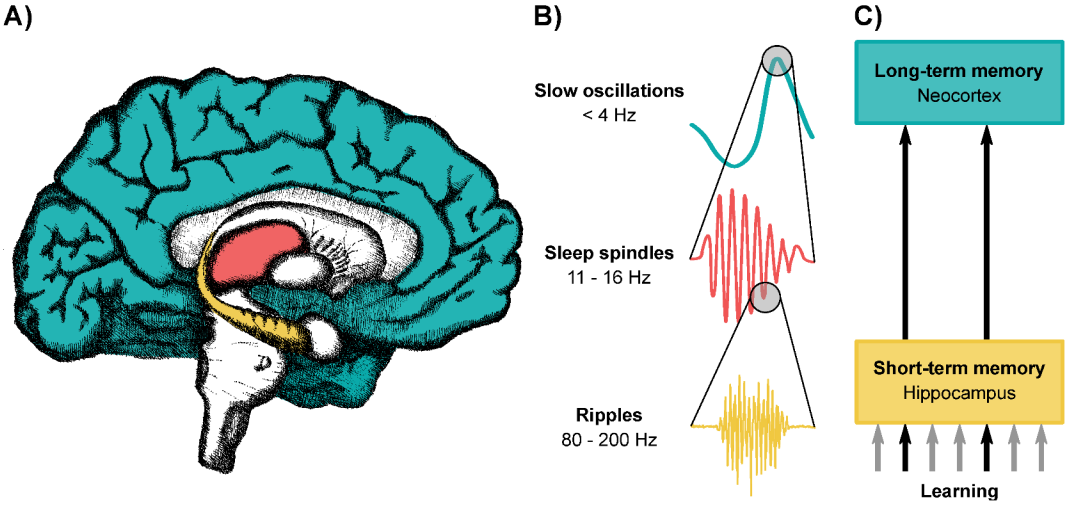

Figure 1.1: The active system consolidation theory proposes that memory consolidation during sleep depends on the precise temporal coordination of three distinct neural oscillations. A) The neocortex (blue) serves as the brain's permanent storage system for both declarative and procedural memories. The thalamus (red) serves as a central hub for the transfer of sensory information projecting widely to both cortical and subcortical structures. It also serves to modulate and filter sensory input, and is integral to higher-level cognition. Early encoding of learning, especially for declarative tasks, occurs within the hippocampus (yellow). The hippocampus underpins encoding, organizing, and temporarily storing new information including temporal sequences via its capabilities in pattern identification, separation, and novelty detection; and its ability to link different elements of an experience to form relational memories. B) From top to bottom, the three main NREM sleep oscillations are represented in the colour associated with the brain regions involved in their generation. Grey circles represent the preferred temporal coupling with sleep spindles nesting in the depolarized 'up-state' of slow oscillations and ripples occurring during the hyperpolarized 'down-state' of sleep spindles. C) This orchestration facilitates the transfer of information between brain regions that are critical for memory formation. The transformation from short-term to long-term memory depends on this hippocampal-neocortical dialogue, with sleep spindles serving as critical mediators in the process. Figure adapted from Fig 1. in Born & Wilhelm (2012). Brain and drawing from EC, used with permission.

1.1.2 Sleep spindles' role in memory consolidation

Sleep is thought to provide the necessary conditions for coordinated neural activity that is essential for memory consolidation (Stickgold, 2005). From animal studies showing replay activity in electrical recordings of place cells in rats (Wilson & McNaughton, 1994) to more recent work using functional magnetic resonance imaging (fMRI) (Boutin et al., 2024), sleep

plays a fundamental role in allowing reorganization of memory traces from temporary storage in the hippocampus to more permanent storage in the neocortex (see Figure 1.1; Rasch et al. 2007; Diekelmann & Born 2010; Rasch & Born 2013; Staresina et al. 2015, 2023).

Understanding the neural mechanisms of memory consolidation during sleep requires first examining the fundamental categories of memory systems themselves. Memories are commonly categorized into two subtypes: declarative memories, which involve information that can be consciously recalled (Tulving et al., 1972; Milner et al., 1998) such as retrieving the Spanish word for 'antepenultimate' or remembering the lyrics of your favourite Celine Dion song; and non-declarative memories, which are typically accessed without conscious awareness (Squire, 1992; Squire & Zola, 1996). An example of non-declarative memory is procedural learning, such as riding a bike or playing the violin. The consolidation of newly acquired memories appears to follow a similar pattern for both types of memories. Sensory information acquired during learning is preserved briefly in sensory memory, and information attended to is passed into short-term memory, allowing manipulation of the information with working memory and other executive functions (Nairne & Neath, 2012). These temporary memories are useful for online computations, but are fragile and evanescent. Through the process of memory consolidation, a subset of short-term memories are reorganized into more stable long-term forms across memory systems (Cabeza & Nyberg, 2000). This process is thought to rely heavily on the brain's ability to undergo structural and functional changes, in a process referred to as 'neuroplasticity'. Such modifications, including the reorganization and strengthening of existing pathways and creations of new connections, are essential for both memory stabilization and improved behavioural performance (Goto, 2022; Walker & Stickgold, 2004). In terms of neuroanatomy, memory consolidation is thought to orchestrate the communication of large neural networks throughout the brain with the hippocampus and neocortex playing central roles. Newly learned information encoded in the hippocampus is gradually transferred to distributed neocortical networks for long-term storage (Neves et al., 2008). Other brain regions are involved in this process such as the amygdala (highlighting the influence of emotions on learning; Phelps 2004), and the prefrontal cortex, which is responsible for working memory and higher-level cognitive processes (Jung et al., 2008; Funahashi & Kubota, 1994).

While declarative and procedural memory share these common neuronal mechanisms (Ullman, 2004; Brown & Robertson, 2007), certain brain regions show preferential activation patterns specific to each memory type. For example, the initial encoding of declarative memory predominantly engages the parahippocampal gyrus, the entorhinal cortex, and the perirhinal cortex within the medial temporal lobe (Manns & Eichenbaum, 2006; Eichenbaum, 2000; Squire & Zola, 1996). In contrast, procedural learning depends more heavily on subcortical and

motor-related structures, including the basal ganglia (particularly the striatum), cerebellum, and various cortical motor areas (Doyon et al., 2002; Barnes et al., 2005; De Zeeuw & Ten Brinke, 2015; Molinari et al., 1997; Censor et al., 2014). The hippocampus may also be involved in early stages of procedural learning (Albouy et al., 2013), either because procedural memory is experienced in the context of specific episodes implicating that they are always embedded into hippocampus-dependent episodic representations (Brodt et al., 2023), or because many procedural skills engage the hippocampus' presumed function of generating sequential content-free structures to access and organize sensory experiences distributed across cortical modules (Buzsáki & Tingley, 2018). In the piano learning task we will later use as a model for complex human neuroplasticity, for example, activity in the right hippocampus in response to hearing music predicted individuals' ability to learn to reproduce simple melodic sequences (Herholz et al., 2015).

Regardless of the specific brain regions involved, memory formation relies on complex interactions between neural systems that work in concert to encode, consolidate, and retrieve information. Researchers have therefore attempted to investigate correlations between the brain's electrical activity during sleep and the strengthening of memory traces. From observational and correlational paradigms to the development of experimental manipulations to evoke brain rhythms, many studies have sought to decipher the functional role of each type of sleep oscillation. Next, I will describe SO's roles only briefly, before turning to known relationships between sleep spindles and memory.

Slow oscillation characteristics (e.g., amplitude, density, and duration) are strongly linked to behavioural improvements in declarative memory tasks (Rasch & Born, 2013). For instance, Born et al. (2006) demonstrated that enhanced slow oscillation power during NREM sleep correlates with improved post-sleep recall in word-pair association and spatial navigation tasks. These types of correlational findings are further supported by studies showing that naturally occurring variations in slow oscillation activity between individuals predict differences in memory retention capabilities (Wilhelm et al., 2011). Furthermore, individual differences in SO-related properties such as the degree of coupling between SOs and spindles present in natural sleep can predict the degree of memory benefit obtained from methods to enhance SOs' occurrence (e.g.,Dehnavi et al. 2021). Invasive recordings in non-human animals have also established mechanisms by which cortical slow oscillations encourage hippocampal input to the cortex, enhancing synaptic strength via preferential replay of cortical firing sequences (e.g., Wei et al. 2016).

Given that modulating sleep spindles is the main novelty of my work, we will take a deeper dive into their known functional relationships with memory. Sleep spindle density has been linked to several cognitive processes such as high-level general mental ability (Bódizs

et al., 2005; Nader & Smith, 2001), performance IQ (Fogel et al., 2007a) and autism-spectrum disorders and schizophrenia via genetic-wide association studies (Krol et al., 2018), but most importantly to the work presented here, in their suggested role in memory consolidation (Clemens et al., 2005; Briere et al., 2000; Gais et al., 2002; Lustenberger et al., 2015; Schabus et al., 2006, 2008; Tucker & Fishbein, 2009).

Sleep spindle power has been correlated with neuronal structural characteristics involved in memory processes such as white matter integrity around the thalamus, corpus callosum, and forceps minor in young adult subjects (Gaudreault et al., 2018; Piantoni et al., 2013). Moreoever, in vitro studies showed that electrically introducing repetitive burst discharges in the thalamus, mimicking sleep spindles, promote neuroplasticity (Rosanova & Ulrich, 2005). As hallmarks of NREM2 sleep, sleep spindles are thought to be responsible for the widely reported role of NREM2 in the learning of both declarative and non-declarative tasks of increasing complexity (for reviews, see Ackermann & Rasch 2014; King et al. 2017). Supporting this association, research has consistently demonstrated that the density of sleep spindles (i.e., the number of sleep spindles detected per unit of time in NREM2 and 3) correlate with various aspects of memory performance, including both consolidation of novel declarative memories (Schabus et al., 2004; Clemens et al., 2005; Schmidt et al., 2006) and their integration into existing knowledge (Tamminen et al., 2010, 2013).

Interestingly, this relationship appears to be bidirectional, as increased learning activity also induces greater spindle density. For instance, in their 2002 study, Gais et al., showed that a word-pair task performed before sleep induced higher spindle activity compared to a task that lacked a learning requirement (e.g., counting letters with curves), with spindle activity positively correlating with post-sleep recall performance (Gais et al., 2002).

Doyon and Ungerleider developed a model explaining how the adult brain's cortico-striatal and cortico-cerebellar systems undergo cerebral plasticity during the acquisition of new motor skills (Doyon et al., 2002). This theoretical framework was later supported in a series of studies highlighting the role of sleep spindles in this process (Morin et al., 2008; Barakat et al., 2011, 2013; Doyon et al., 2009). According to this model, the brain actively reprocesses newly acquired movement sequences through 'offline' mechanisms. This neural reprocessing strengthens the pathways formed during initial learning, significantly improving both performance quality and long-term retention of motor skills—a process believed to depend heavily on sleep spindle activity. In a 2008 study, Morin and colleagues provided compelling evidence that the observed increase in spindle activity following motor learning was related to the consolidation process itself, rather than being a byproduct of nonspecific motor activity during the learning phase (Morin et al., 2008). Additionally, research using targeted memory reactivated paradigms, have shown that changes in sleep spindle characteristics (i.e.,

amplitude, duration and frequency) during reactivation mediate the relationship between experimental conditions and next-day performance improvements (Laventure et al., 2016). Finally, brain imaging research has also provided additional evidence supporting the link between spindles and memory consolidation processes. In their 2012 study, Barakat and colleagues showed a positive correlation between gains in performance and amplitude of sleep spindles (Barakat et al., 2013). They reported higher blood-oxygen-level-dependent (BOLD) signal in both motor-related areas and previously identified memory regions of interest, particularly the hippocampus and various regions of the neocortex. This work provided strong correlational evidence that sleep spindles predict neural changes in motor areas as well as improvement in motor learning, strengthening the link between these brain oscillations and changes in performance.

Although earlier work seemed to support the preferred involvement of slow oscillations in declarative memory (Gais & Born, 2004; Walker, 2009) and of sleep spindles in procedural memory (Choi et al., 2019; Barakat et al., 2013), more recent work challenge this simplistic perspective. For example, Menicucci et al. (2020) reported that slow oscillation activity was correlated with procedural memory. Similarly, the cognitive role of sleep spindles is not limited to procedural learning, as they are also implicated in declarative tasks. For example Schabus et al. (2004) showed that word pair learning improvements correlated with increased overnight spindle activity. Relationships to spindle density or amplitude were also found with improvements in cognitively more complex tasks such as the mirror tracing task (Fogel et al., 2007a,b; Holz et al., 2012; Rasch et al., 2009; Tamaki et al., 2008), a visuomotor learning task (Fogel et al., 2015; Huber et al., 2004), or the tower of Hanoi task (Fogel et al., 2015, 2007b). These results show that while spindles do seem to be involved in memory consolidation, their role is not confined to a specific type of memory. Further evidence for the involvement of sleep spindles in memory consolidation comes from pharmacological studies in animal models. These investigations have shown that increasing sleep spindle density through pharmaceutical interventions in rodents results in enhanced memory consolidation, further supporting the causal relationship between these neural oscillations and memory processes (Kaestner et al., 2013).

While correlative studies have initially suggested separable roles for these oscillations, more recent research indicates a more intertwined relationship (Baena et al., 2024). This theory, referred to as the 'active system consolidation model' emphasizes the importance of their combined action through temporal co-occurrence, rather than individual contributions (Born & Wilhelm, 2012). As described in Section 1.1.1, the coordinated activity of slow oscillations, spindles, and hippocampal ripples may facilitate the transfer of newly acquired information from short-term to long-term memory. In brief, neocortical slow oscillations are hypothesized

to exert control over memory consolidation by orchestrating the transfer of information between neocortex and hippocampus (illustrated in Figure 1.1). The up phases of slow oscillations are believed to trigger memory representation reactivation in the hippocampus, which subsequently generates both sharp-wave ripples and thalamocortical spindles. This precise temporal coordination generates coupled events where sharp-wave ripples carrying reactivated memory information become nested within the troughs of individual spindles. This structured alignment facilitates effective communication between hippocampal and neocortical networks. This triple-oscillation coupling is thought to create an optimal time window for neuronal communication between brain regions, promoting synaptic plasticity and ultimately enhancing memory consolidation processes during NREM sleep.

1.1.3 Sleep spindles' role in protecting the sleep state

Of interest in this work is the brain's responsiveness to auditory stimulation. Auditory processing in sleep has been shown to differ from the wake state (an idea that will be further developed in Section 1.2) as evidenced by reduced sensitivity to external input (Ogilvie et al., 1991), differences in auditory evoked responses (Mai et al., 2019) and limited higher-level processing (Makov et al., 2017), leading to the idea that sound processing might be blocked or attenuated in sleep (Schabus et al., 2012; Mai et al., 2019; Dang-Vu et al., 2011; Lüthi, 2014). This idea is however somewhat at odds with the finding that auditory stimulation has quite strong effects on neurophysiology during sleep (Ngo et al., 2013b). How can sounds be capable of influencing sleep and sleep-dependent cognitive processes, if incoming information is suppressed to protect those same cognitive processes from interference?

The majority of the work suggesting that sleep spindles block sensory information is indirect, as it is based on conceptual understanding of the sensory gating role of the thalamus. Because of the documented role of the thalamus during wakefulness, serving as a selective filter and attentional controller for sensory inputs and modulating their transmission based on relevance and attention (e.g., Koch 1987; Ward 2013; Jaramillo et al. 2019), this regulatory role has been proposed to extend to thalamo-cortically generated sleep spindles. The transition from tonic firing of the thalamic reticular nucleus during wake to bursting mode during spindle generation is thought to prevent normal sensory transmission to cortex. Therefore, sleep spindles are hypothesized to represent a mechanism through which the thalamus restricts external sensory information flow to the cortex, reducing environmental responsiveness (McCormick & Bal, 1994; Dang-Vu et al., 2011; Schabus et al., 2012). This selective gating process is believed to help maintain stable sleep states by preventing awakenings in response to external stimuli. The alleged function of sleep spindles in blocking auditory information

from reaching the cortex is particularly relevant to my ultimate goal of targeting them with auditory stimulation to probe their function. If spindles suppress sensory information, then targeting them with sound might prove futile.

1.2 The auditory system

Sleep stages and their characteristic oscillatory events reflect the brain's internal state changes. They also influence how our brain processes and reacts to incoming sensory information. Of particular interest for the work described in this thesis, auditory stimuli have the capacity to non-invasively influence endogenous sleep oscillations and memory processes (Ngo et al. 2013b; these topics will be discussed in more detail in Section 1.3.

Before diving into the realm of brain manipulation, it is important to first understand how the auditory system works during wakefulness and how it is impacted by sleep. The overall role of the auditory system is to transduce physical energy, in the form of sound waves, into neural information that can be processed by higher cognitive functions (e.g. speech, music, threat detection) through electrical signals in the brain. This rapid process occurs within milliseconds and recruits multiple brain structures, both cortical and subcortical. For an overview of auditory system neurophysiology, please see Eggermont & Ponton (2002).

In summary, sound waves entering the ear canal cause vibrations in the eardrum which then propagate to the cochlea. Vibrations are transformed into neural signals by specialized cells mounted on the cochlea's basilar membrane. These neural signals, which encode properties of sound such as onsets, offsets, frequency, and amplitude, are then sent to the cochlear nucleus (CN) in the brainstem, via the auditory nerve. From this point onward, the central auditory system consists of two ascending pathways: a primary (lemniscal) pathway and a secondary (non-lemniscal) pathway.

The lemniscal pathway, which carries temporally-precise information, continues to the inferior colliculus (IC) and finally to the ventral division of the medial geniculate body of the thalamus (MGB) before reaching the primary auditory cortex (AC) in the the temporal lobe of the cerebral cortex (see Figure 1.2A for an illustration). Far from being merely relay stations, early auditory regions are activity involved in processing, filtering, and integrating acoustic information, via top-down and bottom up connections (see also Figure 2 inMarsh & Campbell 2016 for a wiring diagram of afferent and efferent connectivity in the auditory system). Although additional structures are involved along the auditory pathway (e.g., superior olivary complex, nuclei of the lateral lemniscus), we focus on CN, IC, MGB and AC as these structures include neurons that phase-lock their firing to the periodicity of the signal and can be recorded non-invasively (Coffey et al., 2016b). These characteristics will

prove useful to our exploration on how early sound encoding is affected by sleep. Once the signal arrives at the primary auditory cortex, the information is then processed consecutively in different higher-order pathways to identify the sound's source, interpret information content, or provide information of behavioural relevance to higher-level cognitive functions (see Rauschecker & Scott 2009 for a review).

The non-lemniscal pathway has a more complex (and less well-characterized) structure where neurons form widespread connections between the midbrain, cortex and limbic regions (Lee, 2015). In contrast to the lemniscal pathway's precise, tonotopic representation of acoustic properties, the non-lemniscal system facilitates broader, less frequency-specific auditory processing, contributing to how sounds affect us emotionally and behaviourally, notably through links to the arousal system (Kraus et al., 1994; Anderson & Linden, 2011).

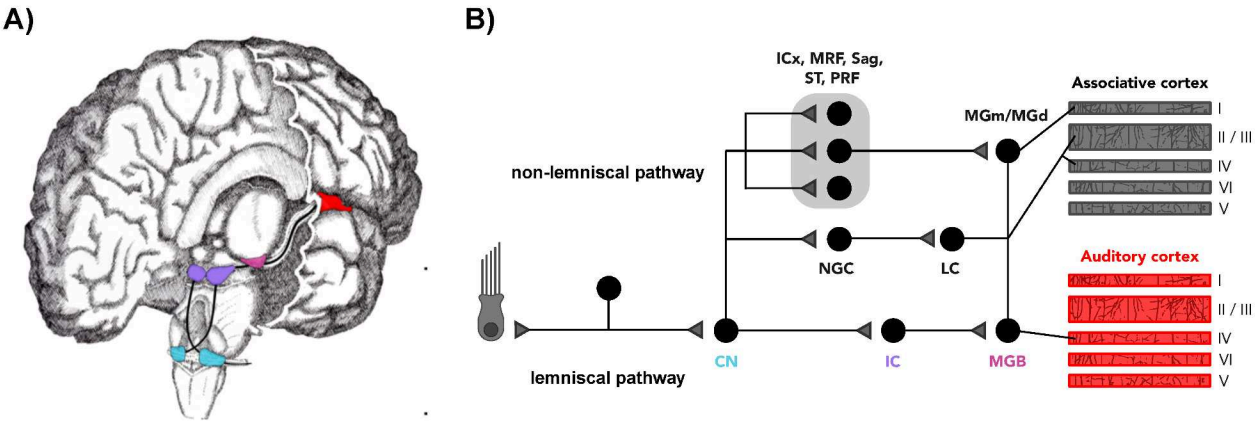

Figure 1.2: A) Schematic anatomical representation of the main structures of the auditory lemniscal pathway. B) Schematic organizational representation of the ascending auditory pathways involved in generating evoked responses during sleep. The auditory system comprises two major pathways: primary (lemniscal) and secondary (non-lemniscal). The lemniscal pathway transmits auditory signals from the cochlear nuclei (CN) through the inferior colliculus (IC) and the medial geniculate body (MGB) of the thalamus to the primary auditory cortex. The non-lemniscal pathway, consists of fibers originating from multiple brainstem regions including the dorsal nucleus of the inferior colliculus (ICx), midbrain reticular formation (MRF), nucleus sagulum (Sag), spinothalamic tract (ST), and pontine reticular formation (PRF). These project to the caudo-medial (MGm) and dorsal (MGd) regions of the medial geniculate body before reaching associative areas surrounding the primary auditory region. Components of the arousal reticular activating system (ARAS), such as the nucleus gigantocellularis (NGC) and locus coeruleus (LC), are also considered part of this secondary pathway due to their activation by auditory stimulation. Figure adapted from Fig 4. in (Bellesi et al., 2014). Brain from the author HRJ, drawing from EC, used with permission.

1.2.1 Auditory evoked responses

Examining sensory processing during sleep is naturally restricted by the lack of behavioural response from the participant. Evoked brain responses give researchers a way to assess the

sensory and cognitive processing of stimuli independent of behavioural response. The majority of research to date on auditory evoked responses has used EEG. EEG signals recorded at the scalp mainly come from the activity of cortical pyramidal cells (layers 3 and 5; Kirschstein & Köhling 2009). This technique's very high temporal resolution, with possible sampling rates up to 20,000 Hz (although sampling rates in the 256 to 512 Hz range are more commonly used), allows the collection of neural signals with sub-millisecond precision. This property allows researchers to investigate high-frequency brain signals involved in human perception and cognition (Kucewicz et al., 2014; Lachaux et al., 2012). By recording brain signals from multiple locations on the scalp simultaneously, researchers can also study the topography of brain activity and to estimate its sources (Stropahl et al., 2018).

Event related potentials (ERPs) are electrophysiological brain responses evoked by a sensory or cognitive event, usually averaged over hundreds of repetitions. They can be elicited by different sensory modalities including auditory stimuli (Gehring et al., 2012), and are frequently used in human neuroscience as they are non-invasive, reliable, consistent, and relatively easy to measure. ERPs are typically presented as averaged time series data, which show peaks and troughs representing cumulative fluctuations in neural activity over time. The different peaks observed in the averaged brain response measured at the scalp correspond to the weighted sum of activity of one or more neural sources in the brain. Peaks and troughs are named based on their polarity ('P' for positive, 'N' for negative), and either based on their approximate timing relative to onset (e.g., P100, a positive deflection approximately 100 ms after onset), or based on their ordinal position ('P1', 'N1', etc.). By comparing ERPs across conditions or subject groups, and by using experimental manipulation (Tanaka & Curran, 2001), researchers can quantify experimentally relevant differences in sensory processing. Peaks evoked by short, relatively standard stimuli such as syllables, words, or tones have been intensively studied and have been attributed to cognitive processes like covert attention (N2pc; Eimer 1996), language processing (N400; Kutas & Hillyard 1980) and categorization (P300; Bashore & Van der Molen 1991).

Changes in the appearance and latency of evoked responses across brain states inform us about the state of the central nervous system and its degree of reactivity to sensory stimulation such as sound. Some of the first evoked response observed in sleep were 'K-complexes' (Colrain & Campbell, 2007; Loomis et al., 1938), a subset of slow oscillations named for their shape, that can be elicited by stimulation or can occur spontaneously (described briefly above, in Section 1.1.1). Evoked K-complexes are used to investigate how sensory processing shifts with varying sleep depth, as detailed in Colrain's review (Colrain & Campbell, 2007).

Subtle changes in amplitude and latency have been reported in the characteristic peaks and troughs (Niiyama et al., 1994; Ogilvie et al., 1991) of auditory ERPs (sometimes

called 'auditory evoked responses', though we will use the more general term 'ERP') as sleep deepens. Notably, the N100 component tends to diminish during sleep, while the P200 component often exhibits increased amplitude in deeper sleep stages (Campbell, 2010). Besides the changes observed on well-known peaks already measured in wakefulness, new evoked potentials occurring later than 300 ms post stimuli only appear during sleep (Bastien et al., 2002). Interestingly, their appearance consistently coincides with the incapacity of subjects to respond to external stimuli (Ogilvie et al., 1991). These peaks labelled N350 and N550 begin to emerge at NREM sleep onset and their amplitude increases with sleep depth until reaching very large values (five times bigger than other components). Their large amplitudes represent synchronized burst firing of many pyramidal cells. N350 is thought to reflect an active inhibition of sensory processing (Ujszászi & Halász, 1988) and N550 amplitude is thought to measure the brain's capacity to generate delta activity, one of the hallmarks of deep sleep (Colrain et al., 2010). Together with the positive peak observed 900 ms post stimulation (i.e. P900), they form part of the very large amplitude elicited K-complex mentioned above. Interestingly, these evoked waves share many similarities with endogenous SOs and have been linked to sleep continuity and arousal (Halász, 2016). Due to their common origin with endogenous slow oscillations and their similar characteristics, it is reasonable to suggest that they might play a similar role in memory consolidation and be the basis of the behavioural effects observed following auditory stimulation paradigms (Ngo et al., 2013b).

Another auditory evoked response used by researchers to probe auditory processing is the 'Frequency Following Response' (FFR). The FFR indexes the brain's ability to encode pitch information. Generated by neurons along the lemniscal pathway, this response is phase-locked to the periodicity in stimuli and is used by researchers and doctors to measure the strength and quality of pitch encoding, which is vital for speech and language functions. It can also be used to measure the long-lasting impact of learning on neuroplasticity such as the difference observed in FFR strength between musicians and non-musicians (Kraus, 2011; Parbery-Clark et al., 2013; Musacchia et al., 2007, 2008). More pertinent to our current focus, FFRs are subtly affected by attention (Galbraith et al., 2003) (likely via corticofugal pathways), and potentially by sleep depth (Mai et al., 2019), making them a valuable tool for investigating how neural encoding and transmission of basic sound features (pitch) up the lemniscal auditory system changes in response to sleep depth and oscillatory events. Furthermore, the neural sources of FFRs can be separated, using magnetoencephalography (MEG), the benefits of which are described in the next selection.

1.2.2 The advantages of magnetoencephalography

A challenge to interpreting results using EEG is that signals originating from different neural populations mix together at the scalp, where they are recorded, meaning that changes in an ERP component's amplitude or latency can not easily be attribute to a specific neural source. Although some source separation is possible using high density EEG (e.g., Stropahl et al. 2018), spatial resolution is inherently limited by the properties of electrical fields; they are influenced by interfaces between tissues through which they pass. Because the complex and highly heterogeneous conductivity profiles of head tissues cannot be measured with precision in vivo (Baillet, 2017), considerable uncertainty remains in any biological model of EEG source origin. Therefore although EEG has excellent temporal resolution and is appropriate to use for research questions that test whether there are differences in evoked responses across groups or experimental conditions, many questions that require knowledge of neural origins cannot be adequately addressed using it. For example, EEG is not well-suited for investigating whether evoked responses are coming from similar sources as endogenous activity, or tying cognitive function to specific brain regions or circuits as a means of developing mechanistic models.

Magnetoencephalography offers a powerful alternative to EEG for investigating these questions (Baillet, 2017). Contrary to the previously-mentioned spatial resolution limitations of EEG source localization due to signal propagation being impacted by brain tissues, MEG source localization maintains its spatial accuracy, because magnetic fields propagate through heterogeneous tissues without significant distortion (Baillet, 2017). This difference between magnetic and electrical signals favours more precise source reconstruction in MEG. While MEG has traditionally been used to study the neocortex, recent evidence (including from our own work, see Appendix C) suggests that, given a sufficient amount of data and source modelling techniques that are optimized for deep sources such as volume models, MEG can also be used to detect sub-cortical activity (Piastra et al., 2021; López-Madrona et al., 2022; Pizzo et al., 2019), including in the hippocampus, amygdala, thalamus and even brainstem – despite these sources being further from sensors (Attal & Schwartz, 2013; Bénar et al., 2021; Pu et al., 2018; Ruzich et al., 2019; Coffey et al., 2016b). By using MEG we are therefore able to measure the neurophysiological activity of the entire brain with sub-millisecond temporal resolution, with excellent spatial and spectral differentiation, and minimum bias (Baillet, 2017). In this thesis, I make use of both EEG and MEG to study evoked auditory responses and their interaction, taking advantage of MEG's superior spatial resolution for research questions that benefit from knowing neural origins, and benefiting from the relative simplicity and low-cost of EEG for questions that do not.

1.3 Manipulating sleep with sound

Non-invasive brain modulation methods, including electrical and magnetic stimulation approaches, have emerged as powerful investigative tools, allowing researchers to systematically manipulate neural activity in healthy individuals. Through either enhancement, disruption, or generation of specific brain events, researchers can now causally manipulate brain activity to examine brain oscillations' functional roles (Kumar, 2021; Occhionero et al., 2020; Antony et al., 2012). Closed-loop brain stimulation is a sub-class of brain stimulation that involves timing sensory, magnetic, or electric stimulation to coincide with and modulate endogenous brain activity. To do so, physiological signals, typically from electroencephalography (EEG), are continuously monitored by real-time algorithms that detect specific neural patterns to rapidly trigger stimulations.

1.3.1 Closed-loop auditory stimulation of slow oscillations

As regards our interest about sleep's role in memory, in a seminal paper, Ngo et al. 2013b showed that closed-loop auditory stimulation of slow oscillations (SO-CLAS) during non-rapid eye movement sleep evoked both additional SOs and spindles, and improved overnight memory performance (see Figure 1.3.1 for a comprehensive table of replication studies). The timing of stimulation proved to be important, with stimulation during SO peaks (up-states) promoting subsequent SO activity and sleep spindles, thereby enhancing sleep-related memory consolidation (Navarrete et al., 2020). Conversely, stimulation during troughs (down-states) decreases spindle activity and delta power (Moreira et al., 2021; Ngo et al., 2013b). While stimulation effectiveness varies across subjects (Nasr et al., 2022), research has relatively consistently shown neurophysiological responses to CLAS, which are linked to behavioural improvements. These findings have been subsequently extended, demonstrating that precisely timed non-invasive auditory stimulation can successfully modulate neural events, establishing its value as a tool for investigating the neural substrates of memory processes (Harrington & Cairney, 2021; Fehér et al., 2021; Choi et al., 2020; Salfi et al., 2020). However, the physiological processes underlying the observed responses – particularly the pathway through which auditory stimulation influences memory processes – is still unknown (Girardeau & Lopes-Dos-Santos, 2021). Furthermore, only a very small subset of stimulation targets and timing variations have been explored, suggesting that the full potential of CLAS to probe the functions of brain circuits has yet to be realized.

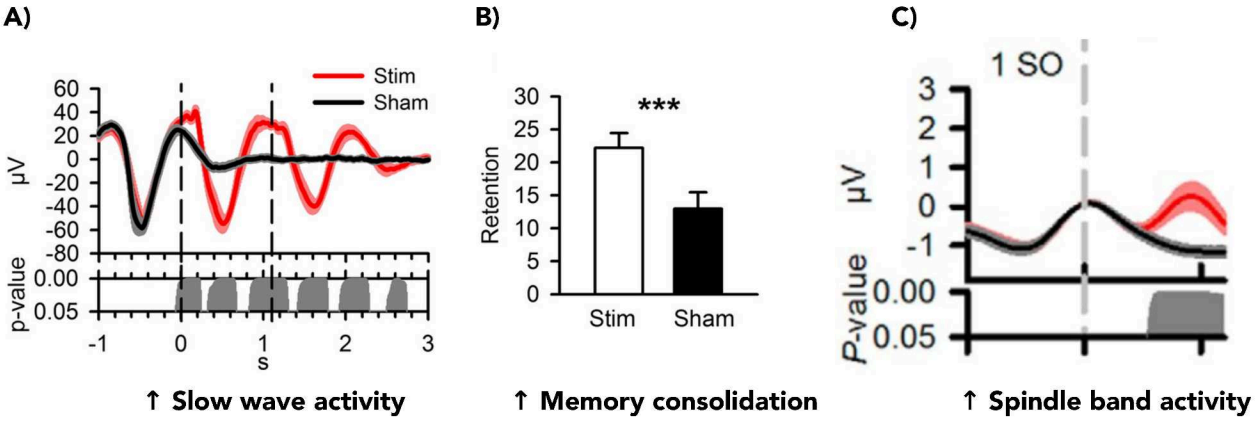

Author	Subjects	Mean age	Target	Stimuli	Measures	Design	Sleep	Evoked	Behaviour
Ngo et al. (2013b)	N = 11	24.2 (0.9)	SO up-state	2 clicks	Declarative	Within	Night	↑ SO	↑ Declarative
Ngo et al. (2015)	N = 18	23.8 (0.6)	SO up-state	2 clicks	Declarative	Within	Night	↑ SO	↑ Declarative
Ong et al. (2016)	N = 16	22 (1.4)	SO up-state	5 clicks	Declarative	Within	Night	↑ SO	↑ Declarative
Leminen et al. (2017)	N = 15	30.5 (N/A)	SO up-state	1 click	Declarative Procedural	Within	Night	↑ SO ↑ Spindle	↑ Declarative only
Papalambros et al. (2017)	N = 13	75.2 (N/A)	SO up-state	5 clicks	Declarative	Within	Night	↑ SO ↑ Spindle	↑ Declarative
Ngo et al. (2019)	N = 34	25.1 (3.4)	SO up-state	7 clicks	Declarative	Within	Night	↑ SO ↑ Spindle	No change
Ong et al. (2018)	N = 37	22.5 (2.3)	SO up-state	2 clicks	Declarative	Within	Nap	↑ SO ↑ Spindle	No change
Henin et al. (2019)	N = 31	23.5 (0.6)	SO up-state	1 click	Declarative Navigation	Within	Night	↑ SO ↑ Spindle	No change
Diep et al. (2020)	N = 24	39.9 (4.2)	SO up-state	continuous clicks*	Declarative Procedural	Within	Night	↑ SO	↑ Working memory in high responders
Schneider et al. (2020)	N = 17	55.7 (1.0)	SO up-state	2 clicks	Declarative Procedural	Within	Night	↑ SO ↑ Spindle	No change
Harrington et al. (2021)	N = 12	20.0 (2.0)	SO up-state	2 clicks	Declarative	Within	Night	↑ SO	No change
Koo-Poeggel et al. (2022)	N = 16	25.6 (0.6)	SO down-to up-state	2 clicks	Declarative	Within	Nap	↑ SO ↑ Spindle	No change
Baxter et al. (2023)	N = 20	29.0 (5.0)	SO up-state	1 click	Procedural	Within	Nap	↑ SO ↑ Spindle	No change

Figure 1.3: Overview of closed-loop auditory stimulation literature. The seminal paper by Ngo et al. demonstrated that precisely timed closed-loop auditory stimulation during slow oscillation up-states produced three main outcomes: A) enhanced slow wave activity compared to sham conditions, B) improved declarative memory consolidation, and C) augmented sleep spindle activity. Since this pioneering work, researchers have attempted to replicate these findings with varying degrees of success, exploring different stimulation methods, neural targets, and memory assessment protocols. The figure presents an illustrative image from Ngo et al. 2013b above and a comprehensive table below. All these studies used 50 ms pink noise. The table has been adapted from Table 1 in Esfahani et al. 2023, retaining only studies involving healthy adult participants while incorporating more recent research findings.

1.3.2 Closed-loop auditory stimulation of sleep spindles

Previous research showed that sleep spindles can be experimentally induced through various brain stimulation approaches, either as an evoked response to SO-CLAS stimulation (Ngo et al., 2013b) or through responses to open-loop (i.e., presented randomly) frequency-modulated stimulation (Antony et al., 2019). In their 2017 study, Antony & Paller (2017) successfully increased spindle activity using white noise that had been modulated at various frequencies (12 Hz, 15 Hz, or 50 Hz) during NREM2 and 3 sleep. Their study also revealed timing dependencies, showing an enhanced effect of stimulation performance when stimulation was delivered 2.5 seconds after spindle offset compared to immediate post-spindle stimulation, suggesting the existence of a spindle 'refractory period' (Antony et al., 2018). Additionally, Lustenberger et al. (2016) demonstrated that transcranial alternating current stimulation (tACS) at 12 Hz led to improvements in motor memory consolidation correlating with changes in fast spindle activity. While their open-loop investigations provided valuable information, technological constraints prevented the direct targeting of sleep spindles, limiting the ability to examine the effects of real-time spindle stimulation. Early work in closed-loop auditory stimulation of sleep spindles was conducted through a series of nap studies by (Choi et al., 2018, 2019, 2020; Choi & Jun, 2022). Despite technical limitations resulting in only 20-23% of stimulations successfully coinciding with target sleep events (even though mostly close to their offset), their findings revealed that spindle stimulation enhanced both slow wave and spindle activity (Choi & Jun, 2022), consistent with general observations about open-loop stimulation during NREM2 and NREM3 (Bastien et al., 2002; Colrain & Campbell, 2007). They reported less fragmented sleep, and tentative improvements in procedural memory consolidation, suggesting that stimulating even towards the end of a spindle might offer some benefit compared to randomly timed stimulation. While these studies have advanced our understanding of the interaction between sleep spindles and auditory stimulation, the technical challenges in achieving precise temporal targeting of spindles has constrained our ability to fully elucidate the timing-dependent effects of stimulation on neural oscillations and their cognitive and behavioural consequences.

1.3.3 Recent technological development

In the pursuit of deciphering the roles of brain oscillations in human cognition, technological advances provide us with new opportunities. For example, the miniaturization of electrical components has made it possible to develop smaller devices without compromising data quality. This development opens new possibilities making data collection more practical both in the laboratory environment and at home. The shift towards portable EEG is particularly

important in sleep research, as traditional polysomnography, while comprehensive, presents significant limitations regarding cost and the requirement for technical expertise for electrode application and signal monitoring. Furthermore, both the amount of equipment applied to the sleeper and the laboratory environment can substantially impact sleep quality. By allowing sleep to be recorded in familiar home environments, portable devices improve the ecological validity of sleep research; by decreasing cost and complexity of use, they make multi-night and longitudinal studies more feasible. In the context of CLAS, portable, low-cost devices are particularly needed as existing real-time equipment is prohibitively expensive and cumbersome. Existing CLAS systems also suffer from insufficient temporal resolution for detecting certain fast oscillations, and lack flexibility in experimental parameters for both detection and stimulation.

Recent advances in artificial intelligence and electrical engineering have led to improved signal processing technology and the development of better, more efficient algorithms, some of which can run with modest computing requirements. This improvement in computational capabilities is particularly relevant for CLAS, as previously available algorithms were not able to detect some neural activity of interest quickly enough to interact with it. By combining these technological developments in both hardware and software, the development of portable, cost-effective closed-loop stimulation systems addresses a significant need in this field, as it will allow for the investigation of new research questions such as the closed-loop stimulation of sleep spindles. While detection performance has been extensively documented in offline analyses (Lacourse et al., 2020, 2019), the physiological responses to precisely timed auditory stimulation during spindles remain to be thoroughly investigated. Understanding these neurophysiological effects and confirming the successful targeting of sleep spindles under experimental conditions represents a critical stepping stone toward applying these techniques to elucidate the roles of spindles in learning and memory processes.

1.4 The present work

My doctoral research investigates the complex interaction between auditory sensory processing and endogenous neural oscillations in the human brain. This dissertation comprises six main studies, with four additional works presented as Appendices that either were directly relevant to development of the tools used in this work (Valenchon, ..., Jourde, et al., 2022; Sobral et al., ..., Jourde, in review), extended our work on sleep in naturalistic environments to extreme conditions (Paas & Jourde et al., 2024), or made use of developments in MEG deep source imaging that were developed in the context of the present work to study thalamocortical spindles in the thalamus (Rattray,..., Jourde et al., in review).

In Chapters 2 and 3, we investigated both the impact of sleep on early auditory processing and the mechanisms by which the auditory system can influence endogenous oscillations in sleep using source-localized magnetoencephalography. In Chapter 4, we addressed a previously accepted hypothesis and educed evidence that auditory input to the cortex is not blocked at the thalamus during spindles and their refractory period. This enabling investigation was needed to pursue our ultimate goal of manipulating them with sound. In Chapters 5 and 6, we explored the neurophysiological effects of the timing of CLAS with respect to coupled and uncoupled SOs and spindles. This work, along with previous studies, lays the foundation for a behavioural study examining the effects of spindle CLAS. In Chapter 7, we therefore compared the behavioural outcomes of SO and spindle stimulation on simple declarative and procedural tasks, as well as on a complex task.

Chapter 2

Sleep state influences early sound encoding at cortical but not subcortical levels

2.1 Abstract

In sleep, the brain balances protecting processes like memory consolidation with preserving responsiveness to significant external stimuli. Although reductions in higher-level auditory processes during deeper sleep have been described, the sleep-dependent changes across levels of auditory hierarchy, particularly as regards early sound representations, remain undefined. The frequency-following response (FFR) is an evoked auditory response that indexes neural encoding of sound periodicity. It is generated by neural populations in the brainstem, thalamus, and auditory cortex that phase-lock to periodic auditory stimuli and encode pitch information. The FFR's neural sources, which can be resolved using magnetoencephalography (MEG), allow evaluation of neural representation strength throughout the auditory neuraxis as a function of sleep state, as well as neural events like slow waves and sleep spindles that are hypothesized to attenuate acoustic processing as a means of preserving the sleep state. We recorded FFRs during a 2.5 hour nap from fourteen healthy male and female human adults to investigate how sleep depth and microarchitecture affect auditory encoding. We show that FFR strength is maintained across non-rapid eye movement sleep stages in subcortical nuclei, yet decreases in deeper sleep in the auditory cortex. FFR strength was not influenced by slow wave or spindle activity, but rather by reduced communication between the thalamus and cortex. This differentiation in sound representation across the auditory hierarchy suggests a means by which the brain might balance environmental monitoring with preserving critical

restorative processes.

2.2 Introduction

Sleep is a unique neurophysiological state that is actively involved in cognition, learning, and memory (Paller et al., 2021; Simon et al., 2022). In deep, non-rapid eye movement (NREM) sleep, people become less responsive to the external world, possibly as a means of protecting these important sleep-dependent processes from disruption (Velluti, 1997; Coenen, 2024). However, sensory stimuli continue to be processed to some degree, and selectively – salient and meaningful sounds such as a person's own name or those charged with emotional prosody are preferentially processed (Perrin et al., 1999; Blume et al., 2018). How the brain navigates the need for protecting sleep-dependent processes with that of preserving responsiveness to significant external stimuli is an unsettled question (Hennevin et al., 2007; Coenen, 2024), with proposals ranging from deeper sleep states reducing the amplitude of encoded sensory activity through thalamic inhibition (Coenen, 2024), specific neural events such as sleep spindles disrupting transfer to cortex selectively when they are present (Schabus et al., 2012), to generation of reactive elements (including as K-complexes and sleep spindles) that might counteract microarousals to stabilize and preserve the sleep state following sensory input (Blume et al., 2018). Clarifying how sensory information is processed by and interacts with the sleeping brain is relevant to several research directions, including those attempting to study or enhance memory processes via neurostimulation (see Harrington & Cairney (2021); Fehér et al. (2021); Choi et al. (2020); Salfi et al. (2020) for reviews), and because abnormalities in arousal patterns are involved in a range of pathologies (Halász et al., 2004).

The effects of sleep depth on auditory processing have been investigated by examining brain responses to sounds of varying complexity across different sleep stages in both human and non-human animals (Colrain & Campbell, 2007). In deeper non-rapid eye movement (NREM) sleep (i.e., stage 3), cortical evoked responses (50–250 ms) generally show similar or only slightly attenuated amplitudes compared to wake states; these signals originate in primary and secondary auditory cortex in the superior temporal gyrus (Colrain & Campbell, 2007; Jourde et al., 2024). Feed-forward information flow to primary and secondary auditory areas seems to therefore remain functional in deeper sleep; however, neural feedback signalling may be reduced (Hayat et al., 2022). Some aspects of higher-level sensory integration and discriminative capacity that are processed further downstream in the auditory hierarchy are preserved even in deeper sleep stages (Hennevin et al., 2007). Meaningful speech is transiently amplified compared to irrelevant signals, but this amplification decreases with sleep depth, with slow waves appearing to suppress neural indices of speech tracking in

deeper sleep (Legendre et al., 2019). In general, brain activation associated with speech processing is increasingly attenuated as sleep deepens, from thalamus in which responses are relatively preserved to high order language representations in inferior frontal gyrus which are absent during NREM sleep (Wilf et al., 2016). While reductions in cortical and higher-order auditory processes during deeper sleep have been reported, the involvement of lower levels within the auditory hierarchy, their interaction with cortical regions, and how specific information-bearing signals such as neural markers of acoustic encoding are affected by sleep states, remains unclear.

The frequency-following response (FFR) is an evoked auditory response indexing neural encoding of sound periodicity associated with pitch information (∼80-400 Hz) (Skoe & Kraus, 2010; Coffey et al., 2019; Krizman & Kraus, 2019). It is generated by neural populations in the brainstem, thalamus, and auditory cortex that phase-lock to periodic auditory stimuli and encode frequency information. The FFR's neural sources, which can be resolved using magnetoencephalography (MEG) (Coffey et al., 2016b; Gorina-Careta et al., 2021), allow evaluation of the strength of neural encoding of sound periodicity throughout the auditory neuraxis. These properties make it suitable to assess auditory encoding in relation to sleep states and to transient neural events that occur during NREM sleep, such as slow waves and sleep spindles.

This study aimed to investigate how sleep depth and microarchitecture influence auditory encoding across the auditory hierarchy. We recorded FFRs during a 2.5 hour nap in 14 healthy young adults using magnetoencephalography (MEG) and electroencephalography (EEG), examining changes in early sound representations with sleep state and specific neural events. Clarifying how, when, and where basic auditory processing is altered in NREM sleep may have implications for our understanding of how the sleeping brain balances environmental monitoring with preservation of critical sleep-dependent neural processes.

2.3 Methods

2.3.1 Participants

Fourteen neurologically healthy young adults who reported being able to sleep in a supine position and being capable of napping mid-afternoon were recruited. One was later excluded due to inability to sleep in the scanner during the experiment. The mean age of the remaining participants was 24.8 years (SD, 4.0; range, 21-36), 9 were female, all were right-handed, and all reported having normal hearing and no history of neurological disorders. We confirmed that all subjects had a regular sleeping schedule (6.5-8.5 hours per night, with habitual

bedtimes). Informed consent was obtained and all experimental procedures were approved by the applicable ethics committees (Montreal Neurological Institute Research Ethics Board and Concordia's University Human Research Ethics Committee), and subjects were compensated for their time.

2.3.2 Study design

Considerations for sample size

Given limited literature relating to our main research questions, which concern changes in FFR magnitude as a function of sleep depth and neural events, our study lacked a basis for calculating an a priori sample size. Sample size and stimulation parameters were therefore selected with reference to previous work on the MEG-FFR (Coffey et al., 2016b; Gorina-Careta et al., 2021; Hartmann & Weisz, 2019; Coffey et al., 2021); with consideration that the study design is within-subjects and therefore has greater statistical power than do between-subjects designs due to reduced variability; noting that the research questions concern basic aspects of physiology that should be conserved across participants; and with consideration for experimental resources (noting that each nap experiment required ∼4 hrs of scanner time). An analysis of the effect of number of epochs on signal-to-noise ratio (SNR) for MEG-FFR suggested that 2000-4000 FFR epochs should be sufficient to achieve SNRs of about 1.5 (FFR strength relative to baseline; see Figure 6.3 in Coffey (2016)), which is sometimes used as an exclusion criterion for FFR signal quality (Skoe & Kraus, 2010). We therefore chose to maximize the nap period and number of stimuli presented for a small group of individuals.

Selection of neurophysiological measures

Our main focus was on assessing where state-dependent changes can be observed in the auditory system's representation of pitch information, for which MEG is most suitable due to its superior spatial properties. However, because much of the FFR work to date has used the EEG-based FFR, and to extend the work of (Mai et al., 2019) showing that EEG-FFR in young adults is sensitive to alertness levels as measured by the occurrence of spindles, we collected both EEG and MEG data, simultaneously. EEG-FFR is a composite signal arising from the summation of multiple generators at the scalp, and can be interpreted as a global measure of FFR strength with multiple contributors (Coffey et al., 2019; Tichko & Skoe, 2017; Coffey et al., 2016b). We thus first assess whether the EEG-FFR magnitude is affected by sleep stages and presence or absence of discrete sleep events, and compare it with

MEG-FFR results. EEG also has a higher SNR, making it suitable for analyses of conditions that have few epochs.

Overview of the experimental procedure

Upon arrival at the laboratory, participants were prepared for EEG and comfortably settled into the MEG scanner in a supine position (as in Jourde et al. (2024)). A 5 min resting state data acquisition with eyes open was collected, as a contribution to an open-access database (Niso et al., 2016). Lights were dimmed, and subjects were asked to close their eyes and relax for a 2.5 h nap opportunity. Sound stimulation was started immediately, with the subject in the awake state, to allow them to get used to the sound and so that the brain response to the wake state could be measured as a baseline for each individual's FFR strength (which can vary considerably even between healthy young adults Coffey et al. (2016a)). Standard T1-weighted anatomical magnetic resonance images were acquired in a separate session to enable distributed source localization of the MEG signals.

2.3.3 Data acquisition

EEG data were collected for several purposes: capturing the EEG-FFR, determining sleep depth (i.e., sleep staging), and detecting sleep events (i.e., sleep spindles and slow oscillations). A three-channel (Cz, C3, C4; 10–20 International System) EEG montage was applied with a forehead ground and earlobe references. Bipolar electrooculography (EOG) electrodes around the eyes and electrocardiography (ECG) electrodes on the chest were applied for later use in detecting corresponding artefacts in the MEG traces. Two pairs of additional electromyography (EMG) channels on the chin and neck were used to assist in sleep scoring. Head shape and the location of head position indicator coils were digitized (Polhemus Isotrak, Polhemus Inc., VT, USA) for co-registration of MEG with anatomical T1-weighted MRI.

Two hundred and seventy channels of MEG (axial gradiometers), along with the five channels of EEG data, EOG and ECG, and one audio channel were simultaneously acquired using a CTF MEG System and its in-built EEG system (Omega 275, CTF Systems Inc.). All data were sampled at 2,400 Hz. The MRI scans acquired in a separate session used a 3T Siemens scanner. The anatomical images were T1-weighted and obtained using an MPRAGE sequence with the following parameters: 176 slices, field of view = 256 x 256, TR/TE/TI = 2300/2.98/900 ms, and 1 mm isotropic voxel size.

2.3.4 Stimulus presentation

To characterize the brain's response to sound over arousal states, we used a 120 ms synthesized speech syllable (/da/) with a fundamental frequency in the sustained vowel portion of 98 Hz. This syllable is favoured by many FFR researchers for its acoustic properties, ecological validity in speech (the fundamental or lowest frequency in human speech typically ranges from 80 to 400 Hz), and its ability to produce robust FFRs in most subjects (Skoe & Kraus, 2010).

The stimulus was presented binaurally at 55 dB SPL, continuously throughout the nap opportunity, in alternating polarity, through Etymotic ER-3A insert earphones with foam tips (Etymotic Research). The sound level is experienced subjectively as quiet but clearly perceivable within the acoustically-shielded imaging chamber. Volume was kept constant for all participants, as the study included only young, healthy individuals with normal hearing. Stimulus onset synchrony (SOA) was randomly selected between 195 and 205 ms from a normal distribution (i.e., stimulus presentation rate of ∼5 Hz). This design maximizes the number of epochs acquired and thus the SNR of the FFR, which is necessary particularly for studying deep FFR sources in the brainstem (Coffey et al., 2016b). The audio signal was recorded as a channel in the EEG/MEG data such that each stimulus onset could be precisely determined. To decrease electromagnetic contamination of the data from the signal transducer, ∼1.5 m air tubes between the ear and the transducer were used such that the transducer could be placed >1 m from the MEG gantry, as in previous work (Coffey et al., 2016b, 2021).

2.3.5 Data processing

Sleep scoring and sleep microarchitecture

Sleep recordings were manually scored according to AASM practices (Iber, 2007) by one researcher and confirmed or challenged by others, with discrepancies being resolved via discussion and consensus. Based on band-pass filtered EEG (.1–20 Hz, channels 'C3', 'C4' and 'Cz' referenced to right mastoid), EOG (.1–5 Hz) and EMG (10–58 Hz) signals; each 30 s window of data was visually inspected and categorized into Wake, N1 (NREM sleep stage 1) to N3 (NREM sleep stage 3) and REM sleep. Sleep events (i.e. sleep spindles and slow oscillations) were detected on a down-sampled version of the EEG data (250 Hz) from a central EEG electrode (position 'Cz'), referenced to the right mastoid. In the case of three subjects, signal quality at 'Cz' was of poor quality for at least part of the recording; another central electrode ('C3'), which received very similar signals due to the broad spatial

distribution of both auditory and sleep oscillations across the dorsal and frontal scalp, was used as an alternative.

Spindles were detected across N2 and N3 sleep (Schulz, 2008) using a freely available algorithm which emulates human scoring (Lacourse et al., 2019). The detection method uses four key criteria: absolute power in the sigma frequency band (the range associated with sleep spindles), relative sigma power, and both correlation and covariance between the sigma band-filtered signal and the original EEG recording. The default parameters were used. Slow oscillations were detected in N3 sleep only using the method described in Carrier et al. (2011). Four criteria were used for detection: peak-to-peak amplitude exceeding 75 μV, negative peak amplitude greater than 40 μV, negative peak duration between 125 and 1500 ms, and positive peak duration under 100 ms (Rosinvil et al., 2021).

EEG and MEG pre-processing

Data pre-processing was performed using Brainstorm (Tadel et al., 2011) and custom Matlab scripts (The Mathworks Inc., MA, USA). MEG channel signal quality was confirmed by visual inspection; one channel in one subject was removed due to poor signal quality (MRT51). Cardiac artefacts were removed from MEG data using Brainstorm's in-built cardiac detection algorithm, and source signal projection algorithm (Tesche et al., 1995), using the recommended procedure: projectors were removed when they captured at least 12% of the signal and the topography of the components matched those of ocular or cardiac origin upon visual inspection. Eye blinks were not detected nor removed, as participants had their eyes closed during the recording.

Both EEG and MEG data were bandpass filtered in the FFR frequency range, to remove the low frequency components of the evoked response (80-450 Hz; 43,506-order linear phase FIR filter with a Kaiser window and 60 dB stopband attenuation; the order is estimated using Matlab's kaiserord function and filter delay is compensated by shifting the sequence to effectively achieve zero-phase and zero-delay, as per Brainstorm default settings (Tadel et al., 2011)), and a notch filter to remove power line noise was applied at 120 and 180 Hz (power line harmonics falling into the frequency band of interest for FFR). A simple threshold-based artefact rejection was applied ($\pm$500 fT in MEG or $\pm$50 μV in EEG) for each channel and epoch, noting that the same epochs were retained for both EEG and MEG analyses. This step removed approximately 5% of epochs (final numbers of retained epochs are presented in Table 2.1).

MEG source modelling

As in previous work (Coffey et al., 2016b, 2021), we used FreeSurfer (Fischl et al., 2002; Fischl, 2012) to prepare cortical surfaces and automatically segment subcortical structures from each subject's T1-weighted anatomical MRI scan, imported the anatomy into Brainstorm (Tadel et al., 2011), and combined the brainstem and thalamic structures with the cortex surface to form the image support of MEG distributed sources: the mixed surface/volume model included a triangulation of the cortical surface (∼15,000 vertices), and brainstem and thalamus as a three-dimensional dipole grid (∼18,000 points). We computed an overlapping-sphere head model for each run, which explains how an electric current flowing in the brain would be recorded at the level of the sensors. A noise covariance matrix was computed from 2-min empty-room recordings taken before each session. The inverse imaging model estimates the distribution of brain currents that account for data recorded at the sensors. We computed the MNE source distribution, which is robust and frequently used in literature (Hämäläinen, 2009), with unconstrained source orientations for the subcortical volume and constrained sources of the cortical surface elements of the model, for each run using Brainstorm default parameters.

Region of interest definition

The auditory cortex regions of interest (ROIs) were defined using the Destrieux atlas (Destrieux et al., 2010), by combining the regions labelled as 'S_temporal_transverse', 'G_temp_sup-Plan-tempo', and 'G_temp_sup-G_T_transv' for the left and right hemispheres, respectively. The left and right auditory cortex regions (rAC, lAC) cover the posterior superior temporal gyrus, as has been used in previous work (Coffey et al., 2021; Jourde & Coffey, 2024; Jourde et al., 2024). The rAC ROI is depicted in Figure 2.3D. We used small spherical regions centred on each subcortical nucleus, as subcortical regions were modelled as a volume. The centre of each subcortical ROI was defined using standard space (MNI152) coordinates, transformed to the subjects' T1-weighted MRI image, and visually inspected to confirm location. The coordinates of subcortical ROIs were: rCN: 8 -36 -38; lCN: -4 -36 -38; rIC: 6 -36 -10; lIC: -4 -36 -10; rMGB: 14 -30 6 and lMGB: -10 -32 6. Each ROI was between 0.4 and 0.5 cm^3, as in previous work (Coffey et al., 2021). The locations of the subcortical structures are depicted in Figure 2.4A.

FFR extraction

Data from each auditory cortex (AC) and bilateral pairs of subcortical auditory system region of interests (ROIs; medial geniculate nucleus, MGB; inferior colliculus, IC; and cochlear

nucleus, CN), were extracted and categorized in two steps: first by the sleep stage during which they occurred, and then by whether they coincided with sleep spindles or slow oscillations. Events that occurred during N2 or N3 stages without overlapping with these discrete sleep events were classified into a 'Clear' comparison condition. Epochs were created around each auditory stimulation, spanning from 50 ms before to 250 ms after sound onset.

To quantify magnitude of the brain's phase-locked response to sound at the sound's fundamental frequency (98 Hz), FFR averages were first computed by averaging epochs of each polarity and then summing negative and positive polarity averages, for each subject, condition, and region of interest. A Fast Fourier Transform was then applied to each FFR average (0 to 140 ms) to obtain frequency spectra. For subcortical structures the left and right hemisphere homologues were averaged. Based on previous work (Coffey et al., 2016b) showing stronger FFR response in the right auditory cortex (due to lateralization of pitch encoding; Coffey et al. 2017b; Albouy et al. 2020), we focused our cortical analysis on the right hemisphere only (spectra for the lAC are also reported in Supplementary Figure S1C). We then extracted the magnitude at a peak within a 88-108 Hz frequency band (i.e., surrounding the stimulus' fundamental frequency) for each subject and condition. Note that individuals' average peaks can be slightly offset from the stimulation frequency of 98 Hz, likely due to entrainment; Coffey et al. 2021).

FFR signal conduction delay by sleep stage in the rAC

To assess the effects of deepening sleep stage on the timing of the MEG-FFR at the cortical level (i.e., that extracted from rAC), we used a cross-correlation algorithm to compute relative timing between the FFR timeseries during the wake state vs. each of the sleep states. Correlation maxima were selected by constraining the search window to ± 3 ms, which is highly likely to encompass any timing differences in the FFR caused by differences in brain state, whilst avoiding potential confounds of selecting an alignment with the subsequent cycle in a periodic signal, and which is unbiased as regards the direction of potential time-shift. After extracting the values for each subject across pairs of states, we test one-tailed hypotheses at the group level that NREM sleep causes the pitch representation to be delayed in the auditory cortex. Although the same approach is not possible in the present study with the subcortical regions, due to difficulty reconstructing a single clear FFR time series from the three dimensions derived from volume-based models, prior results from intracranial recordings suggest that delays due to sleep stage are unlikely at subcortical levels (Amadeo & Shagass, 1973; Murphy & Starr, 1971); we therefore focus on the cortical level.

Thalamocortical functional connectivity

To examine how sleep stages influence communication within the lemniscal pathway, we analyzed functional connectivity between the right auditory cortex (rAC) and the right medial geniculate body (rMGB). We used imaginary coherence (iCOH) to measure this connectivity, focusing on the steady-state portion of the frequency-following response within the (25-125 ms) time window. We then also calculated it in overlapping 50 ms segments to track changes over time. Since the rMGB is a three-dimensional structure, we computed iCOH between the rAC and each dimension, then used the maximum value to represent the overall functional connectivity between these regions.

2.3.6 Signal quality and statistical approach

The study design focused on comparing FFR strength across sleep stages, within-subject. We opt for non-parametric statistical tests throughout, as the normality assumption required by parametric tests is difficult to confirm in small sample sizes, and becuase FFR magnitudes in a population tend to be non-normally distributed.

We first report the number of epochs after sorting into each sleep stage, for each participant, noting that averaged FFRs in EEG are typically obtained from averaging ∼2000 epochs (Skoe & Kraus, 2010). Due to lower SNRs in the source-localized MEG signal, a higher number is needed (i.e., at least ∼3000-4000 epochs) to achieve similar SNRs (Coffey, 2016), though signal clarity also depends on the neural source, with thalamus (MGB) typically yielding the weakest signal (Coffey et al., 2016b, 2021) – and the strength of an individuals' FFR, which can vary considerably even amongst healthy young adults (Coffey et al., 2016a). As a measure of signal clarity, we compute the SNR as the ratio between the FFR strength at its fundamental frequency; selected by taking the peak between 88-108 Hz; and the mean magnitude between the 3rd and 4th harmonics (320–380 Hz), both during stimulus presentation. Within this frequency range, the averaged spectra are relatively flat, lacking meaningful signals, and can therefore be used as a proxy of the background noise levels of the filtered data (as in Coffey et al. (2021)).

For each of the analyses concerning the main research questions, we compute FFR magnitude differences with respect to the wake period, as a within-subjects baseline normalization, using Wilcoxon signed rank tests for independent samples [W] (effect sizes are reported using rank biserial correlation [r_{rb}]). This approach allows us to determine the effects of each individual sleep stage on the standard wake FFR.

To investigate how the impact changes across successively deeper sleep stages, we performed a second analysis, using a Friedman test [X^2_F], and Conover's Post Hoc Comparisons [T] to

identify statistically significant pairwise comparisons. In each set of tests, we correct for False Discovery Rate (FDR) using the Benjamini-Hochberg correction (alpha = .05; Thissen et al. (2002)). Corrected p-values are reported unless otherwise indicated.

2.4 Results

2.4.1 Sleep

Sleep scoring analysis confirmed that all subjects except for one were able to sleep in the scanner during the nap opportunity. The time spent in each brain state varied, with the majority of time spent in wake (∼60 mins) and stage 2 sleep (∼45 mins; see Figure 2.2, and Figure 2.1). REM sleep was observed in only a few participants and in very small amounts, likely due to the timing and duration of the nap. REM is therefore not included in the analysis, which focuses on NREM sleep depth. On average, subjects spent 100.5 minutes sleeping (SD, 44.6) in NREM sleep stages (combined), and 293 spindles (SD, 184) and 370 slow oscillations (SD, 360) were detected per subject.

	Sleep stages durations (min)					Sleep stages conditions (#)				Detected sleep events (#)		Sleep events conditions (#)		
	Wake (min)	N1 (min)	N2 (min)	N3 (min)	REM (min)	daWake	daN1	daN2	daN3	SO	Spindles	daSpindles	daClear	daSO
S01	64.5	72.5	57	0	0	18126	21695	12900	0	0	197	1031	13549	0
S02	90	14.5	45.5	0	0	18247	4339	13315	0	0	532	1430	9308	0
S03	79.5	12.5	29	33.5	0	23593	3740	8671	9933	748	223	1706	10509	4754
S04	100.5	20	40	19.5	0	30057	5986	11973	5834	381	243	2713	10394	1794
S05	47.5	23	18.5	60	0	14190	6867	5225	17889	795	186	2056	13979	4854
S06	94	42	15.5	3.5	0	27724	12401	4643	1048	34	108	538	3984	217
S07	17.5	46.5	96.5	21.5	0	4350	10313	24520	4874	225	317	1391	13918	1613
S08	127.5	21.5	13.5	0	0	37861	6429	3886	0	0	53	553	2219	0
S09	24	36	52.5	53.5	15.5	6978	10766	15685	15850	846	178	1976	20165	5439
S10	40.5	34.5	72	24	0	12111	10323	21555	7027	305	253	1244	23537	1820
S11	9.5	20.5	71	58	6	2541	5971	21200	17211	974	641	3607	22104	3868
S12	87.5	18.5	43	5	0	20704	3215	7182	0	0	538	645	5016	0
S13	20.5	17	58.5	15	0	5376	4626	14738	4476	204	342	1181	11054	1291
Average	61.8	29.2	47.1	22.6	1.7	17066.0	8205.5	12730.2	6472.5	369.5	293.2	1543.9	12287.4	2047.5
SD	37.3	17.2	25.4	23.2	4.6	10740.8	5122.5	7039.9	7042.1	360.0	184.2	918.4	6946.4	2061.4

Figure 2.1: Time spent in different sleep stages per subject, as well as the number of stimuli presented, number of spindles and SOs detected, and the number of sound presentations which occurred during spindles, slow oscillations, and in N2 or N3 in the absence of sleep events.

2.4.2 Signal quality

As a measure of FFR signal clarity, we examined the SNR of the FFR's fundamental frequency. As expected, the EEG-FFR had a very clear signal particularly in the Wake condition (see Supplementary Figure S1A), which included on average over 17,000 epochs (mean SNR, 40.2; SD, 21.1). Signal quality was maintained even in N3 sleep, for those participants (9) who attained this sleep depth in the scanner (mean SNR, 33.6; SD, 17.3). On average, ∼370

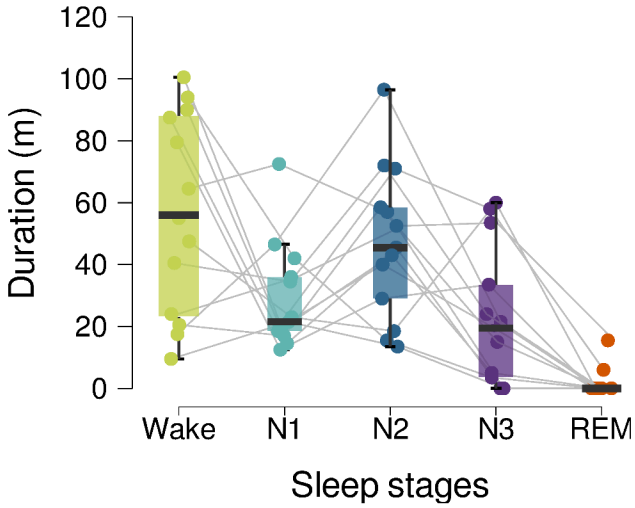

Figure 2.2: Time spent in each sleep stage; all subjects slept. Four subjects were excluded from analyses of N3 sleep due to insufficient time spend in N3 sleep. REM sleep was not analyzed. Lines connect data points from the same subject.

stimulations were co-incident with slow oscillations (mean SNR, 23.8; SD, 12.5) and ∼290 were co-incident with spindles (mean SNR, 24.5; SD, 16.0). These results provide strong confidence in the EEG-FFR signal quality, even for the secondary analyses that involve using vastly reduced number of epochs (see Table 2.1 and Supplementary Figure S3).

In MEG, at the cortical level (rAC), all subjects also had strong FFRs (though with considerable variability across subjects; mean SNR, 17.4; SD, 19.3), even in the N3 condition (mean SNR, 6.8; SD, 5.4); all subjects' SNRs were well above 1.5 (which is sometimes used as a criterion for FFR; Skoe & Kraus 2010) in all conditions (see Supplementary Figure S1B). As expected, the MEG-FFR signal at the subcortical levels was discernible (see Supplementary Figure S2) in the spectra but with lower SNRs (Coffey et al., 2016b, 2021). The signal from the deepest source (CN) was clear in the Wake condition (mean SNR, 3.17; SD, 2.6) and deeper, N2 sleep (mean SNR, 2.8; SD, 1.4), and in the N3 sleep stage for the subjects who achieved it (mean SNR, 2.3; SD, 1.0), with the SNR in only one subject in one condition (N3) not achieving and SNR of 1.5. The SNRs of signals from the IC and MGB were somewhat less clear in some subjects and conditions, though were on average higher than 1.5.

These results support the inclusion of all regions and sleep states in the analyses, although nuanced by the different degrees of signal clarity. Because of the relatively low number of stimulations occurring during spindles and slow oscillations (∼300) and the lower SNR found in MEG, we elect to investigate the effect of these sleep events only in the more global EEG-FFR, as it yields the highest SNRs.

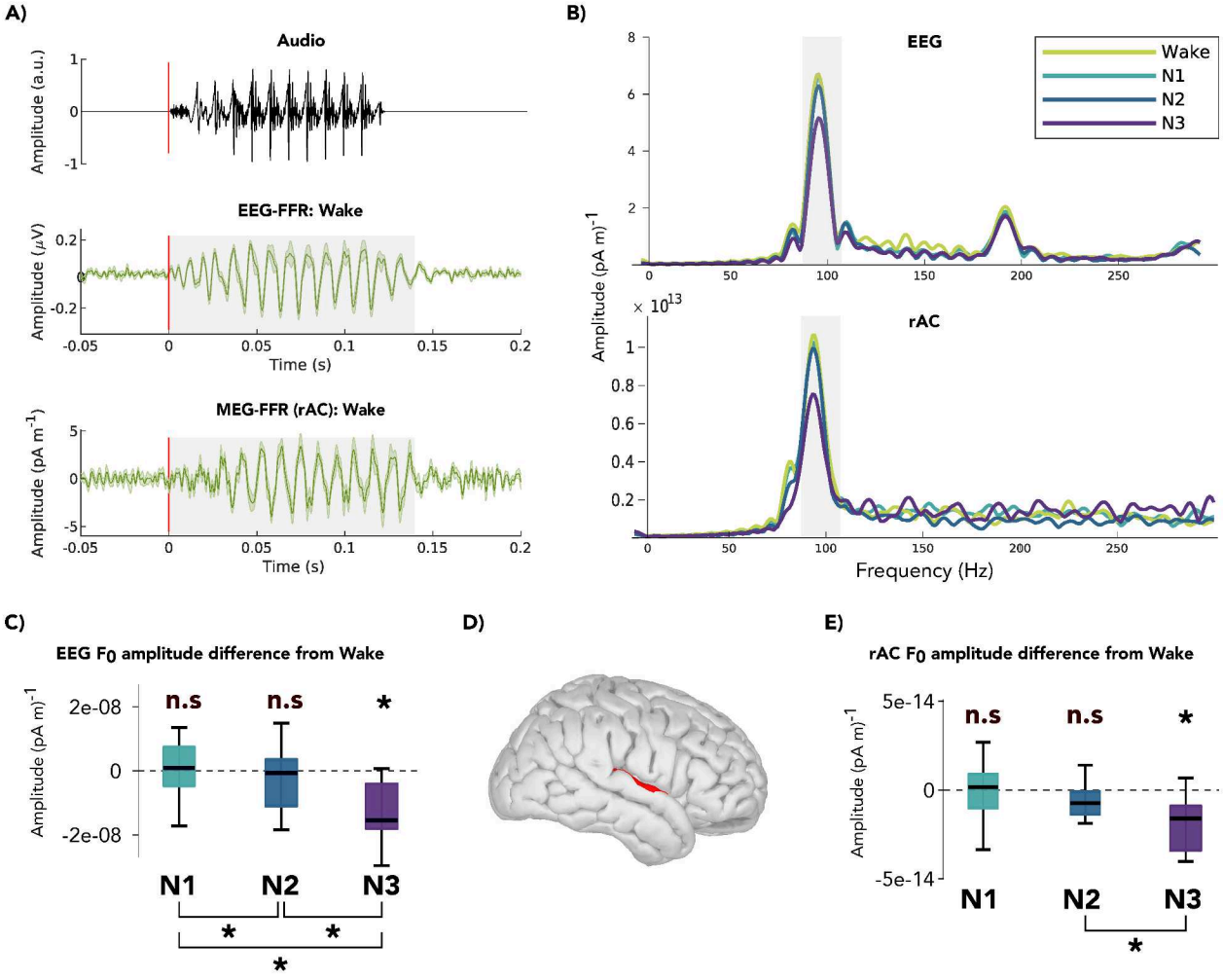

Figure 2.3: Effects of non-rapid eye movement sleep depth on encoding of auditory frequency information. A) Auditory stimulus (/da/) (top), and the brain's frequency-following response (FFR) to that stimulus, as measured using single-channel electroencephalography (EEG; middle), and extracted from the right auditory cortex (rAC) using magnetoencephalography (MEG; bottom) in the Wake condition, showing preservation of frequency information at the fundamental frequency (98 Hz). Grey shading indicates the 0 to 140 ms time range range over which the FFR spectra are computed. B) Spectra averaged across participants for each sleep stage, for EEG (top) and MEG at the rAC (bottom); grey shading indicates the 88-108 Hz frequency range surrounding the fundamental frequency in which subject maxima are selected. Comparison of magnitude at the fundamental frequency in C) the EEG-FFR and E) the MEG-FFR at rAC. The rAC region of interest is depicted in D). Error bars = standard error. * p-values $< .05$, 'n.s.' refers to non-significant comparisons.

2.4.3 Global FFR strength by sleep stage

We use the EEG-FFR as a global measure of FFR strength, as it comprises signal from a mixture of FFR-generating neural sources. The strength of the fundamental frequency representation decreases in EEG (see Figure 2.3C) during deep sleep as compared with Wake (N3 vs Wake: W = 1.00, p = .012, r_{rb} = -.96), but did not differ from Wake in N1 and N2 sleep (N1 vs Wake: W = 53.00, p = .706, r_{rb} = 1.65; N2 vs Wake: W = 32.00, p = .282, r_{rb} = -.29).

The results of the Friedman test indicated a statistically significant difference between sleep stages ($X^2_F(2) = 14.89$, $p < .001$), with a large effect size (Kendall's W = .83). Post-hoc analyses showed a statistical difference between N1 and N2 (T(16) = 2.67, p = .02, r_{rb} = .56), N1 and N3 (T(16) = 8.56, $p < .001$, r_{rb} = 1), and N2 and N3 (T(16) = 5.88, $p < .001$, r_{rb} = 1).

2.4.4 Cortical FFR strength by sleep stage

We use source analysis of the MEG signal to measure FFR strength at both cortical and subcortical levels. The FFR extracted from the right auditory cortex showed a similar pattern to that observed in the EEG-FFR (see Figure 2.3E), with a significant difference between deep sleep and Wake (N3 vs Wake: W = 3.00, p = .03, r_{rb} = -.87). The difference between N1 and Wake (N1 vs Wake: W = 49.00, p = .61, r_{rb} = .07) was not significant, and the difference between N2 and Wake (N2 vs Wake: W = 20.00, p = .06, r_{rb} = -.56) did not reach significance after correction.

The results of a Friedman test indicated a statistically significant difference between sleep stages ($X^2_F(2) = 6.89$, p = .03), with an effect size (Kendall's W) of .38. Post-hoc analyses showed a statistical difference between N2 and N3 (T(16) = 3.11, p = .03, r_{rb} = .82). The differences between N1 and N2 (T(16) = 1.13, p = .36, r_{rb} = -.02) as well as N1 and N3 (T(16) = 1.98, p = .13, r_{rb} = .60) did not reach significance.

2.4.5 Subcortical FFR strength by sleep stage

The FFR extracted from the subcortical sources of the FFR in the lemniscal pathway (i.e., the medial geniculate body (MGB), the inferior colliculus (IC) and the cochlear nucleus (CN); see Figure 2.4A), showed a different pattern. We observed no differences in FFR strength in these subcortical sources as a function of sleep depth (see Figure 2.4B; **MGB**: N1 vs Wake: W = 15.00, p = .09, r_{rb} = -.67; N2 vs Wake: W = 29.00, p = .27, r_{rb} = -.36; N3 vs Wake: W = 10.00, p = .24, r_{rb} = -.56; **IC**: N1 vs Wake: W = 16.00, p = .12, r_{rb} = -.64; N2 vs Wake:

W = 28.00, p = .24, r_{rb} = -.38; N3 vs Wake: W = 11.00, p = .30, r_{rb} = -.51; **CN**: N1 vs Wake: W = 15.00, p = .09, r_{rb} = -.67; N2 vs Wake: W = 32.00, p = .38, r_{rb} = -.29; N3 vs Wake: W = 13.00, p = .45, r_{rb} = -.42). These results suggest that sound processing in subcortical regions is maintained across brain states.

The results of the Friedman tests did not indicate a statistically significant difference between sleep stages in any region of interest (**MGB**: ($X^2_F(2)$ = 2.00, p = .37) ; **IC**: ($X^2_F(2)$ = 1.56, p = .46) ; **CN**: ($X^2_F(2)$ = 4.22, p = .12)).

2.4.6 FFR signal conduction delay by sleep stage in the rAC

To assess whether deepening sleep causes delays in processing periodic sound at the cortical level, we applied a cross-correlation analyses to pairs of FFRs between Wake and each NREM sleep stage, extracted from the rAC, for each subject. In this analysis, the two timeseries are progressively shifted against one another in time, to determine the delay at which correlation is maximum. The mean delay of N1 relative to Wake was -0.26 ms (SD, 0.671); mean delay of N2 vs Wake was 0.16 ms (SD, 0.60) and the mean delay of N3 vs. Wake was 0.463 ms (SD, 0.79).

Wilcoxon signed-rank tests did not show significant differences from zero in these inter-stage latency comparisons (N1 vs Wake: W = 12.0, p = .91, r_{rb} = -.47; N2 vs Wake: W = 36.5, p = .19, r_{rb} = .33; N3 vs Wake: W = 23.0, p = .07, r_{rb} = .64). However, a trend was observed in that within-subject, successively deeper NREM sleep stages appeared to result in increasing delays (see Figure 2.5). To assess the consistency of this observation, we included only subjects who had FFRs for all 3 sleep stages (N=9) in a non-parametric repeated measures Friedman Test.

The results of the Friedman test indicated a statistically significant difference between sleep stages ($X^2_F(2)$ = 8.97, p = .011), with an effect size (Kendall's W) of .63. Post-hoc analyses showed a statistical difference between N1 and N2 (T(16) = 2.70, p = .03, r_{rb} = -.91) as well as between N1 and N3 (T(16) = 3.89, p = .004, r_{rb} = -1). The difference between N2 and N3 (T(16) = 1.18, p = .34, r_{rb} = -.29) did not reach significance. These results show that deeper sleep results in slower transmission of periodic information to the cortex.

2.4.7 Thalamocortical functional connectivity

To evaluate whether functional connectivity between thalamus (MGB) and cortex differed as a function of sleep stage, we used imaginary coherence to measure non-zero phase-lag functional connectivity between these two regions of interest, focusing on the maximally-different states: Wake and N3.

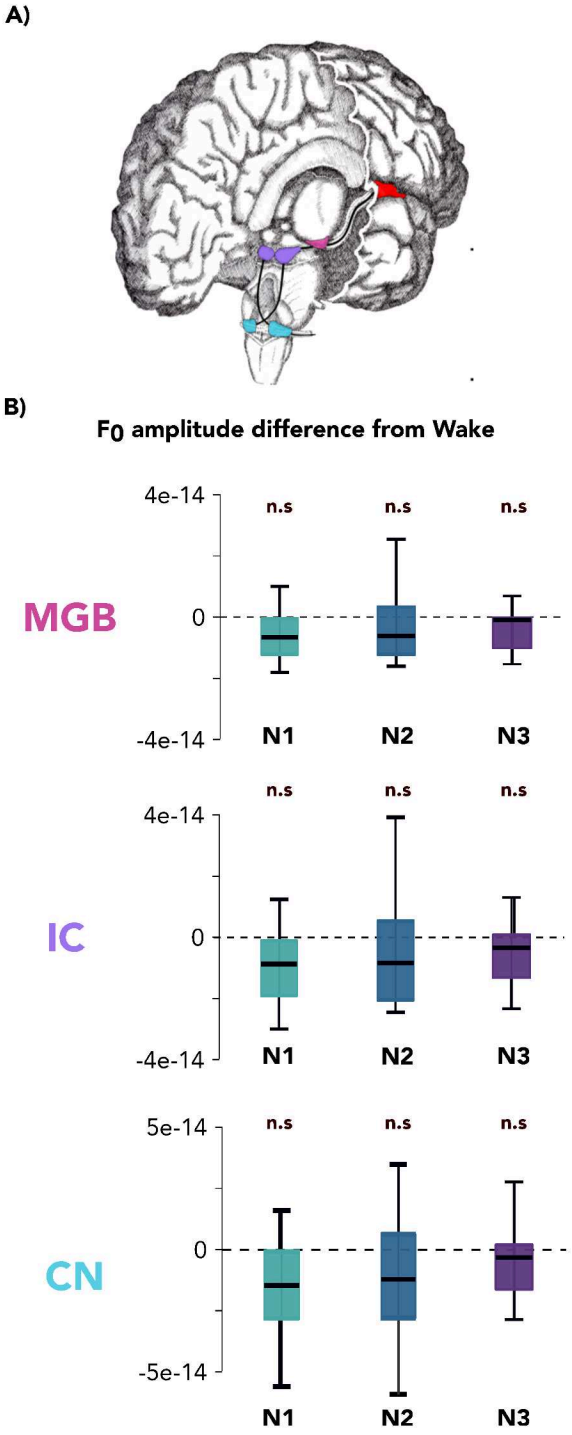

Figure 2.4: Impact of sleep depth on FFR strength in subcortical regions of the auditory lemniscal pathway. A) Schematic representation of the lemniscal pathway highlighting the locations of structures included in the analysis. B) Difference between sleep stages in FFR magnitude within the medial geniculate body (MGB), the inferior colliculus (IC) and the cochlear nucleus (CN). Error bars = standard error. 'n.s.' refers to non-significant comparisons, p-values > 0.05

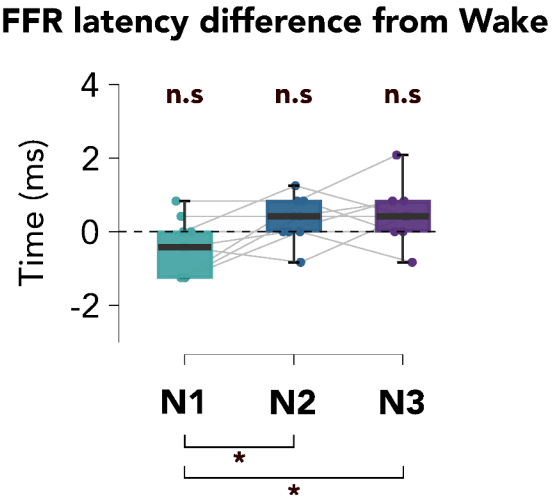

Figure 2.5: Latency of FFR from the right auditory cortex (rAC) as compared with Wake. Delay increases in deeper sleep stages. Error bars = standard error. * p-values < .05, 'n.s.' refers to non-significant comparisons.

When analyzing the entire FFR time window (25–125 ms post-stimulation onset), we did not observe significant differences between Wake and N3 sleep (see Figure 2.6A) (W = 32.00, p = .301, r_{rb} = .42). However, the strength of the FFR and the nature of its frequency representation evolves over its course (see Coffey et al. (2021)). A more detailed analysis of the temporal evolution of brain responses revealed a significant decrease in functional connectivity in N3 compared to Wake during the middle time window (25–75 ms post-stimulation onset) (W = 39.00, p = .027, r_{rb} = .36) (see Figure 2.6B). Differences during other time windows did not reach significance (**[-50:0] ms**: W = 24.00, p = .455, r_{rb} = .07; **[0:50] ms**: W = 31.00, p = .180, r_{rb} =.38; **[50:100] ms**: W = 33.00, p = .125, r_{rb} = .47; **[75:125] ms**: W = 18.00, p = .715, r_{rb} = -.20).

2.4.8 EEG-FFR strength as a function of discrete sleep events

Finally, given the decrease in FFR strength observed in deeper sleep stages and the ongoing debate about the interaction between sleep events and sensory stimulation, we examined how the presence of sleep spindles (detected in N2 and N3) (see Figure 2.7A) and slow oscillations (detected in N3) (see Figure 2.7B) influences the magnitude of the EEG-FFR. Due to the small number of stimulations coinciding with slow oscillations and sleep spindles, we used the clearest FFR signal, which is derived from EEG, for this analysis.

By comparing FFRs to stimulation co-occurring with these events and responses to 'Clear' conditions we concluded that neither the presence of sleep spindles (Clear vs Spindle: W = 47.00, p = .47, r_{rb} = .03) nor slow oscillations (Clear vs Slow Oscillation: W = 33.00, p = .13, r_{rb} = .46) impacted the FFR magnitude. Thus, these events are unlikely to explain the

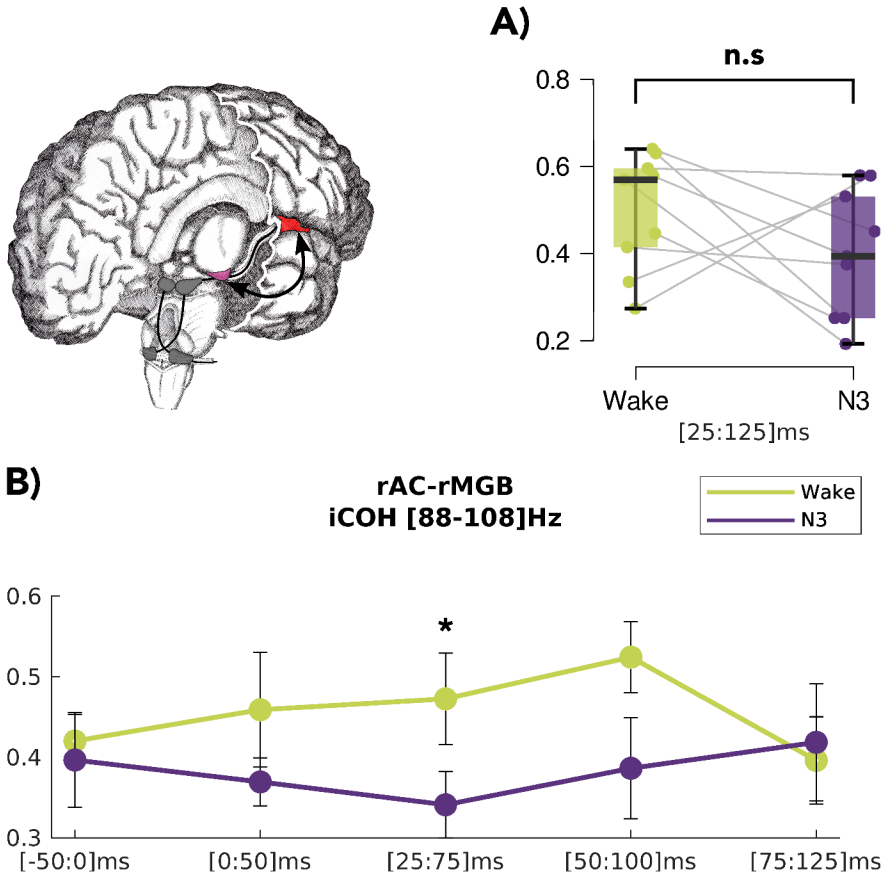

Figure 2.6: Functional connectivity (FC) (imaginary coherence) within the range of the stimulus' fundamental frequency between right auditory cortex and right medial geniculate body (in the 9 subjects who entered deep [N3] sleep). A) Overall FC was not different when measuring the entire FFR time windows. B) However, connectivity trended towards a reduction during deep sleep during the FFR, reaching significance during a window of time 25-70 ms post stimulus onset. Error bars = standard error. * p-values $< .05$, 'n.s.' refers to non-significant comparisons.

general decrease in auditory response observed in deeper sleep stages.

2.5 Discussion

In this study, our primary objective was to investigate how sleep depth (across NREM sleep stages) and the presence of slow oscillations and sleep spindles influence basic, pitch-relevant auditory encoding throughout the auditory hierarchy. This work has implications for our understanding of how the brain balances environmental monitoring with protecting sleep-dependent processes such as memory consolidation from disruption.

2.5.1 Global FFR strength decreases in deep sleep

Previous research on auditory processing during sleep in humans has primarily focused on linguistic and higher-order processing of auditory stimuli. Available evidence suggests that neural responses to speech and other sounds are modulated by sleep depth in cortical regions, showing reduced activity during deeper sleep in brain regions responsible for higher-level processing, including prefrontal cortex (Czisch et al., 2002; Wilf et al., 2016; Czisch et al., 2004). Mai et al. (2019) were the first to investigate lower-order or early auditory processing during sleep using the FFR, documenting a systematic decrease in its strength as a function of arousal state as study participants drowsed and periodically fell asleep during a long, passive listening experiment. This study did not deliberately include a sleep element, but rather used the density of sleep spindles as an indication that participants had fallen asleep. To extend this work, we examined a broader range of sleep stages and neural events in a nap study design. We first investigated the effect of sleep depth on periodicity encoding of auditory stimuli, using EEG-FFR as a composite measure of frequency encoding across the brainstem, thalamus, and cortex (Coffey et al., 2016b). Compared to the waking state, EEG-FFR fundamental frequency magnitude was significantly reduced during stage N3 sleep. No significant differences were observed between N2 or N1 and Wake states when directly compared, but successively deeper sleep stages had significantly lower EEG-FFR magnitude (see Figure 2.3C). These results confirm that non-rapid eye movement sleep depth attenuates frequency encoding in the human brain.

2.5.2 Strength of FFR decreases in deep sleep only in cortical structures

Scalp-recorded EEG-FFR captures global evoked responses from multiple sources along the auditory pathway, including subcortical structures (cochlear nucleus, inferior colliculus, and medial geniculate nucleus) and cortical regions (Coffey et al., 2016b). By using source-localization approaches in magnetoencephalography, we are able to extracted FFRs directly from regions of interest along the auditory pathway and thereby more precisely identify which cortical or subcortical regions are modulated by sleep depth. We found that FFR magnitude in the rAC was significantly reduced during deeper sleep compared to wakefulness (N2 and N3), while no significant differences were observed during lighter sleep (N1). This pattern of results is similar to that observed in the global EEG-FFR (a finding that is consistent with previous work suggesting that the EEG-FFR includes a strong contribution from the auditory cortex; Coffey et al. (2016b)).

In contrast, we observed that FFR magnitude remained stable across all sleep stages in all

subcortical regions of interest (Figure 2.4). These results suggest that the representation of pitch within the auditory brainstem and thalamus is preserved during sleep. Maintenance of subcortical auditory processing aligns with previous research in invasive non-human animal recordings showing that early, subcortical responses are generally preserved while later responses vary considerably as a function of sleep depth (Meeren et al., 2001). For example, Morales-Cobas et al. (1995) reported that in cellular recordings from the guinea pig IC, the majority of neurons showed no change in discharge rates in deep sleep as compared to wake.

2.5.3 Cortical sound processing may be attenuated by changes in thalamocortical connectivity across sleep stages

In a seminal study, Massimini et al. (2005) demonstrated reduced signal propagation during NREM sleep compared to wakefulness, indicating a breakdown in cortical connectivity. Subsequent research has corroborated these findings. For instance, Jobst et al. (2017) documented a global decrease in cortical interactions during slow-wave sleep, measured through fMRI functional connectivity. Thalamocortical functional connectivity was also reported to decrease during deep sleep, correlating with responsiveness to sensory stimulation Hale et al. (2016); Picchioni et al. (2014).

Further evidence came from a follow-up transcranial magnetic stimulation (TMS) study by Massimini et al. (2010), in which the neural responses to magnetic stimulation were examined for complexity and timing as a means of assessing global neural communication patterns. The authors reported that in deeper NREM sleep, thalamocortical circuits remain active and reactive but lose their ability to interact and to produce complex, long-range patterns. The brain's response to stimulation by TMS in deep sleep evokes a simpler wave than it does when participants are awake, an observation which is consistent with local processing (conversely, levels of connectivity in REM sleep remain comparable to those observed in wakefulness).

Because sleep stages coincide with broader changes in brain neural communications patterns, we investigated changes in functional connectivity between the auditory thalamus (i.e., MGB) and the primary auditory cortex (represented by rAC) as a function of sleep depth, specifically in the FFR frequency range. Functional connectivity analysis revealed reduced thalamocortical interactions during the steady-state portion of the FFR (Figure 2.6B).

Furthermore, comparison of response latencies in the auditory cortex between wake and deep sleep showed increased response latency (Figure 2.5). Together, these findings suggest that neurophysiological states characteristic of deeper sleep underly the FFR magnitude reduction we observe in auditory cortex.

2.5.4 Slow oscillations and sleep spindles are not responsible for decrease in EEG-FFR strength

Slow oscillations appear to play a role in reshaping these communication patterns, disrupting the dynamic processes needed for complex long-range information processing. The observed decrease in FFR magnitude in both EEG and right auditory cortex occurred during sleep stages characterized by slow oscillations events, suggesting a possible relationship. Furthermore, previous work using a combination of EEG and fMRI suggested that sound might be selectively attenuated in the presence of sleep spindles (Dang-Vu et al., 2011). Mai et al. (2019) also hypothesized that, because FFR attenuation was correlated with sleep spindle density, spindles might play a direct role in decreasing transfer of auditory information to cortex. Our findings showed decreased FFR magnitude in cortical levels and decreased thalamocortical connectivity in deeper sleep, in which discrete events such as sleep spindles and slow oscillations are present. We therefore investigated whether EEG-FFR magnitude was affected by the presence or absence of these events. After sorting epochs according to whether each type of sleep event occurred and compared the evoked responses with epochs from N2 and N3 sleep in which no event was present, we found no direct effect of either spindles or slow oscillations on FFR magnitude. These results suggest that neither spindles nor slow oscillations drive the observed attenuation across sleep stages (see also Jourde & Coffey (2024) for further discussion of sleep spindles' role in attenuating sound processing).

Limitations and future directions

While MEG has considerable advantages as regards being able to non-invasively record neural signals from the whole brain with decent spatial resolution (Baillet, 2017), it is also resource-intensive, particularly for longer experiments such as those needed to record naps. The physical constraints also make it challenging to record REM sleep, which is most abundant towards the end of a night's sleep. Nevertheless, the high number of observations per participant produced robust results, as evidenced by the strong signal-to-noise ratios across our analyses (in-line with studies using similar techniques; e.g., Coffey et al. (2016b, 2021); Hartmann & Weisz (2019); Gorina-Careta et al. (2021)). Future research could benefit from recruiting participants specifically based on their ability to sleep comfortably in a supine position. Additionally, while our very high stimulation rate was optimized for FFR analysis, several methodological changes could enhance future studies. For instance, separating the Wake and Sleep data collection sessions could minimize the impact of continuous auditory stimulation on sleep onset.

Finally, our study investigated one aspect of basic auditory processing, pitch encoding,

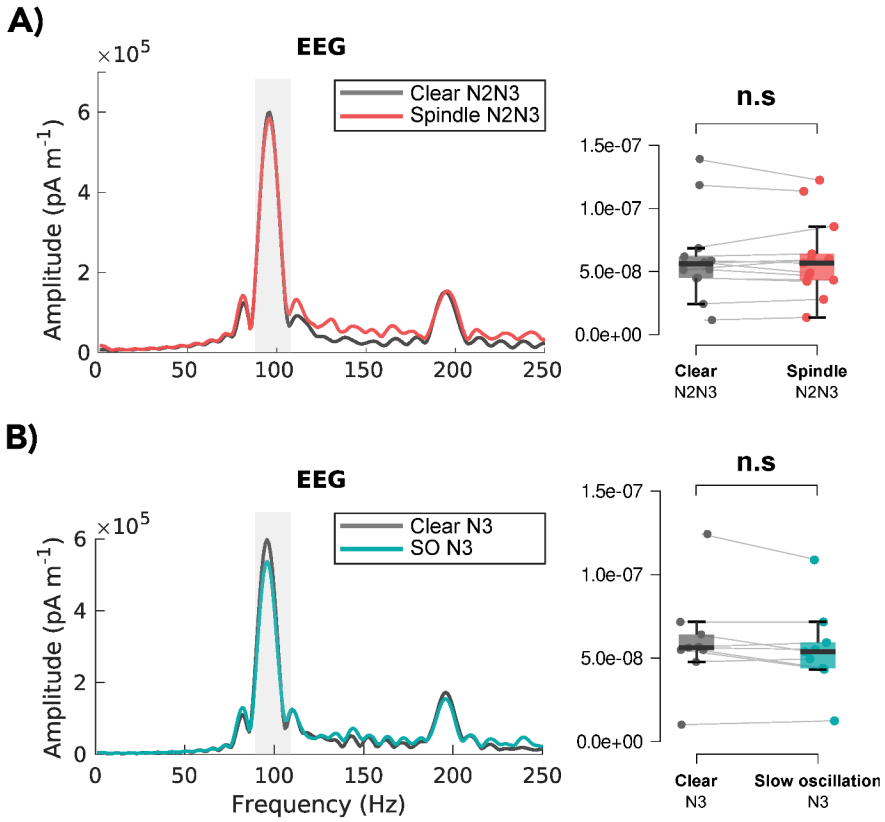

Figure 2.7: Effects of sleep microarchitecture on global FFR magnitude as measured using EEG. Neither A) the presence of sleep spindles nor B) the presence of a slow oscillations significantly reduced the magnitude of the FFR. Grey shading indicates the 88-108 Hz frequency range surrounding the fundamental frequency in which subject maxima are selected. Error bars = standard error. 'n.s.' refers to non-significant comparisons, p-values > 0.05.

which is accessible to temporally resolved electromagnetic methods such as EEG and MEG because populations of neurons phase-lock their activity to periodicity in acoustic stimuli. While a useful window into early sound processing (Murphy & Starr, 1971; Krizman & Kraus, 2019), the FFR represents only one aspect of auditory sensory information, which includes onsets and offsets, timbre, spectral content, and dynamics. Not all of this information is encoded in ways that are temporally-precise enough to be measured using evoked responses in non-invasive recordings. More studies will be needed to confirm that the observations described herein, i.e., that of preserved subcortical processing and disrupted transmission to cortex, are more broadly applicable to parallel information streams within the auditory system, and extended to other sensory modalities.

Future work could also tackle the perhaps most interesting is the question of why sensory processing decreases during sleep. Is this reduction merely a biproduct of broader changes in brain activity that are incompatible with wake-like sensory processing, or does it serve a specific purpose in protecting sleep's restorative and consolidative functions, many of which

seem to take place during N2 and N3 sleep?

2.6 Conclusion

Our results revealed a dissociation between subcortical and cortical auditory processing during sleep. While early auditory encoding in subcortical regions remained stable across sleep depths, both indices of cortical pitch representation (i.e., FFR magnitude extracted from the right auditory cortex) and the more global EEG-FFR measurements, showed significant magnitude attenuation as sleep deepened. These results were not directly attributable to the interaction between sensory processing and specific sleep events, but rather may reflect broader sleep-depth-dependent changes in information flow and cortical processing. This interpretation is supported by our observation that reduced activity was limited to higher-order structures in the auditory pathway, while subcortical responses remained intact. Furthermore, our additional analyses indicate that the changes in auditory processing during sleep, previously documented in previous studies, likely arise from alterations in cortical effective connectivity rather than a reduced ability for sensory processing linked to the loss of consciousness. The current study advances our understanding of how the brain processes sensory information during deeper sleep stages.

2.7 Supplementary material

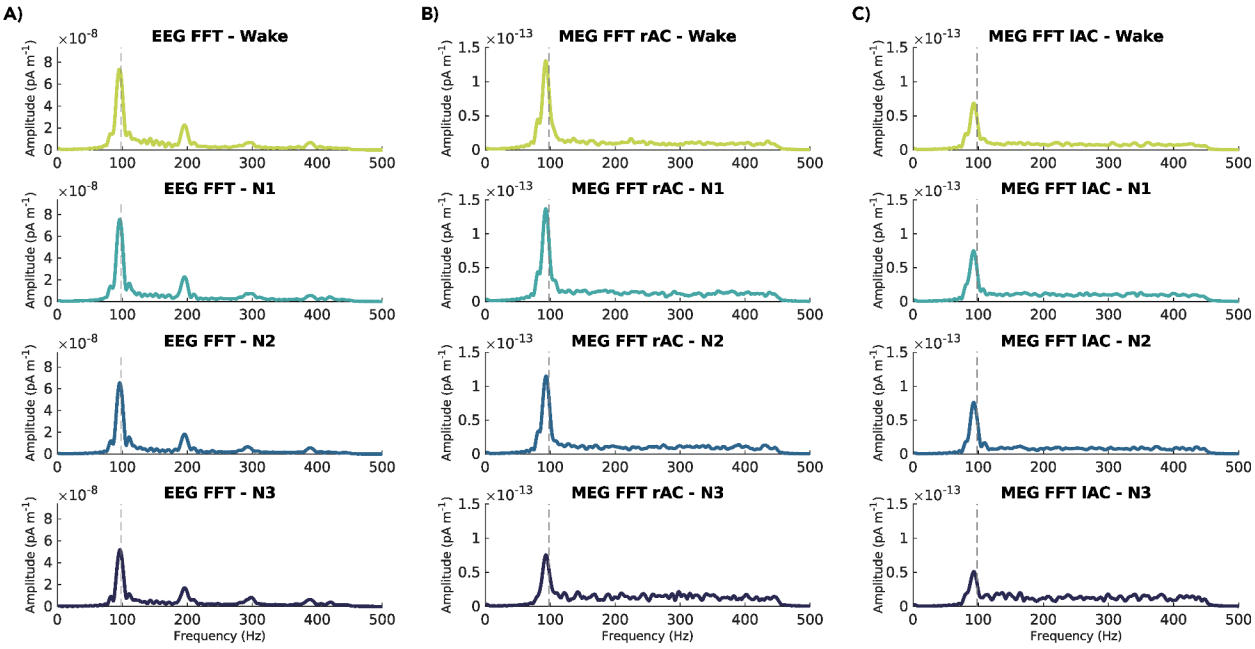

Figure 2.8: FFR spectra averaged across participants for each sleep stage in subcortical regions of interest. A) The composite EEG-FFR response as well as the signal extracted from the B) right auditory cortex (rAC) and C) left auditory cortex (lAC) in MEG are presented. Vertical dashed grey line represents the fundamental frequency of the incoming stimulus (98 Hz).

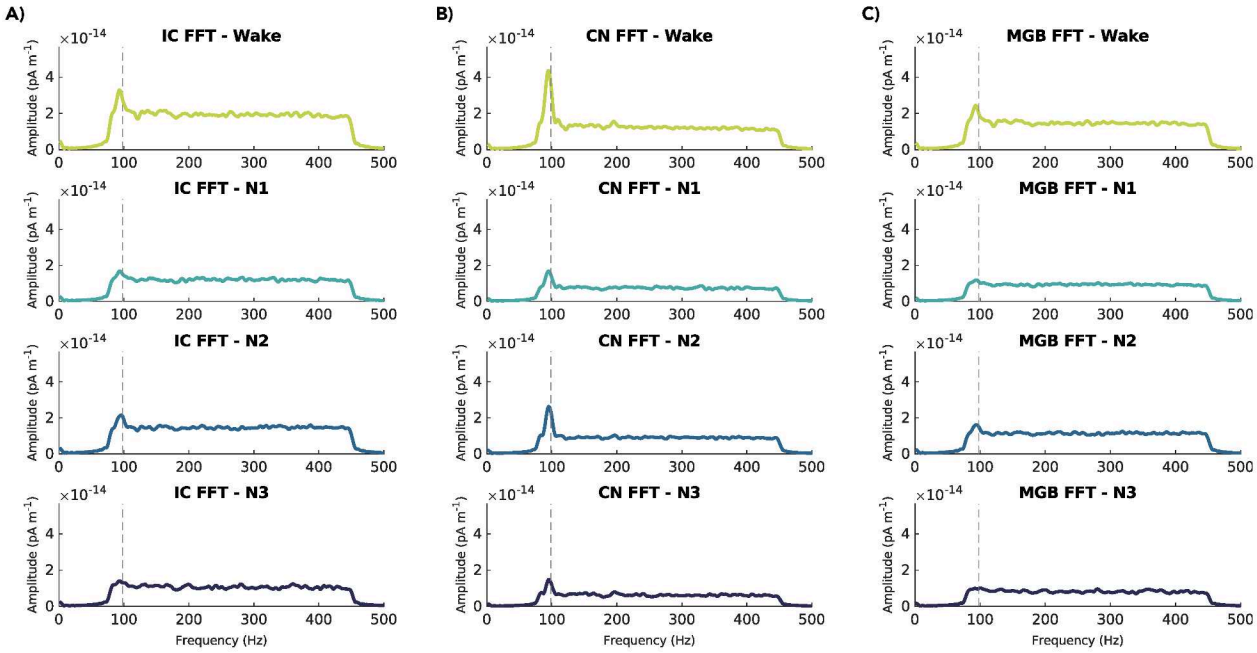

Figure 2.9: FFR spectra averaged across participants for each sleep stage in subcortical regions of interest: A) Inferior colliculus (IC), B) the cochlear nucleus (CN), and C) the medial geniculate nucleus (MGB) are presented. Vertical dashed grey line represents the fundamental frequency of the incoming stimulus (98 Hz).

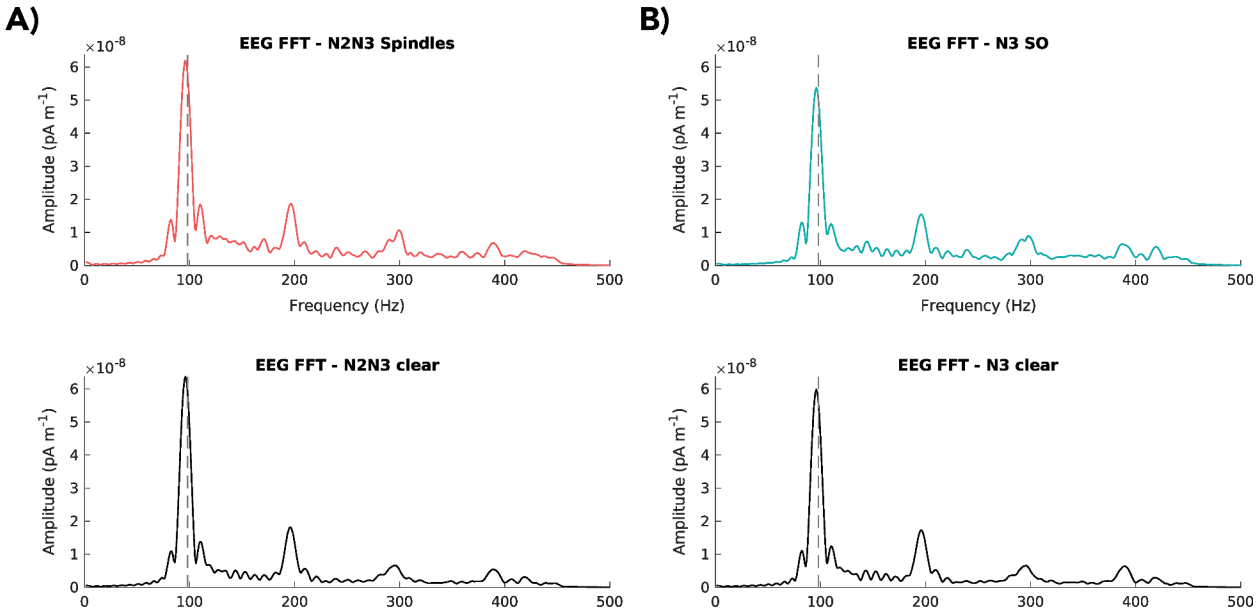

Figure 2.10: EEG-FFR spectra averaged across participants for each condition related to the analysis of sleep oscillations: A) for sleep spindles (top) compared to the 'clear' condition in sleep stages N2 and N3 (bottom); and B) slow oscillations (top) compared to 'clear' in N3. Vertical dashed grey line represents the fundamental frequency of the incoming stimulus (98 Hz).

2.8 Acknowledgements

The authors would like to thank Raphaëlle Merlo, Camille Bouhour, Meredith Rowe, Alix Noly-Gandon and Keelin Greenlaw for help collecting data; Robert Zatorre, Christopher Steele and Julien Doyon for discussion; Karine Lacourse for advice on spindle detection, and Marc Lalancette and Sylvain Baillet for assistance and support at the McConnell Brain Imaging Centre. This work was supported by a research grant from Natural Sciences and Engineering Research Council of Canada (NSERC). EBJC is supported by a Concordia University Research Chair, and HRJ is supported by a scholarship from the Fonds de recherche du Québec (FRQ).

Chapter 3

The neurophysiology of closed-loop auditory stimulation in sleep: a magnetoencephalography study

3.1 Abstract

Closed-loop auditory stimulation (CLAS) is a brain modulation technique in which sounds are timed to enhance or disrupt endogenous neurophysiological events. CLAS of slow oscillation up-states in sleep is becoming a popular tool to study and enhance sleep's functions, as it increases slow oscillations, evokes sleep spindles, and enhances memory consolidation of certain tasks. However, few studies have examined the specific neurophysiological mechanisms involved in CLAS, in part because of practical limitations to available tools. To evaluate evidence for possible models of how sound stimulation during brain up-states alters brain activity, we simultaneously recorded electro- and magnetoencephalography in human participants who received auditory stimulation across sleep stages. We conducted a series of analyses that test different models of pathways through which CLAS of slow oscillations may affect widespread neural activity that have been suggested in literature, using spatial information, timing, and phase relationships in the source-localized magnetoencephalography data. The results suggest that auditory information reaches ventral frontal lobe areas via non-lemniscal pathways. From there, a slow oscillation is created and propagated. We demonstrate that while the state of excitability of tissue in auditory cortex and frontal ventral regions shows some synchrony with the EEG-recorded up-states that are commonly used for CLAS, it is the state of ventral frontal regions that is most critical for slow oscillation generation. Our findings advance models of how CLAS leads to enhancement of slow oscillations, sleep

spindles, and associated cognitive benefits, and offer insight into how the effectiveness of brain stimulation techniques can be improved.

3.2 Introduction

Closed-loop brain stimulation is a technique in which sensory, magnetic or electric stimulation is timed to modulate endogenous brain activity or states (see Antony et al. (2022) for a discussion of terminology). Its main appeal to neuroscientists is the ability to test relationships between brain activity and function causally, thus adducing strong evidence for the roles of neural events and processes. Closed-loop auditory stimulation (CLAS) of slow oscillations during non-rapid eye movement (NREM) sleep has enjoyed particular attention, perhaps due to the unique (and still somewhat mysterious Girardeau & Lopes-Dos-Santos 2021) physiological processes that take place in sleep.

Sleep is a collection of neurophysiological states with several crucial functions including cleaning waste produced during wakeful activity (Hauglund et al., 2020), rescaling synapses (Blanco et al., 2015; Timofeev & Chauvette, 2017), and transforming temporarily-stored memories into lasting ones in a process known as memory consolidation (Diekelmann & Born, 2010; Schabus et al., 2004; Antony et al., 2019; Klinzing et al., 2019). These processes seem to rely on sleep-specific neurophysiological events that are most often measured in EEG: slow oscillations, K-complexes (also referred to as 'N550-P900 complexes' when evoked by external stimuli), and sleep spindles. Slow oscillations (SOs) refer to low frequency brain activity that is defined variously as <1.0, 1.5, 2, or 4 Hz (Carrier et al., 2011; Ngo et al., 2013b; Jaar et al., 2010; Vyazovskiy & Harris, 2013). These high-amplitude fluctuations in cortical and subcortical excitability occur during NREM sleep (stages N2 and N3) and appear to be involved in all three processes (Neske, 2016; Timofeev & Chauvette, 2017; Hauglund et al., 2020; Klinzing et al., 2019). N550-P900 complexes are a particular kind of evoked slow oscillation that also occur during stage N2 and N3 sleep (about 550 to 900 ms after sensory input) (Bellesi et al., 2014; Latreille et al., 2020; Riedner et al., 2011). They are highly related to and often considered to be K-complexes, although K-complexes can be generated in the absence of external stimulation. N550-P900 complexes have been linked to sleep continuity and arousal (Halász, 2016). Sleep spindles are transient (<2.5 s) 11-16 Hz bursts of activity that are generated through thalamocortical interactions. They frequently co-occur with slow oscillations, may be evoked by sensory stimulation (Sato et al., 2007), and are linked to memory and consolidation processes (see Fernandez & Lüthi (2020) for a comprehensive review).

Closed-loop auditory stimulation of slow oscillations, and subsequent enhancement of memory consolidation of performance on a declarative memory task (e.g. word list learning), was first reported by Ngo et al. (2013b). CLAS of SOs has since been repeatedly used in sleep research due to its convenience, ease of use, and temporal precision (see recent reviews Harrington & Cairney (2021); Choi et al. (2020)). As with other forms of brain stimulation, effectiveness can vary considerably across subjects (Nasr et al., 2022). Timing of stimulation seems crucial, and stimulation close to SO peaks (i.e., the 'up-state') evokes subsequent SO activity, as well as sleep spindles, and best enhances sleep-related memory consolidation processes (Navarrete et al., 2020). Stimulation during the trough (i.e., the 'down-state') can result in a decrease in spindle activity and delta power (Ngo et al., 2013b; Moreira et al., 2021). It is thought to be through evoked neural events that memory consolidation is enhanced (Bellesi et al., 2014); however, the neurophysiological mechanisms underlying the effects of CLAS to slow oscillation up-states are poorly understood, and thus it is difficult to optimize and improve stimulation effectiveness. Notably, states are measured most often using a single EEG channel (frontal or central electrode referenced to earlobe or mastoid); this technique captures large-scale, global changes in excitability of cortical tissue. During up-states, neurons are thought to be closer to their firing thresholds, meaning they are more readily activated upon auditory stimulation. However, slow oscillations are not homogeneous phenomena; they originate at different sites and travel along the cortex (Massimini et al., 2004). These dynamics are poorly captured in single-channel EEG. Spatially-resolved techniques such as magnetoencephalography (MEG), which yields information about the relative timing and amplitude of brain responses across brain regions (Baillet, 2017), are needed to explore regional differences in tissue state when stimulation occurs, and to localize its effects.

Evoked brain responses (i.e., event-related potentials in electroencephalograpy; ERPs) are used in sleep research to characterize the evolution of sensory processing according to the depth of sleep (reviewed in Colrain & Campbell (2007)). The amplitude and latency of typical patterns of peaks and troughs, sometimes called 'components', are somewhat affected by deepening sleep stage (Niiyama et al., 1994; Ogilvie et al., 1991). The N100 component (i.e., a negative peak occurring about 100 ms after sound onset), is often reported to be attenuated during sleep, whereas P200 (i.e., a positive peak about 200 ms after onset) increases in deeper sleep (Campbell, 2010). Some evoked components occurring more than 300 ms after stimulation only appear during sleep (Bastien et al., 2002). Three of these components, labelled N350, N550 and P900 (i.e., negative deflections occurring at about 350 and 550 ms and a positive deflection at about 900 ms post onset) begin to emerge at NREM sleep onset (stage N1) and their amplitude increases with sleep depth (stages N2 and N3). The N550-P900 complex has an asymmetrical shape composed of a trough in which cortical

neurons are hyperpolarized, followed by a longer rebound of cortical activity during which neurons are comparatively depolarized and thus more excitable (Latreille et al., 2020). Recent work using electrical source localization models suggests that the spontaneous K-complex, which is similar to the sensory-evoked N550-P900 complex (Halász, 2016), originates in ventral limbic cortex, including medial temporal and caudal orbitofrontal cortex (OFC) (Morgan et al., 2021).

Because the specific auditory pathway involved in closed-loop auditory stimulation is not yet well understood, we must consider the anatomy of the auditory system. There are two main ascending auditory pathways: the lemniscal or primary pathway, and the non-lemniscal or secondary pathway. In the lemniscal pathway, the primary auditory cortex receives projections from the cochlear nucleus via the central nucleus of the inferior colliculus and the ventral division of the medial geniculate body of the thalamus. The non-lemniscal pathway consists of many sets of fibres that send and receive feed-forward and feedback projections widely in midbrain, cortical and limbic areas (Lee, 2015). Of interest here are fibres originating in the brainstem which project to the dorsal division of the medial geniculate body of the thalamus and to secondary auditory cortex, and those which interact with the ascending reticular activating system (ARAS). The ARAS is comprised of many nuclei with connections to the rest of the cortex (Yeo et al., 2013). It also has connections to the locus coeruleus, a group of large nuclei in the brainstem (Poe et al., 2020; Bellesi et al., 2014). The locus coeruleus is the principal source of norepinephrine/noradrenaline in the brain and has widespread (though sparse) projections to the cortex. Both the locus coeruleus and ARAS are involved in transitioning among arousal states, meaning that there is overlap between the auditory non-lemsniscal pathways and the arousal-promoting systems (Bellesi et al., 2014; Wijdicks, 2019).

Evidence suggests that elements of the auditory system, as well as general arousal mechanisms that are independent of the auditory modality (Riedner et al., 2011), are involved in generating the slow oscillations observed in the CLAS effect (Bellesi et al., 2014). However; how, where, and when these systems conspire to produce SOs is unknown, and their contributions to the more commonly-studied cortical EEG evoked responses are not yet understood. Next, we define four possible variations of models of auditory-arousal system interactions, based on the auditory system anatomy described above, ideas proposed in Bellesi et al. (2014), and extent research concerning the origins of evoked and endogenous slow oscillations (e.g., Riedner et al. 2011; Halász 2016; Morgan et al. 2021). Each leads to different predictions in the location, amplitude, and timing of evoked responses to sound in NREM sleep, which can be assessed with temporally- and spatially-resolved neuroimaging methods.

The four models, which vary in the timing and involvement of arousal networks and the location of initial SO generation, are illustrated in Figure 3.1. In the first model, auditory sensory information reaches the auditory cortex (AC) through lemniscal auditory pathways, where it generates a slow oscillation that propagates locally. In this case, only the auditory cortex should exhibit early auditory evoked components (P100, N100, P200), and in NREM sleep, the evoked slow oscillations should occur earlier and with higher amplitude in auditory cortex as compared with other regions. In the second model, auditory information reaches auditory cortex as above, but then propagates to other cortical regions including frontal areas via structural connections (see Plakke & Romanski (2014)). Upon arrival in the ventral frontal regions, the neural impulse induces a slow oscillation locally, which then propagates across the cortex as previously reported for endogenously-generated SOs (Massimini et al., 2004). In this case, the auditory cortex is not the primary generator of evoked slow oscillations, but the process of SO generation is dependent upon a robust response in the auditory cortex. This model would predict a delayed or absent auditory response in the OFC (orbitofrontal cortex), and that late components would appear first and strongest in ventral frontal regions (like OFC), and then later in other cortical regions. In the third model, as auditory information travels simultaneously through the lemniscal and non-lemniscal pathways, non-lemniscal neurons interact with arousal systems in the brainstem (possibly involving LC) and/or thalamus, which then result in diffuse changes in cortical excitability, leading to the generation of slow oscillations throughout the brain. An early auditory-like response followed by a slower late component should be observed throughout the cortex, although due to the previously-observed tendency for ventral limbic areas (including OFC) to generate endogenous slow oscillations (Massimini et al., 2004; Morgan et al., 2021), we would expect larger-amplitude SOs in the OFC.

In the fourth model, as in the third, auditory information primarily generates the CLAS effect via the non-lemniscal auditory pathway. Contrary to Model 3, in Model 4 the impulse would preferentially stimulate SOs in the OFC, which then propagate to other cortical areas. In Model 3, the SOs would be generated locally (in each region of interest) via common ARAS inputs, whereas in Model 4, the slow OFC activity would induce SOs in other cortical areas. These models can be differentiated using directional functional connectivity metrics in the slow frequency band.

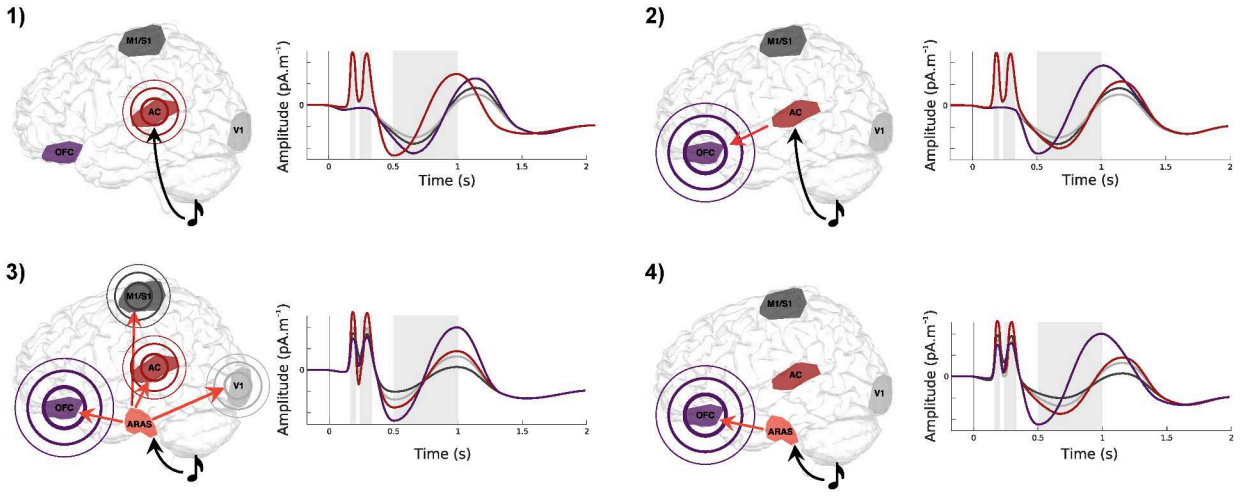

Figure 3.1: Four models of information flow leading to generation of evoked slow oscillations. 1) SO is evoked by arrival of auditory information in the AC via auditory pathways, from which it propagates. 2) Auditory information arrives in the AC, spreads in cortico-cortical networks to the OFC, which is sensitive to stimulation in sleep and generates SOs, from whence they propagate. 3) The arousal networks in brainstem and thalamus are stimulated, and generate widespread and simultaneous SOs, most strongly in OFC due to its sensitivity. 4) Arousal system is activated as in 3, but SOs are generated first in OFC, from which they propagate to other brain areas. Grey shading indicates the evoked responses components P200, N350 and N550-P900. SO: slow oscillations, AC: auditory cortex, OFC: orbitofrontal cortex. Grey shading indicates time windows of interest that are used in later analyses

In the present work, we recorded magnetoencephalography (MEG) and EEG data simultaneously in an overnight design, in five healthy young adults, while short, quiet sounds were presented. We first replicate previous results showing that sleep-specific evoked response components emerge in deeper sleep stages. We then take advantage of MEG's spatial and temporal resolution to explore the distribution of evoked responses over the cortex, their temporal evolution, and their co-occurrence with evoked sleep spindles. We then evaluate evidence in favour of each of these models using MEG. Finally, we explore the relationship of the MEG results to the signal observed in single-channel EEG, as it is most frequently used both to detect SOs and assess the impact of CLAS-SO on evoked oscillations in extent research. Clarifying how sound evokes slow oscillations and sleep spindles has important implications for using CLAS as a causal tool to explore mechanisms of memory, and optimizing its effectiveness in fundamental research and in potential clinical applications.

3.3 Methods

3.3.1 Participants

Six neurologically healthy young adults without sleep or neurological conditions were recruited from the local community. One dataset was unusable due to a technical problem with the EEG system that precluded scoring. The mean age of the five remaining participants was 21.2 (SD: 1.33; range 19-23), and 3 were female. All subjects reported being in good health with normal hearing, were non-smokers, were not taking medication, had not changed time zones or conducted shift work in the 6 weeks preceding the experiment, and had a normal 6-10 hour sleeping pattern in the three days prior to the experiment (confirmed by sleep log). The night prior to the experiment, participants were asked to stay up one hour later than their habitual bedtime to increase sleep pressure. The day of the experiment they were asked to refrain from consuming caffeine, alcohol, nicotine, and cannabis. Subjects gave written informed consent, and were compensated for their time. The experimental protocol was approved by Concordia University's Human Research Ethics Committee, and the Research Ethics Board at McGill University. This study was not pre-registered.

3.3.2 Study design

On the experimental evening, participants first completed a health questionnaire to confirm eligibility; the Munich Chronotype Questionnaire (MCTQ) to document their habitual diurnal rhythms (Roenneberg et al., 2003); and the Pittsburgh Sleep Quality Index (PSQI) (Buysse et al., 1989), which contains 19 self-rated questions which are scored from 0-3 points, where '0' indicates no difficulty, and '3' indicates severe difficulty. The PSQI seven component scores are added to yield a global score between 0 and 21 points. Scores of 5 or more indicates poor sleep quality; the higher the score, the worse the quality. Participants also completed a subjective fatigue scale concerning their current state, which consisted of 7 questions rated on a 5 point Likert-scale. Items on the scale asked about subjects' levels of tiredness, activity, motivation, interest, concentration, relaxation and general feeling; all ratings were moderate.

Participants were prepared for EEG with electrodes positioned at Cz, C3, and C4; 10-20 system (Homan et al., 1987), noting that the majority of closed-loop studies (whose effects we are trying to better understand) used similar frontal-central electrode positions. To avoid discomfort due to contact with the MEG helmet, occipital electrodes were not used. Participants settled into the MEG scanner in a supine position. A five-minute resting state data acquisition with eyes open was collected, as a contribution to an open-access database (which also houses the current dataset (Niso et al., 2016)). Lights were dimmed to full

darkness, and subjects were asked to close their eyes and relax. Sound stimulation was started immediately, with the subject in the awake state, to allow them to get used to the sound and so that the brain response to the wake state could be measured. Standard T1-weighted magnetic resonance anatomical images (1 mm^3 isotropic voxels) were acquired in a separate session to enable distributed source localization of MEG signals.

3.3.3 Auditory stimulation

We used a 120 ms synthetic speech syllable (/da/, 10 ms consonant burst, a 30 ms formant transition, and an 80 ms steady-state vowel with a fundamental frequency of 98 Hz), to facilitate comparison of the evoked responses in simultaneously acquired EEG and MEG with previous work (Coffey et al., 2016b, 2017a, 2021). The stimulus was presented binaurally through Etymotic ER-3A insert earphones with foam tips (Etymotic Research), at 55 dB SPL, which we determined through pilot testing was clearly audible but did not awaken sleeping participants. The stimulus onset interval range was 2800 to 3000 ms (mean ∼2900 ms), where jitter was selected randomly from a uniform distribution.

One of our main goals is to better understand the neurophysiology behind the CLAS effect, and how it can be optimized. Stimulating only up-states as measured by single-channel EEG would a) limit the total number of stimulations sent, and b) limit our ability to explore the optimal phase of stimulation with respect to excitability state in specific brain locations using MEG, which is not well-captured in the global electrical fields measured using single-channel EEG. We therefore elected to use a continuous sound presentation rather than exclusively stimulating EEG up-states. This design has some potential limitations.

The first is that regular sound presentation might limit the depth of sleep achieved. We started presenting sound before sleep, and confirmed that participants were able to fall asleep, and slept adequately, using polysomnography. All participants achieved deep sleep (and even some REM sleep; (see Table 3.2), suggesting that the auditory stimulation did not impair sleep quality. Second, it is possible that brain responses were reduced due to the frequency and regularity of sound presentation. We included some temporal jitter to reduce predictability, but the inter-stimulus interval is nonetheless kept short in an effort to maximize the number of trials. Bastien et al. found that some components of the evoked responses in sleep are affected by presentation rate (i.e., N350, N550), but not others (P900) (Bastien & Campbell, 1994), suggesting that the slower evoked responses is preserved even with shorter intervals (of around 5 s). We confirmed that we were able to observe these evoked responses across sleep stages using the present inter-stimulus interval (Figure 3.3). Third, it is possible that brain state at the moment of stimulation is impacted by the previous stimulation, when

using short inter-stimulus intervals. In the present study, baseline levels of activity appeared to be restored before 2.5 s following stimulation, implying that processing of new incoming sounds was not strongly influenced by residual activity caused by the preceding sound.

Notably, existing studies that have used closed-loop stimulation and have found memory effects (e.g. Ngo et al. 2013b) often stimulate either pairs or trains of SO peaks, resulting in even shorter inter-stimulus intervals of around ∼1 s, sometimes with no-stimulation periods of only ∼2.5 s (Ngo et al., 2013b, 2015). For similar reasons, although it is possible that short inter-stimulus interval results in less spindle activity generation due to some stimulations arriving towards the tail end of a spindle refractory period (Fernandez & Lüthi, 2020; Antony et al., 2018), past results with short intervals in a closed-loop setting did successfully generate spindles. We can therefore conclude that the auditory stimulation parameters are compatible with existing CLAS studies and are appropriate for addressing the present questions.

3.3.4 EEG and MEG data collection

Two hundred and seventy MEG channels (axial gradiometers), five EEG channels (C3, C4, Cz, M1 and M2), two bipolar EMG channels (chin and neck), EOG, ECG, and one audio channel were simultaneously acquired using a CTF MEG System and its in-built EEG system (Omega 275, CTF Systems Inc.). All data were sampled at 2400 Hz, and were recorded in 30-minute 'runs'. Prior to each run, the head was localized, and head position was stored for use in MEG source localization. Data pre-processing was performed with Brainstorm (Tadel et al., 2011), and using custom scripts (The Mathworks Inc., MA, USA), according to recommended practices (Gross et al., 2013).

3.3.5 Sleep scoring

Sleep scoring of the data, in which 30 s windows of data are visually inspected and categorized into wake, non-REM sleep stages 1-3, and REM sleep, was accomplished according to AASM practices (Iber, 2007) based on band-pass filtered EEG (0.1-20 Hz, channels 'C3', 'C4', and 'Cz' referenced to left mastoid), EOG (0.1-5 Hz), and EMG (10-58 Hz) channels, which were then down-sampled for ease of handling to 150 Hz. Each epoch was scored by one researcher and confirmed or challenged by a second observer. Discrepancies were resolved via discussion.

3.3.6 Statistical approach

We elected to study a small number of subjects in an overnight design rather than a larger number of subjects for shorter sleep periods (as is used in most nap studies and studies

inve (Baker et al., 2021)stigating behavioural correlates) so as to be able to capture brain responses across all sleep stages, and to have a very high number of stimulations per subject that hit sleep features of interest (e.g. SO troughs and peaks), or missed them (e.g., stimulations that occurred in the absence of SOs, spindles, and their refractory periods). This design also facilitated an in-depth exploration of phase relationships between EEG and specific brain regions. It is increasingly being recognized that statistical power is dependent upon the amount of data available per subject, particularly in cases in which the within-participant variance is larger than the between-participants variance (Baker et al., 2021). The approach of collecting a large amount of data in a small number of subjects is best suited to research questions that address low-level mechanisms that are likely to be highly similar across participants. It has a long history in non-human primate research, in which research resources and ethical considerations limit sample sizes (please see Smith & Little (2018); Brysbaert & Stevens (2018); Baker et al. (2021) for a discussion and demonstration of the trade-offs between number of subjects and number of observations).

Analysis for basic confirmations of well-established results (e.g., the presence of an evoked N550-P900 complex in NREM sleep stages 2 and 3) were conducted using non-parametric Wilcoxon signed-rank tests on subject means. With our small number of subjects, these results are valid, but are only significant if all five subjects show the same pattern of results. They serve only to confirm that well-replicated phenomena (like the existence of a N550-P900 complex in sleep) are clearly and consistently observed across subjects in this study, as a starting point for addressing the study's specific objectives. Each subject's mean values across sleep stages were normalized by dividing by their maximum value, for visualization purposes; this approach was used in Figures 3.3 and 3.6.

For the main research questions, we applied linear mixed effects (LME) models (Pinheiro & Bates, 2006), which model the relationship between dependent data and independent data when there is a correlation between observations (e.g., multiple measurements taken from each subject; subject is modelled as a random factor). This class of models takes advantage of the high number of observations per subject (i.e., between 5,000 and 116,000 depending on the research question). LME analyses were conducted in R using the lme4 and emmeans packages (Bates et al., 2015; Lenth, 2022). Alpha values of .05 were used throughout, and FDR corrections for multiple comparisons were applied over the dimensions of interest (e.g., frequency bins) when necessary, using the Benjamini-Hochberg procedure (Thissen et al., 2002). For each linear mixed effects models used in analysis, we visually inspected the histograms and quantile-quantile (Q-Q) plots of the residuals for deviations from normality and homoskedasticity. In models in which clear deviations were present, we excluded outliers by removing values based on thresholds that were defined as 1.5 times the interquartile range

(i.e., below Q1 and above Q3; this methods removes data which lie beyond 2.7 σ from the mean), and re-ran the models. The use of outlier removal is indicated for each analysis.

3.3.7 EEG auditory evoked responses across sleep stages

For EEG analysis, we used a 'Cz' to left mastoid channel. We first filtered the raw data between 0.1 and 200 Hz (87010-order linear phase FIR (finite impulse response) filter with a Kaiser window and 60 dB stop-band attenuation; the order is estimated using the MATLAB 'kaiserord' function, and filter delay is compensated by shifting the sequence to effectively achieve zero phase and zero delay, as per Brainstorm default settings (Tadel et al., 2011)). Data were then down-sampled to 500 Hz, epochs from 1 second pre-stimulus onset to 3 seconds post-stimulus onset were extracted, and the mean during the pre-stimulus baseline period was subtracted from each epoch. Epochs were separated according to the sleep stage during which they occurred, and grouped across an individual's runs. Subject averages were computed for each sleep stage, a 40 Hz low-pass filter was applied to the average so as to maximize comparability with previous work looking at auditory evoked responses, and mean values from -0.5 s to 0 s were subtracted for better visual alignment across sleep stage time series. Grand average means and standard error were computed for each time series, for visualization purposes.

To quantify the amplitude of the P200 ERP component, we computed average amplitude for each stage between 165 and 205 ms (based on a previously-observed P200 peak in both EEG and MEG to the same stimulus at ∼185 ms (see Coffey et al. (2017a)). The latency of the N350 component appeared to increase in deeper NREM sleep stages (see Figure 3.3). For Wake, N1, and REM, we used a window of 240 to 280 ms; for N2, the window was defined as 265 to 305 ms, and for N3, 290 to 330 ms after sound presentation. To compute the amplitude of the slowest evoked responses, we first averaged a time window 500 to 600 ms to capture the N550 component, and 800 to 1000 ms for the P900 component. We then subtracted the N550 mean value from the P900 value to get an amplitude measure of the N550-P900 complex. Note that we favour this terminology when referring to activity occurring within this time window to avoid assumptions about whether or not K-complexes are evoked on individual trials. However, 'P900-N550' is used in figures to indicate the direction of subtraction in the case the amplitude difference between the two components is measured (i.e., P900 amplitude minus N550 amplitude, which results in a positive peak-to-trough value in case of a successful evoked response).

Later components have broader peaks and are generally less temporally-aligned across subjects, motivating the use of longer windows. We used simple non-parametric Wilcoxon

signed-rank tests (one-tailed) to test whether the amplitudes of P200, N550, and N550-P900 complexes differed in N2 and N3 sleep as compared with responses within each time window during wakefulness. We calculated effect sizes for between-condition comparisons used the probability of superiority (PSdep), which is calculated as the number of positive difference scores divided by the total number of paired scores (Grissom & Kim, 2012).

Because CLAS is thought to affect memory through the generation of not only slow oscillations, but also sleep spindles nested within them (Ngo et al., 2013b), we also investigated changes in spindle band power following sound stimulation, across sleep stages. For each epoch, we computed time-frequency power over a 1-30 Hz frequency band (central frequency: 15 Hz, full-width half-maximum: 0.2 s), using spectral flattening (i.e., power values are multiplied by frequency), in Brainstorm (Tadel et al., 2011). All epochs were averaged by sleep stage within subjects, and a subject grand average difference for N3 minus Wake was computed to define a time and frequency window of interest for further analysis, by visual inspection, which was 0.6-1.2 s after sound onset in a 11-14 Hz frequency band. We then computed the difference between this window and an equivalent window preceding sound offset (-0.6 -0 s after sound onset, 11-14 Hz), for each subject and sleep stage.

It is worth noting that the time window used to measure baseline activity occurs $/sim$2s after the onset of the previous sound, which could mean that an incoming sound overlaps with long-range responses to the previous sound. However, as mentioned in the description of auditory stimulation above, baseline levels of EEG activity, including sigma power, seem to be restored $/sim$2 s following stimulation making this specific time-window (2.3-2.9 s) adequate for baseline measurement (see (Figure 3.6b). As above, we used a non-parametric Wilcoxon signed-rank test (one-tailed) to confirm that spindle power amplitude increased across subjects following sound presentation as compared with baseline, specifically in N3 when the effect should be most prominent, and in N2 as a basis for merging of N2 and N3 epochs. These EEG-based analyses serve to select parameters (e.g., time and frequency windows) for further analysis in MEG source space.

In past work, epochs have sometimes been divided into those which produce a strong response (K-complex), and those which do not (e.g., Bastien & Campbell (1992); Dang-Vu et al. (2011)). To explore whether evoked responses are unimodally or bimodally distributed, as would be the case in an all-or-nothing response, we selected stimulations which fell into N2 and N3 sleep stages, yet coincided neither with a slow oscillation nor sleep spindle (as measured in the Cz-to-mastoid EEG channel). We extracted average amplitudes for each epoch during the N550 and P900 windows (as in the analysis above), and computed their difference as a measure of the strength of the N550-P900 complex. We then plotted the distribution of trough-to-peak amplitudes for each subject. Epochs were then sorted

into those containing the top 25% and bottom 25% amplitude values. To investigate the relationship between elicited N550-P900 complex and spindle generation, time-frequency plots were computed and averaged for each condition and each subject. Each subject's mean values across conditions were normalized by dividing their maximum value, for visualization purposes.

3.3.8 SO detection and phase-binning

We used a Cz-to-mastoid channel to detect slow oscillations using an offline detection algorithm developed by Carrier et al. (2011). In brief, EEG was filtered between 0.16 and 4 Hz and four criteria were evaluated to detect the emergence of a slow oscillation: a peak-to-peak amplitude greater than 75 μV, a negative peak amplitude higher than 40 μV, a duration of the negative peak between 125 and 1500 ms, and a positive peak lasting less than 100 ms (Rosinvil et al., 2021). Detected slow oscillations were then divided into bins representing cortical states.

To explore the impact of up-states and down-states of slow oscillations and question the mechanism of CLAS, 150 ms time windows centred on the detected peak and trough of each oscillation were defined and stimulation occurring approximately simultaneously (defined as occurring within a 150 ms window centred on the detected peak or trough) were sorted accordingly 'Up-state' and 'Down-state' categories. Stimulation occurring during N2 and N3 NREM sleep stages and outside of a detected slow oscillation (or sleep spindles and their associated refractory periods) was sorted into an additional bin referred to as 'Clear'. Based on the definition by Antony et al. (2018), the spindle refractory period was defined as a fixed time window lasting 2.5 seconds after the offset of the detected sleep spindle. To maximize the number of stimulations per bin, we combined N2 and N3 NREM sleep stages. On average, the number of stimulations during detected slow oscillations per subject across all phases was 411.8 (SD = 180.7, range = 196-608), and the number of stimulations during the 'Clear' condition was 2055.5 (SD = 535.6, range = 1474-2764).

3.3.9 Spindle detection

Sleep spindles were detected as input to sort stimulations into the Clear condition, such that they coincided neither with a slow oscillation nor with a spindle. Sleep spindles were detected on the Cz (referenced to mastoid) channel, because it is centrally located, near where spindles peak (Cox et al., 2017). Spindles were detected offline using an algorithm which emulates human scoring (Lacourse et al., 2019). In brief, the algorithm filters the EEG signal in the sigma band, 11-16 Hz (as per Lacourse et al. (2019)), and applies four criteria: absolute

sigma power (default = 1.25), relative sigma power (default = 1.6), and both correlation (default = 0.6) and covariance (default = 1.3) of the sigma band-passed signal to the original EEG signal. After consultation with the authors, we adjusted the parameters slightly to work better with our EEG data (absolute sigma power = 0.8; relative sigma power = 1.0; covariance = 1.0; correlation = 0.4), and a trained expert confirmed successful detection visually for each subject. As in the analysis of slow oscillations, N2 and N3 sleep stages were merged.

3.3.10 MEG data processing

Cardiac artifacts were removed from MEG data using Brainstorm's in-built cardiac detection and source signal projection algorithms (Tesche et al., 1995). Projectors were removed when they captured at least 12% of the signal and the topography of the components matched those of ocular or cardiac origin upon visual inspection. Eye blinks were not detected nor removed, as participants generally had their eyes closed during the recording. Data were filtered between 0.1 and 200 Hz, and down-sampled to 500 Hz. For ERP and ERF analyses, data were further low-pass filtered below 40 Hz, which is common practice to measure the amplitude of evoked auditory response components (e.g., P200).

Auditory event markers were used to define epochs that started 1 s before sound onset and ended 3 s after sound onset as in the EEG analysis. Similar to previous work (Coffey et al., 2021), we used a distributed source-modelling approach. This process estimates activity originating throughout the brain, constrained by spatial priors derived from each subject's T1-weighted anatomic MRI scan (Baillet et al., 2001; Gross et al., 2013). We imported anatomical data into Brainstorm, and cortical and subcortical (thalamus, hippocampus, and amygdala) structures were combined with the cortex surface (∼15,000 vertices). An overlapping-sphere head model was computed for each run; this forward model explains how an electric current flowing in the brain would be recorded at the level of the sensors (Tadel et al., 2011). A noise covariance matrix was computed from 2 min empty-room recordings taken before each session. We computed the minimum-norm estimate (MNE) source distribution model using source orientations constrained to brain structure surfaces, for each run (Hämäläinen, 2009). Source models for each run were averaged within-subject.

3.3.11 MEG topographies

To explore the topography of the evoked slow oscillations (as indexed by N550-900 complex amplitude), we prepared subject averages in source space for stimulations occurring in Wake, N2, and N3 sleep stages, and extracted time series using the Destrieux brain atlas (Destrieux

et al., 2010). As our source models included thalamus, hippocampus, and amygdala in addition to the cortex, we created ROIs for these areas. Because the first two structures are large and averaging source-spaced signals over large, elongated or round regions can degrade the signal, we divided them each into three equally-sized ROIs, and visually confirmed that each subject's divisions were similarly positioned and numbered, thus roughly corresponding across subjects and allowing for meaningful group averages. To maximize the number of trials and thus signal clarity for the sleep analyses, we calculated a weighted average across N2 and N3 sleep stages, proportional to the amount of N2 and N3 sleep collected for each participant (see Table 3.2). We then created weighted grand averages for each of the Destrieux regions of interest for Wake and combined N2 and N3 sleep ('N2 & N3'), taking into consideration the proportion of data recorded for individual participants. Each ROI time series was baseline-corrected (-0.5 to 0 s relative to stimulus onset). The amplitude of the N550-P900 complex was computed as described in the EEG analysis (i.e., an average over 500-600 ms was subtracted from an average over 800-1000 ms), and the absolute value was taken. A difference was then computed between the Wake and N2 & N3 conditions. ROIs having outlying values +/- 3SD of the mean across all ROIs was set to +/-3SD, and the values were mapped to colour scales such that red indicates greater activity change relative to pre-stimulation baseline, in sleep). To explore the spatial trajectory of brain activity over time in NREM sleep, we conducted a similar analysis, except that brain activity was computed over six consecutive 500 ms windows starting at -0.5 s relative to stimulation, and the absolute value over each window was displayed on a black-to-red colour scale where red indicates more activity change relative to the pre-stimulus baseline period.

To explore the topography of evoked responses in the spindle range, we computed spindle band power as in the EEG window in Wake and NREM (N2&N3) for each region of interest, and mapped the power difference to a blue-red scale where red indicates more spindle activity in sleep. These average activity topographies were used to present spatial information concerning evoked responses qualitatively, and as input to confirm and select regions of interest for further investigation of evoked responses in source space.

For a visual comparison of the topography of the evoked slow responses and spindle band activity, we used the FOOOF algorithm (https://fooof-tools.github.io/fooof/) as implemented in Brainstorm (frequency range of analysis: 1-40 Hz; otherwise using default parameters: peak width limits: 0.5-12 Hz, maximum number of peaks: 3, min peak height = 3 dB, proximity threshold: 2 standard deviations) to separate oscillatory from 1/f (frequency) brain activity (Donoghue et al., 2020), and averaged peak values for slow oscillations (0.5-1.5 Hz) and spindles (11-17 Hz) separately. We used the wider spindle frequency range here for best comparison with prior literature, although it is slightly different than the 11-14 Hz

range selected based on the evoked spindle power in our own dataset. Note that due to the study design, brain activity captured in this analysis includes a combination of evoked and endogenous activity, meaning that we limit our analysis to a qualitative observation of similarities; a specialized study design that clearly separates evoked from endogenous oscillations would be needed to quantitatively investigated questions of similarity more thoroughly. Note that endogenous slow oscillations and stimulus-evoked K-complexes share many similarities and there is currently no normative data for discriminating evoked responses from other slow waves (Halász, 2016).

3.3.12 MEG time series analysis

Based on the models that we propose to evaluate (Figure 3.1) as well as the topographical analysis showed in Figure 3.5, five bilateral cortical regions of interest (ROIs) based on the Destrieux atlas (Destrieux et al., 2010) were defined in subject space for each participant. The selected ROIs are based on: 'pre-central gyrus', 'post central gyrus', 'occipital lobe', and 'sub-callosal gyrus', and the 'transverse temporal' and 'planum temporale' gyri, which were merged to capture the auditory cortex. Each ROI was defined in each hemisphere. The size of each ROI was manipulated by progressively increasing or decreasing ROI area, so as to be similar across ROIs and hemispheres (across all ROIs, all subjects, mean area: 10.3 cm^2, SD: 0.2 cm^2, range: 9.99 to 10.88 cm^2). We preferred to use ROIs of similar size, as we extract the mean activity from each ROI. In general, we kept left and right hemisphere homologue ROIs separate during the analyses so as to explore the possibility of hemispheric differences, for which there is some limited support. For example, Morgan et al. (2021); Achermann et al. (2001) found that slow oscillatory activity was stronger in left than right ventral limbic areas, using EEG.

For MEG analysis investigating the contribution of specific ROIs, we sorted epochs (i.e., -1 to +3 s relative to sound onset) by sleep stage, and produced evoked response plots, as in the EEG analysis (see Supplementary Figure 1). We have not included SNR measurements, because they are confounded by the nature of the evoked design. That is, if we measure an evoked response we can be confident that we have adequate SNR to measure it, but if we do not, we cannot clearly distinguish between a region not producing a response and our inability to pick it up due to insensitivity (note that we compare results within-region whenever possible). To evaluate the presence or absence of specific peaks in the evoked response, we then measured the mean amplitude over a window centered on P200 in EEG (165 and 205 ms post stimulation) as well as the difference in amplitude within a time window capturing the N550-P900 slope as observed in EEG ERPs (i.e., the average amplitude over

500ms to 600 ms subtracted from the average amplitude from 800ms to 1000ms) for each run and for each ROI. Extracted values for each epoch were then used in LME statistical models to assess the impact of sleep stage on responses elicited by sound across sleep stages.

3.3.13 Directed phase-transfer entropy

Functional connectivity between the AC and OFC was estimated using directed phase-transfer entropy (Lobier et al., 2014), in N2 and N3 sleep only, as these contain the evoked responses of interest (i.e., SOs and sleep spindles). In brief, the time series is described by its instantaneous phase, in a similar fashion to Wiener-Granger causality (Hillebrand et al., 2016).

We used common frequency band divisions: 'delta', 'theta', 'alpha', 'beta' and 'low gamma', with the additional separation of 0.5−1.5 Hz and 11−17 Hz as 'slow oscillation' and spindle or 'sigma' bands, due to their relevance to the research questions, and because there is some evidence that very slow oscillations (<1.5) are somewhat distinct in characteristics and function from 2–4 Hz oscillations (Steriade et al., 1993; Brodt et al., 2023; Kim et al., 2019). Note that while slow oscillations within the 0.1 to 0.5 Hz range have been included in our slow oscillation analyses elsewhere, for example to detect slow oscillations or visualize time-locked evoked responses, the 4 s epochs used for the connectivity analysis only allow us to characterize frequencies above about 0.25 Hz (i.e., 1/4 s); we therefore raised the filter to 0.5 Hz. In sum, signals were band-pass filtered in the following frequency bands: 0.5−1.5, 2−4, 5−7, 8−10, 11−17, 18−29, and 30−58 Hz.

Directed phase-transfer entropy was computed for each pair of ROIs within each frequency band, and normalized between -0.5 and 0.5. The sign of the result indicates the dominant direction of functional connectivity. Directed phase-transfer entropy results for each trial were then entered in LME statistical models.

3.3.14 Up-state and down-state detection in EEG and MEG

We explored the role of tissue state in specific regions and its relationship to EEG by detecting up and down-states in extracted time series from each ROI over each ∼30 min recording. We used the same detection algorithm for the MEG data (extracted from regions of interest in source space) as had been used for EEG (Cz) signals, to maximize comparability. We first isolated periods of sleep that had been manually scored as N2 or N3, and filtered the data in the slow wave frequency band (0.1 to 2 Hz). Troughs and peaks were automatically detected (using the 'findpeaks' function implemented in MATLAB), and the amplitude difference between peak and trough amplitude was computed for each detected peak. Trials were sorted by amplitude differences, and epochs containing the top 25% of peak-trough amplitude for

each subject were selected as our Up-state condition for further analyses. Similar processing pipeline was used to select troughs (Down-states) by detecting peaks after inverting the signal (i.e., multiplication by -1).

Epochs were defined around the detected peak (Up-state) in the EEG signal (-2 to +2 s) to examine the correlation between the EEG signal and MEG signal extracted from ROIs. Correlation of the signal from the EEG sensor Cz and each extracted signal was then computed and the correlational relationship between signals was investigated using LMEs. The instantaneous phase of the signal in EEG as well as in each ROI was extracted using the Hilbert transform of the signal.

Finally, to investigate the role of cortical tissue excitation state on EEG brain evoked responses, incoming sounds were sorted according to whether they coincided with a local up-state or down-state in each ROI (as defined by a 150 ms window centred on the detected peak or trough), and as before, 4 s epochs (-1 s pre-stimulation onset to 3 s post-stimulation onset) were defined. The elicited N550-P900 complex amplitude was measured as previously described and the sigma power post-stimulation was calculated using the root mean square (RMS) value of the signal filtered between 11 and 14 Hz, 0.6 to 1.2 s after stimulation from which a pre-stimulus value (-0.6 to 0 s) was subtracted to emphasize sound-evoked spindle band power, as in previous analyses.

3.4 Results

3.4.1 Sleep

Although sleep quality was not optimal, all subjects were able to sleep sufficiently in the physically-restricted and unfamiliar scanner environment so as to have a large number of trials (see Table 3.2). Sound stimulation was started before sleep onset and all subjects were able to fall asleep, but as sleep pressure wore off, participants sometimes reported that when they awakened, the stimulation distracted them from falling asleep again. Participants could ask for the stimulation to be turned off until they were once again asleep. Two of the five participants availed themselves of this option. Once they were sleeping, turning on the sounds did not re-awaken them. Unstimulated periods were not included in the analyses and 30 s epochs containing movement were discarded. On average, participants had 246.6 mins of movement-free, stimulated recordings in sleep (including NREM and REM sleep, but not Wake; SD = 26.6 mins). Every subject, except one ('Sub2'), had >10 mins of N3 and REM sleep. See Table 3.2 for details. In analyses which combined N2 and N3, weighted averages within-subject were used to account for the differences in sleep stage duration. As the study

concerns physiological rather than behavioural research questions, these results are sufficient to investigate auditory brain responses during sleep.

	Wake	N1	N2	N3	REM
	min (#)	min (#)	min (#)	min (#)	min (#)
Sub1	30.5 (610)	12 (235)	99 (1979)	107.5 (2157)	21 (420)
Sub2	32 (487)	152 (2439)	83 (1479)	7 (137)	0 (0)
Sub3	125 (2493)	31 (607)	66.5 (1321)	89 (1766)	21.5 (431)
Sub4	15 (145)	6.5 (46)	55.5 (579)	186.5 (3368)	23.5 (470)
Sub5	49.5 (913)	55 (994)	121 (2236)	82 (1601)	13.5 (272)
Average	50.4 (929.6)	51.3 (864.2)	85 (1518.8)	94.4 (1805.8)	15.9 (318.6)
SD	43.43 (916.3)	59.4 (952.4)	26.05 (642.3)	64.18 (1161.1)	9.7 (193.3)

Figure 3.2: Sleep staging results from usable recordings during which sound stimulation was present, for each subject. Sleep was staged into 30 s epochs, and reported in minutes per stage. The number of auditory stimulations occurring during each stage is reported in parentheses.

3.4.2 Effect of sleep stage on brain responses evoked by auditory stimulation

Auditory evoked responses in EEG

To confirm that the study design and amount of sleep stimulations acquired across sleep stage were adequate to observe previously reported state-dependent differences in evoked responses, we analyzed evoked responses across brain states in EEG. The evoked responses for each observed sleep stage in EEG, averaged across subjects, are presented in Figure 3.3a. Qualitatively, the early evoked responses that are associated with auditory processing in wake states (i.e., P100, N100, P200) do not appear to be strongly influenced by sleep stage, whereas the later components (i.e, N350, N550, P900) that appear only in sleep are stronger in deeper NREM stages.

We used simple non-parametric Wilcoxon signed-rank tests (one-tailed) to evaluate whether evoked response amplitudes differed between wakefulness and deeper NREM sleep stages (N2 & N3), which are the brain states in which CLAS of SOs is normally used. P200, as a representative measure of the classical auditory evoked response, was significantly greater in N2 sleep as compared to wake ($Z = 15$, $p = .03$, $PSdep = 1.0$), but the Wake vs. N3 difference was not significant ($Z = 3$, $p = 0.31$, $PSdep = 0.8$). The N350 component, instead, was significantly larger in NREM sleep stages 2 and 3 ($Z = 15$, $p = .03$, $PSdep = 1.0$ for both). The N550-P900 complex (i.e., P900 - N550 amplitude) was significantly greater in N3 sleep than Wake ($Z = 15$, $p = .03$, $PSdep = 1.0$), but did not reach significance in N2 sleep ($Z = 14$, $p = .06$, $PSdep = 0.8$). These results are used to confirm that the slow evoked responses

that emerge in deeper sleep (N2 and N3) and have been previously reported (see Colrain & Campbell 2007; Bastien et al. 2002) are present in our sample, as a starting point for spatially-resolved MEG analyses. To increase the number of trials for subsequent analyses, we combine N2 and N3 sleep stages, as N350 and N550-P900 components are observed in both stages (Colrain & Campbell, 2007) (although noting that the N2 effects are smaller than in deeper, N3 sleep). Importantly for the purposes of using LME models, the number of observations included in the statistical analyses for the main questions concerning the effects of sound stimulation in N2 and N3 sleep are over 16,000 per region of interest (see Table 3.2).

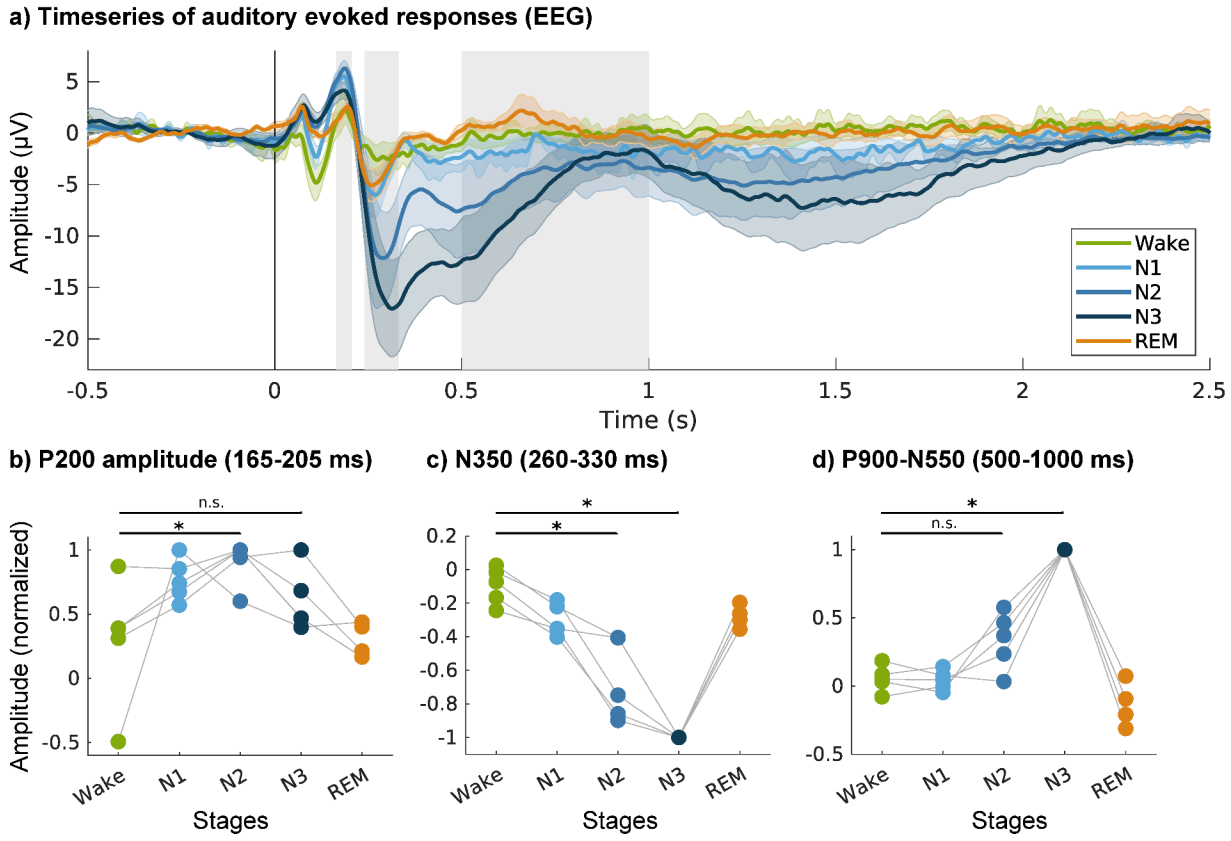

Figure 3.3: Evoked responses over sleep stages, in EEG (Cz). a) Time series of the auditory evoked responses showing the appearance and evolution of late evoked components (N350, N550, P900) in deeper NREM sleep stages. Coloured lines show means across participants; shaded areas indicate standard error. Grey shading indicates the evoked responses components P200, N350 and N550-P900. b) Amplitudes of the P200 component show little change across sleep stages. Conversely, amplitudes c) at N350 and d) peak-to-trough differences between P900 and N550 are stronger in deeper NREM sleep stages than in Wake. Asterisks denote significant differences between Wake and deeper sleep conditions (Wilcoxon signed-rank test on the means) * p ¡ .05). EEG: electroencephalography; NREM: non-rapid eye movement sleep, REM: rapid eye movement sleep; N1-3: stage 1-3 NREM sleep.

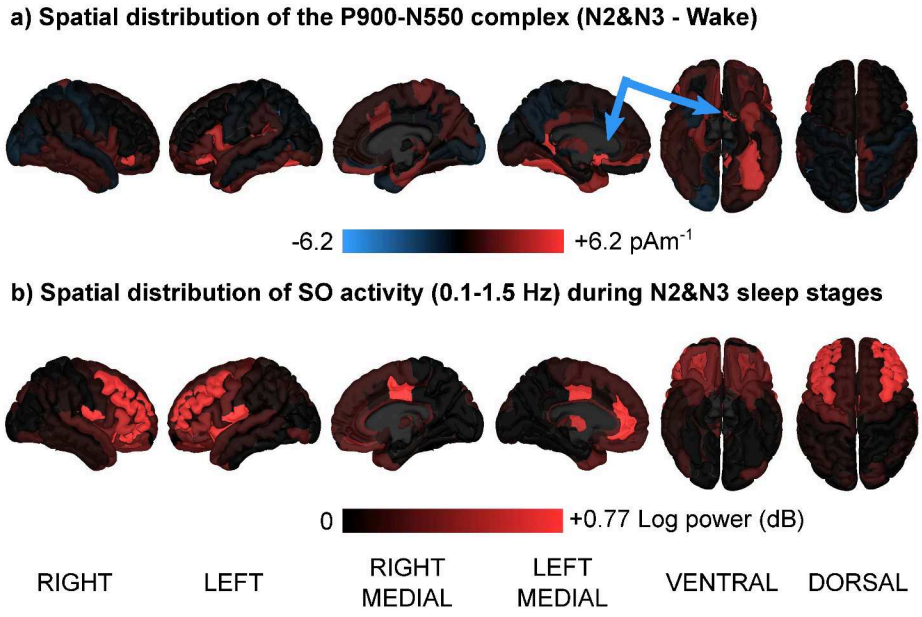

Figure 3.4: Topographies of a) evoked activity differences between wake and NREM sleep (stages N2 and N3 combined). Red indicates more activity change relative to pre-stimulus baseline during the auditory-evoked N550-P900 complex in sleep as compared to wake. The evoked N550-P900 complex is specific to sleep and shows widespread activity change in ventral and orbital frontal areas (see also Figure 3.3b,d for topographies of evoked activity in NREM sleep over time). b) Topography of slow frequency oscillatory activity during N2 & N3 sleep stages (as indexed using FOOOF), for reference; note that due to the study design, both spontaneous and evoked slow oscillations are represented. Blue arrows indicate activity in the orbitofrontal cortex. FOOOF: fitting oscillations & 1/F; SO: slow oscillation; N2-3: stage 2-3 NREM sleep.

Slow oscillations evoked by sound in sleep in MEG source space

To confirm that the orbitofrontal regions of interest is involved in the evoked response to sound, we computed the topography of evoked activity differences between Wake and N2 & N3, displayed in Figure 3.4a. Widespread activity differences are observed in ventral and orbital frontal regions (blue arrows), and inferior frontal gyrus (e.g., Destrieux regions 'G_subcallosal L', 'Lat_Fis-ant-Vertical L', 'G_cingul-Post-ventral L', 'G_front_inf-Orbital R', 'S_circular_insula_ant L'). On the basis of these observations, we selected Destrieux atlas regions ('G_subcallosal' left and right) as representative of ventral regions exemplifying the SO evoked response (see Methods for details, and Figure 3.7b for a visualization of the resulting ROI). For visual comparison only, we plotted topographies of slow frequency oscillatory activity during N2 & N3 stages (using the FOOOF algorithm) (Figure 3.4b). In general, we observed some overlap between the evoked N550-P900 complex topography (Figure 3.4a) and the slow oscillation activity (Figure 3.4b). There was more SO activity in dorsolateral frontal regions in b; however, as noted in methods, the specific study design does not allow us to clearly separate (and therefore quantitatively compare) evoked vs. endogenous SO

topographies. We also take advantage of MEG's temporal resolution to visualize the time course of the evoked responses, see Figure 3.5. In the earlier time window (0 to 0.5 s), the auditory cortex is bilaterally active (blue arrow). In later periods (e.g., 1.5 to 2.0 s), the orbitofrontal regions show greater change with respect to pre-stimulus baseline. The auditory regions also show activity changes in later periods. Note that the P900 component is not prominent in this representation, which displays difference from baseline, because as shown in the time series average (Figure 3.5 (bottom)), amplitude peaks close to the pre-stimulus level (at 0.9 s) before once again decreasing (at 1.5 s). We nonetheless see activity in the OFC related to the late component of the EEG response around 1.5-2 s (blue arrow). The evoked response returns to baseline ∼2-2.5 s post stimulation, which is prior to the next stimulation (∼2.9 s).

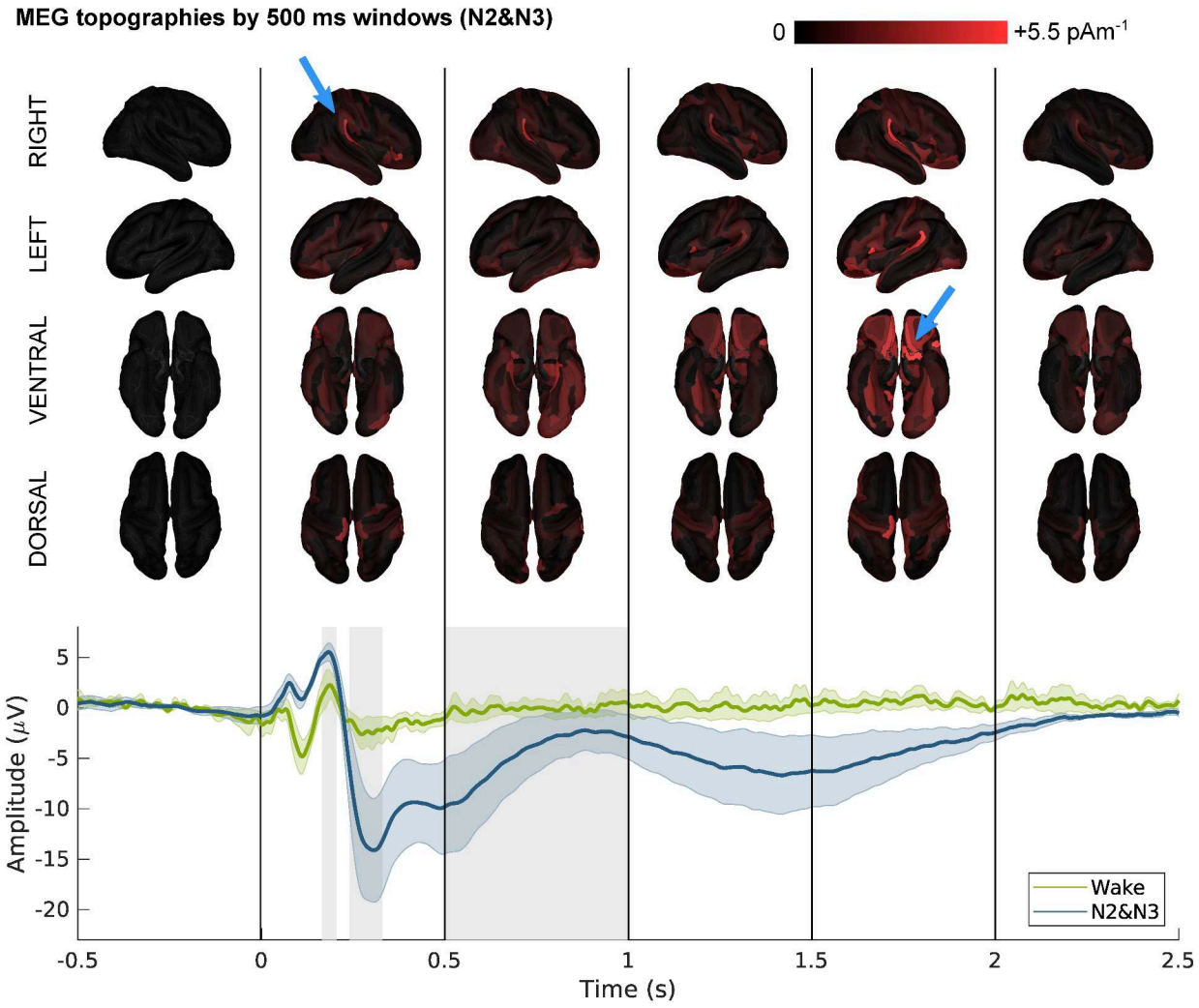

Figure 3.5: Topographies of evoked activity in NREM sleep over time (stages N2 & N3 are combined). Brighter red indicates relatively more activity change relative to pre-stimulus baseline. The EEG time series of evoked responses for Wake and N2&N3 is shown (bottom) for reference. Coloured lines show means across participants; shaded areas indicate standard error. Grey shading indicates the evoked responses components P200, N350 and N550-P900. Blue arrows note where the activation occurs. Grey shading indicates the evoked responses components P200, N350 and N550-P900. MEG : magnetoencephalography;EEG: electroencephalography; NREM: non-rapid eye movement sleep; N2-3: stage 2-3 NREM sleep.

To better characterize the sound-evoked N550-P900 complex, we investigated whether it represents an 'all-or-none' response, as suggested by some previous work in which epochs have been separated according to the presence or absence of an elicited N550-P900 complex (e.g., Bastien & Campbell (1992); Dang-Vu et al. (2011); Laurino et al. (2014)). In closed-loop auditory stimulation applications, up-states are preferentially stimulated as they produce the

greatest enhancement in slow oscillations and evoked spindle power (Ngo et al., 2013b). In the current analysis, however, we focused on periods of time in which sound presentation did *not* coincide with slow oscillations or sleep spindles (in EEG), to observe the evolution of the evoked response in the absence of endogenous sleep-related events (later sections explore the effect of cortical tissue excitability on the EEG evoked response).

We first identified trials that occurred within spindle and SO-free stage N2 & N3 sleep (as identified by automatic detection algorithms). The mean number of trials included per participant was 2284.2 (SD = 650; individual totals: Sub1 = 2762, Sub2 = 1325, Sub3 = 1910, Sub4 = 2850, Sub5 = 2574). In general, each subject's N550-P900 complex amplitude distribution was centred around zero (means (SD) by subject: Sub1: 4.76 μV (43.2), Sub2 = -.04 μV (22.1), Sub3 = 4.54 μV (42.5), Sub4 = 14.89 μV (54.3), Sub5 = 4.26 μV (37.7)). Interestingly, we do not observe a bimodal distribution that might suggest that sound produces a clear evoked slow oscillation in a binary fashion (see Supplementary Figure 2). This analysis does not bear directly on our main research questions concerning the information flow leading to generation of evoked slow oscillations, but rather contributes to an ongoing discussion of the nature of 'successful' sound stimulation, and the optimization of the CLAS technique. We further investigate the relationship between evoked N550-P900 amplitude and spindle-band activity in the next section, using the present analysis to separate trials into those producing relatively higher amplitude N550-P900 complexes (i.e., top 25%) and those which had lower values during the same time window (i.e., bottom 25%).

Sleep spindles evoked by sound in sleep

To evaluate differences in how sound evokes sleep spindles across stages of consciousness, we calculated mean time-frequency plots for Wake and N2 & N3 across all subjects and epochs, and computed their difference, to identify a time and frequency window for further analysis (see Figure 3.6a). Evoked responses were maximally different between Wake and N2 & N3 starting about 0.6 s and ending about 1.2 s after sound onset, and within a 11-14 Hz frequency band, by visual inspection. All subjects showed greater spindle power in N2 and N3 than Wake using simple non-parametric Wilcoxon signed-rank tests (one-tailed) across subject means (Z = 15, p = .031, PSdep = 1.0 in both cases; see Figure 3.6a (right)).

To more robustly evaluate differences in evoked spindle power as a function of the N550-P900 complex's amplitude, we conducted LME analyses at the single trial level, using subjects as a random effect. We removed outliers from each Condition (Top 25%, Bottom 25%) by excluding values based on thresholds defined as 1.5 times the interquartile range (i.e., below Q1 and above Q3). The mean percentage of retained epochs across subjects was 95.8% (SD = 4.0). We compared a model with N550-P900 complex's amplitude Condition

(either Top 25% or Bottom 25%) as a fixed effect to a null intercept-only model and found that the addition of Condition significantly increased model fit ($\chi^2(1) = 67.04$, p ¡ .0001). The intercept estimates the mean spindle power increase post-stimulation generating low amplitude N550-P900 complexes (Bottom 25% condition). There was a significant main effect of Condition, indicating statistically stronger spindle power in the Top 25% of epochs than in the Bottom 25% of epochs (β = 3.83e-01, SE = 4.66e-02, t(5454) = 8.21, p < .0001) (see Figure 3.6b).

The topography of evoked spindle activity differences between Top vs. Bottom 25% of evoked N550-P900 complexes is displayed in Figure 3.6c. Increased activity was observed mainly in medial regions (e.g., Destrieux regions 'G_cingul-Post-dorsal', 'G_and_S_cingul-Mid-Ant', 'G_cingul-Post-dorsal , 'S_subparietal'), and also in lateral occipital regions (e.g., 'G_and_S_occipital_inf'). An increase in thalamic activity is also observed. For visual comparison only, we plotted topographies of spindle-band (11-17 Hz) oscillatory activity during N2 & N3 stages (using FOOOF). In general, we observed considerable overlap between the evoked spindle topography as described above (Figure 3.6c) and activity measured in the spindle band across N2 and N3 sleep stages using the FOOOF algorithm (Figure 3.6d), with the strongest activity observed in medial regions. As noted in Methods, the study design does not allow us to cleanly separate and therefore quantitatively compare evoked vs. endogenous spindle topographies. These analyses take advantage of our MEG approach to inform us about the spatial distribution of the co-occurrence of the strongest evoked SOs and coupled spindles.

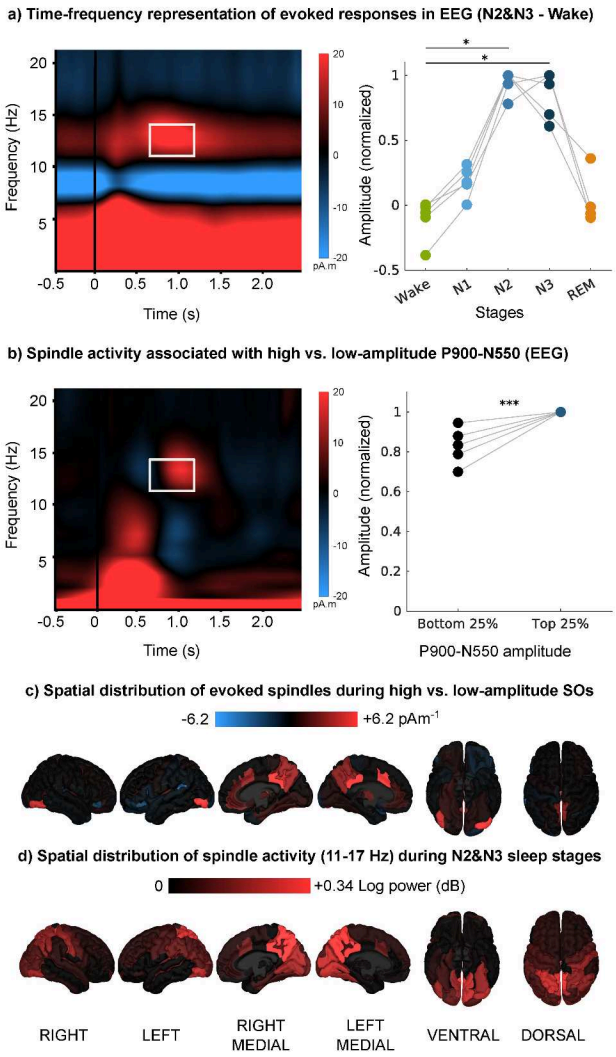

Figure 3.6: Sound-evoked sleep spindles in EEG (Cz). a) The time-frequency plot averaged across all subjects (left) shows increased spindle power in N2 & N3 sleep 0.6 to 1.2 s after sound onset in a frequency band of 11 to 14 Hz (white rectangle). Spindle power in that frequency range as compared with spindle power in the pre-stimulus baseline (-0.6 to 0 ms) is shown at right. Each subject is represented by its mean. Asterisks denote significant differences between Wake and N2 & N3 (* $p < .05$). b) The difference time-frequency plot averaged across all subjects (left) comparing spindle activity when epochs are divided according to the strength of the N550-P900 complexes that they produce (i.e., Top minus Bottom 25%). Stronger spindle power is observed to be coincident with stronger N550-P900 complexes in the EEG time-frequency plot, suggesting that spindle activity is positively related to evoked N550-P900 complex amplitude. Extracted values (white rectangle shown on left) of spindle power in the Top 25% are higher across subjects (right).Each subject is represented by its mean. Asterisks indicate a significant difference between the Top vs. Bottom 25% (*** $p < .001$). c) The topography of spindle power differences (in MEG) according to evoked N550-P900 complex strength (Top vs. Bottom 25% of N550-P900 complexes averaged across subjects) shows increased activity in thalamus and frontal midline structures coincident with stronger N550-P900 complexes. d) The topography of spindle power in the 11-17 Hz range across all N2 & N3 sleep epochs, for comparison; note that due to the study design, both spontaneous and evoked sleep spindles are represented. EEG: electroencephalography; N2-3: stage 2-3 non-rapid eye movement sleep 2 and 3, SO: slow oscillations.

Temporal evolution of auditory evoked responses in MEG source space

To address the main research questions evaluating evidence for slow oscillations generation models, we first explore the time course of neural events in specific brain regions to compare activity within cortical regions between sleep and wake states. We extracted time series from cortical regions thought to be involved in the generation of cortical auditory evoked responses (AC and OFC) as well as other sensory regions used as controls (S1/M1 and V1). We averaged the extracted signals across trials and hemispheres according to sleep stage and measured the amplitude of activity during specific time windows (P200 and the N550-P900 complex), for each subject (see Figure 3.7). We observed peaks of activity in the AC and OFC at about 100 and 200 ms after sound onset (P100, P200), with OFC peaking slightly later than AC, and troughs in OFC and AC occurring around 350-550 ms post-onset (N350, N550). There is some evidence of brain activity in V1, M1 and S1 within 300 ms of sound onset, but peaks appeared delayed or indistinct with respect to AC and the EEG timeseries (in Figure 3.3).

We then conducted LME analyses on P200 amplitude, using subjects as a random effect to compare amplitude between Wake and N2&N3. We removed outliers from each ROI by excluding values based on thresholds defined as 1.5 times the interquartile range (i.e., below Q1 and above Q3). The mean percentage of retained epochs across subjects was 90.4% (SD = 5.90). Using a null-intercept linear mixed effect model we found that only AC ($\beta = 10.14$, SE = 0.48, z(5.63) = 21.14, $p < .0001$) and the OFC ($\beta = 2.81$, SE = 0.48, z(5.6707) = 5.84, p = .001) across Condition (Sleep and Wake merged) are statistically greater than zero, as suggested by Figure 3.7. This analysis shows that auditory information is present at P200 across sleep and wake states only in the OFC and AC regions of interest, and motivates focusing on them to assess the impact of sleep state (Condition).

Using a new linear mixed effects model with ROI as fixed effect and Subject as random effect (Amplitude $\sim$ 1+ ROI +(1—Subject)), we found a main effect of ROI, meaning that both AC and OFC are significantly different across the sleep and wake Conditions (F(1,76138) = 832.77, $p < .0001$). Adding the interaction between Condition and ROI improved model fit (Amplitude $\sim$ 1+ ROI + Condition + ROI * Condition + (1—Subject)) as compared with fixed effects of ROI and Condition only ($\chi^2(1) = 29.87$, $p < .0001$). We do not find a main effect of Condition (Wake, Sleep on P200 amplitude across ROIs (F(1, 72083) = 0.18, p = 0.67) but there is a main effect of ROI (F(1, 76138) = 832.77, $p < .0001$) as in the ROI-only model, with AC estimated mean amplitude (M = 10.17, SE = 1.08) being higher than OFC estimated mean amplitude (M = 2.78, SE = 1.08). There is a main effect of interaction between ROI and Condition (F(1, 76134) = 29.46, $p < .0001$), meaning that the ROIs do not behave similarly across wake and sleep states. Post-hoc analysis using estimated means

showed that AC amplitude in Sleep is lower than in Wake (Sleep-Wake difference, M = -1.80, SE = 0.44, p = .0003) and that OFC amplitude is higher in Sleep than Wake (Sleep-Wake difference, M = 1.52, SE = 0.46, p = .0052).

This pattern of results shows that auditory information is present in the AC and OFC in both wake and sleep states. However, these regions are differently impacted by sleep state, with AC showing smaller P200 responses and OFC showing larger P200 responses in NREM sleep as compared with wake. This result is most consistent with Models 3 and 4, in which auditory information coming from the non-lemniscal pathway is leading to changes in excitability of tissues within the OFC. At this stage we cannot rule out Models 1 and 2, because feed-forward information via the lemniscal pathway could subsequently reach OFC from AC, albeit with a neural conduction delay. However, diminished P200 amplitude in the AC during sleep suggests a lower likelihood of the lemniscal pathway through AC playing the key role in SO generation in OFC in sleep.

In an exploratory basis, we also tested Hemisphere (Left and Right) as a fixed effect, as compared with the null model ($\chi^2(1) = 71.49$, $p < .0001$). The results suggest that on average across Condition and ROI, P200 amplitude is greater in the left hemisphere than in the right hemisphere (Left-Right difference, M = 2.17, SE = 0.26, $p < .0001$).

Next, we conducted LME analyses to investigate the elicited N550-P900 complex amplitude, testing our hypothesis that change in amplitude would be greater in Sleep than in Wake (as seen in the time series average, see Supplementary Figure 1). We removed outliers from each ROI using the same process as defined in the P200 analysis. The mean percentage of retained epochs across subjects was 89.4% (SD = 6.18). First, using a null-intercept linear mixed effect model we found that only the OFC across Condition (Sleep and Wake merged) is statistically greater than 0 ($\beta = 1.15$, SE = 0.26, z(8.1545) = 4.5, p = .002). Focusing on the OFC only (Amplitude $\sim$ 1 + Condition +(1—Subject)), we found a main effect of Condition ($F(1, 3946.3) = 20.7$, $p < .0001$). Post-hoc analysis using estimated means showed that OFC N550-P900 complex amplitude in Sleep is higher than in Wake (Sleep-Wake difference, M = 2.17, SE = 0.48, $p < .0001$).

The absence of a significant N550-P900 complex in the AC argues against Models 1 and 3, which both posit AC generating a local SO. The absence of N550-P900 complex in V1, M1 and S1 further argues against Model 3, which posts the generation of widespread, simultaneous SOs. The biggest change in late components occurs in the OFC, in-line with models that propose that the SO generator is primarily in orbitofrontal regions, consistent with Models 2 and 4.

On an exploratory basis, we also tested Hemisphere (Left and Right) as a fixed effect, as compared with the null model ($\chi^2(1) = 9.66$, p = .002). The results suggest that on average

across Condition, elicited N550-P900 complex amplitude is greater in the left OFC than in the right OFC (Left-Right difference, M = 1.19, SE = 0.38, p = .002).

Together, the data also suggest that regional contributions to the global cortical ERP differ by brain state (Wake vs. Sleep), with earlier components (as measured via the amplitude of P200) being associated mainly with activity in the auditory cortex and to a lesser extent other regions including the OFC, and later EEG components (as measured via the amplitude of the N550-P900 complex) generated primarily in the OFC. For subsequent analyses of evoked oscillations and functional connectivity, we focused on the OFC and AC regions, as they seem most affected by brain state and are most relevant to evaluating evidence for and against the remaining SO generation models (i.e., 2 and 4; Figure 3.1).

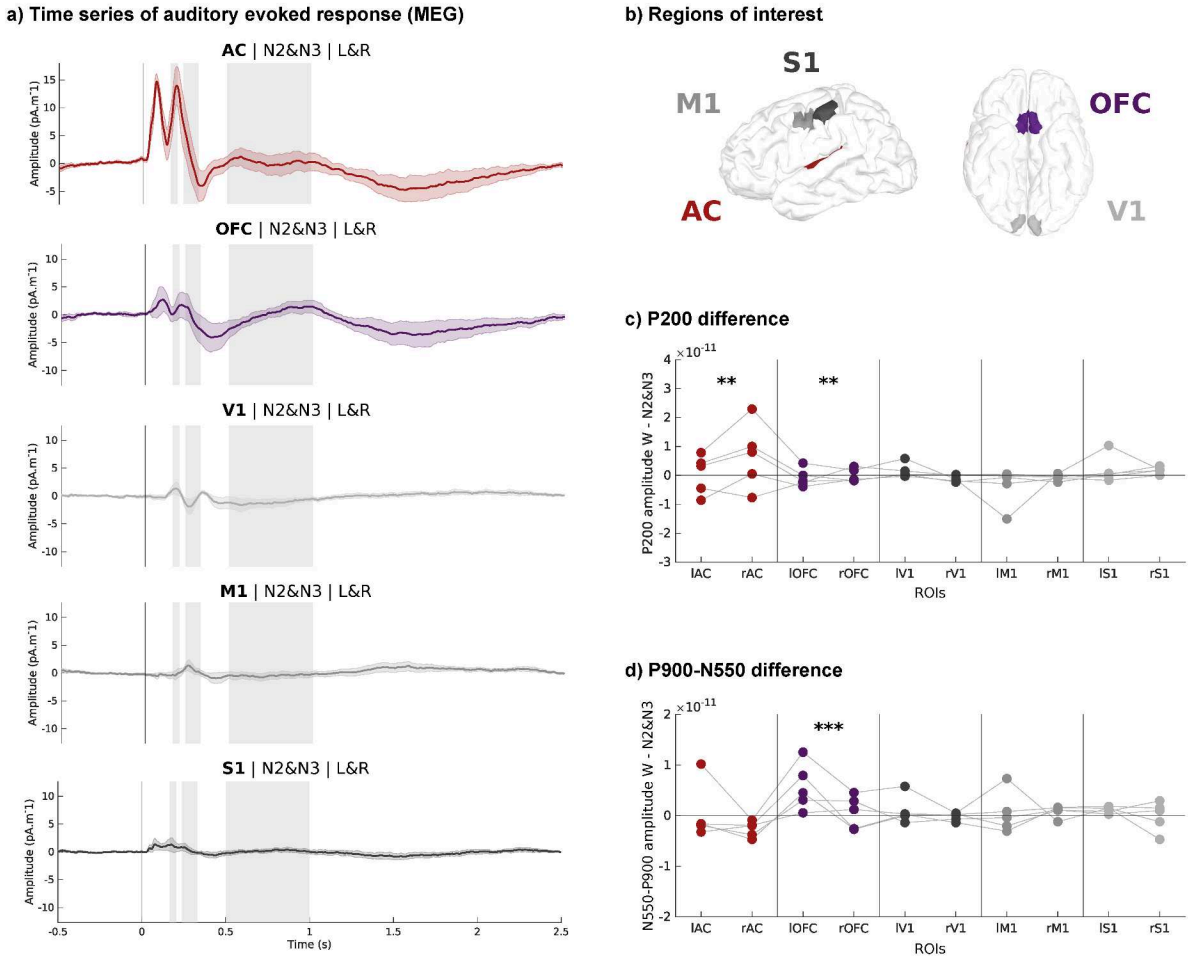

Figure 3.7: Evoked responses in N2 & N3. a) Time series, averaged across subjects and hemispheres, for each region of interest. Coloured lines show means across participants; shaded areas indicate standard error. Grey shading indicates the evoked responses components P200, N350 and N550-P900. b) Schematic view of regions of interest. c) P200 amplitude differences between Wake and N2 & N3 for each region of interest and each hemisphere. Each subject is represented by its mean. Asterisks denote significant differences between Wake and N2 & N3 (** $p < .01$) d) N550-P900 complex amplitude differences between Wake and N2 & N3 for each region of interest and each hemisphere. Each subject is represented by its mean. Asterisks denote significant differences between Wake and N2 & N3 (*** $p < .001$). MEG: magnetoencephalography; N2-N3: non-rapid eye movement sleep stages 2 and 3; L&R: Left and Right brain hemisphere homologues

Functional connectivity between auditory and orbitofrontal cortex following sound stimulation in sleep

The results of the connectivity analysis are represented schematically in Figure 3.8. LME analyses were conducted to investigate functional connectivity between AC and OFC in successive non-overlapping frequency bands (0.1-1.5 Hz, 2-4 Hz, 5-7 Hz, 8-10 Hz, 11-17 Hz, 18-29 Hz, 30-58 Hz). Functional connectivity was computed separately in each hemisphere. The mean percentage of retained epochs after outlier removal across subjects was similar in both hemispheres (Left, M = 98.7% SD = 0.9 and Right, M = 98.8%, SD = 0.6).

In both the right and left hemisphere, directed phase-transfer entropy values were significantly lower than 0 in the 0.1-1.5 Hz frequency band, indicating connectivity from OFC to AC (Left: β = -2.22e-02, SE = 6.89e-04, t(5.99) = -32.24, p < .0001; Right: β = -2.46e-02, SE = 9.54e-04, t(5.53) = -25.77, p < .0001). In the higher frequency ranges, the pattern is reversed, with modest but statistically significant directional connectivity from AC to OFC (between 5 Hz and 29 Hz on the left and similarly for the right side except that the 11-17 Hz bin was non-significant; see Figure 3.8 for trends and Supplementary Table 1 and 2 for numerical values).

Together these results provide evidence for an OFC to AC directed connectivity in the slow oscillation frequency band. This indicates that the N550-P900 component is generated in the OFC before propagating to other cortical areas, including the AC. These functional connectivity measurements in the low frequecies therefore are consistent with Models 2 and 4. However, we cannot rule out Model 2 at this stage, due to the possibility that information carried from AC to OFC in higher frequency bands stimulates a slow oscillation in OFC upon its arrival (which would be mediated by the lemniscal pathway). After exploring the relationship between the single-channel EEG timeseries and regional extracted time series from MEG in the next section, we will present a final analysis that is informative to distinguish Models 2 and 4.

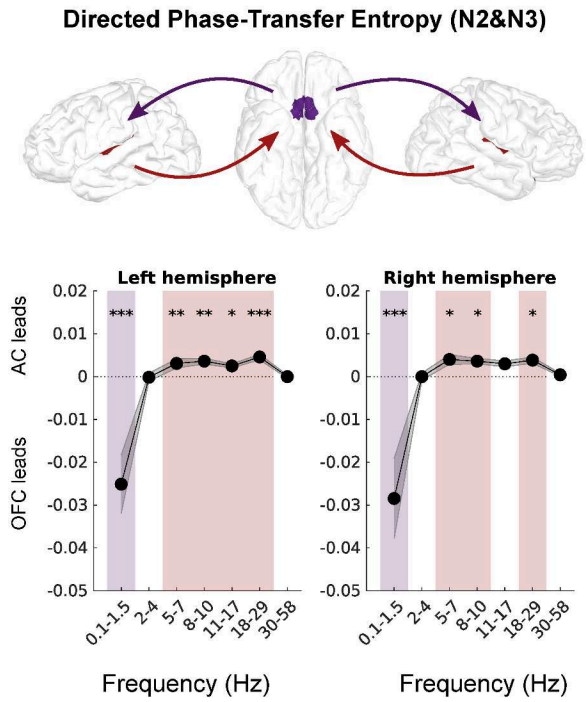

Figure 3.8: Functional connectivity (directed phase-transfer entropy) between auditory (red) and orbitofrontal (purple) cortices. Frequency bands that have significant directed connectivity are shaded in the colour of the leading region of interest. Asterisks denote significance (* $p < .05$,** $p < .01$,*** $p < .001$). N2-3: non-rapid eye movement sleep stage 2 and 3; AC: auditory cortex; OFC: orbitofrontal cortex

3.4.3 Effect of regionally-specific cortical states on responses

Investigation of region of interest contributions to EEG up-states

Closed-loop auditory stimulation usually targets EEG up-states (i.e., peaks in the slow frequency range of about 0.1-2.0 Hz) using single-channel scalp EEG, on the assumption that SO up-states in EEG are indicative of global peaks in cortical tissue excitability. In the following analyses we take advantage of MEG's spatial and temporal resolution to explore the specificity of up-state slow wave activity as measured in single-channel scalp EEG. These analyses are intended to provide researchers using EEG for CLAS with additional information concerning the neural originals of the scalp-recorded signal, and may aid efforts to optimize stimulation effectiveness (e.g., (Navarrete et al., 2020)).

To compare the EEG recordings to the signals extracted from the AC and OFC ROIs, we first detected slow oscillation up-states in the EEG signal and defined 4-second windows ($+/-2$ s) around each detected peak. We then computed (zero phase lag) correlations between the EEG and each of the four source-space MEG time series (rAC, lAC, rOFC and

lOFC). The average time series for EEG and the ROIs are presented in Figure 3.9(top). Consistent with the assumption of most CLAS studies, when the EEG is in an up-state, AC and OFC also generally seem to be in an up-state.

We conducted LME analyses using subjects as a random effect to identify which ROI's activity correlates most with scalp EEG recorded at Cz, a commonly used electrode placement in SO-CLAS paradigms. Due to the intrinsic property of correlation values to be bounded between -1 and 1, no outlier removal process was implemented. Using a null-intercept linear mixed effect model with ROI as fixed effect and Subject as random effect, we found that correlations of both AC (β = 0.11, SE = 0.02, t(5.02) = 4.87, p = .005) and OFC (β = 0.08, SE = 0.02, t(5.02)= 3.35, p = .02) activity with EEG activity were significantly greater than 0 across subjects. Using a new linear mixed-effect model to compare ROI (Correlation $\sim$ 1 + ROI + (1 — Subject), we found a main effect of ROI. The EEG-OFC correlation was significantly lower than EEG-AC correlation (β = -3.49e-02, SE = 2.68e-03, t(6.590e+04) = -13.03, p < .0001). The strong representation of AC in this EEG montage is consistent with the scalp distribution of brain activity generated in auditory cortex (Stropahl et al., 2018); frontal activity may be less well represented due to distance from sensors or tissue orientation (Ahlfors et al., 2010).

We also further explored the lateralization effect noted in the previous analyses. Adding Hemisphere as a second fixed effect increased model fit ($\chi^2(1)$ = 483.62, p < .0001), with overall EEG activity being more correlated with ROI activity in the left hemisphere (F(1, 65899) = 485.40, p < .0001). This result is coherent with the previously observed dominance of the left hemisphere in other analysis.

Investigation of phase relationships between regions of interest and EEG up-state

To further explore the relationship between single-channel EEG and regional brain activity, we calculated the instantaneous phase of the extracted ROI signals at the time EEG up-states were detected. Because phase angles are bounded between $-\pi$ and π rad, no outlier removal process was implemented. As shown in Figure 3.9 (bottom), phase distribution from the four key regions of interest were far more dispersed than in the EEG, and only a small percentage of trials were aligned with a simultaneous EEG up-state (phase difference between EEG and ROI $+/-\frac{\pi}{6}rad$; lAC M = 11.5 % SD = 0.9; rAC M = 12.7 %, SD = 1.6; lOFC M = 13.7 %, SD = 4.6; rOFC M = 9.5 %, SD = 1.7). We then computed F-scores to compare the variance of the EEG distribution with that of each ROI. The variance of phase distribution (i.e., dispersion) of each ROI was significantly greater than that of EEG (F(16487) = 0.33, p < .001), lAC phase distribution (F(16487) = 0.33, p < .0001), lOFC phase distribution (F(16487) = 0.26, p < .001) and rOFC phase distribution (F(16487) = 0.31, p < .001). These

results indicate that up-states in EEG only partially coincide with local up-states in key cortical regions.

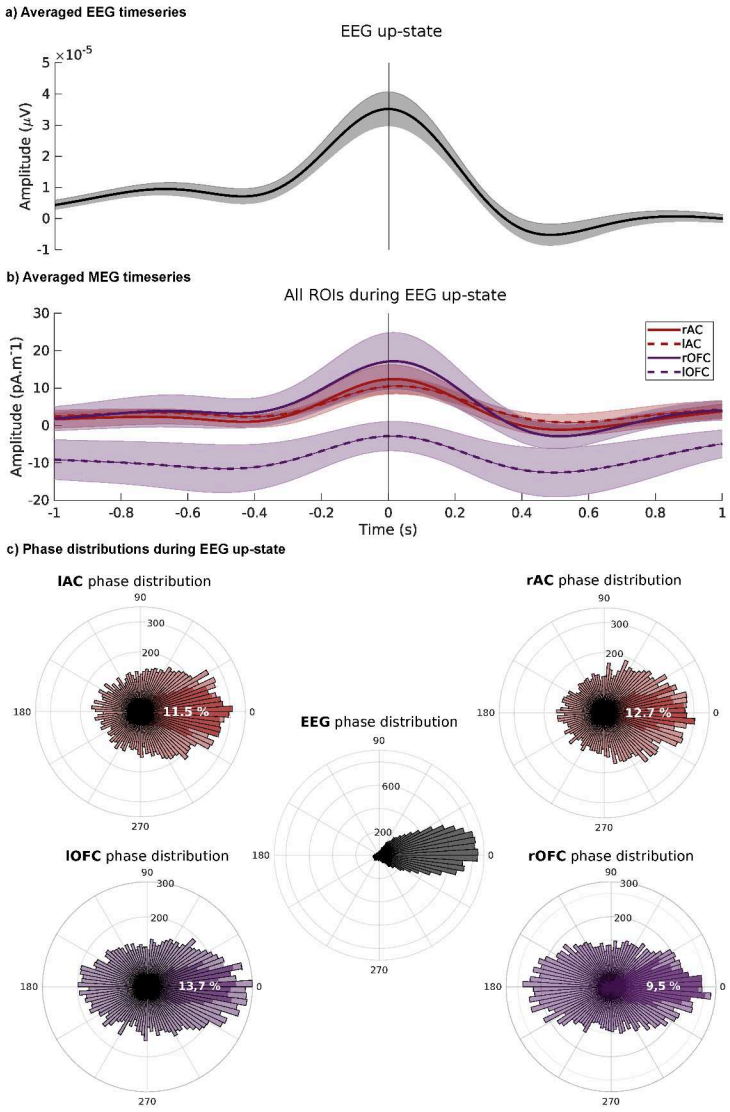

Figure 3.9: Comparison of EEG (Cz) and MEG activity from auditory (lAC, rAC) and orbitofrontal (lOFC, rOFC) regions of interest. a) EEG averages across subjects, aligned by up-state as detected in EEG. b) MEG ROI averages across subjects, aligned by up-state as detected in EEG. Coloured lines show means across participants; shaded areas indicate standard error. c) Polar histograms indicating phase distribution of EEG and ROIs during up-state as detected in EEG. The percentage of trials with aligned phase between each ROI and EEG is indicated schematically in darker shading, and numerically in superimposed white text ($+/-\frac{\pi}{6}rad$). Shaded bars indicate SEM in a) and b). EEG: electroencephalography; MEG: magnetoencephalography; AC: auditory cortex; OFC: orbitofrontal cortex; r and l refers to the right and left hemispheres.

Comparison of EEG evoked responses as a function of regional tissue state

Returning to the main research questions concerning models of information flow leading to evoked slow oscillations, we now investigate the effect of tissue excitability on amplitude of the evoked response, a measure of stimulation success. Two pieces of information from previous analyses make this analysis relevant: first, evoked N550-P900 amplitude is normally distributed (see Supplementary Figure 2), indicating that auditory stimulation varies on a trial-to-trial basis in its effectiveness; this observation suggests room for optimization. Second, because up-states in EEG only partially coincide with local up-states in key cortical regions (Figure 3.9), it is possible that stimulation effectiveness could depend on the phase of tissue in specific regions.

To identify the impact of regionally-specific cortical tissue excitability level on the evoked brain response, we take advantage of the open-loop nature of the study design, which allows us to observe the effects of stimulations occurring over the full cycle of tissue excitability. We detected up-states and down-states of slow activity (0.1 - 2.0 Hz) in each key region of interest. We then computed the amplitude of the elicited N550-P900 complex and spindle activity across condition (Up-state vs. Down-state). We focused on evoked responses as measured in EEG for comparability with previous literature. Concerning the elicited N550-P900 complex amplitude, we conducted LME analyses to investigate the impact of up and down-states of both the OFC and the AC.

Including Condition (Up-state vs. Down-state) as a fixed effect in a linear mixed-effect model increased model fit (Amplitude $\sim$ 1 + Condition +(1—Subject)) as compared to a null intercept-only model ($\chi^2(1) = 4.08$, p = .043), indicating across ROIs, stimulation occurring during an up-state elicited a larger-amplitude N550-P900 complex as observed in EEG, compared to down-states. Adding the interaction of ROI and Condition (Amplitude $\sim$ 1 + Condition*ROI +(1—Subject)) resulted in a better-fitting model ($\chi^2(2) = 15.34$, p = .0005). Post-hoc analysis using estimated means showed that tissue state in the OFC was critical to the generation of N550-P900 complex (OFC: Up vs. Down-state difference, M = 8.43, SE = 2.01, p = .0002), whereas tissues state in the AC did not significantly affect N550-P900 complex amplitude as measured in EEG (AC: Up vs. Down-state difference, M = -2.56, SE = 1.96, p = 0.56).

These results provide additional evidence for a critical role of the OFC in SO generation. Auditory cortex excitability state instead does not seem to matter, further implicating the non-lemniscal auditory pathway in the CLAS effect and decreasing the likelihood of Model 2, in which the auditory information passes first to the AC via the lemniscal pathway. Together, these results are best explained by Model 4.

On an exploratory basis, we also tested Hemisphere (Left and Right) as a fixed effect,

as compared with the previous model ($\chi^2(1) = 0.03$, p = 0.86). The comparison suggests that Hemisphere does not account for more variance in the data, meaning that differences in tissue state across left and right OFC does not clearly impact the N550-P900 complex as observed in EEG.

Recalling the importance of elicited sleep spindles in the memory consolidation effects of CLAS (Ngo et al., 2013b; Harrington & Cairney, 2021; Fernandez & Lüthi, 2020), and that stronger N550-P900 complexes are related to greater evoked spindle activity (Figure 3.6b), we investigated the effect of cortical state in ROIs on spindle activity. For each epoch, root mean squared values of the EEG sigma filtered in the previously defined frequency band of interest (11-14 Hz) was computed in the time windows of interest (0.6 to 1.2 s post-stimulation), as well as before stimulation to serve as baseline (-0.6 to 0 s). Note that these analyses do not assist us in distinguishing between models of information flow leading to generation of evoked slow oscillations, but as spindles are integral to memory consolidation processes, they are nonetheless helpful to better understand the CLAS effect.

We first investigated the conditions affecting the production of spindle power via auditory stimulation, using zero-intercept models (Spindle Power Change $\sim$ 0 + ROI + (1 — Subject) and Spindle Power Change $\sim$ 0 + Condition + (1 — Subject)). In each ROI, across Condition (Up and Down-state merged), auditory stimulation statistically increased spindle power as compared to a pre-stimulation baseline (AC, $\beta = 0.51$, SE = 0.19, t(5.3522) = 2.74, p = .04 and OFC, $\beta = 0.55$, SE = 0.19, t(5.42) = 2.82, p = .04). Collapsing instead across ROIs, auditory stimulation statistically increased spindle power in Up-states ($\beta = 0.58$, SE = 0.18, t(5.31) = 3.16, p = .02), but not Down-states ($\beta = 0.44$, SE = 0.19, t(5.51) = 2.35, p = .06).

To compare between ROIs, we used a LME with Subjects as random effect (Spindle Power Change $\sim$ 1 + Condition + (1 — Subject)). We find a main effect of Condition (tissue excitability as measured with ROI Up and Down-state, (F(5716) = 4.14, p = .04)) with Up-state stimulation eliciting greater spindle power, as measured in EEG, than Down-state stimulation. Adding the interaction between ROI and Condition (Amplitude $\sim$ 1 + Condition*ROI +(1—Subject)) did not improve model fit ($\chi^2(2) = 2.18$, p = 0.34). These results show that while being in an up-states in either regions of interest when sound arrives is associated with greater evoked spindle activity, we do not observe regional dependencies.

For completeness, we also tested Hemisphere (Left and Right) as a fixed effect (Spindle Power Change $\sim$ 1 + Condition + Hemisphere + (1 — Subject)), as compared with the Condition-only model ($\chi^2(1) = 1.69$, p = 0.19). The comparison suggests that Hemisphere does not account for additional variance in the data, meaning that differences in tissue state across left and right OFC do not clearly impact spindle generation.

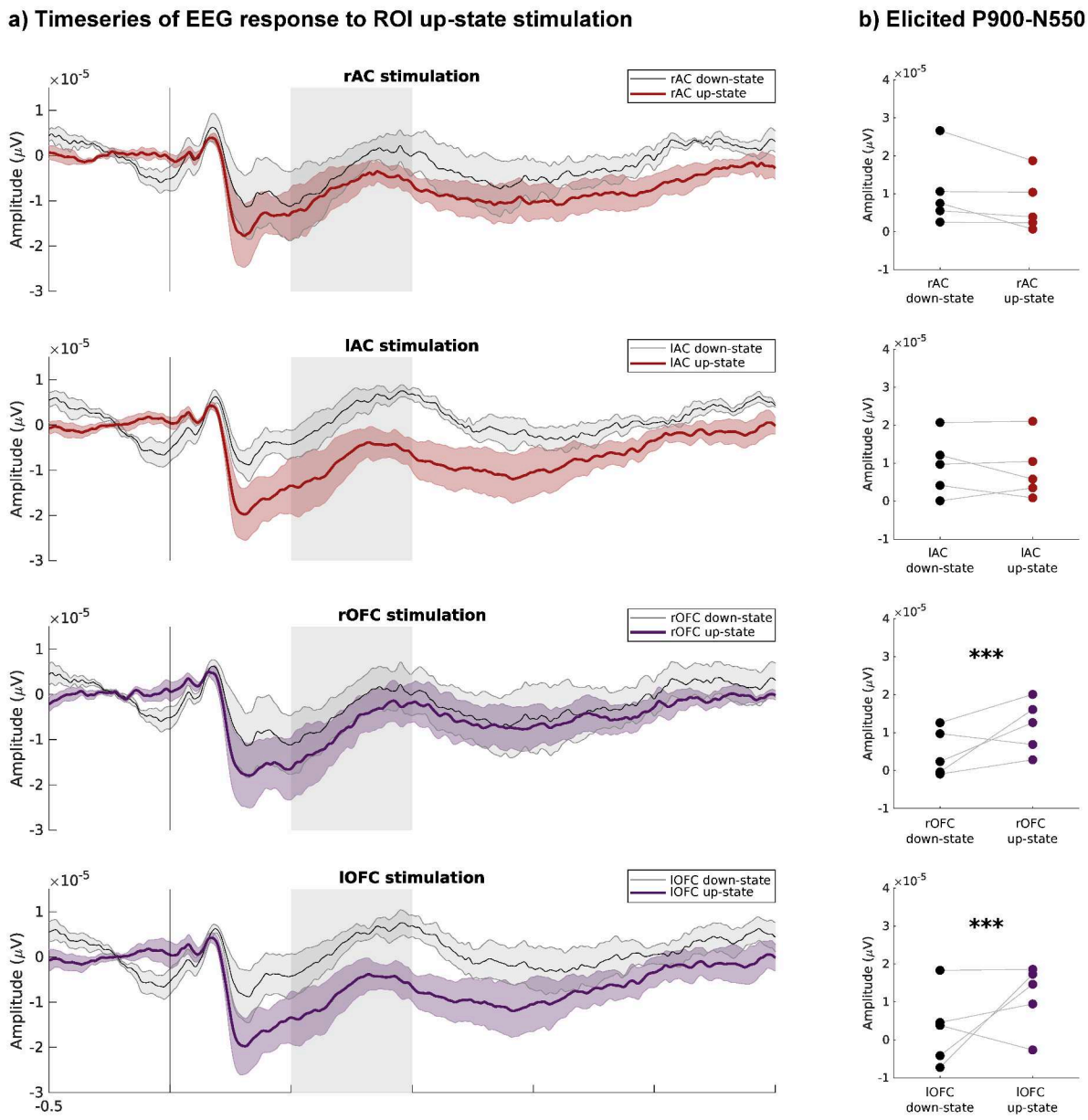

Figure 3.10: Evoked responses in EEG divided according to the excitability state of local tissue in auditory (rAC, lAC), and orbitofrontal (rOFC and lOFC) regions of interest, as measured in MEG. a) Comparison of the EEG time series for up-state and down-state stimulations, which have been defined by the state of excitability in MEG extracted timeseries from auditory and orbitofrontal ROIs. Coloured lines show means across participants; shaded areas indicate standard error. Grey shading indicates the evoked responses components P200, N350 and N550-P900. b) Mean N550-P900 complex amplitude for each ROI in each condition. Each subject is represented by its mean. Asterisks denote significant differences between up-state and down-state stimulation using LME statistical models (*** $p < .001$). MEG: magnetoencephalography; AC: auditory cortex; OFC: orbitofrontal cortex; r and l refers to the right and left hemispheres.

3.5 Discussion

Evaluating evidence for SO generation models

Understanding the neurophysiology of closed-loop auditory stimulation requires identification of the origin of auditory evoked brain responses during sleep. The main goal of this work was to define potential mechanistic models based on previous literature (Figure 3.1) and to evaluate their ability to explain spatially-resolved evoked brain responses in the sleeping brain, including slow oscillations and sleep spindles, and by association, the beneficial effects on memory consolidation that have been reported in literature (Harrington & Cairney, 2021; Choi et al., 2020; Nasr et al., 2022), as well as other sleep-related physiological functions (Besedovsky et al., 2017; Kelley et al., 2022).

According to the first potential model we described (Figure 3.1), slow oscillations would be generated locally within the auditory cortex upon the arrival of sound information through lemniscal auditory pathways at primary auditory cortex in the superior temporal gyrus. If this were the case, we would expect SOs to occur first in this region before propagating to subsequent cortical regions. Although we do observe clear evoked auditory responses in sleep that are similar to those in the Wake state up to and including 200 ms (P200), the evoked slow oscillations appear strongest in the orbitofrontal region (Figure 3.5, 3.7). Additional evidence against this model comes from the functional connectivity analysis (see Figure 3.8), which shows that in the slow oscillation frequency range (0.5-1.5 Hz), information flows in the reverse direction; from OFC to AC (replicated in both left and right hemispheres). These findings align with previous reports that the primary generator of (endogenous) SOs is found in ventral frontal areas (Morgan et al., 2021).

In the second of the proposed models (Model 2 in Figure 3.1), sound information would arrive at the auditory cortex via primary auditory pathways and would then be passed forward to frontal regions, which would generate slow oscillations. This model relies on the progression of auditory information from auditory cortex to ventral frontal regions. Although we did observe connectivity from AC to OFC in higher frequencies (i.e., $>$ 5Hz), it was of very low strength. The majority of the energy in auditory evoked responses is captured in the $<$ 5 Hz frequency range (confirmed by applying filters with different band pass limits). Although it cannot entirely be ruled out on the basis of the present analysis, it seems unlikely that the modest AC to OFC connectivity we observed in high frequency ranges is the trigger for SO generation in OFC. Additionally, the finding that early auditory evoked components in AC and OFC are differentially impacted by sleep state, with amplitude in AC decreasing and OFC increasing, suggests that auditory information travelling through lemniscal pathways

to AC may not be the most critical to activate SOs within OFC. Moreover, the observation that SOs are more likely to be generated when tissue in OFC is in an up-state at the time of stimulation as compared with AC, suggests that the non-lemniscal auditory pathway is most relevant for the CLAS effect.

Models 3 and 4 consider the involvement of the non-lemniscal pathway as a potential mechanism for auditory evoked responses as suggested by Bellesi et al. (2014). They hypothesized that CLAS is likely mediated by the activation of the non-lemniscal ascending auditory pathway, which projects broadly to association areas including frontal regions and secondary auditory areas (Bellesi et al., 2014; Kjaerby et al., 2022). They proposed that the modulation of noradrenaline levels by the locus coeruleus is critical for the generation of N550-P900 complexes, and that low noradrenaline levels might be a necessary factor for the emergence of an evoked N550-P900 complex, whereas elevated levels of noradrenaline would result in arousal.

In Model 3, a signal generated in the arousal network via interactions with the non-lemniscal auditory system in the brainstem and thalamus would cause changes to neural activity in widespread areas, and generate slow oscillations throughout the cortex. Although this domain-generality is plausible from work showing that visual, tactile, and auditory stimulation can all generate slow oscillations (Riedner et al., 2011), we do not find that slow oscillations are generated via auditory stimulation in any of the other selected cortical regions (V1, M1, S1), nor do we observe activity within the whole brain maps during the evoked N550-P900 complex (Figures 3.5 and 3.7). Moreover, the significant functional connectivity in the slow wave frequency band from OFC to AC would not be observed if both the OFC and the AC were generators of slow oscillation receiving simultaneous stimulation from a common source (Figure 3.8).

Finally, in Model 4, the general arousal system is implicated, but it is the ventral frontal regions that generate slow oscillations. This model is supported by the finding that frontal and ventral regions show the strongest SOs (Figures 3.5, 3.4, 3.7), as well as the functional connectivity analysis, which shows that information flows from OFC to AC bilaterally in the slow wave frequency range (Figures 3.8). Furthermore, the result that tissue excitability state in OFC significantly affects the success of stimulation to generate a strong N550-P900 complex but AC does not, further supports Model 4 (Figures 3.10).

Evoking sleep spindles

Although the primary objective of this work is to evaluate evidence in support of the four models of information flow leading to the generation of evoked slow oscillations, we also

investigated the generation of spindles evoked by auditory stimulation, due to their importance in sleep's memory consolidation function and in the CLAS effect (Fernandez & Lüthi, 2020; Ngo et al., 2013b). Previous research focused on the increase in spindle activity when auditory stimulation is time-locked to the up-state of the targeted slow oscillation (Ngo et al., 2013b). However, a study by (Sato et al., 2007) showed that non-arousing stimulation using different sensory modalities (somatosensory, auditory, or visual) during light non-rapid eye movement (stage N2) sleep also induced higher spindle activity in related sensory cortical areas. Spindle generation is often not reported in sleep studies focusing on ERPs (Colrain & Campbell, 2007), as they are not precisely time-locked to stimulation events and disappear when independent trials are averaged (in the time domain). By using time-frequency analyses and analyzing sigma power within specific time windows following stimulation, we replicated the observation that sleep spindles are elicited in N2 and N3 sleep (Ngo et al., 2013b). Furthermore, we showed that spindle amplitude was bigger in trials that successfully generated higher N550-P900 complexes. MEG topographies of these evoked spindles show a pattern of activation in medial and dorsal brain regions including the precuneus, which is similar to the pattern of activity in the spindle frequency range throughout N2 and N3 sleep stages (see Figure 3.6).

Interestingly, even if their presence is linked to the amplitude of the evoked N550-P900 complex (as seen the Figure 3.6b), the elicited spindle activity does not seem to depend on the local activity of the key regions of interest we selected for our analysis; both AC and OFC up-state stimulation induces an increase in spindle activity which is greater than down-state stimulation. We can hypothesize that even if the spindle and the N550-P900 generation mechanisms are intertwined, they are not identical. Other factors, potentially the state of activity in other regions, might modulate the degree of spindle activity generated. This observation opens the possibility that the two mechanisms might be independently manipulated, which could be useful for restoring ideal functional coupling between SOs and sleep spindles, which degrades with age and is linked to memory consolidation (Hahn et al., 2020; Helfrich et al., 2018).

Improving the effectiveness of CLAS

While the effect of CLAS on physiology and memory largely replicates across studies (Wunderlin et al., 2021; Choi et al., 2020; Harrington & Cairney, 2021), there are inter-individual differences in the effectiveness of non-invasive brain stimulation (Ziemann & Siebner, 2015; Guerra et al., 2020), and effectiveness appears to change over the lifespan (Schneider et al., 2020). Attempts have therefore been made to identify the best timing for CLAS with respect to tissue excitability state as detected in a single EEG channel (in younger and older

populations) (Navarrete et al., 2020), and to target local SOs in different brain regions using the spatial information that is available in multichannel EEG data (Ruch et al., 2022). Our investigation of phase in EEG and MEG makes several contributions to this area. Notably, we found that although EEG up-states detected in single channel over frontal areas does on average correlate with up-states in both AC and OFC (Figure 3.9a), only ∼10-15% of slow oscillation up-states detected in EEG correspond to up-states in each of these regions (Figure 3.9b). As the state of the OFC is most critical to successful generation of N550-P900 complexes and their associated spindles (Figure 3.10), which both play important roles in memory consolidation, particularly when they are coupled (Mikutta et al., 2019; Muehlroth et al., 2019; Hahn et al., 2020; Helfrich et al., 2018), it is likely that increased efficiency and reliability of CLAS can be obtained by selectively targeting up-states in ventral frontal regions. This goal could be achieved by detecting patterns in multichannel EEG (e.g., (Ruch et al., 2022)), and/or machine learning-approaches that can detect fine-grained signatures on one or several channels to stimulate the brain with optimal timing (e.g., Valenchon et al. (2022)), and perhaps adapt detection parameters in real time to an individual's idiosyncratic neural signals. These ideas are in alignment with the emerging concepts of 'precision neuroimaging' and 'person specific methods', in which reliable individual differences in brain activation or connectivity are studied to understand (and sometimes make use of) individual differences in brain function and behaviour Michon et al. (2022).

As regards the origins of the auditory evoked responses in sleep, our results suggest the following contributions: the first components (i.e., P100, P200) originate mainly in bilateral auditory cortex (as expected (Stropahl et al., 2018)), perhaps with some contribution from other brain regions including OFC via non-lemniscal pathways. Later components of the observed brain response in the EEG appear to come mainly from the OFC upon its activation through a non-lemniscal pathway (Figure 3.5).

Limitations and next steps

A limitation of our investigation of is that while we have evidence against Models 1 and 3 and there is generally stronger evidence for Model 4 as best explaining information flow leading to the generation of evoked slow oscillations, we cannot entirely rule out Model 2, because we do observe some feed-forward activity from AC to OFC in the higher frequency ranges (i.e., above 5 Hz). Notably, auditory information does not pass through the lemniscal *or* non-leminiscal branches, but rather both on its way to other cortical regions, in both sleep and wakefulness. It seems likely that the small amount of connectivity we observed from AC to OFC may be capturing information flow that is unrelated to SO generation in OFC.

However, invasive methods would be required to confirm this hypothesis. For example, if auditory stimulation continued to generate SOs in OFC when bilateral AC had been ablated or disconnected would provide definitive evidence against Model 2. Another limitation of our study is that due to the nature of its design, we were not able to distinguish between elicited (evoked) and endogenous brain activity. The topographies of endogenous SOs and spindles offered in Figures 3.4b and 3.6d for visual comparison with the evoked activity are therefore approximations that are strongly weighted towards endogenous activity, but nonetheless also capture evoked activity. Comparing periods of evoked oscillations in stimulated sleep and endogenous oscillations in unstimulated sleep in the same individuals would allow for a more rigorous evaluation of the similarities and differences in slow oscillations and spindles generated by sound (which was not an aim of the present work). The current work does not empirically address how generating slow oscillations through sound stimulation causes the memory consolidation processes that have been observed in previous work Ngo et al. (2013b, 2015); Choi et al. (2020); Harrington & Cairney (2021), because we did not have a memory-related experimental manipulation. The apparently common origin of evoked and endogenous slow oscillations in ventral frontal brain regions Riedner et al. (2011); Morgan et al. (2021) suggests that memory consolidation processes are activated through stimulation in the same way as they occur spontaneously (see Brodt et al. (2023); Staresina et al. (2023)). However, direct comparison of spontaneous vs. evoked memory processes is needed to confirm this assumption.

Nonetheless, the study aims to investigate the evoked responses which have been causally implicated in memory processes in previous work (e.g., (Ngo et al., 2013b; Harrington & Cairney, 2021)). The overnight design allowed us to record data in all sleep stages and have large numbers of trials in N2 and N3 sleep, which is difficult to achieve in a nap design. Our LME-based statistical approach allowed us to investigate our research questions within a small sample size, but as we only record data in five participants, we cannot account for the range of human variability in brain responses to sound in sleep (limiting generalizability). It would be interesting to explore individual differences across populations and over the lifespan, in a larger sample. This research direction could help to explain why sensitivity to CLAS differs between individuals (Ziemann & Siebner, 2015; Guerra et al., 2020) and in older adults (Navarrete et al., 2020).

Several of our analyses suggest a leftward lateralization in OFC involvement. We caution against over-interpreting these findings, as hemispheric differences in brain folding and ROI placement can affect the strength of observed signals in MEG source space; however, other studies using EEG have also found that low frequency oscillations in ventral limbic areas are more frequent on the left side (Morgan et al., 2021; Achermann et al., 2001), suggesting that

a more focused analysis of lateralization may be an interesting focus for future work. Finally, we opted to use standard surface-based cortical source localization models. Previous work has demonstrated that brain signals associated with information in the auditory lemniscal pathway can be extracted using MEG source space volume models (Coffey et al., 2016b); however, signals extracted from these models are more difficult to work with and their use with functional connectivity metrics has not been validated. As MEG modelling and connectivity techniques develop, it may be possible to explore the involvement of brainstem regions and more directly test the involvement of the ARAS in brainstem-OFC interactions, to further refine models of SO generation. As we collectively push the limits of methodology, preregistration may facilitate reproducible results and reduce publication bias (Logg & Dorison, 2021).

3.6 Conclusion

In summary, our data suggest a crucial orbitofrontal contribution to the auditory-evoked N550-P900 complex that underlies the effect of closed-loop auditory stimulation on physiology and memory. Previous research mainly detected high states of excitability based on single channel scalp EEG, making the assumption that activity over frontal regions represents a global up-state of high brain tissue excitability. Our results suggest that targeting up-states in ventral frontal regions has potential to improve the effectiveness of CLAS. Clarifying how sound stimulates the brain has important implications for making causal manipulation tools like CLAS more effective in fundamental research, and in potential clinical applications.

3.7 Supplementary material

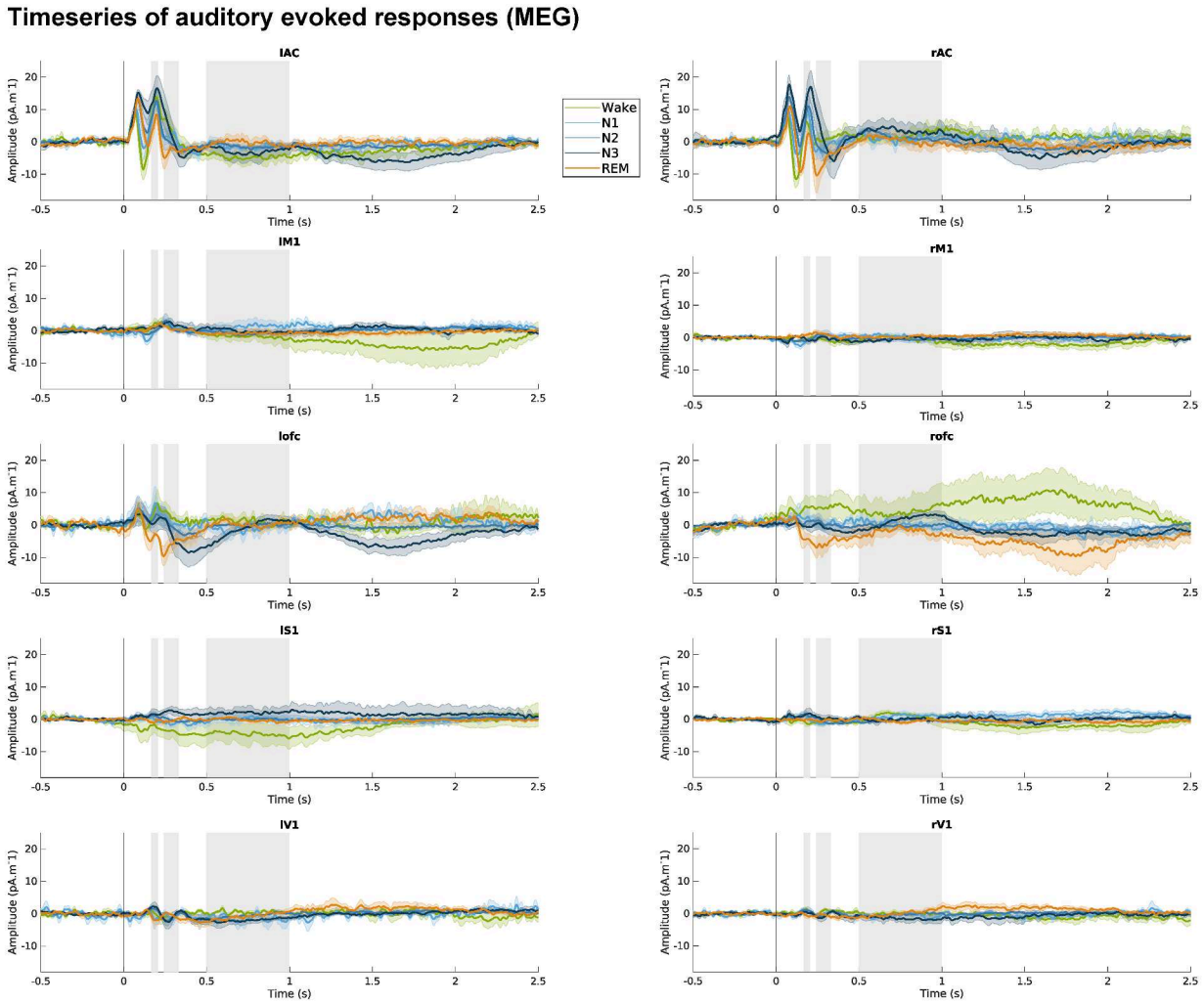

Figure 3.11: Evoked responses across sleep stages. Time series, averaged across subjects, for each region of interest. Coloured lines show means across participants; shaded areas indicate standard error. Grey shading indicates the evoked responses components P200, N350 and N550-P900.

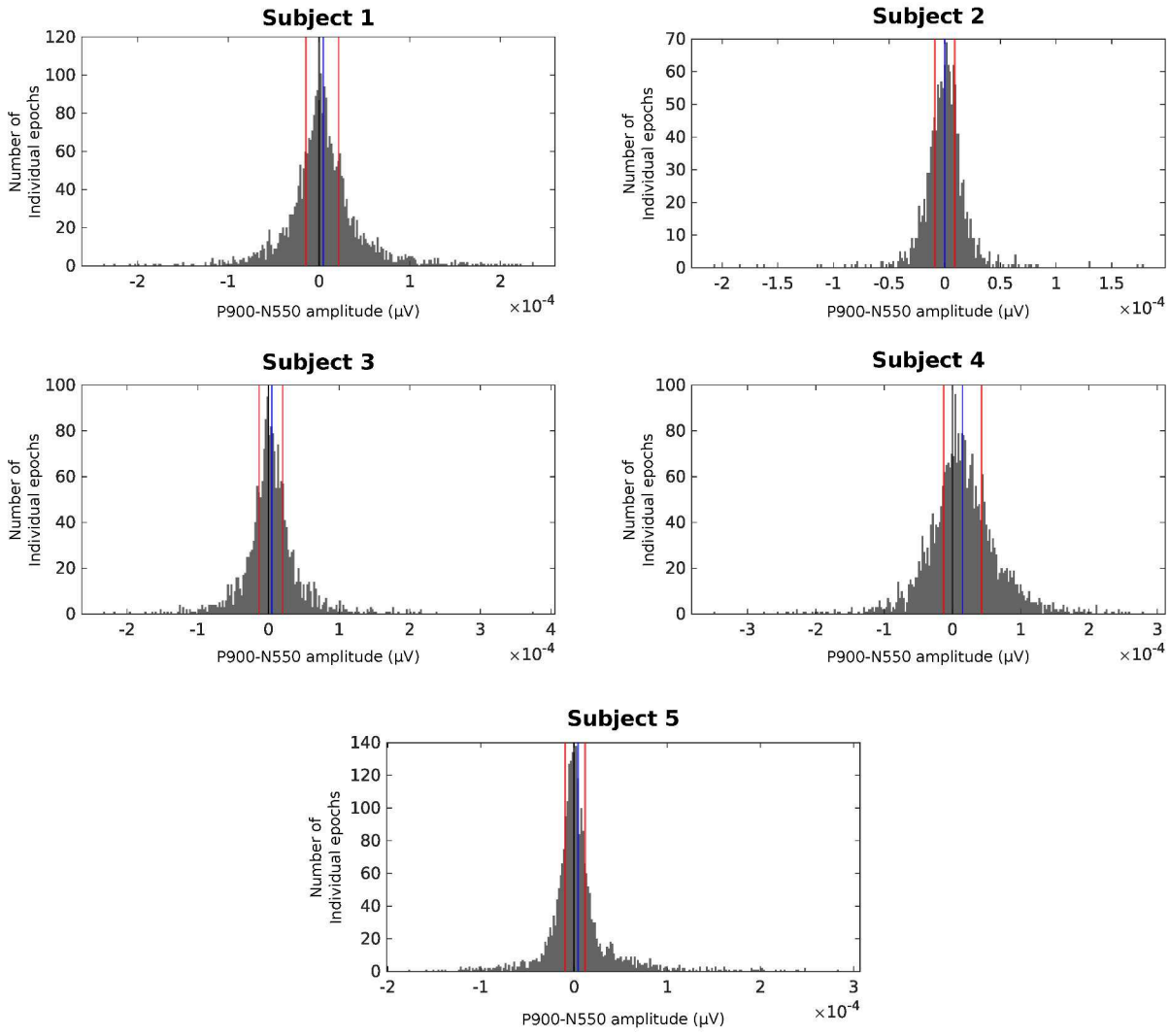

Figure 3.12: Histograms of P900-N550 amplitude for each subjects. Black lines represent 0, blue lines represent the average value for each subject. Red lines represent the Top vs. Bottom 25% for each subject

Fixed effects:	Estimate	Std. Error	df	t value	Pr(>|t|)
FrequencyBand1 (0.1-1.5 Hz)	-2.22e-02	6.89e-04	5.98	-32.236	6.06e-08
FrequencyBand2 (2-4 Hz)	-5.547e-04	6.89e-04	5.96	-0.805	0.45150
FrequencyBand3 (5-7 Hz)	2.83e-03	6.89e-04	5.96	4.106	0.00640
FrequencyBand4 (8-10 Hz)	3.28e-03	6.89e-04	5.96	4.759	0.00318
FrequencyBand5 (11-17 Hz)	2.21e-03	6.89e-04	5.96	3.214	0.01843
FrequencyBand6 (18-29 Hz)	4.15e-03	6.89e-04	5.96	6.033	0.00096
FrequencyBand7 (30-58 Hz)	-3.31e-04	6.89e-04	5.96	-0.481	0.64784

Figure 3.13: Fixed effects of the connectivity analysis for the left hemisphere.Negative estimate values indicate OFC leading and positive estimate values indicate AC leading. Degrees of freedom (df) are approximate and estimated using Satterthwaite's method.

Fixed effects:	Estimate	Std. Error	df	t value	Pr(>|t|)
FrequencyBand1 (0.1-1.5 Hz)	-2.46e-02	9.54e-04	5.53	-25.78	5.62e-07
FrequencyBand2 (2-4 Hz)	-3.45e-04	9.54e-04	5.51	-0.36	0.7307
FrequencyBand3 (5-7 Hz)	3.50e-03	9.54e-04	5.51	3.68	0.0121
FrequencyBand4 (8-10 Hz)	3.11e-03	9.54e-04	5.51	3.26	0.0195
FrequencyBand5 (11-17 Hz)	2.45e-03	9.54e-04	5.51	2.57	0.0456
FrequencyBand6 (18-29 Hz)	3.31e-03	9.54e-04	5.51	3.48	0.0151
FrequencyBand7 (30-58 Hz)	-5.02e-05	9.54e-04	5.51	-0.05	0.9599

Figure 3.14: Fixed effects of the connectivity analysis for the right hemisphere. Negative estimate values indicate OFC leading and positive estimate values indicate AC leading. Degrees of freedom (df) are approximate and estimated using Satterthwaite's method.

3.8 Acknowledgements

The authors would like to thank Sylvain Baillet and Mark Lalancette for assistance with MEG technical matters, Robert Zatorre for assistance with funding acquisition and consultation concerning results, Alexander Albury, Charlotte Emma Moore, Keelin Greenlaw and Marie-Anick Savard for help with statistical modelling, Marie-Anick Savard and Anita Paas for helpful comments on the manuscript, Alix Noly-Gandon for helping with several data recordings and confirming the sleep scoring, and lab members for general support. This work was financially supported by a Natural Sciences and Engineering Research Council of Canada (NSERC) Discovery grant, a grant from the Fonds de recherche du Québec – Nature et technologies (FRQNT), the 'Healthy Brains for Healthy Lives' Canada First Research Excellence Fund (CFREF) at McGill University, and a Concordia (New Scholar) Research Chair in 'Sleep and Sound' to EBJC. HRJ was supported by a Graduate Scholar Stipend from the Centre for Research on Brain, Language and Music.

Chapter 4

Auditory processing up to cortex is maintained during sleep spindles

4.1 Abstract

Sleep spindles are transient 11-16 Hz brain oscillations generated by thalamocortical circuits. Their role in memory consolidation is well-established, but how they play a role in sleep continuity and protection of memory consolidation against interference is unclear. One theory posits that spindles or a neural refractory period following their offset act as a gating mechanism, blocking sensory information en route to the cortex at the level of the thalamus. An alternative model posits that spindles do not participate in the suppression of neural responses to sound, although they can be produced in response to sound. We present evidence from three experiments using electroencephalography and magnetoencephalography in humans that examine different evoked responses in the presence of and following sleep spindles. The results provide convergent empirical evidence suggesting that auditory processing up to cortex is maintained during sleep spindles, and their refractory periods.

4.2 Introduction

Sleep has important functions in removal of waste metabolites produced during wakefulness (Hauglund et al., 2020), synaptic rescaling (Blanco et al., 2015), and in actively consolidating memory (Diekelmann & Born, 2010; Schabus et al., 2004; Antony et al., 2019; Klinzing et al., 2019). These functions could not efficiently occur if sleep were constantly interrupted. Empirical support for the presence of a protective mechanism ensuring sleep continuity comes from studies demonstrating a reduced capacity to process external stimuli

(e.g., Wang et al. 2022; Andrillon et al. 2016; Kállai et al. 2003; Badia et al. 1990) and a reduced propensity for arousal by them during sleep (reviewed in (Andrillon & Kouider, 2020)). The nature of such a protective mechanism and how the sleeping brain might maintain a balance between monitoring the surroundings and reducing sensory interference with other sleep-dependent processes remains unclear (Andrillon & Kouider, 2020).

Neural events that occur only in sleep and whose presence correlates with reduced arousability are prime candidates as potential mechanistic explanations. Several such sleep-specific neural events occur during non-rapid eye movement (NREM) sleep (stages 2 and 3), among them sleep spindles and slow oscillations (SOs). Spindles are transient (<2.5 s) 11-16 Hz brain oscillations that are generated through thalamocortical interactions (Fernandez & Lüthi, 2020) (see Figure 1A), and SOs are low frequency (usually < 1.5 Hz), large-scale fluctuations in cortical and subcortical excitability (Neske, 2016; Ngo et al., 2013b; Vyazovskiy & Harris, 2013). Spindles in particular are a credible candidates for interrupting sensory transmission through thalamus to cortex, because they are observed when neurons within the thalamic reticular nucleus shift their activity from a tonic to burst mode of firing (Fernandez & Lüthi, 2020). As tonic mode firing is present during normal wakeful sensory processing, it follows that quite a different firing pattern may not allow normal sensory transmission to cortex.

Further conceptual support for this idea comes from other known thalamic roles; in wakefulness, the thalamus acts as a selective filter and attentional controller for sensory inputs, regulating their transmission based on task relevance and attention (e.g., Koch (1987); Ward (2013); Jaramillo et al. (2019)). This concept has been proposed to extend to sleep spindles, where the thalamus continues its gating role but in a different context. During sleep, sleep spindles are believed to represent a mechanism by which the thalamus limits the influx of external sensory information to the cortex, dampening responsiveness to the environment (McCormick & Bal, 1994; Dang-Vu et al., 2011; Schabus et al., 2012). This selective gating mechanism is thought to help sustain a stable sleep state, protecting against full awakenings caused by external stimuli (see Figure 1B).

Evidence concerning this proposal is, however, equivocal, as some sensory-evoked brain responses appear to be unaffected by the presences of spindles (reviewed in Andrillon & Kouider 2020; Fernandez & Lüthi 2020). Much of the work suggesting a role of spindles in blocking sensory information is indirect. For example, sleep stage or overall spindle density might be correlated with brain responses (e.g., Mai et al. 2019), without considering specifically when a stimulus arrives relative to the appearance of a spindle. To date, there are few studies using time-resolved methods in healthy humans that directly investigate whether and how sleep spindles, or subsequent spindle refractory periods (Antony et al.,

2018), influence gating of sensory information between thalamus and cortex (but see Dang-Vu et al. 2011; Schabus et al. 2012 for evidence that hemodynamic responses to sound presented during spindles are reduced). If sensory information is gated by spindles (or their refractory periods Antony et al. 2018) at the thalamic level, the neural representation of the stimulus or reaction to it should be weaker or absent in the cortex when sleep spindles occur as compared to periods of time in which they do not. In sum, there are two competing explanations for the patterns of results reported in previous literature: 1) that spindles (or their refractory periods) gate sensory access to the cortex to protect the sleep state, and 2) that other mechanisms are responsible for diminished sensory processing and arousal observed during sleep.

The auditory sensory modality lends itself particularly well to investigating whether spindles block sensory information, as peripheral auditory structures remain accessible during the sleep state, and the origin and timing of specific neurological responses evoked by sound within the auditory pathway are quite well understood (see Figure 1C) (Coffey et al., 2016b, 2017a). Notably, recent developments in techniques to capture early responses to sound using magnetoencephalography (MEG) and electroencephalography (EEG) offer a means of measuring the effects of brain state on sensory process as sensory information ascends the central nervous system (Coffey et al., 2016b; Hartmann & Weisz, 2019; Coffey et al., 2021, 2017a; Wang et al., 2022).

An interesting property of the auditory system is that stimulation at specific times during neural events, notably during peaks in slow oscillations (SOs), generates additional SOs and sleep spindles in the following seconds, and thereby enhances sleep-related memory consolidation processes. This technique is called closed-loop auditory stimulation, or CLAS (for recent reviews, see Harrington & Cairney 2021; Choi et al. 2020). Evidence suggests this phenomenon is likely to be mediated through the activation of non-lemniscal ascending auditory pathways, which project broadly to association areas including frontal regions (along with secondary auditory areas), likely also involving the ascending reticular activating system (Bellesi et al., 2014; Jourde et al., 2022). Measuring the ability of CLAS to generate additional SOs and spindles therefore offers the prospect of assessing how this pathway functions in the presence of sleep spindles, in addition to measuring auditory-modality-specific evoked responses.

In the present work, we conducted three experiments to assess the impact of sleep spindle occurrence and their refractory period on different measures of auditory cortical processing (see Figure 1C right). First, we used combined MEG-EEG and distributed-source modeling techniques in a nap experimental design and measured frequency-following responses (FFR), a brain response used in auditory and cognitive research to measure the fidelity and precision of sound encoding (FFR; for reviews, see Coffey et al. 2019; Skoe & Kraus 2010; Krizman

& Kraus 2019). Critically, this signal is an early sound response that can be measured in the auditory cortex using MEG (Coffey et al., 2016b), and so allows us to investigate how periodicity encoding of auditory stimuli in the primary auditory (lemniscal) pathway is affected by the presence of sleep spindles. In a second experiment, overnight recordings allowed us to acquire sufficient trials (with the necessary inter-trial intervals) to measure slower cortical evoked response components extracted from right auditory cortex (namely P100, P200) in the presence of sleep spindles (Colrain & Campbell, 2007), and quantify their amplitude as a function of spindle presence. Finally, using a closed-loop auditory stimulation design based on EEG detection of slow oscillations, we investigated the impact of auditory stimulation in the presence and absence of spindles which were coupled to SO up states. Coupling between SOs and spindles is reported to occur in less than 10% of SOs (Hahn et al., 2020, 2022); we therefore collected 5 whole-night recordings per participant to achieve high statistical sensitivity. In addition to clarifying one of the putative roles of sleep spindles, the results have practical use for optimizing the timing of brain stimulation delivery relative to endogenous neural events (Ramot & Martin, 2022; Van den Bulcke et al., 2023).

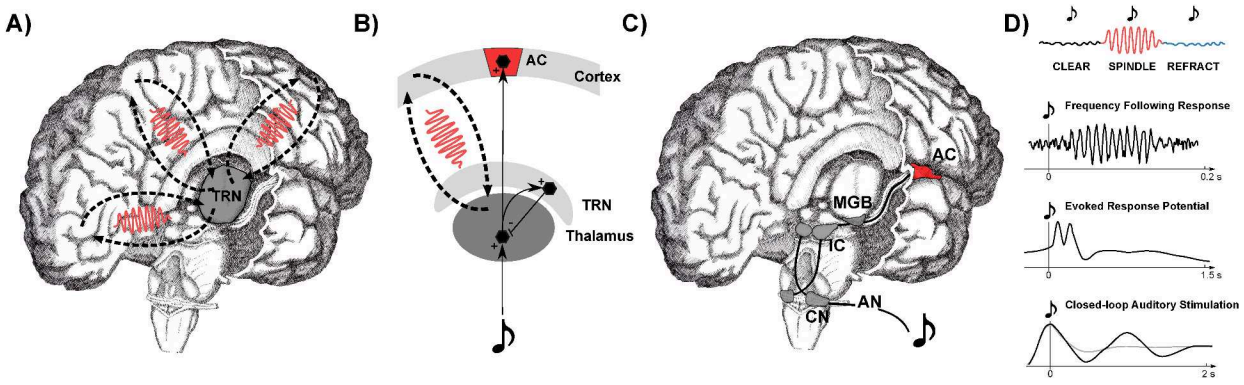

Figure 4.1: Proposed mechanisms by which sleep spindles might gate access of auditory information to the cortex. A) Schematic representation of the thalamocortical loops involved in the generation of sleep spindles. The thalamic reticular nucleus (TRN), which wraps around the thalamus, is responsible for the initiation of sleep spindles (in NREM2 and NREM3 sleep stages). B) According to the thalamic gating hypothesis, the TRN is thought to modulate the flow of information through the thalamus to cortex (Crabtree, 2018), protecting the sleep state by disrupting transfer of sensory information through thalamus to cortex. C) Diagram of the ascending auditory pathway (right dorsolateral view), showing the auditory nerve (AN); cochlear nucleus (CN) and inferior colliculus (IC) in the brainstem; medial geniculate body (MGB) of the thalamus; and the auditory cortex (AC) in the temporal lobe. D) The thalamic gating hypothesis is tested in the current work by comparing the magnitude of three types of evoked auditory responses localized to or known to involve cortical brain regions (FFR, ERP and effects of CLAS) during spindles as identified using EEG (labelled 'Spindle'), during their refractory periods ('Refract'), and during stage 2 and 3 sleep when neither a spindle nor refractory period is occurring ('Clear'). FFR: frequency-following response; ERP: evoked response potential; CLAS: closed-loop auditory stimulation.

4.3 Methods

Sections A to C describe methods common to all three experiments. Sections D, E and F detail methods specific to each of the the three experiments.

4.3.1 Participant recruitment and selection

For all experiments, adults aged 18-45 were recruited from the local community. Participants were screened for neurological and auditory conditions using a medical questionnaire. All participants reported being in good neurological health with normal hearing, were non-smokers, reported not having changed time zones or conducted shift work in the 6 weeks preceding the experiment, and had a normal sleeping pattern in the three days prior to the experiment by sleep log (i.e., 6-9 hours). Participants confirmed they were not taking any sleep or wakefulness-altering drugs, which can affect sleep characteristics such as spindle density (e.g., Plante et al. 2015). For the MEG experiments (Experiments 1 and 2) participants were asked to stay up one hour later than their habitual bed time the night prior to the recording session, to increase sleep pressure and the prospect of attaining sleep in the scanner environment. The day of the experiment, as well as the day prior to it, they were asked to refrain from consuming caffeine, alcohol, nicotine, and cannabis. Subjects gave written informed consent, and were compensated for their time. All experimental protocols were approved by Concordia University's Human Research Ethics Committee, and concerning the MEG experiments, also by the McGill University Research Ethics Board.

4.3.2 Statistical approach

In this work we used both frequentist and Bayesian statistics. Baysian statistical approaches were used to assess evidence in favour of both an alternative and null hypothesis. Bayesian statistic are gaining acceptance as an alternative or complement to traditional frequentist null hypothesis significance testing in psychology (Aczel et al., 2018; Wagenmakers et al., 2016; Marsman & Wagenmakers, 2017; Kelter, 2020). The resulting metric, known as a Bayes factor (BF), is a likelihood ratio of the marginal likelihood of two competing hypotheses (e.g., the null hypothesis and an alternative). Bayes factors are expressed as a positive number on a continuous scale. For BF10 values, numbers greater than 1 are interpreted as evidence in favour of an alternative hypothesis, where bigger numbers indicate stronger evidence. On the other hand, small BF10 values, between zero and 1, indicate evidence in favour of the null hypothesis instead. BF10 and BF01 values operate symmetrically; thus BF01 values greater than 1 is another measure of support for the null hypothesis (i.e., small BF10 values). (Lee

& Wagenmakers, 2014; Aczel et al., 2018). We adopt the classification scheme used in JASP to interpret Bayes factors, i.e., separating between "anecdotal", "moderate", "strong", etc. relative evidence for an hypothesis based on the size of the Bayes factor obtained (Kelter, 2020). In addition, we report frequentist statistics for the main research questions, as many readers are more familiar with them, noting that in contrast to Bayesian statistics they cannot be used to test null models.

For Experiment 2, we opted to conduct an overnight study with a limited number of subjects, as opposed to including a larger subject pool with shorter sleep duration. This choice was made to maximize the number of stimulations per subject that co-occur with sleep features of interest (like sleep spindles and their refractory periods) or captured instances where those features were absent (as seen in the Clear condition defined earlier). The recognition is growing that the statistical power of a study depends upon the volume and quality of data available per subject, especially when within-participant variability outweighs between-participant variability (Baker et al., 2021). This strategy of gathering extensive data from a small group of subjects is most suitable for inquiries into fundamental mechanisms that are likely to be highly consistent across participants. This approach finds its roots in non-human primate research, which often faces constraints on sample size due to resource limitations and ethical considerations (see Smith & Little (2018); Brysbaert & Stevens (2018); Baker et al. (2021) for an in-depth discussion and illustration of the trade-offs between subject numbers and observations). To analyze the data, we employed linear mixed effects (LME) models (Pinheiro & Bates, 2006). These models capture the relationship between dependent and independent variables, accounting for correlations between observations, such as multiple measurements taken from each subject. In our case, the subject was treated as a random factor. This category of models capitalizes on the substantial number of observations per subject (ranging from 1,560 to 3,700, depending on the specific research question). The LME analyses were performed using the *lme4* and *emmeans* packages in the R programming language (Bates et al., 2015; Lenth, 2022). Throughout the analyses, a significance level (alpha) of 0.05 was maintained, and we employed false discovery rate (FDR) corrections for multiple comparisons across relevant dimensions (e.g., frequency bins) when deemed necessary. The Benjamini-Hochberg procedure was applied for FDR correction (Thissen et al., 2002). For each linear mixed effects model used in our analysis, we visually examined histograms and quantile-quantile (Q-Q) plots of the residuals to detect deviations from the assumptions of normality and homoscedasticity. In instances where noticeable deviations were observed, we identified and excluded outliers by employing a threshold criterion of 1.5 times the interquartile range (IQR), corresponding to values below the first quartile (Q1) or above the third quartile (Q3). This approach eliminates data points lying beyond 2.7 standard

deviations (σ) from the mean. Subsequently, the models were rerun, and the decision to remove outliers was indicated for each analysis.

4.3.3 Sleep event detection and condition assignment

In all three studies, the same spindle detection strategy was used. As our research questions focus on sleep spindles, which are present in both NREM2 and NREM3 sleep, we detected sleep spindles across both stages stages (Schulz, 2008). Sleep spindles were detected on a central EEG electrode (position 'Cz'), referenced to the right mastoid. Only in case of bad quality signal on the preferred electrodes was an alternative, nearby electrode chosen ('C3'; this affected only 3 subjects in Experiment 1, see below). Spindles were detected offline using a freely available algorithm which emulates human scoring (Lacourse et al., 2019). In brief, four criteria are used: the absolute sigma power (frequency band of spindle activity), the relative sigma power, and both the correlation and covariance of the sigma band-passed signal to the original EEG signal.

For Experiment 3, which used a specialized closed-loop stimulation EEG device (Endpoint Connected Hilbert Transformation (ecHT); Elemind Technologies, Inc., Cambridge, USA; see below) in participants' home environments. Slow oscillations were detected in real-time adapting a previously validated method (Carrier et al., 2011). In brief, EEG was filtered between 0.16 and 4 Hz and the following criteria were assessed to detected the presence of a slow oscillaton: a peak-to-peak amplitude greater than 75 μV, a negative peak amplitude higher than 40 μV, a duration of the negative peak between 125 and 1500 ms and a positive peak lasting less than 100 ms (Rosinvil et al., 2021). We detected SO to ensure that the Clear condition did not include any stimulation occurring concurrently with them; the Clear condition therefore contained only epochs of NREM2 and NREM3 without any specific sleep oscillations.

Sleep spindles were detected offline using a modification of the initial sleep spindle detection algorithm (Lacourse et al., 2019) to account for differences in broadband noise in the ecHT signal with respect to standard EEG systems. In this case one of the four original detection criteria, the absolute value of sigma power, was ignored. The quality of the resulting detection was then confirmed by a trained sleep scorer by visually inspecting random epochs.

For Experiments 1 and 2, the spindle refractory period was defined as a fixed time window lasting 2.5 seconds after the offset of the detected sleep spindle. The 'Clear' condition was defined as the absence of slow oscillations, spindles, and their refractory periods. For Experiment 3, in which the sound stimulation occurred only during SO up-states, no Clear condition was defined because a slow oscillation was always present at sound onset.

Stimulations were divided between Solitary and Coupled depending on the absence or presence of a sleep spindle nested in the up-state (coupling was defined as the occurrence of a sleep spindle in a time window of 1.2s around the trough of a SO).

4.3.4 Experiment 1: Evidence that the lemniscal auditory pathway operates during spindles

	Sleep stages durations (% of TST)				Detected sleep events density (events/min)		Stimulation conditions (#)		
	% N1	% N2	% N3	%REM	SO	Spindles	Spindle	Refractory	Clear
S01	56.0%	44.0%	0.0%	0.0%	0.8	3.5	1031	2115	13549
S02	24.2%	75.8%	0.0%	0.0%	0.5	11.7	1430	2289	9308
S03	16.7%	38.7%	44.7%	0.0%	12.0	3.6	1706	2900	10509
S04	25.2%	50.3%	24.5%	0.0%	6.4	4.1	2713	3534	10394
S05	22.7%	18.2%	59.1%	0.0%	10.1	2.4	2056	3185	13979
S06	68.9%	25.4%	5.7%	0.0%	1.8	5.7	538	852	3984
S07	28.3%	58.7%	13.1%	0.0%	1.9	2.7	1391	2090	13918
S08	61.4%	38.6%	0.0%	0.0%	1.9	3.9	553	710	2219
S09	22.9%	33.3%	34.0%	9.8%	8.0	1.7	1976	3599	20165
S10	26.4%	55.2%	18.4%	0.0%	3.2	2.6	1244	2145	23537
S11	13.2%	45.7%	37.3%	3.9%	7.6	5.0	3607	5332	22104
S12	27.8%	64.7%	7.5%	0.0%	4.1	11.2	645	914	5016
S13	18.8%	64.6%	16.6%	0.0%	2.8	4.7	1181	1997	0
Average	31.7%	47.2%	20.1%	1.1%	4.7	4.8	1543.9	2435.5	11437.1
SD	18.0%	16.6%	18.9%	2.8%	3.7	3.1	886.1	1292.5	7486.0

Figure 4.2: Experiment 1: Sleep duration, detected sleep events and number of epochs in each condition for each subject

Participants

Fifteen neurologically healthy young adults who reported being able to nap in a supine position were recruited. Sample size and stimulation parameters were selected to be in-line with previous work on the MEG-FFR (Coffey et al., 2016b), as estimations of possible effect sizes for FFR were not available. Subjects were first screened for neurological and auditory conditions using a custom medical questionnaire. We used the Munich Chronotype Questionnaire (MCTQ) to document their habitual diurnal rhythms (Roenneberg et al., 2003) and confirm that all subjects had a regular sleeping schedule (6.5-8.5 hours per night, with habitual bedtimes clustering around midnight). The Pittsburgh Sleep Quality Index (PSQI) (Buysse et al., 1989), which contains 19 self-rated questions assessing sleeping difficulty and yields a global score of between 0 and 21 points, was used to confirm that the sampled did not have sleep difficulties; scores of 5 or more indicate poor sleep quality and would have been grounds for exclusion. Participants also completed a subjective fatigue scale concerning their current state, which consisted of 7 questions rated on a 5 point Likert-scale. Items on

the scale asked about subjects' levels of tiredness, activity, motivation, interest, concentration, relaxation and general feeling; all scores were moderate. One participant was excluded due to inability to sleep in the scanner during the experiment. The mean age of the remaining participants was 24.8 years (SD: 4.0; range: 21-36), 9 were female, and all were right-handed, and had no history of neurological, auditory, nor sleep disorders.

Study design and participant preparation

After filing out questionnaires and changing into comfortable clothing, participants were prepared for EEG. A three-channel (Cz, C3, C4; 10–20 International System) EEG montage was applied with a forehead ground and mastoid reference. We limited EEG recordings to central channels to improve comfort and reduce preparation time, and because SOs and spindles are typically detected on these channels. Bipolar electrooculogram (EOG) electrodes around the eyes and electrocardiogram (ECG) electrodes on the chest were applied for later use in detecting and cleaning corresponding artefacts in the MEG traces. Two pairs of additional electromyogram (EMG) channels on the chin and neck were used during sleep scoring (for detecting REM sleep). Head shape and the location of head position indicator coils were digitized (Polhemus Isotrak, Polhemus Inc., VT, USA) for co-registration of MEG with a standard anatomical T1-weighted magnetic resonance image (MRI), which was acquired in a separate session.

Participants were then settled onto a mattress placed on the MEG scanner bed in a supine position, and were covered with blankets if they wished. A 5 min resting state data acquisition with eyes open was collected, as a contribution to an open-access database (Niso et al., 2016). Lights were dimmed, and subjects were asked to close their eyes and relax for a 2.5 h nap opportunity. Sound stimulation was started immediately, with the subject in the awake state, to allow them to get used to the sound and so that the brain response to the wake state could be measured. Standard T1-weighted MRI anatomical images ($1mm^3$ isotropic voxels) were acquired in a separate session to enable distributed source localization of MEG signals.

Stimulus Presentation

To characterize the brain's response to sound over arousal states, we used a synthesized speech syllable (/da/; 120 ms, comprised of a 10 ms consonant burst, a 30 ms formant transition, and an 80 ms steady-state vowel with a fundamental frequency of 98 Hz). This syllable is favoured by many FFR researchers for its acoustic properties, ecological validity in speech (n.b., fundamental frequencies in human speech range from 80 to 400 Hz), and its ability to

produce robust FFRs in most subjects (Coffey et al., 2016b; Skoe & Kraus, 2010).

The stimulus was presented binaurally at 55 dB SPL, ∼45,000 times in alternating polarity, through Etymotic ER-3A insert earphones with foam tips (Etymotic Research). We used a constant sound level across participants after selecting young, healthy participants with normal hearing (noting that personalized sound levels are preferable for some research designs, e.g. with older adults, or to optimize stimulation for an individual (Esfahani et al., 2023)). Stimulus onset asynchrony (SOA) was randomly selected between 195 and 205 ms from a normal distribution. Stimuli were thus presented continually at ∼5 Hz, to maximize the number of trials. The rapid rate of this presentation was essential as it enabled us to collect a sufficient number of epochs (over 1000, as suggested by previous literature (Coffey et al., 2016b; Skoe & Kraus, 2010)), thereby allowing us to produce a clear FFR response for each subject in each condition. Note that the study design optimizes the signal-to-noise ratio for deep sources in the brainstem but not analysis of the slower cortical evoked responses in the 0.1-40 Hz range, as the responses overlap with the 5 Hz presentation rate. Longer SOAs are used for studying the entire evolution of lower frequency cortical evoked potentials (Coffey et al., 2017a), as in Experiment 2.

To decrease the possibility of electromagnetic contamination of the data from the signal transducer, ∼1.5 m air tubes between the ear and the transducer were used such that the transducer could be placed >1 m from the MEG gantry, as in previous work (Coffey et al., 2016b, 2017a, 2021).

Data Acquisition and Definition of Conditions

Two hundred and seventy channels of MEG (axial gradiometers), five channels of EEG data, EOG and ECG, and one audio channel were simultaneously acquired using a CTF MEG System and its in-built EEG system (Omega 275, CTF Systems Inc.). All data were sampled at 2,400 Hz. In three subjects, the electrode Cz did not have consistent quality for the entire recording, and was replaced for sleep scoring and event detection by C3.

Data pre-processing was performed with Brainstorm (Tadel et al., 2011), and using custom Matlab scripts (The Mathworks Inc., MA, USA). Sleep scoring, in which 30 s windows of data are visually inspected and categorized into wake, non-REM sleep stages 1-3, and REM sleep, was accomplished according to AASM practices (Iber, 2007) based on band-pass filtered EEG (0.1-20 Hz), EOG (0.1-5 Hz), and EMG (10-58 Hz) channels, which were then downsampled for ease of handling to 150 Hz. Each epoch was scored separately by the same two trained researchers, and discrepancies were resolved via discussion.

Sleep events were detected using the detection methods defined earlier on a down-sampled version of the EEG data (250 Hz) (See Sleep event detection and condition assignment).

Auditory stimulation events were first binned according to the sleep stage in which they occurred, and then further binned by their co-occurrence with sleep spindles, refractory periods, or slow oscillations. Auditory stimulation occurring in NREM2 and NREM3 but not coinciding with any of the previously defined categories were labelled as Clear.

The data acquisition was part of a larger project with additional research questions. For the present analyses, we used epochs occurring in NREM2 and NREM3 sleep, and combined them to maximize the number of trials within the Sleep, Refractory, and Clear conditions.

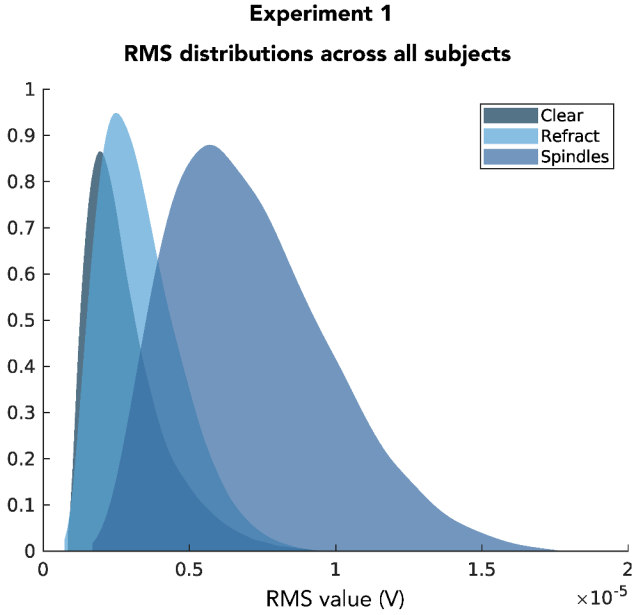

Figure 4.3: Experiment 1: Normalized distribution of sigma power (i.e., root mean square), averaged across subjects and sorted according to the presence (Spindle), recent history (Refract) or absence (Clear) of a spindle at the moment of auditory stimulation. The median sigma (spindle) power in the Clear condition was 2.64e-6 V (SD: 5.94e-7); in the Spindle condition it was 5.65e-6 V (SD: 1.27e-6); and in Refract condition it was 3.94e-6 V (SD: 7.41e-7). These data confirm that the analysis successfully separated brain responses by condition.

MEG FFR Analysis

Channel signal quality was confirmed by visual inspection; one MEG channel in one subject was removed due to poor signal quality (MRT51). Cardiac artefacts were removed from MEG data using Brainstorm's in-built cardiac detection algorithm, and source signal projection algorithm (Tesche et al., 1995), using the recommended procedure: projectors were removed when they captured at least 12% of the signal and the topography of the components matched those of ocular or cardiac origin upon visual inspection. Eye blinks were not detected nor removed, as participants had their eyes closed during the recording.

MEG data were then bandpass filtered in the FFR frequency range, to remove the low

frequency components of the evoked response (which are the focus of Experiment 2) (80-450 Hz; 43,506-order linear phase FIR filter with a Kaiser window and 60 dB stopband attenuation; the order is estimated using Matlab's kaiserord function and filter delay is compensated by shifting the sequence to effectively achieve zero-phase and zero-delay, as per Brainstorm default settings (Tadel et al., 2011)), and a notch filter to remove power line noise was applied at 120 and 180 Hz. All data were sampled at 6 kHz and downsampled to 2.4 kHz for analysis.

Auditory event markers binned by neural event (Spindle, Refractory, Clear) were used to define epochs that started 50 ms before sound onset and 250 ms after sound onset.

A simple threshold-based artefact rejection was applied (±1,000 fT) for each epoch across MEG channels; this step removed approximately 5% of epochs (final number of retained epochs are presented in all Tables). The FFR measured on the scalp using EEG (EEG-FFR) is a composite signal arising from the summation of multiple generators at the scalp (Coffey et al., 2019; Tichko & Skoe, 2017; Coffey et al., 2016b). To assess where state-dependent changes observed in the FFR are present in the auditory system along the lemniscal pathway, we used distributed source models, which estimate the amplitude of a large set of dipoles on the cortical surface or within the entire brain volume(Daunizeau et al., 2006). These models require constraints imposed by spatial priors. As in previous work (Coffey et al., 2016b), we used FreeSurfer (Fischl et al., 2002; Fischl, 2012) to prepare cortical surfaces as well as automatically segmented subcortical structures from each subject's T1-weighted anatomical MRI scan. We then imported the anatomy into Brainstorm (Tadel et al., 2011), and combined the brainstem and thalamic structures with the cortex surface to form the support of MEG distributed sources. This mixed surface/volume model included a triangulation of the cortical surface (∼15,000 vertices), and a three-dimensional dipole grid (∼18,000 points) for the brainstem and the thalamus. An overlapping-sphere head model was computed for each run, to predict how an electric current generated in the brain would be recorded at the level of the different sensors. This inverse imaging model estimates the distribution of brain currents that account for data recorded at the sensors level. A noise covariance matrix was then computed from 2-min empty-room recordings taken before each session to assess baseline level of magnetic activity in the room. Finally, to separate the contributions of subcortical and potential cortical FFR sources, we used minimum-norm estimate (MNE) modelling of head tissues with unconstrained source orientation based on individual anatomy which is a robust and frequently used technique in literature (Hämäläinen, 2009).

The auditory cortex ROIs were defined using the Destrieux atlas (Destrieux et al., 2010), by combining the regions labelled as 'S_temporal_transverse', 'G_temp_sup-Plan-tempo', and 'G_temp_sup-G_T_transv' for the left and right hemispheres, respectively. The left and right auditory cortex regions (rAC, lAC) cover the posterior superior temporal gyrus, as has been

used in previous work (Coffey et al., 2021; Jourde et al., 2022) and which captures P100 and P200 activity (see Figure 3d in (Coffey et al., 2017a)). Data from each auditory cortex (AC) for each epoch was extracted from the surface model.

To quantify magnitude of the brain's phase-locked response to sound at the sound's fundamental frequency (e.g. 98 Hz), FFR averages were first computed by averaging epochs of each polarity and then summing negative and positive polarity averages, for each subject, condition, and region of interest (ROI) using custom scripts. A Fast Fourier Transform (FFT) was then applied to each FFR average to obtain frequency spectra. Using a custom script in Matlab (Mathworks, Natick, MA, USA), we extracted the mean amplitude surrounding the observed grand average peak at 94 Hz (mean amplitude in the 84-104 Hz frequency range) for each subject and each condition. Note that as in previous work (Coffey et al., 2016b), the peak frequency of the FFR averaged across the entire window tends to be somewhat lower than the 98 Hz stimulation frequency, due to a phenomenon of oscillatory convergence (Coffey et al., 2021); the 94 Hz peak nonetheless captures the frequency-following phenomena of interest. To ensure a sufficient signal-to-noise ratio, we performed the same analysis on a time window preceding the auditory stimulation for each subject and each condition. SNR was computed to be higher than 5:1 for each subject and condition, indicating high quality FFR signals. We then statistically compared the mean magnitude of the FFT within our frequency band of interest, within subjects, for our 3 conditions: Spindles, Refractory, and Clear (please see Statistical approach).

4.3.5 Experiment 2: Evidence that sleep spindles do not greatly affect early cortical sound processing

	Sleep stages duration (% of TST)				Detected sleep events density (events/min)		Stimulation condition (#)		
	% N1	% N2	% N3	%REM	SO	Spindles	Spindle	Refractory	Clear
S01	5.0%	41.3%	44.9%	8.8%	19.4	2.0	276	612	2762
S02	62.8%	34.3%	2.9%	0.0%	19.9	0.8	85	149	1325
S03	14.9%	32.0%	42.8%	10.3%	24.1	5.0	289	425	1910
S04	2.4%	20.4%	68.6%	8.6%	8.4	8.0	228	614	2850
S05	20.3%	44.6%	30.2%	5.0%	28.4	1.3	246	499	2574
Average	21.1%	34.5%	37.9%	6.5%	20.0	3.4	224.8	459.8	2284.2
SD	24.4%	9.4%	24.0%	4.2%	7.4	3.0	81.8	191.2	650.5

Figure 4.4: Experiment 2: Sleep duration, detected sleep events and number of epochs in each condition for each subject

Experiment 2 follows largely the same design as Experiment 1; only differences are therefore reported.

Participants

Six neurologically healthy young adults were recruited from the local community, and screened as described in Experiment 1. One dataset was unusable due to a technical problem with the EEG system that precluded sleep scoring. The mean age of the five remaining subjects was 21.2 (SD: 1.33; range 19-23), and 3 were female.

Study design and participant preparation

In contrast to Experiment 1, recordings in Experiment 2 were made overnight in the MEG scanner rather than during afternoon naps, and stimuli were presented less frequently (i.e., using a longer SOA), so as to measure the slower evoked response potential components (see Stimulus Presentation below).

Participants were prepared for recordings and the data acquisition was as described above in Experiment 1. Although it is possible to make relatively continuous overnight MEG recordings in the constrained scanner environment, this is achieved through adaptation nights, and with considerable dropout (e.g., 17% (Himmer et al., 2021)). The added disturbance of sound stimulation leads to more disrupted sleep. Several participants found it difficult to achieve the sleep state after an initial sleep cycle with the sound stimulation on, and were able to ask to have it paused until they regained sleep. We discontinued the recording when the participant believed that they would not be able to fall asleep again, usually around six in the morning. The dataset therefore represents a shorter and less continuous night of sleep than they might habitually experience at home, but nonetheless all participants achieved considerable amounts of NREM sleep, which were rich in sleep spindles and slow oscillations.

Stimulus Presentation

The same auditory stimulus was used as in experiment 1. However, to measure low frequency components of the evoked response, the interval between stimulations (SOA) was lengthened and stimuli were presented continually every ∼2900 ms plus up to an additional 460 ms (selected from a uniform distribution) of jitter.

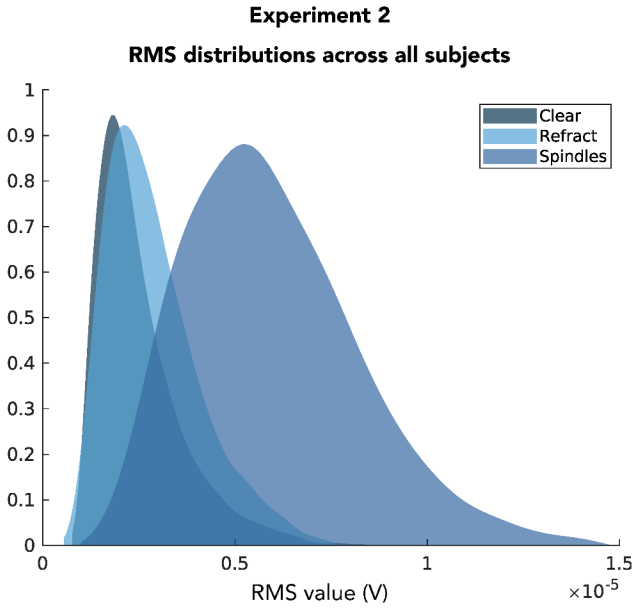

Figure 4.5: Experiment 2: Normalized distribution of sigma power (i.e., root mean square), averaged across subjects and sorted according to the presence (Spindle), recent history (Refract) or absence (Clear) of a spindle at the moment of auditory stimulation; the sorting approach results in similar distributions in Experiment 2 as compared with Experiment 1. The median sigma power in the Clear condition was 2.24e-6 V (SD: 6.26e-7) in the Spindle condition was 5.62e-6 V (SD: 2.01e-6); in Refract it was 2.62e-6 V (SD: 6.93e-7). These data confirm that the analysis successfully separated brain responses by condition, as in Experiment 1.

Cortical evoked response analysis

The MEG processing and analysis steps were as described in Experiment 1, except that a filter of 0.1-200 Hz was used, data were resampled to 500 Hz, epochs were defined as -1 before to 3 seconds after stimulus onset, and a baseline correction of -1 to 0 was used. We did not apply a threshold-based artefact detection step, because SOs measured in sleep, which are of interest in the present work and are retained using the filter parameters appropriate for looking at ERPs, frequently exceed rejection limits. Furthermore, movements and arousals were minimal when considering only NREM2 and NREM3 sleep stages.

Using distributed source modelling data as in Experiment 1, timeseries of the evoked response were exported from the right auditory cortex region of interest using a surface model of the cortex. Mean amplitude of these extracted signals during specific time windows defined on the subjects' average measured for each subject and each condition (e.g. 0.7 to 0.9s for P100 and 1.9 to 2.1s for P200). We selected P100 and P200 as measures of early cortical auditory processing, as they are robustly observed in signals extracted from bilateral auditory cortex using MEG (Figure 3a in (Coffey et al., 2017a); Figure 6a in (Jourde et al., 2022)).

P100rAC	BF01 Clear <->Spindle	BF10 Clear <->Spindle	95% CI	BF01 Clear <->Refract	BF10 Clear <->Refract	95% CI
OL01	2.61	0.38	[-0.01,0.25]	17.98	0.06	[-0.11,0.08]
OL02	3.85	0.26	[-0.35, 0.08]	5.56	0.18	[-0.07, 0.26]
OL03	5.28	0.19	[-0.04, 0.22]	7.86	0.13	[-0.04, 0.18]
OL05	11.75	0.09	[-0.11, 0.16]	6.94	0.14	[-0.02,0.15]
OL06	10.15	0.09	[-0.18, 0.09]	0.95	1.05	[-0.22, -0.02]
Mean	6.73	0.20		7.86	0.31	
SD	4.01	0.12		6.25	0.42	

P200rAC	BF01 Clear <->Spindle	BF10 Clear <->Spindle	95% CI	BF01 Clear <->Refract	BF10 Clear <->Refract	95% CI
OL01	0.04	28.33	[0.09, 0.36]	18.00	0.06	[-0.11,0.08]
OL02	1.80	0.56	[-0.03, 0.41]	0.09	10.21	[0.09, 0.43]
OL03	13.50	0.07	[-0.14,0.12]	14.57	0.07	[-0.13,0.09]
OL05	8.01	0.13	[-0.07, 0.20]	12.76	0.08	[-0.13, 0.05]
OL06	3.22	0.31	[-0.25, 0.02]	0.81	1.24	[-0.23, -0.03]
Mean	5.31	5.88		9.25	2.33	
SD	5.45	12.55		8.25	4.43	

Figure 4.6: Experiment 2: Bayesian factors for each analysis, each condition and each subject

		Detected sleep events (#)			Stimulation conditions (#)					
	Night recordings (#)	SO	Spindles	Coupling rate	Stim_SO	Sham_SO	Stim_CoupledSO	Sham_CoupledSO	Stim_SolitarySO	Sham_SolitarySO
S01	4	8,166	6,088	8.66%	4,347	3,819	382	325	3,965	3,494
S02	5	9,890	6,863	4.94%	5,390	4,500	247	242	5,143	4,258
S03	4	7,448	6,688	6.43%	4,016	3,432	229	250	3,787	3,182
S04	5	12,710	7,360	5.39%	6,881	5,829	394	291	6,487	5,538
S05	5	9,566	4,518	3.87%	5,077	4,489	165	205	4,912	4,284
S06	6	12,596	15,019	11.46%	6,905	5,691	733	710	6,172	4,981
S07	5	10,355	11,495	8.52%	5,698	4,657	471	411	5,227	4,246
S08	5	7,780	6,983	6.40%	3,992	3,788	226	272	3,766	3,516
S09	6	11,728	3,752	2.99%	6,349	5,379	185	166	6,164	5,213
S10	4	9,962	5,981	11.30%	5,248	4,714	613	513	4,635	4,201
S11	5	23,495	6,666	2.17%	12,603	10,892	255	256	12,348	10,636
S12	5	13,426	6,102	3.40%	7,134	6,292	237	220	6,897	6,072
S13	4	8,594	7,869	10.96%	4,443	4,151	471	471	3,972	3,680
S14	3	10,520	8,750	14.30%	5,520	5,000	746	758	4,774	4,242
S15	4	13,741	6,902	4.58%	6,994	6,747	304	326	6,690	6,421
S16	5	23,559	6,278	3.29%	12,076	11,483	375	401	11,701	11,082
S17	5	13,083	6,792	1.89%	6,767	6,316	117	130	6,650	6,186
Mean	4.71	12,154.06	7,300.35	6.50%	6,437.65	5,716.41	361.76	349.82	6,075.88	5,366.59
SD	0.77	4,722.08	2,587.37	3.74%	2,463.19	2,271.22	190.96	177.67	2,483.97	2,287.78

Figure 4.7: Experiment 3: Sleep duration, detected sleep events and number of epochs in each condition for each subject

Participants

Participants were recruited for a 5-night home study using a closed-loop auditory stimulation device. The multi-night design aimed to ensure that a sufficient number (>100) of SOs coupled to sleep spindles would coincide with the sound stimulation, as coupled SOs represent a relatively low proportion of SOs (<10% (Hahn et al., 2020, 2022)). We recruited 23 healthy young adults for Experiment 3. Two participants dropped out of the study due to discomfort sleeping with the apparatus, or technical issues. We further removed four subjects for having fewer than 100 clean epochs in at least one of the conditions, so as to achieve a clear averaged

evoked response with reliable and high SNR peaks (Thigpen et al., 2017). The final sample comprised 17 subjects (9 female; M= 27.56 years, SD = 9.39, range = 22-43 years).

Participants completed the MCTQ (Roenneberg et al., 2003) as in previous studies, and also filled in a sleep diary for three nights prior to the first recording night, and prior to each subsequent experimental night.

Study design and participant preparation

Data collection for Experiment 3 was conducted during a period of COVID-19 health restrictions which necessitated contact-free research designs. Participants first met remotely with a research assistant via video conference, during which time they gave oral consent to participate. Upon agreement, participants received a package of study materials at their home: an Endpoint Connected Hilbert Transformation Box (ecHT) box for closed-loop stimulation (Elemind Technologies), a portable battery, a laptop computer on which to collect data, EEG materials, and written instructions needed to conduct the recording. A second video-chat session was organized prior to the beginning of the data collection with the experimenter to go through the entire protocol, answer any question participants could have and to ensure the instructions about electrodes placement were understood.

Participants were then asked to use the equipment for five nights. Instructions directed the participant to prepare the skin with alcohol swabs, an abrasive strip, and exfoliating paste, to ensure good contact and low impedance during the recording and then apply a disposable electrode to the forehead (at approximately Fpz; 10–20 International System), and a reference electrode on the left mastoid (M1). The Fpz placement was selected for ease of preparation (i.e., skin), and because both slow oscillation and sleep spindles can be captured at this site (Campos-Beltrán & Marshall, 2021). The ecHT box has an in-built impedance indicator, which is red in the event of poor signal quality ($< 5KOhm$). Participants were instructed to repeat the process of applying the electrodes if the red indicator light was on. Assistance was available throughout the duration of the experiment until 10:00pm by video conference. If questions arose later the participants were asked to note them down, skip the experimental night and reach out to the researcher the following morning. Participants were permitted to take breaks between recording nights if they wished. In total, 10 days were allocated for the completion of five nights of sleep with the apparatus.

Stimulus Presentation

The endpoint-corrected Hilbert Transformation v2 box (ecHT; Elemind Technologies, Inc., Cambridge, USA) is a closed-loop auditory stimulation device which monitors a single channel

of EEG activity and outputs sound bursts via connected headphones (Schreglmann et al., 2021). Online detection of slow oscillation peaks was possible by an algorithm designed by D. Lesveque and implemented on the ecHT, which, as validated during pilot testing, approximates the performance of offline SO detection algorithms. EEG data were sampled at 500 Hz, filtered online using a 50-sample sliding-window average. Slow oscillation peaks were detected when -40 μV troughs were followed by a peak-to-peak change of at least 75 μV.

The sound stimuli (40 ms pink noise, with a 5 ms linear rising and falling ramps, respectively) was presented binaurally at 55 dB SPL at SO peaks through Etymotic ER-3C earphones with insert foam tips (Etymotic Research). Pink noise was used instead of the speech syllable used in Experiments 1 and 2 as the ecHT due to the system's technical capabilities, and because pink noise bursts have been used in the majority of closed-loop auditory stimulation studies (including (Ngo et al., 2013a,b)), which increases comparability with previous CLAS results. We used a within-nights design to ensure that a similar number of trials was collected under equivalent experimental conditions across stimulation and sham conditions. The closed-loop system was programmed to first start with 30 minutes of silence to allow the participants to fall asleep, and then go through 5 minute cycles of detecting and stimulating slow oscillation ('Stim' condition), followed by 5 minutes in which SOs were detected and marked but no sound was presented ('Sham' condition), resulting in approximately equal numbers of Stim and Sham condition epochs. The two conditions were separated by a 5 s pause.

Data acquisition and definition of conditions

EEG data was recorded from the Fpz-M1 channel at a sampling rate of 500 Hz using the ecHT box. Data were first visually inspected for general signal quality. As anticipated, due to the in-home nature of the recordings, not all recordings were usable due to electrode displacement (see Table 4 for the number of retained nights). Retained data were then analysed using custom scripts in Matlab. Due to the research questions addressed, and because full polysomnographic recording needed for sleep scoring was not available in this in-home design, the night recordings were not sleep-scored.

Sleep spindles were detected offline (see Sleep event detection and condition assignment). Epochs were defined as -1 s before stimulation to 4 s after stimulation and were sorted according to the presence or the absence of a sleep spindle when detection (for both stimulation and sham conditions) occurred. Epochs from the five individual nights were then pooled. The entire raw signal was then bandpass-filtered in three frequency bands: (1) between 70 and 150 Hz to estimate muscle activity, (2) between 0.5 and 1.5 Hz to characterize the slow wave activity (SWA) range, and (3) between 12 and 15 Hz to measure the fast sigma activity

(FSA). To avoid measuring brain responses in which stimulation might have been erroneously triggered by movement, we first excluded 5 percent of epochs with the highest activity in this frequency band, at the subject level. To evaluate the effect of spindle-coupled vs. solitary slow oscillations on subsequent SOs and spindle activity we measured differences in EEG activity between the Stim and Sham conditions, for all SOs, Solitary SOs and Coupled SOs, in both the SO and spindle bands. Root mean square (RMS) of the slow frequency (0.5 - 1.5 Hz) signal was computed with a moving average and used to assess slow wave activity. Average RMS values post stimulation (onset+0.5 s to onset+1.5 s) were compared between sound and sham conditions within this time interval. Root mean square (RMS) of the fast sigma signal (12 - 15Hz) was used to assess evoked spindle activity. Average RMS values post stimulation (onset+0.75 onset+1.25s) were compared between sound and sham conditions within this time interval in order to characterize the effect on sigma signal. For visualization purposes, we z-scored the envelope of the fast sigma signal for each subject (across both conditions), to account for inter-subject variability in overall sigma amplitude (Figure 4B).

4.4 Results

4.4.1 Experiment 1: Evidence that the lemniscal auditory pathway operates during spindles

Fourteen subjects were included in a nap study (mean age: 24.8 (SD: 4.0; range: 21-36), 9 females).

Sleep scoring analysis confirmed that all subjects included in the analysis slept during the 2.5 hr nap opportunity. On average, subjects spend 70 minutes (SD: 35) in NREM2 and NREM3 sleep stages (combined), in which sleep spindles occur. On average 293 spindles (SD: 177) and 370 slow oscillations (SD: 348) were detected per subject using EEG (NREM2 and NREM3). Please see Table S1 for time spent in other sleep stages.

Brain responses to incoming sounds were cut into 300 ms epochs (from -50 ms prior to the sound to 250 ms post sound) and sorted according to their timing with respect to spindle onset and offset (i.e., 'Spindle'), and a refractory period defined as a fixed window of 2.5 seconds post offset, as in previous work (i.e., 'Refract' (Antony et al., 2018)). The 'Clear' condition was defined as the absence of a slow oscillation, spindle, or its refractory period at the time of stimulation, only considering NREM2 and NREM3 sleep stages. After sorting the auditory stimulation events, the mean number of epochs in the Spindle condition was 1,540 (SD: 880), in the Refractory condition 2,430 (SD: 1,290), and in the Clear condition, 11,430 (SD: 7,480; see Table S1 for further details).

To confirm that the detection (at Cz) and sorting procedure was successful to separate time periods that included high and low spindle activity, we compared the electroencephalography absolute sigma band power (root mean square of the amplitude within 11-16 Hz; see Methods) during each of the three epoch types in 2 second windows centred on the sound presentation. Both absolute spectral power and relative spectral power (i.e., selected frequency band divided by broadband activity) are commonly used metrics, we favoured the absolute power approach for its simplicity of interpretation and lack of dependency on power differences in other spectral bands, throughout the paper. We confirmed that the distributions (see Figure S1) were statically different using a repeated measures ANOVA $F(2, 24) = 144.64$, $p < 0.001$). Post hoc pairwise comparisons revealed that sigma band power was significantly greater in Spindle as compared with Clear (mean difference = 3.00e-6, SE = 2.33e-7, 95% CI = [2.36e-6 3.65e-6], $p < 0.001$), Refractory as compared with Clear (mean difference = 1.30e-6, SE = 1.14e-7, 95% CI = [9.86e-7 1.62e-6], $p < 0.001$), and Spindle as compared with Refractory conditions (mean difference = 1.71e-6, SE = 1.65e-7, 95% CI = [1.25e-6 2.16e-6], $p < 0.001$).

To test the main hypothesis that spindles (or their refractory periods) play a protective role in sleep by impeding the transmission of auditory information between thalamus and cortex, we investigated the strength of acoustic periodicity encoding in the right auditory cortex (i.e., the amplitude of the fundamental frequency in the FFR, which is associated with pitch information) using magnetoencephalography, across Spindle, Refractory, and Clear epochs. To test whether the cortical FFR was affected by the presence of a spindle, we focused on the right auditory cortex. Due to hemispheric specialization in the auditory system (Albouy et al., 2020), the strongest phase-locked neural response to pitch information (FFR) is found in this region (Coffey et al., 2017a, 2016b; Lerousseau et al., 2021).

To confirm that the FFR was of sufficient quality and clarity to be used as a basis for investigating the main research questions, we statistically compared the amplitude of the FFR at the fundamental frequency (98 Hz) with the amplitude at the same frequency during the pre-stimulus period (50 ms), as in previous work (Coffey et al., 2016b). The mean signal-to-noise ratio (SNR) for the Clear condition was 11.75 (SD: 7.24), Spindle condition: 5.11 (SD: 6.28); Refractory: 10.39 (SD: 20.15); with a minimum SNR across all conditions of 1.28. We confirmed that the strength of the FFR during the stimulus was well above the baseline period in all three conditions (for each of Clear, Spindle, Refract: $V = 91.00$, $p < .001$, rank-biserial correlation: $r_{rb} = 1.00$, 95% CI $[1.00, +\infty]$; Wilcoxon signed-rank tests were used due to a violated Shapiro-Wilk test of normality).

We then compared the magnitude of the fundamental frequency in the FFR between our conditions (Spindle, Clear, Refractory). A non-parametric equivalent of a repeated-measures ANOVA was used (due to a violated normality assumption). A Friedman's Test did not show

any significant difference between FFR magnitude in the rAC across Clear, Spindles and Refractory conditions ($\chi^2(2) = 0.154$, p = 0.926). The FFR amplitude from right auditory cortex was therefore not significantly reduced during spindles, nor refractory periods, as compared with clear periods of NREM sleep (see Figure 4.8).

The frequentist statistical approach used thus far does not allow us to evaluate evidence in favour of a null hypothesis, here being that the strength of the cortical pitch representation is not systematically diminished by the presence of a spindle or its refractory period. Baysian statistical approaches allow for assessing evidence in favour of both an alternative and null hypothesis (Aczel et al., 2018; Wetzels et al., 2009; Wagenmakers et al., 2016; Marsman & Wagenmakers, 2017; Kelter, 2020). The resulting metric, known as a Bayes factor (BF), is a likelihood ratio of the marginal likelihood of two competing hypotheses (e.g., the null hypothesis and an alternative). Bayes factors are expressed as a positive number on a continuous scale. For BF10 values, numbers greater than 1 are interpreted as evidence in favour of an alternative hypothesis, where bigger numbers indicate stronger evidence. On the other hand, small BF10 values, between zero and 1, indicate evidence in favour of the null hypothesis instead. BF10 and BF01 values operate symmetrically; thus BF01 values greater than 1 is another measure of support for the null hypothesis (i.e., small BF10 values). (Lee & Wagenmakers, 2014; Aczel et al., 2018).

We first ran a Bayesian version of a repeated measures ANOVA comparing our 3 conditions (Clear, Spindle and Refractory). The analysis revealed substantial evidence in favour of the null hypothesis, with a BF01 value of 4.27, indicating strong support for the absence of an effect of conditions. We then ran post hoc tests comparing Spindle and Refract to Clear.

In agreement with the frequentist statistics, there was little evidence in favour of the hypothesis that spindle presence affects FFR amplitude ($BF_{SpindleEffect} = 0.313$, error = 0.009, 95% CI: [-0.621, 0.372]), nor of an effect of the Refractory period ($BF_{RefractoryEffect} = 0.299$, error = 0.009, 95% CI: [-0.397, 0.593]), on FFR strength. Conversely, there was moderate to strong evidence supporting the absence of a protective role of the presence of spindle ($BF_{NoSpindleEffect} = 3.200$, error = 0.009, 95% CI: [-0.621, 0.372]), and similarly, there was moderate to strong evidence in favour of there being *no* change in amplitude due to the refractory period ($BF_{NoRefractoryEffect} = 3.343$, error = 0.009, 95% CI: [-0.397, 0.593]).

4.4.2 Experiment 2: Evidence that sleep spindles do not greatly affect early cortical sound processing

The FFR examined in Experiment 1 represents periodicity encoding in the right auditory cortex, which is isolated from other evoked responses based on its high frequency range (>80

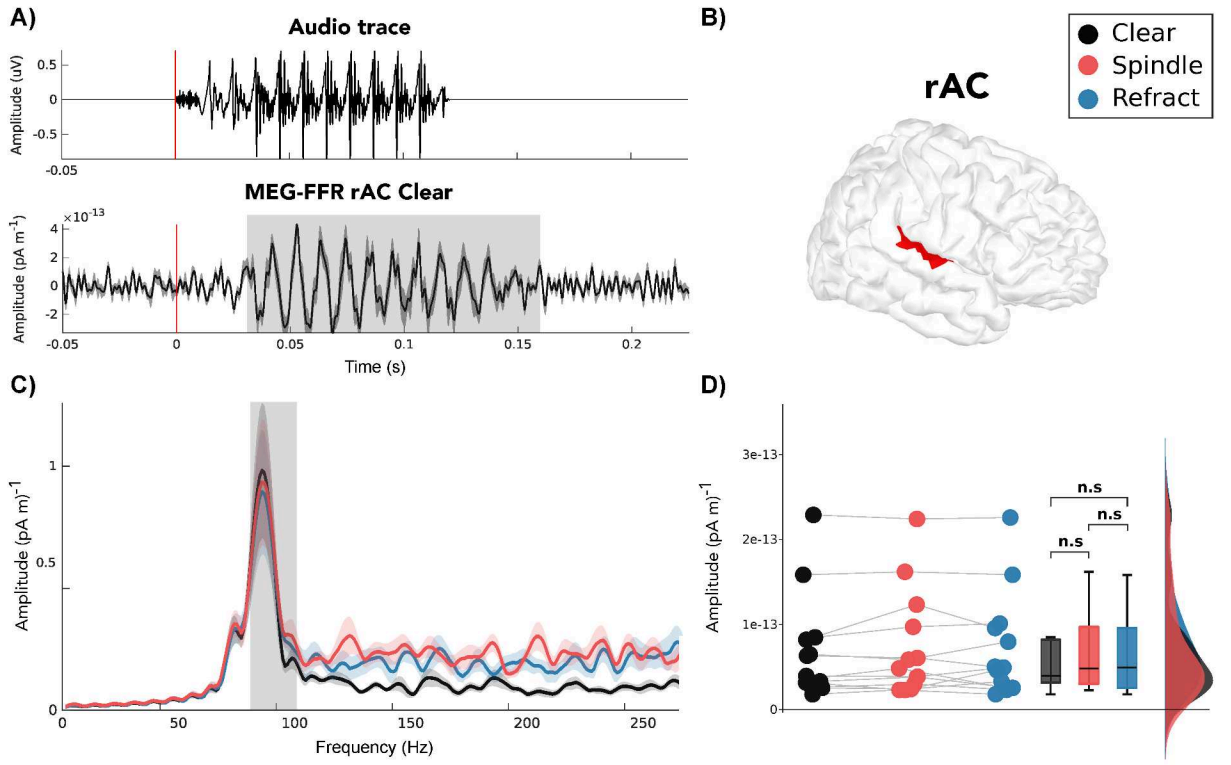

Figure 4.8: The presence of neither a spindle nor its refractory period impedes propagation of fine auditory information through the lemniscal system from thalamus to cortex. A) Timeseries of the auditory stimulus (speech syllable /da/), and its the neural phase-locked evoked response extracted from the right auditory cortex in NREM2 and 3 sleep (combined). B) Location of the right auditory cortex region of interest from which data are extracted. C) Frequency domain plot of FFR amplitude across conditions. D) FFR fundamental frequency (98 Hz) amplitude during Spindle, Clear and Refractory periods. FFR: frequency-following response; Spindle: responses during a spindle; Refract: responses measured during the refractory period; Clear: responses measured during neither a spindle nor refractory period.

Hz). Filtering the same data in lower frequency ranges (i.e., 1.5 and 40 Hz Jourde et al. 2022; Eggermont & Ponton 2002) reveals "long latency" evoked responses (i.e., P100, P200) that are associated with other aspects of sound processing in the primary and secondary auditory cortex. The study design of Experiment 1 is unsuitable for examining these slower evoked components, as a too-short inter-stimulus interval is used to maximize the number of trials (Skoe & Kraus, 2010); more time must be left between sound stimulations to observe the brain's extended response to sound, which is in the order of seconds rather than hundreds of milliseconds as for the FFR. Getting a sufficient number of stimulations while leaving an inter-stimulus interval long enough to observe these long latency components require a longer sleep opportunity than a nap timeframe. We therefore adopted an overnight study design with a limited number of subjects and conducted statistics within-subject, assessing the consistency of results by repeating the process independently on multiple subjects using

linear mixed effect models (see Methods). Five neurologically healthy young adults without sleep conditions or taking medication were included in an overnight study. The mean age was 21.2 (SD: 1.33; range: 19-23), and 3 were female.

As in Experiment 1, sleep scoring analysis confirmed that all subjects slept reasonably well despite the constraints of the scanner. Importantly for the present analysis due to the presence of spindles, subjects spent 179 minutes (SD: 59) in NREM2 and NREM3 sleep stages (combined; see Table S2 for further details on sleep duration). On average, 690 spindles (740) and 1,655 slow oscillations (SD: 890) were detected per subject using EEG from NREM2 and NREM3 combined. During stages NREM2 and NREM3, an average of 224.8 stimulus presentations coincided with sleep spindles (SD: 81.8; range: 85-289) and 459.8 were presented during the refractory period (SD: 191.2; range: 149-614). An average of 2284.2 epochs were sorted into the Clear condition, in which stimuli did not arrive concurrently with a slow oscillation, or within nor immediately after a spindle (SD: 650.5; range: 1,325-2,850).

To confirm that the detection (at Cz) and sorting procedure was successful to separate time periods that included high and low spindle activity, we compared the electroencephalography absolute sigma band power (root mean square of the amplitude within 11-16 Hz; see Methods) during each of the three epoch types in a 2 second windows centred on the sound presentation. We confirmed that the distributions were statically different using a repeated measures ANOVA $F(2, 8) = 25.543$, $p < 0.001$) (see Figure S2). Post hoc analyses were conducted to confirm that each conditions was statistically different from the comparison (Clear) condition.Post hoc pairwise comparisons revealed that sigma band power was significantly greater in Spindle as compared with Clear (mean difference = 3.37e-6, SE = 5.18e-7, 95% CI = [1.81e-6 4.96e-6], $p < 0.001$) and Spindle as compared with Refractory (mean difference = 3.00e-6, SE = 5.18e-7, 95% CI = [1.44e-6 4.56e-6], $p < 0.001$). The Clear and Refractory conditions were not significantly different (mean difference = -3.71e-7, SE = 5.18e-7, 95% CI = [-1.93e-6 1.19e-6], $p = 0.495$).

To visualize whether the presence of a spindle or its refractory period influences the low-frequency cortical response, we first produced subject average evoked responses from extracted signals from the rAC for each of the three conditions (Clear, Spindle, Refractory period), within the 0.5-40 Hz frequency band; see Figure 4.9A. Following a similar logic to the FFR experiment, the unaltered appearance of cortical responses when sound onset coincides with an endogeneous sleep spindle would indicate that auditory information has passed through the thalamus and arrived at the cortex, unimpeded. The first components of evoked auditory responses (e.g., P100 and P200), i.e., those occurring within about 200 ms of sound onset, originate in auditory cortical areas (see Figure 3 in (Coffey et al., 2017a) for group-level whole-brain MEG topographies of the P1 and P2 components, see also Colrain

& Campbell 2007; Campbell 2010) and are reliably produced by the right auditory cortex during sleep (see Figure 6 in Jourde et al. (2022)). For statistical analysis of the amplitude of early components, we extracted both P100 and P200 amplitudes for each epoch based on their peak timing as observed in the group averages (20 ms windows centered on 80 ms for P100 and 200 ms for P200, in agreement with previous work (Lijffijt et al., 2009)). To confirm that P100 is observed in the absence of spindles and refractory periods (i.e., Clear condition), in the signal extracted from the right auditory cortex in each participant, we used simple non-parametric Wilcoxon signed-rank tests (one-tailed) to test the distribution of amplitude values across all single-trials epochs. For every subject, they were significantly higher than 0, meaning that a P100 component was clearly present (Sub 1: V = 1.96e6, p < .001; Sub 2: V = 0.69e6, p < .001; Sub 3: V = 1.06e6, p < .001; Sub 4: V = 2.95e6, p < .001; Sub 5: V = 1.95e6, p < .001). We conducted the same analysis for P200. For every subject, amplitudes were significantly higher than 0, meaning that a P200 component was clearly present (Sub 1: V = 1.54e6, p < .001; Sub 2: V = 0.68e6, p < .001; Sub 3: V = 1.08e6, p < .001; Sub 4: V = 2.59e6, p < .001; Sub 5: V =1.66e6, p < .001). Note that the P200 component in Figure 4.9A appears to be of lower amplitude in the Spindle condition because a single subject had a lower number of detected spindles and less evident P200 component (see Figure 4.9B and Table S2).

To robustly evaluate potential differences in amplitude of the P100 component depending on the presence of a spindle, its refractory period or its absence, we conducted LME analyses at the single trial level, using subjects as a random effect. We removed outliers from each Condition (Clear, Spindle and Refractory) by excluding values based on thresholds defined as 1.5 times the interquartile range (i.e., below Q1 and above Q3). The mean percentage of retained epochs across subjects was 93.7% (SD = 4.7). We compared a model with Condition as a fixed effect to a null intercept-only model and found that the addition of Condition did not significantly increase model fit ($\chi^2(2) = 1.62$, p = .44). Post-hoc analysis using estimated means did not show any statistically significant differences between conditions. (Clear-Refract difference, M = 2.04e-13 $pAm^{-}1$, SE = 8.68e-13, p = 0.97) and (Clear-Spindle difference $pAm^{-}1, M = 1.52e-12, SE = 1.19e-12, p = 0.41$).

We conducted the exact same analysis for P200 amplitude and found similar results. The mean percentage of retained epochs across subjects was 93.2% (SD = 4.6). We compared a model with Condition as a fixed effect to a null intercept-only model and found that the addition of Condition did not significantly increase model fit ($\chi^2(2) = 5.95$, p = .05). Post-hoc analysis using estimated means did not show any statistically significant differences between conditions. (Clear-Refract difference, M = -1.47e-12, SE = 1.06e-12, p = 0.35) and (Clear-Spindle difference, M = 2.63e-12, SE = 1.44e-12, p = 0.16). For completeness, we also

ran Bayesian statistics on each subject on epoch-level data, finding coherent results (please see Table S3). These results indicate that the occurrence of spindles and their refractory period does not affect auditory cortical responses associated with early sound processing in the primary and secondary auditory cortex (P100, P200).

Later components (N550-P900) associated with widespread changes in brain activity and evoked slow oscillations (Jourde et al., 2022), which are integral to sleep-dependent memory consolidation particularly when they are coupled to sleep spindles (i.e. co-occurring in a phase-amplitude relationship), have been shown to be dependent upon brain activity at the time of sound onset (Ngo et al., 2013b, 2015, 2019; Choi et al., 2020; Harrington & Cairney, 2021)). As auditory stimulation has been used to alter memory processes non-invasively in a technique known as closed-loop auditory stimulation (CLAS), it is of interest to further explore the influence of spindles on how well CLAS generates additional slow oscillations and spindles in a reactive fashion.

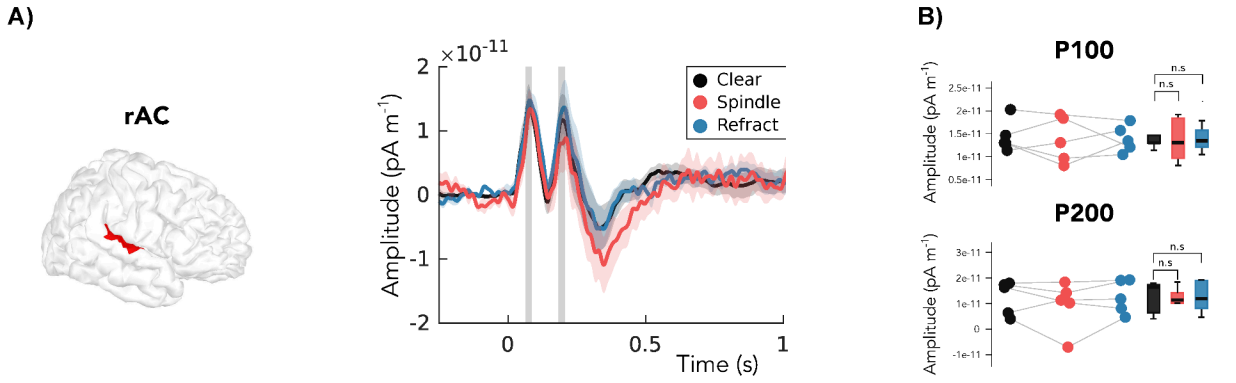

Figure 4.9: The presence of neither a spindle nor its refractory period greatly affects the slow cortical evoked responses 'P100' and 'P200' (filter: 0.5-40 Hz). A) Timeseries of the auditory evoked responses in electroencephalography (Cz electrode), by condition. The right auditory cortex region of interest is shown at left. B) Within-subject means across all epochs are indicated by horizontal lines; amplitudes were similar across all three conditions.

4.4.3 Experiment 3: Evidence that sleep spindles do not reduce the effect of closed-loop auditory stimulation

Because slow oscillation-spindle coupling, i.e co-occurrence of the spindle and the up-state of the slow oscillation, is thought to be particularly important for memory consolidation (Staresina et al., 2023)), and because sound presented during up states provokes additional slow wave and spindle activity and boosts memory performance (closed-loop auditory stimulation) (Ngo et al., 2013b, 2015, 2019)), we investigated whether the co-occurrence

of spindles during CLAS affects its effectiveness (i.e., ability to generate slow oscillations and spindle activity). As <10% of slow oscillations are coupled with spindles (Hahn et al., 2020)), and each stimulation must be separated by several seconds to allow for the analysis of the slower evoked components (Jourde et al., 2022), more data per participant are needed to address this research question. Experiment 3 used an at-home design so as to record 5 nights per subject.

Seventeen participants were included in this multiple-night experiment. The mean age was 27.56 (SD: 9.39; range 22-43), and 9 were female. On average, the mean number of usable recordings per subject for the remaining 17 subjects was 4.71 (SD: 0.77) (see Table S4). On average 7,300 spindles (SD: 2,590) and 12,150 slow oscillations (SD: 4,720) were detected (at Fpz) per subject using EEG (NREM2 and NREM3). The mean number of total stimulations was 6,437.65 (SD: 2,463.19), and sham stimulations (in which a SO peak was detected but not stimulated, for comparison) was 5,716.41 (SD: 2,271.22). The mean number of spindles occurring during stimulated SOs was 361.76 (SD: 190.96), and spindles occurring during sham stimulations was 349.82 (SD: 177.67). In accordance with previous observations, the mean percent coupling across all detections was 6.50% (SD: 3.74).

To confirm that CLAS generates a subsequent SO, as has been observed in previous work (e.g., (Ngo et al., 2013b; Harrington & Cairney, 2021; Choi et al., 2020)), we first filtered the signal in the slow wave activity (SWA) range (0.5 to 1.5 Hz) and compared the amplitude of the generated slow oscillation between all Stimulation and Sham trials. A paired sample t-test was conducted to assess the differences in mean amplitude in the SO range between 0.5 and 1.5 second post stimulation (Ngo et al., 2013b) in both Stimulation and Sham conditions. It revealed a significant difference in amplitude between the Stim and Sham conditions ($t(16) = 5.69$, $p < .001$, Cohen's $d = 1.38$). These results replicate previous findings (Ngo et al., 2013b) showing that the mean amplitude in the stimulation condition was significantly higher than in the sham condition (see Figure 4.10A).

Next, we split epochs according to the presence or absence of spindles (Coupled SO and Uncoupled SO) to assess the impact of the presence of a sleep spindle at the time of stimulation. A paired sample t-test revealed a significant difference in amplitude between the Coupled Stim and Coupled Sham conditions ($t(16) = 4.30$, $p < .001$, Cohen's $d = 1.04$). This result suggests that the presence of a sleep spindle nested in the SO up-state does not prevent the physiological effect induced by auditory stimulation.

To confirm that CLAS also increases fast spindle activity as has been observed (Ngo et al., 2013b), we first filtered the signal in the fast sigma range (12-15 Hz; Ngo et al. 2013b) and compared the route mean square within that band during the generated SO (0.75 to 1.25 s post SO upstate detection), between Stimulation and Sham across all trials. Spindle

activity following stimulated SOs was significantly larger than that after unstimulated SOs ($t(16) = 4.14$, $p < .001$, Cohen's $d = 1.00$) We then split epochs according to the presence or absence of spindles to assess the impact of the effect of sleep spindle presence at the time of stimulation. A paired sample t-test was conducted to assess the differences in both Coupled Stimulation and Coupled Sham conditions; it revealed a significant difference in amplitude between the Coupled Stim and Coupled Sham conditions ($t(16) = 2.28$, $p = 0.01$, Cohen's $d = 0.55$). This result suggests that the presence of a sleep spindle nested in the SO up-state does not prevent the physiological effect induced by auditory stimulation (see Figure 4.10B). In sum, sleep spindles do not impede the physiological enhancement of SOs and spindle activity by CLAS.

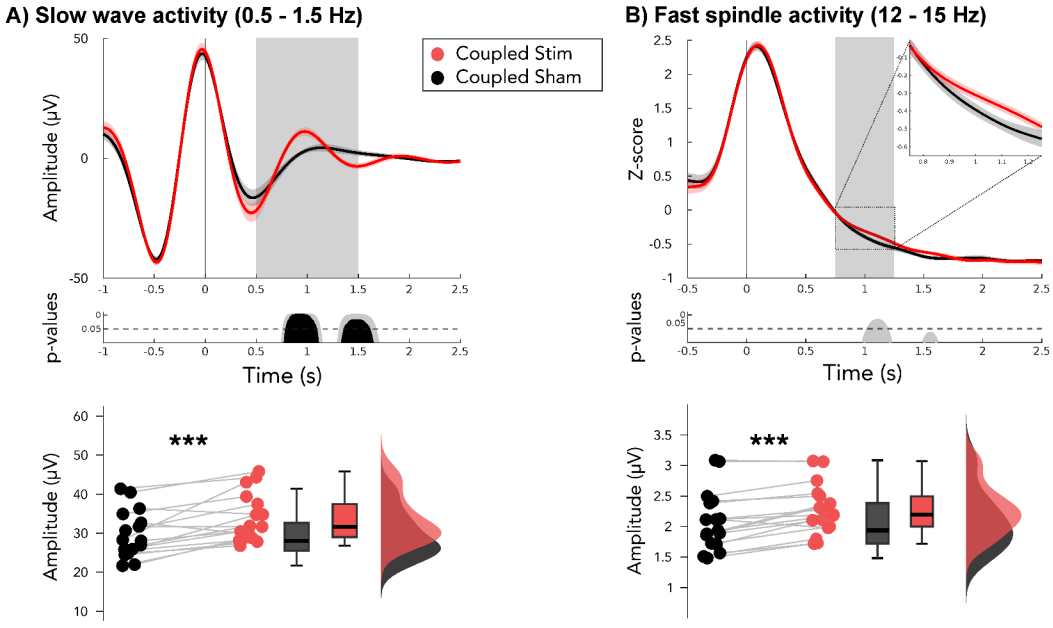

Figure 4.10: The presence of a spindle coupled to a slow oscillation up-state does not impede closed-loop auditory stimulation effects on slow wave nor fast sigma activity at electrode Cz. A) Timeseries of low-frequency EEG time-locked to the detected SO up state in both Stim and Sham conditions only when the detected slow wave was coupled to a sleep spindle. Statistical significance of the difference between conditions is represented below. Grey shading represent uncorrected p-values and black shading represent these p-values after Benjamini-Hochberg correction. Amplitude (RMS) of the subsequent (generated) SO across conditions are reported for each subject, below. B) Timeseries of amplitude (z-score of root mean square) in the fast sigma band (12-15 Hz) for both stimulated and non-stimulated coupled slow oscillations. Statistical significance of the difference between conditions is represented below the timeseries. Amplitude (RMS) of the subsequent (generated) fast sigma activity across condition are reported for each subject, below. Red = Stimulation, Black = Sham. Error bars = standard error. *** p-values < 0.001

4.5 Discussion

Our results suggest that neither the co-occurrence of sleep spindles nor their refractory periods decrease time-resolved indices of auditory processing in healthy adults. In the first experiment we showed that the amplitude of the frequency-following response extracted from the right auditory cortex was conserved across conditions. These data indicate that the lemniscal pathway that carries fine sound information from the auditory periphery to primary auditory cortex (via the auditory nerve, cochlear nucleus and inferior colliculus in the brainstem, and medial geniculate body in the thalamus), operates independently from spindle dynamics (Figure 4.8).

In the second experiment, we measured the more commonly-recorded long-latency evoked responses, P100 and P200. P100 in humans is thought to be generated in non-primary regions of the superior temporal gyrus that are innervated by extra-lemniscal auditory input from non-specific thalamic nuclei (e.g., medial pulvinar, nucleus limitans and suprageniculate nuclei), wheres P200 is generated by downstream processing steps over an extended area of the auditory cortex (Stroganova et al., 2013; Yvert et al., 2005; Kaas et al., 1999; Eggermont & Ponton, 2002). As with the FFR, neither the P100 nor P200 evoked components were noticeably diminished by the presence or recent history of a spindle (Figure 4.9). This result indicates that a second branch of the auditory processing pathway, which is dependent upon different thalamic regions than the FFR, is also not strongly affected by spindle activity.

In the third experiment, we investigated how physiological responses to closed-loop auditory stimulation of cortical slow oscillations are affected by the presence of spindles. The process of generating slow oscillations and sleep spindles is thought to be mediated via the ascending reticular activating system sending inputs to ventral frontal regions that are strong generators of slow waves in sleep Bellesi et al. (2014); Jourde et al. (2022). Under the hypothesis that sleep spindles serve in part to suppress sound and preserve the sleep state, their presence would be expected to reduce or eliminate the previously demonstrated effect of the auditory stimulation on slow wave activity and fast spindle activity. However, instead we find that stimulation during spindles generates additional slow oscillation and spindle-band activity, as has been noted in previous work that did not distinguish between slow oscillations that were coupled with spindles and those that were not (e.g., (Ngo et al., 2013b)). This result suggests that a third means through which sound can influence cortical activity is also functional during spindles and their refractory periods (Figure 4.10).

The idea that sleep spindles play a protective role in sleep comes from several lines of research (summarized in (Fernandez & Lüthi, 2020)). In undisturbed NREM sleep, the density of spindles correlates with the duration of NREM2 sleep (Purcell et al., 2017), and people who

generally have more spindles exhibit higher tolerance for sleeping in noisy conditions (Dang-Vu et al., 2010). In rodents, optogenetic manipulations that increase spindle activity increase the duration and stability of NREM2 sleep (Kim et al., 2012; Ni et al., 2016). A relationship between sleep spindles and sleep continuity is also observed in aging human populations, in whom sleep spindle amplitude and density are reduced (Crowley et al., 2002; Clawson et al., 2016). Sleep spindle density is correlated with sleep efficiency and stability across the lifespan (Li et al., 2022; Mander et al., 2014; Pace-Schott & Spencer, 2014). Studies experimentally investigating arousability in humans and rodents also implicate sleep spindles in protecting the sleep state. Enhancing sleep spindles causally, either pharmacologically (using benzodiazepines) in humans (Johnson et al., 1976), or through genetic manipulations in animal models (Wimmer et al., 2012), elevates arousal thresholds. Another line of work looks at how the brain's responses to sensory input changes over brain states. For example, Mai et al. noted that frequency-following response amplitude was lower during recordings in which more sleep spindles were present (Mai et al., 2019). As regards longer-latency auditory evoked responses, results are unclear. Elton et al. observed some difference in gross ERP morphology of responses to sounds occurring close to spindles vs. when they were absent, when sounds were presented to 6 participants (at 65 dB sound pressure level). P100 and P200 appeared to have higher amplitude during spindles (Elton et al., 1997). Cote et al. investigated P200 amplitude in response to different sound levels across sound levels of 60, 80, and 100 dB in eight participants. They did not observe differences between responses to sounds that were concurrent with spindles vs. those which were not (although they did find a difference at high sound intensities with a third condition, in which spindles occurred after sound presentation - possibly related to the CLAS effect) (Cote et al., 2000).

One reason for lack of clarity on the relationship between spindles and sensory information might be a matter of definition. Many studies invoking the thalamic gating hypothesis (according to which the thalamus filters sensory input during sleep spindles) do not differentiate between the potential roles of spindles in preventing sensory information from reaching cortex; or alternatively, in producing a subsequent, reactive response that could stabilize the sleep state itself (preventing an arousal from a subsequent sensory event). The terms 'protective' and 'reactive' were used to distinguish these ideas in a recent review (Fernandez & Lüthi, 2020); however, they may still be ambiguous. For example, 'protective' might refer to shielding endogenous sleep-related cognitive processes (like memory consolidation) from external interference. Or, 'protective' could mean maintaining the sleep state itself, which could include generating slow oscillations and spindles in the seconds following a response (which would also fit under the 'reactive' term) - or even just not causing an arousal, as in studies that evaluate propensity to waking following sensory input. In the latter case, a

mechanism is still lacking, returning us to the question of whether sleep spindles modulate the strength of sensory input to higher-level processes.

Importantly, auditory transmission is fast; information travels from ear to cortex in less than 15 ms (Parkkonen et al., 2009). If the spindle were to gate sensory information to cortex as a protective mechanism, the spindle must already have started when sound information arrives at the thalamus for a blocking mechanism to make sense. For this reason, study designs that specifically separate brain responses according to their co-occurence with spindles are critical to clarify the question of whether spindles play a protective role by impeding sound transmission.

To date, few studies have directly assessed responses to sound presented during a spindle. In addition to the two ERP studies presented above (Elton et al., 1997; Cote et al., 2000), a notable exception is a pair of studies which used simultaneous EEG to mark the timing of sleep spindle and functional magnetic resonance imagining (fMRI) to investigate brain responses to tones during wakefulness and NREM sleep Dang-Vu et al. (2011); Schabus et al. (2012). The authors showed that whereas elicited responses were observed in the thalamus and the transverse gyrus during wakefulness as well as during NREM, responses were smaller and more variable when sounds were presented during a sleep spindle, suggesting that sound information is less prone to be faithfully transmitted to the cortex. They concluded that changes in sensory processing at the thalamic level during spindles allows for functional isolation of brain circuits from incoming stimuli, to promote and protect cellular interactions underpinning brain plasticity. However, other researchers have suggested that the higher response variability observed in these studies may also reflect a low number of trials recorded during sleep spindles (Sela et al., 2016).

A potential issue for the idea that spindles impede sensory transmission is that quite a lot of cortical sensory processing seems to take place during sleep, including spindle-rich sleep stages (NREM2 and NREM3; reviewed in (Andrillon & Kouider, 2020)). In mice, presenting meaningful sounds (especially those previously associated with aversive tasks), can lead to disruptions in sleep-associated brain oscillations without necessarily causing full behavioural arousal (van Kronenberg et al., 2022). In-line with these findings and the observation that voice familiarity is processed in NREM (and also REM) sleep stages, Blume et al. proposed that the auditory system acts as a 'sentinel system' by continuing to evaluate environmental stimuli and initiate awakenings when necessary to respond to potential threats (Blume et al., 2018). While some of these processes, particularly those involving fear conditioning, may be mediated by subcortical structures (e.g., thalamo-amydala circuitry (Goosens & Maren, 2001)), evidence for higher-order (cortical) information processing in humans has also been reported during spindle-rich NREM sleep. For example, sleepers are able to selectively amplify

informative vs. meaningless competing speech streams in NREM (and REM) sleep (Legendre et al., 2019; Koroma et al., 2020). It is hard to reconcile a role for intermittent spindle activity in generally suppressing sensory transmission to cortex with a role for the auditory system to monitor the environment, particularly if higher-level cognitive processing such as recognizing and separating sound sources is needed.

To our knowledge, only one group has conducted time-resolved spindle analyses investigating auditory processing with direct recordings from the auditory cortex. In 2016, Sela et al. measured local field potentials and multi-unit activity responses to auditory stimuli in rat primary auditory cortex. They reported that when sleep spindles (measured locally) co-occurred with the stimulus, neural responses were nearly identical in terms of local field potential morphology (latency and amplitude) and multiunit activity firing rate to those observed across NREM sleep (<6% difference). Even when narrowing their analysis to a subset of the highest amplitude sleep spindles so as to maximize the sensitivity of the analysis to amplitude modulations, they did not observe weakening of the responses, nor was there a correlation between strength of auditory response and sigma power Sela et al. (2016). These results make a strong case against spindles impairing auditory thalamocortical transmission, although the authors acknowledge the restriction of the conclusions to auditory activity in primary auditory cortex (likely through the lemniscal pathway), leaving open the possibility that sleep spindles impair auditory processing downstream in other auditory (or nonauditory) regions Sela et al. (2016). The view that spindles play an active role in blocking sound continues to be prevalent, particularly in human literature Mai et al. (2019); Fernandez & Lüthi (2020); Nicolas et al. (2022); Weiner et al. (2023). In the present work, we investigated this question in humans using MEG and EEG to assess auditory processing in the presence of sleep spindles through the main leminiscal pathway (see Figure 4.8) as well as other non-lemniscal auditory pathways (see Figures 4.9 and 4.10).

Our results using time-resolved and whole-brain techniques suggest that the presence of sleep spindles doesn't significantly impede auditory information from reaching the cortex through neither lemniscal nor two non-leminiscal auditory pathways. Previous work has shown that evoked responses to sound do however change considerably across NREM and REM sleep stages (Jourde et al., 2022; Colrain & Campbell, 2007). One explanation that might reconcile the discrepancy between our observations from EEG/MEG showing that evoked responses are preserved and those from earlier work showing that hemodynamic responses are reduced during spindles (Dang-Vu et al., 2011; Schabus et al., 2012) could be that it is not the thalamic relay itself that impedes sound transmission but rather the state of the cortex upon arrival of sensory information that determines its cognitive fate (the cortical gating hypothesis (Esser et al., 2009; Andrillon & Kouider, 2020)). Overall

differences in levels of neurotransmitters within the system, which do vary considerably across sleep state and affect neural firing patterns (Datta, 2010), could perhaps affect the ability of auditory information to propagate within the cortex due to changes in tissue properties and/or functional connectivity between brain areas during sleep (Massimini et al., 2005).

Recent work highlighted that sleep spindles are organized temporally according to an infraslow rhythm of around 0.02 Hz. This would correspond to sleep spindles being clustered within spindle-rich and relative spindle-free periods of 50 seconds alternating throughout the night. Interestingly, this pattern aligns with the alternating organization of NREM sleep into fragility and continuity periods, distinguished by acoustic arousability (Lecci et al., 2017) and also observed in autonomic physiological fluctuations such as heart-rate rhythm in humans (Lecci et al., 2017) but also pupil diameter (Yüzgeç et al., 2018) and brain temperature in rodents (Csernai et al., 2019). This prevalent 0.02 Hz rhythm then might reflect a widespread brain-body rhythm impacting behavioural arousal, brain activity, and cortical cellular dynamics. In that case, the decrease in auditory cortex activity observed in previous neuroimaging studies might come from a decrease in general functional connectivity during deeper sleep and perhaps specific windows of time during which spindles happen to be more common, rather than due to thalamic gating during the spindle itself. We propose that spindles are one of many consequences of this sleep protective mechanism rather than its cause. Further work might consider assessing auditory processing comparing epochs not based on the presence or absence of a spindle but rather on their timing relative to other physiological processes (e.g., infraslow rhythm, phase of slow oscillation, evolution of spindle envelope), and using complementary study designs which quantify sleep fragmentation as a function of sensory stimulation (e.g., with longer inter-stimulus intervals and varied stimulus intensity), using sensitive measures of arousal (Stepanski, 2002). Furthermore, the physiological and behavioural impact of targeting spindles with different properties (i.e., fast vs. slow; Mölle et al. 2011) and from different brain regions (Vantomme et al., 2019) remains to be explored.

4.6 Conclusion

Altogether, our data suggest that auditory information reaches the cortex through multiple pathways even during the presence of a sleep spindle (and its refractory period). These data therefore do not support a direct role of sleep spindles in protecting the sleep state by impeding its interruption by auditory input. This view is coherent with Sela et al.'s observation that cellular-level responses to sound in auditory cortex in rats are unchanged by sleep spindles Sela et al. (2016), and with the idea that the roles of sleep spindles lie in other directions, for example in active memory consolidation as has been suggested in previous

work (reviewed in (Fernandez & Lüthi, 2020)). More research is needed to clarify whether these results might extend to other sensory modalities (e.g., vision, touch), which seems likely considering that non-arousing somatosensory and visual stimuli generally evoke similar brain responses to auditory stimuli in sleep (Sato et al., 2007; Riedner et al., 2011), and to evaluate the hypothesis that electrochemical changes in cortical tissue are responsible for observed differences in evoked responses across sleep stages. It also raises questions that can only be answered using more granular levels of investigation, i.e., concerning how distinct firing modes in thalamus during spindles can in fact still allow for transmission of sensory information. Finally, our results show that sounds presented during concurrent slow oscillations and sleep spindles generate additional slow oscillations and spindle activity, as has been shown when slow oscillation up-states are stimulated randomly with respect to spindle presence (Ngo et al., 2013b). As closed-loop auditory stimulation has generated a lot of interest for its potential to causally investigate the roles of neural oscillations and restore them in disease states (Van den Bulcke et al., 2023; Grimaldi et al., 2020; Romanella et al., 2020; Harrington & Cairney, 2021; Choi et al., 2020), this result encourages further exploration into how and when sound can be used to modulate and improve sleep-dependent brain processes (Valenchon et al., 2022).

4.7 Acknowledgements

The authors would like to acknowledge team members past and present who assisted in data collection: Arina Ujevco, Noam Thillou, Meredith Rowe, Keelin Greenlaw, Alix Noly-Gandon and Raphaëlle Merlo. We thank Karine Lacourse for advice concerning spindle detection; David Levesque and Latifa Lazzouni for developing and testing the SO detection algorithm on the ecHT; and David Wang for technical assistance with the ecHT; Sylvain Baillet and Marc Lalancette for assistance with MEG access and technical matters.

Chapter 5

Neurophysiological effects of targeting sleep spindles with closed-loop auditory stimulation

5.1 Abstract

Sleep spindles are neural events unique to non-rapid eye movement sleep that play key roles in memory reactivation and consolidation. However, much of the evidence for their function remains correlational rather than causal. Closed-loop brain stimulation uses real-time monitoring of neural events (often via electroencephalography; EEG) to deliver precise auditory, magnetic, or electrical stimulation for research or therapeutic purposes. Automated online algorithms to detect and stimulate sleep spindles have recently been validated, but the time and frequency-resolved physiological responses generated by them have not yet been documented. Building on the recent findings that sleep spindles do not block the transmission of sound to cortex, the present work investigates the neurophysiological responses to closed-loop auditory stimulation of sleep spindles. EEG data were collected from 10 healthy human adults (6 nights each), whilst sleep spindles were detected and in half the nights, targeted with auditory stimulation. Spindles were successfully stimulated before their offset in 97.6% of detections, and did not disturb sleep. Comparing stimulation with sham, we observed that stimulation resulted in increased sigma activity (11 to 16 Hz) at about 1 s post stimulation, but that stimulation occurring at the beginning of the spindle also resulted in early termination of the spindle. Finally, we observed that stimulating an evoked spindle did not elicit additional sigma activity. Our results validate the use of closed-loop auditory stimulation targeting sleep spindles, and document its neural effects, as a basis for future

causal investigations concerning spindles' roles in memory consolidation. This paper is part of the Festschrift in honor of Dr. Robert Stickgold Collection.

5.2 Introduction

Sleep spindles are transient (0.5 to 2.5 s) neural events with frequencies of 11 - 16 Hz, which are specific to non-rapid eye movement sleep. They are believed to be instrumental for sleep-dependent memory reactivation and consolidation (see Fernandez & Lüthi 2020 for a recent review of spindle function, and Rasch & Born 2013; Brodt et al. 2023 for current thinking about sleep's role in learning and memory). There has been much pioneering work describing sub-types of sleep spindles Cox et al. (2017), how spindles differ between individuals Purcell et al. (2017), and how they are related to memory deficits in clinical populations (for example in schizophrenia Wamsley et al. 2012; Manoach et al. 2016; Manoach & Stickgold 2019). However, the majority of evidence concerning their roles is either from invasive investigations using non-human animals (Latchoumane et al., 2017), or from correlational studies in humans (Tamminen et al., 2010; Payne et al., 2008).

Non-invasive brain stimulation techniques offer the possibility of precisely interacting directly with neural brain processes so as to educe evidence for their roles in complex, real-world learning which is relevant to human cognition (Kumar, 2021; Occhionero et al., 2020; Antony et al., 2012). Closed-loop brain stimulation is a technique in which neural events of interest for research or therapeutic purposes are measured (frequently using electroencephalography; EEG) and quickly identified in real-time, such that auditory, magnetic or electrical stimulation can be used to interact with brain processes in a temporally-precise fashion. This technique has been used successfully to enhance slow oscillations (SOs: 0.5 - 1.5 Hz), which, like spindles, are involved in memory consolidation (Staresina et al., 2015). By stimulating SO up-states, when cortical neurons are partly depolarized and more excitable, Ngo et al. enhanced the amplitude of SOs and reported an overnight improvement in memory performance (Ngo et al., 2013b). These results have now been replicated and extended (see Harrington & Cairney 2021; Fehér et al. 2021; Choi et al. 2020; Salfi et al. 2020 for reviews), demonstrating the effectiveness of precisely-timed non-invasive auditory stimulation in modulating neural events – and the techniques' scientific value for investigating the neural substrates of memory processes. In previous work, Jourde et al. (2024), investigated the neural mechanism by which sound influences slow oscillations and found it likely to be related to a domain-general activation of the ascending reticular activating system, in accordance with prior hypotheses (Bellesi et al., 2014). It has also been confirmed that sleep spindles do not significantly attenuate brain responses to acoustic information (Jourde & Coffey, 2024; Sela et al., 2016), which

would have precluded using auditory stimulation as a means of interacting with endogenous processes associated with sleep spindles.

Sleep spindles can be induced by brain stimulation in an open-loop fashion, either as part of an evoked response to an impulse (e.g., as seen in Ngo et al. 2013a), or in the form of entrainment to frequency-modulated stimulation. Lustenberger et al. (2016) applied transcranial alternating current stimulation (tACS) within the spindle frequency range (12 Hz) and observed enhanced cortical synchronization. The degree of stimulation-induced change in fast spindle activity was correlated with enhancement of motor (but not declarative) memory consolidation. Using a similar approach but in the auditory modality, Antony & Paller (2017) explored the induction of spindles using auditory steady-state stimulation. Their design involved presenting white noise modulated at 12 Hz, 15 Hz, or 50 Hz, intermittently during NREM2 or NREM3; the intervention did increase spindle activity. In a follow-up study, the same team investigated how the timing of stimulation affected memory performance in a spatial location task. They concluded that stimulation delivered well after a spindle (i.e., 2.5 sec after a spindle offset) resulted in better performance compared to stimulation sent immediately after the spindle (i.e., within 0.25 s of spindle offset; Antony et al. 2018), suggesting a post-spindle refractory period.

A series of nap experiments by Choi et al. (Choi et al., 2018, 2019; Choi & Jun, 2022) regroups initial attempts at the challenging task of detecting spindles in real-time and stimulating them, with short bursts of pink noise (i.e., closed-loop auditory stimulation; CLAS). Due to detection latency of the equipment, however, the majority of auditory stimulations occurred after the spindles had already ended, with only 20 - 23% of stimulations hitting the desired target sleep event. They showed that stimulating towards the end or after a spindle enhances both slow wave and sleep spindle activity (Choi & Jun, 2022), as occurs generally with stimulation during NREM sleep stages 2 and 3 (Bastien et al., 2002; Colrain, 2005; Jourde & Coffey, 2024). Their results also suggested that stimulation at the end of the spindle rather than presented in a randomized fashion might reduce sleep fragmentation in a nap setting, and potentially increase procedural memory consolidation. Because spindles have proven difficult to target, and because fine-grained analysis requires many stimulations and thus multiple nights of recordings, there remain few studies and many open questions on the neurophysiological effects of the timing of stimulation on evoked neural oscillations (and their cognitive and behavioural consequences). Furthermore, it is unknown whether spindles evoked by sound can in turn be stimulated to generate additional, trained spindles.

Automated online algorithms to detect and stimulate sleep spindles in real-time have recently been validated (Hassan et al., 2022; Valenchon et al., 2022). In our previous work, we introduced the Portiloop, a deep learning-based, portable and low-cost closed-loop stimulation

system able to target specific brain oscillations, and validate its ability to detect spindles in a large database of sleep recordings in a simulated online context (Valenchon et al., 2022). However, work to date was conducted offline to document detection performance; the physiological response to single-pulse auditory stimulation successfully delivered selectively during spindles has not yet been documented. Confirming that sleep spindles can effectively be targeted under experimental conditions and measuring the neurophysiological effects of auditory stimulation is a necessary precursor to applying these techniques to questions about the roles of spindles in learning and memory.

In the present work, we collected EEG data from 10 healthy human adults (6 nights each), whilst sleep spindles were detected, and in half the nights, targeted with auditory stimulation. We document the neurophysiological effect of closed-loop auditory stimulation across frequencies in the seconds following stimulation, and further evaluate when and how stimulation timing affects spindle and slow oscillation activity, which have been tied to processes of memory consolidation in literature. Our results validate the method of closed-loop auditory stimulation targeting sleep spindles, and document the neural effects as a basis for future causal investigations concerning spindles' roles in memory consolidation.

5.3 Methods

5.3.1 Participants

Ten neurologically-healthy adults were recruited from the local environment (6 female, M= 28.9 years, SD = 7.4, range = 23-45). Participants were screened via self-report for neurological, hearing, sleep problems, and sleep or wakefulness altering drug usage (which can affect spindle density; Plante et al. 2015). Participation was on a voluntary basis. This research received approval from Concordia University's Research Ethics Board.

5.3.2 Study design

Participants were first screened for neurological conditions and briefed about the nature of their involvement. Following recruitment, participants received a kit containing the required equipment (i.e., Portiloop, electrode bundle, battery, skin cleaning supplies, electrode paste, tape, earphones, etc.), and detailed instructions as regards equipment operation, electrode placement, sound testing, and factors affecting signal quality. Each participant met with an experimenter to be trained on the handling of the material and data collection was closely monitored by the experimenter in the morning after each recording, ensuring proper electrodes

placement and optimal data quality for an at-home multi-night design. If the data quality was suboptimal, the experimenter contacted the participant to remind them of the procedure. Participants were asked to select 6 nights during which they expected to have a normal sleep schedule. We elected to collect multiple nights of sleep data on a small group of subjects to buffer against data loss due to electrode detachment or improper placement in the home environment, and to obtain a large number of epochs per subject. Subjects were asked to alternate between stimulation and sham nights (i.e., during which sleep spindles were detected and marked, but no sound was delivered).

5.3.3 Closed-loop auditory stimulation

Closed-loop auditory stimulation was accomplished using the Portiloop v2, a portable EEG system that is capable of stimulating sleep spindles with sound within about 300 ms of spindle onset as detected using offline algorithms (Valenchon et al., 2022). In brief, the detection algorithm running on the Portiloop is a model based on a Convolutional Neural Networks (CNN) followed by a Recurrent Neural Networks (RNN), trained on a gold-standard annotated dataset (Massive online data annotation; Lacourse et al. 2020) to provide a real time confidence score of the presence or absence of a sleep spindle. Based on performance evaluation and validation work described in Valenchon et al. (2022), we set a confidence threshold of 0.75 for the current experiment. Portiloop is in active development, with recent additions including online sleep scoring subject-specific adaptation (Sobral et al., 2025); the current work uses the architecture described in Valenchon et al. (2022). Portiloop plans are available to the community as an open science initiative to encourage further development and advance closed-loop neuroscience research[1].

The electrode montage consisted of four midline positions (Fpz, Fz, Cz, Pz), with a unilateral (left) reference placed on the left mastoid and a ground electrode placed on the left earlobe. A 'right-leg-drive' circuit (i.e., the built-in bias drive amplifier' in the Portiloop's EEG amplifier; Texas Instruments ADS1299) is used to ensure good common-mode rejection ratio (CMRR) performance, removing sources of environmental noise that are common across electrode sites (Yang, 2021). In brief, the signal from the electrodes that are not used for detection (i.e., Fpz, Fz and Pz) are averaged and reinjected at the left earlobe ground electrode. This configuration greatly reduces signal contamination from environmental sources such as 60 Hz power line noise and enhances signals that are relatively focal to Cz, notably fast spindles, allowing for their detection even in electrically unshielded environments. The midline configuration of the electrodes as selected in the current study also has the

[1] `https://github.com/Portiloop`

effect of slightly modulating the appearance of the evoked responses recorded using the same configuration as compared to that observed in a standard Cz-mastoid channel; specifically, neural patterns with a focal topography close to Cz (such as first components of the auditory evoked response) have higher relative amplitude to neural patterns with a more distributed topography such as evoked slow oscillations (note that amplitudes from different montages across studies are not directly comparable). The Cz electrode was used for spindle detection. Electrodes were secured with tape or gauze, according to hair coverage. Data were recorded locally on the Portiloop device at a sampling rate of 250 Hz and were transferred to the experimenter upon equipment return.

Sound stimulation consisted of 15 ms pink noise bursts (with 5 ms cosine ramps to avoid earphone clicks; normalized to -1 to +1 μV and sampled at 48,000 Hz), presented binaurally at 55 dB SPL, a sound level that generates robust evoked neural responses yet does not awaken participants (Jourde et al., 2024).

The minimum interval between stimulations was set to 400 ms (selected based on pilot testing, to minimize the likelihood of a single spindle being detected and stimulated twice). Broadband (pink) noise was selected for similarity to the majority of CLAS work published to date, and because it generates a robust response that is likely invariant to minor differences in hearing sensitivity between subjects due to broad recruitment across the basilar membrane, noting that the underlying mechanism by which CLAS influences endogenous oscillations does not seem to depend on the type of noise used (Debellemanière et al., 2022; Bellesi et al., 2014; Jourde et al., 2024). Sound was delivered through commercially-available earbuds (Hiro: wired, Wicked Audio) which were secured in the ear using medical tape. This design choice was made to support our wider goals of making closed-loop research tools widely available and cost-effective (Valenchon et al., 2022). All participants used the same earphones, with the same configuration.

5.3.4 EEG processing and analysis

We analyzed data from three our of the four electrodes (Fpz, Fz and Cz) due to the high heterogeneity in data quality on the fourth electrode (Pz), which is located towards the back of the scalp and frequently becomes detached. All data were analyzed in Python using custom scripts based on freely accessible packages. NumPy was used for array manipulation, SciPy's signal module (scipy.signal) for filtering operations (including notch, bandpass, and band-specific filtering with butter and filtfilt), and Matplotlib for visualizing both the frequency response of the filters as well as the average brain responses. A 4th order Butterworth band-pass filter (0.5 to 30 Hz) was applied to look at event-related potentials

and to compute the event-related spectral perturbations. Epochs were extracted (-15 s to 15 s following spindle detection), baseline-corrected over the mean amplitude of the signal prior to the detection (from -1.5 s to -1 s). This window was defined to avoid capturing the potential change in amplitude generated by slow oscillations occasionally coupled with the detected sleep spindle (Clemens et al., 2007).

To control for data quality, a custom artifact rejection script was applied to each recording, which automatically removed poor sections of data by detecting both the absolute amplitude of the signal (for electrode-off detection) and sudden changes in amplitude (such as those caused by movements). Epochs with amplitudes exceeding +/- 200 μV were excluded. Due to the design choice of setting the minimum stimulation delay to 400 ms, note that it is not possible to definitively differentiate between detected sleep spindles that are endogenous and those that are evoked by stimulation. To ensure that each epoch contained only a single stimulation event, so as to characterize brain responses uninterrupted by additional stimulation, only stimulations spaced at least 2.5 seconds apart were included in the main analysis.

Event-related spectral perturbation plots were computed using the Python package scipy, with segments of 100 datapoints (approximately 0.4 seconds) and a 50 % overlap. Statistical comparisons were computed across subjects for each time-frequency bin and corrected for False Discovery Rate using a Benjamini-Hochberg correction (alpha = 0.05). Concerning the analysis of the impact of stimulation in the slow-wave band, analysis was similar except the use of a different 4th order Butterworth band-pass filter (0.1 to 4 Hz), which was applied to the raw data. Similarly, analysis of the spindle band activity followed a similar procedure with a third filter (same parameters with a 11-16 Hz frequency band). For each analysis, the filters were applied before defining epochs to avoid border effects. Because phases of both the detected and evoked sleep spindles can vary, we used the envelope of the signal as our metric to estimate instantaneous spindle power.

To quantify the distribution of stimulation delays achieved by the online detection algorithm, we implemented an offline detection method based on sigma power deviation, as defined in the work by Choi & Jun (2022) (see Supplementary Figure S1 for a detailed characterization of our online sleep spindle detection).

To investigate the long-term effects of stimulation and ensure the maintenance of sleep continuity, we calculated the cumulative sigma power for both STIM and SHAM conditions by summing the amplitude of the envelope signal during the 15 seconds following stimulation. For this and subsequent analyses, we focused on Cz, which showed clear evoked responses in both frequency ranges of interest. Temporal statistical comparison was computed using subjects averages and corrected similarly using the Benjamini-Hochberg procedure (both

uncorrected and corrected p-values are represented below the timeseries figures).

We also investigated the interaction between stimulation timing and electrophysiological outcomes by sorting epochs based on the relative position of the stimulation to the peak of sigma activity for each detected spindle (as measured by the peak of the envelope signal). If stimulation occurred more than 50 ms prior to the peak, it was sorted into the first category (referred to as 'before the peak'). If it occurred 50 ms after the peak, it was sorted into the second category: 'after the peak'. In addition to analyzing the effects of spindle timing on evoked sigma power as in the main analysis, we explored differences between the conditions in cumulative sigma power over the subsequent 15 s, as a means of observing overall differences in the amount of evoked sigma activity.

To explore the effect of stimulating the *evoked* sleep spindles, we isolated epochs in which two detections occurred consecutively (within -1.5 to -0.5 seconds; see Supplementary Table 1 for the number of epochs included per subject). The second of the two spindles is likely to have been evoked, a) on the basis of our average results Figure 2D; and b) because the rhythms of endogenously-produced spindles follow a longer (∼0.02 Hz) cycle (Lecci et al., 2017). The strength of evoked sigma activity following the second stimulation was evaluated by statistically comparing the mean sigma envelope amplitude 1.5 to 2.5 after the onset of the first spindle.

Finally, to investigate the potential disruptive (or stabilizing; Choi & Jun 2022) effects of CLAS to sleep spindles, we statistically compared the number of overall detections in the STIM and SHAM conditions, and computed cumulative sigma power over the 15 s epochs, which as they are overlapping collectively cover the duration of NREM2 and 3 sleep (noting that a validated sleep scoring procedure for Portiloop's unique montage has not yet been validated).

5.4 Results

5.4.1 Spindle detection

We first confirmed the effectiveness of spindle detection. As anticipated, improper electrode placement or loss in the in-home recordings resulted in poor signal quality for some time intervals. However, a large amount of data was usable; on average, 2.6 (SD: 0.5) stimulation and 2.2 (SD: 0.6) sham nights per subject were retained in the analysis (i.e., 20% data loss). Across all nights, the mean number of epochs included in the main analyses in the STIM condition which met the criteria for inclusion in the main analysis (i.e., no additional stimulation in the subsequent 2.5 s) was 958.2 (SD: 621.6), and in the SHAM condition it

was 891.9 (SD: 467.2; please see Supplementary Table 1 for per-subject values). A Wilcoxon Signed Rank Test confirmed that the number of spindles detected during sham and stimulation nights did not differ systematically (W = 31, z = 0.36, p = .770). The effect size (r = 0.127) was measured using Rank-Biserial Correlation.

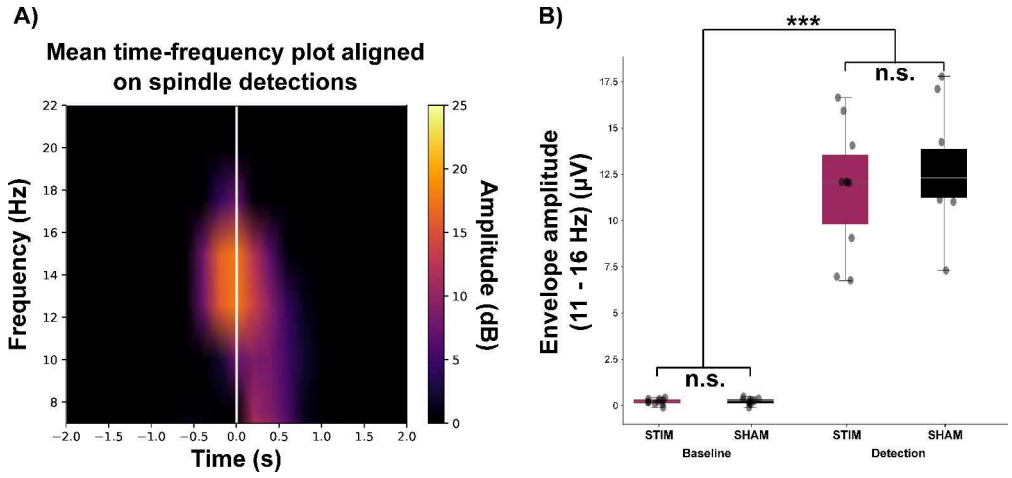

Figure 5.1: Successful real-time detection of sleep spindles. A) Mean time-frequency plot shows a clear burst of sigma activity at the time of detection. B) Comparison of the envelope of the sigma activity (11 - 16 Hz) 1 second prior to the detection (Baseline) and at the time of the detection suggests the presence of a spindle. '***' indicates significance at p<0.001, FDR-corrected.

As observed in Figure 1, the in-home Portiloop approach was successful in detecting spindles, and in stimulating them before they ended, with 97.6% of stimulations arriving before the end of the spindle as determined using an offline detector (see Supplementary Figure S1D). Spindle power at time of detection and at baseline level (Baseline STIM: Mean: 0.21, SD: 0.14; Baseline SHAM: Mean: 0.23, SD: 0.16; Detection STIM: Mean: 11.76, SD: 3.20; Detection SHAM: Mean: 12.75, SD: 2.89) did not differ significantly between stimulation and sham conditions (Baseline STIM vs SHAM: t(18) = -0.30, p = 0.77, Cohen's d = -0.13; Detection STIM vs SHAM: t(18) = -0.69, p = 0.75, Cohen's d = -0.31) but is significantly higher than one second prior to detection (Baseline vs Detection: t(38) = -16.97, p < 0.001, Cohen's d = -5.36). The mean spindle duration as computed by the offline algorithm (see Methods) was 958.7 ms with the bulk of stimulations falling between about 300 to 500 ms, in accordance with expectations from offline estimates (Valenchon et al., 2022). Supplementary Figure S1B illustrates the distribution of delays between (offline-detected) spindle onset and stimulation. These results confirm that the Portiloop device successfully detected spindles, and did so similarly for the stimulation and sham conditions, such that differences in post-detection neurophysiology may be meaningfully be compared.

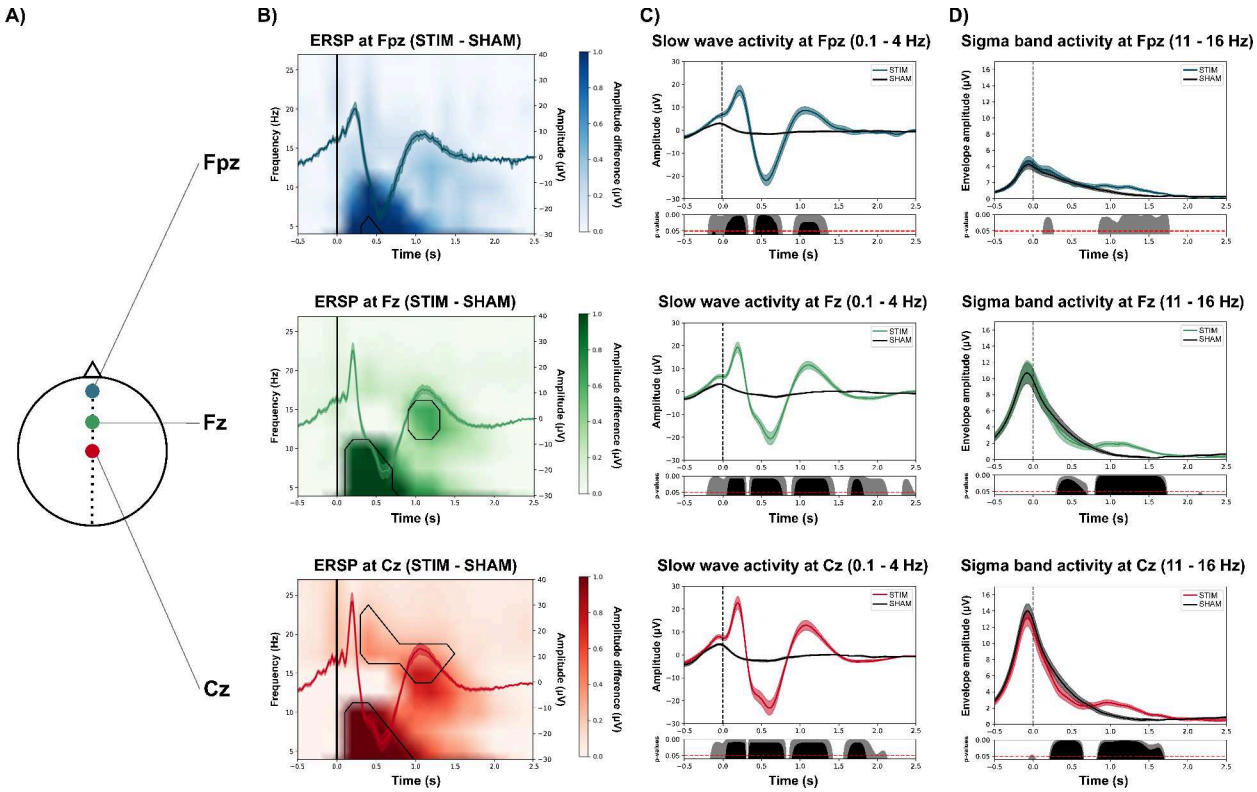

Figure 5.2: Effects of closed-loop auditory simulations of sleep spindles (detected at Cz). A) Position of the three electrode sites. B) Event-related spectral perturbation following closed-loop auditory stimulation of sleep spindles as compared to sham. Black contours highlight the significant differences between conditions (for visualization purposes only significant clusters bigger than a single time-frequency bin are represented). The overlaid line represents the broadband (0.5 - 30 Hz) mean evoked response potential (shaded area: standard error of the mean). C) Slow wave-filtered evoked responses. D) Spindle-band activity. In C and D, solid lines indicate group mean and shaded lines represent standard error of the mean. Statistical differences (STIM vs. SHAM) are represented in the bottom panels. Grey areas represent uncorrected p-values and black areas represent corrected p-values.

5.4.2 Effects of stimulation vs. sham

To document the effects of auditory stimulation to sleep spindles without bias as to frequency band or time window, we used an event-related spectral perturbation approach to assess the strength of changes in oscillatory activity locked to the stimulation, between stimulation and sham conditions for each of the three electrodes of interest (averaged broadband evoked response potentials for the stimulation condition are overlaid, see Figure 2B). Statistical analyses confirm an increase in high theta immediately following stimulation (from around 100 ms to 500 ms) and an increase in spindle power about one second post stimulation. This pattern was most prominent at the Fz and Cz electrode sites, and did not reach significance at the most frontal site (Fpz). Effect sizes are reported in Supplementary Figure S4.

Next, we evaluated the effects of stimulation specifically on slow wave activity (0.1 - 4 Hz). A clear evoked auditory response and subsequent slow oscillation is observed when sound is delivered during spindles, with statistically-significant differences from sham for the majority of the duration between stimulation and 2 s at Fz and Cz (Figure 2C). The most frontal site (Fpz) also showed a significant evoked response, though with fewer clear differences from the sham condition.

In the spindle range (11 - 16 Hz), we observe a significant decrease in power towards the end of the detected spindle (around 500 ms), possibly indicating early termination (Sela et al., 2016), followed by a strong increase in activity between 750 ms and 1.75 s post stimulation (see Figure 2D). As in the previous analysis, the pattern was more pronounced at the central electrodes than the frontal electrode.

5.4.3 Effects of stimulating the beginning vs. the end of a sleep spindle

To investigate the interaction between stimulation timing and evoked brain activity in the sigma range, we compared the difference between STIM and SHAM trials for epochs in which stimulation occurred before or after the spindle peak (as defined in Methods). As observed in Figure 2D in which all epochs were considered, stimulation occurring before the peak of sigma activity also resulted in an early termination of the current spindle (<0.5s post-stimulation) and a subsequent increase in evoked activity around 1 s after stimulation. In contrast, when stimulation occurred after the peak of the sigma activity, there was no early termination of the current spindle, but clear evoked activity was still generated ∼1 second post-stimulation (see Figure 3). Interestingly, when investigating the long-lasting effects through cumulative sigma analysis, we observe that while targeting stimulation before the peak did not modify overall sigma power, stimulating the end of the sleep spindle enhanced sigma activity as

observed in the 15 seconds post-stimulation. This difference was statistically significant at uncorrected alpha values from 4 seconds onward, but did not survive the Benjamini-Hochberg procedure.

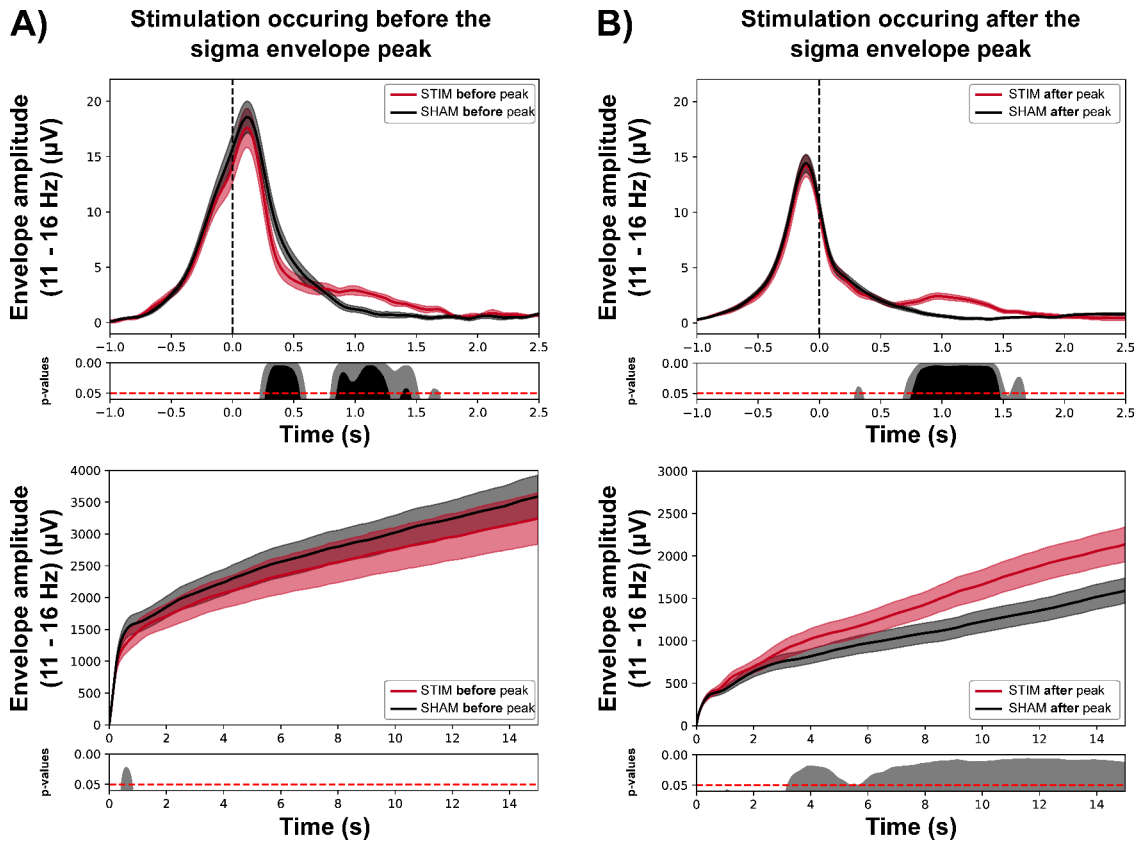

Figure 5.3: Timing relative to the ongoing sigma activity impacts the neurophysiological response to stimulation. A) Top: Comparison of the envelope of the sigma activity (11 - 16 Hz) for both STIM and SHAM conditions when stimulation occurred before the peak of the detected spindle. Bottom: cumulative sigma power in the 15 seconds following stimulation. B) Top: Comparison of the envelope of the sigma activity for both STIM and SHAM conditions when stimulation occurred after the peak of the detected spindle. Bottom: Cumulative sigma power in the 15 seconds following stimulation. Dashed vertical line represent timing of auditory stimulation. Grey areas represent uncorrected p-values and black areas represent corrected p-values.

5.4.4 Effects of stimulating evoked sleep spindles

Due to the design of our experiment in which the minimum inter-stimulus interval was set to 400 ms, some evoked spindles occurring one second after stimulation were also detected and subsequently stimulated. By filtering for these specific epochs, we can investigate the effect of auditory stimulation on spindles that are most likely *evoked* (see Figure 4). Interestingly, we observed an absence of evoked activity following the *second* stimulation. This result was statistically confirmed by comparing the extracted values between STIM and SHAM

conditions from 1.5 to 2.5 seconds post the original stimulation (t(9) = -0.593, p =0.58, Cohen's d = -0.19).

5.4.5 Effects of whole-night spindle stimulation on sleep microarchitecture

To investigate the potential disruptive or stabilizing consequences of whole-night spindle stimulation, we computed average difference time-frequency plots extended to 10 s, and found no evidence of increased high frequency activity that might indicate arousals as would be expected if the sound stimulation disturbed sleep. Next, we statistically evaluated the overall number of spindle detections between conditions. Across all nights, the mean number of spindles detected in the STIM condition (comprising those before and after 2.5 s, to allow for a total detection count including evoked responses) was 1050.8 (SD: 677.1), and in the SHAM condition it was 939.0 (SD: 492.5) (see Supplementary Table 1 for details). A Wilcoxon Signed Rank Test confirmed that the number of spindles detected during sham and stimulation nights did not differ systematically (W = 34, z = 0.663, p = 0.557). The effect size (r = 0.236) was measured using Rank-Biserial Correlation. Finally, we computed the overall cumulative sigma power across a 15 s window following each stimulation onset (see Supplementary Figure S3). Results showed no significant difference after correction for multiple comparisons, and showed only a short window (400 - 800 ms) of decreased sigma activity in the stimulation condition, corresponding to the spindle termination described above (Figure 2D), at uncorrected statistical levels.

5.5 Discussion

The aim of this work was to document the neurophysiological effects of auditory spindle stimulation on neural activity. We first confirmed that our method of stimulating spindles successfully detected spindle-band activity (i.e., using the Portiloop; Valenchon et al. 2022 ; Figure 1), and that it was able to stimulate spindles prior to their termination (with almost all stimulations hitting spindles). Comparing stimulation with sham conditions, we found that the earliest difference between stimulation and sham is an increase in lower frequency activity (i.e., up to about 11 Hz), between 100 and 500 ms post detection (Figure 2B). While some results suggests that this activity is associated with memory functions (Wüst et al., 2021; Gonzalez et al., 2018), its function has not been been causally explored.

In the slow oscillation band, we observe a strong sleep-specific evoked response resembling that reported in open-loop studies (Latreille et al., 2020; Riedner et al., 2011; Jourde et al.,

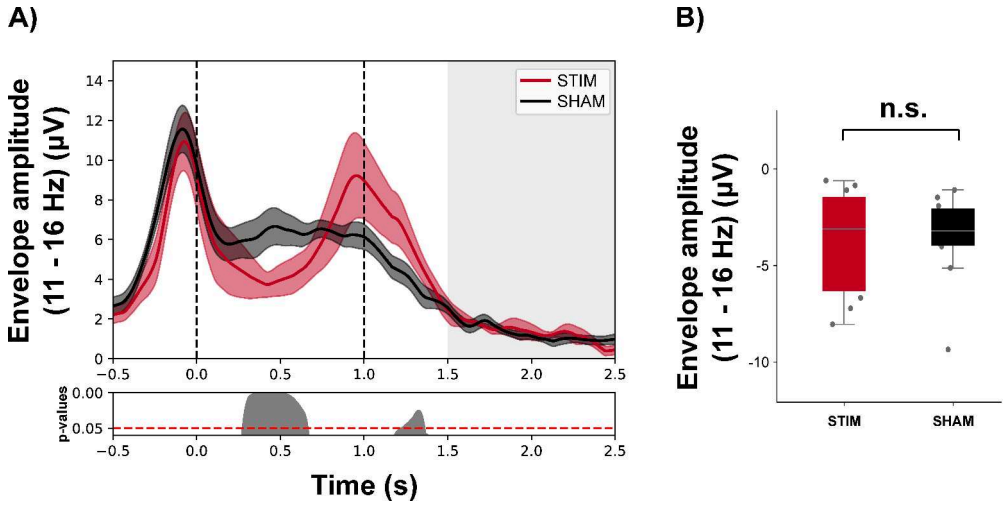

Figure 5.4: Effect of trains of spindle stimulation showing that stimulating evoked spindles (i.e., two stimulations in a row) does not appear to elicit additional sigma activity A) as observed in the envelope amplitude timecourse, and B) confirmed statistically within a window 1.5-2.5 s (grey shading in A) following the first sound onset. Dashed vertical lines represent timing of auditory stimulations. Grey areas represent uncorrected p-values and black areas represent corrected p-values.

2024), closed-loop auditory stimulation studies that target SO up-states (Ngo et al., 2013b), and in studies that stimulated the end or following the offset of spindles (Choi et al., 2019; Choi & Jun, 2022). In brief, the auditory evoked response components observed in wakefulness within about 300 ms following stimulus presentation are followed in the sleep state by a pronounced negativity from about 300 - 600 ms (sometimes referred to as components N350 and N550), and then a positive component after 900 ms (P900). As spindles were present during stimulation in this experiment, the results support prior observations that their presence does not impede the CLAS effect (Jourde & Coffey, 2024).

Most importantly given our focus on manipulating sleep spindles experimentally, we observed two clear changes in the spindle frequency band. First, stimulated spindle is truncated around 500 ms post-stimulation. This observation is consistent with work showing that stimulating the locus coeruleus, a brainstem nucleus that produces the neuromodulator noradrenaline and projects broadly to frontal brain regions (Poe et al., 2020; Kjaerby et al., 2022), suppressing sleep spindle activity (Swift et al., 2018). As the locus coeruleus is connected to the ascending auditory pathway and is thought to be critical for generating the evoked N550-P900 complexes, it has been implicated in a proposed mechanism by which CLAS to slow oscillations induces more slow oscillations, sleep spindles, and consequently, memory benefits (Bellesi et al., 2014; Jourde et al., 2024). Spindle activity power increased between 750 ms and 1.75 seconds post stimulation, which coincided with the induced SO upstate. As the degree of temporal coupling between spindles and slow oscillations is predictive of successful memory consolidation (Muehlroth et al., 2019), this result suggests that it will be

possible to manipulate and perhaps enhance memory processes.

Our results also demonstrate that the specific timing of stimulation may have different physiological effects. If stimulation hits the early portion of the spindle, the spindle is most likely to terminate early (Figure 3A). Early termination of spindles as a result of sound stimulation in sleep has been previously observed in the rat auditory cortex (Sela et al., 2016). Sela et al. noted that termination occurred within about 150-200 ms post-stimulation and was more likely for louder sounds. In the present work, early termination was followed by an increase in sigma activity relative to the sham condition (between 900 and 1500 ms), yet did not lead to overall changes in cumulative sigma activity (nor awaken the participants). If stimulation hits the later, waning part of the spindle, there is no appreciable influence on the present, detected spindle, but a clear increase in sigma band activity is elicited, also from about 800 to 1500 ms (Figure 3B), similar to observations by Choi et al. (2019). The overall cumulative sigma band activity appears greater in the stimulation vs. sham conditions over the subsequent sleep period (though at uncorrected significance levels).

An intriguing result emerged when we separated cases in which an evoked spindle was strong and clear enough to be detected by the detection algorithm, and itself stimulated – although the second consecutive stimulation did evoke a response in the slow frequency band (see Supplementary Figure S2), no concurrent evoked sigma activity was observed (Figure 4B). This finding suggests a limit to the temporal frequency with which spindles can be successfully evoked, in line with the concept of a post-spindle refractory (Antony et al., 2018; Fernandez & Lüthi, 2020), and hints that constraints on externally driving spindles and slow oscillations may be set by different underlying mechanisms (Ngo et al., 2015). These results also corroborate the observation made by Ngo et al. (2015), which stated that the phase-locked increase in spindle activity was restricted to the first stimulus presentation.

An open question is whether sound stimulation alters the architecture of sleep. Noise has been investigated both for its disruptive properties in the context of unwelcome environmental noise (e.g., in hospital settings or in neighbourhoods adjacent to heavy transportation routes), and as a means of intentionally stabilizing sleep (e.g., by playing white or coloured noise, music, or sound bursts). While recent reviews have emphasized in both cases that heterogeneity of study design make general conclusions difficult to draw (see Basner & McGuire 2018; Capezuti et al. 2022), the effects may depend on sound intensity, predictability, meaning, sleep depth, and individual factors such as hearing ability. In the current work, we concluded that presenting short bursts of pink noise devoid of semantic content at low intensity has little effect on sleep continuity or overall depth (as measured by the number of spindles detected and lack of observed arousals). However, it does appear to alter the temporal organization of sigma activity (Figure 3).

It is noteworthy that while random sound stimulation and CLAS targeting different sleep features during NREM sleep have broadly similar physiological effects (i.e., evoked SO and sigma activity), subtle differences in neurophysiological responses arise due to timing variations with respect to the phase of endogenous activity. These differences, however, may have distinct consequences for memory processes (Ngo et al., 2013b).

Comparing the outcomes of stimulating different neural oscillations and examining phase and timing-specific effects would help determine whether CLAS mechanisms are fundamentally the same but vary in intensity, or if they differ qualitatively, by enhancing or disrupting specific processes. In any case, it will be necessary to establish the optimal stimulation paradigms and their behavioural effects through direct empirical comparison (i.e., using the same equipment and methods). Future work could also personalize detection parameters (Sobral et al., in review) and explore the optimal stimulation features (i.e., sound content, level and duration). Developments such as online sleep scoring will enable the detector to activate only during the targeted sleep stages for better precision (Sobral et al., in review).

5.6 Conclusion

The present work supports the value of research tools that can detect and stimulate neural events quickly and flexibly along their time courses. Practically-speaking as regards spindles, our results suggest that they might be experimentally repressed by targeting them early after onset, possibly using pairs of stimulations to also disrupt the evoked sigma activity at ~ 1 s. Sigma activity might instead be enhanced by targeting spindles' waning phase, leaving several seconds between stimulations so as to avoid the refractory period and benefit from the evoked sigma activity.

Although much work lies ahead, the present results represent advances in demonstrating that stimulating sleep spindles with sound is technically and biologically possible, with distinct effects depending on stimulation timing. It supports the use of closed-loop auditory stimulation to causally manipulate sleep spindles, as a means of investigating their roles in learning and memory, health and disease, and potentially as a means of restoring processes degraded by disease state (Manoach & Stickgold, 2019; Wamsley et al., 2012) or aging (Crowley et al., 2002; Clawson et al., 2016). We hope that the closed-loop auditory stimulation technique will facilitate the expansion of much previous research by Professor Robert Stickgold on sleep spindles' functions (Cox et al., 2017; Denis et al., 2021; Tamminen et al., 2010; Stickgold, 2013; Stickgold & Walker, 2007, 2005, 2013) to the non-invasive and non-pharmacological causal domain, and thereby help deepen our understanding of sleep's role in memory.

5.7 Supplementary material

	Number of epochs included in each analysis									
	#STIM all epochs	#SHAM all epochs	#STIM main	#SHAM main	#STIM before peak	#SHAM before peak	#STIM after peak	#STIM after peak	#STIM evoked	#SHAM evoked
S01	605	879	571	852	90	91	291	480	34	27
S02	2085	2066	1881	1955	312	255	831	923	204	111
S03	460	362	383	333	52	47	162	161	77	29
S04	1079	682	969	637	150	96	489	318	110	45
S05	1533	416	1386	389	288	45	536	178	147	27
S06	1927	1245	1804	1202	307	194	859	542	123	43
S07	231	629	226	624	34	87	116	320	5	5
S08	170	927	157	890	20	119	78	434	13	37
S09	1280	1087	1219	1052	116	115	607	572	61	35
S10	1138	1097	986	985	149	103	443	437	152	112
Mean	1050.8	939	958.2	891.9	151.8	115.2	441.2	436.5	92.6	47.1
Std dev	677.1	492.5	621.6	467.2	112.9	64.3	279.62	220.7	65.7	35.7

Figure 5.5: Supplementary Table 1 lists the number of epochs included in the main analysis (left), in which only stimulations that were followed by a 2.5 s gap were included so as to observe the undisturbed evolution of the evoked response (i.e., represented in Figure 2). The middle columns indicate the number of epochs included in the analysis of the effect of stimulation timing within the spindle, and the right column indicate the number of spindles included in the analysis of the effects of stimulating evoked sleep spindles.

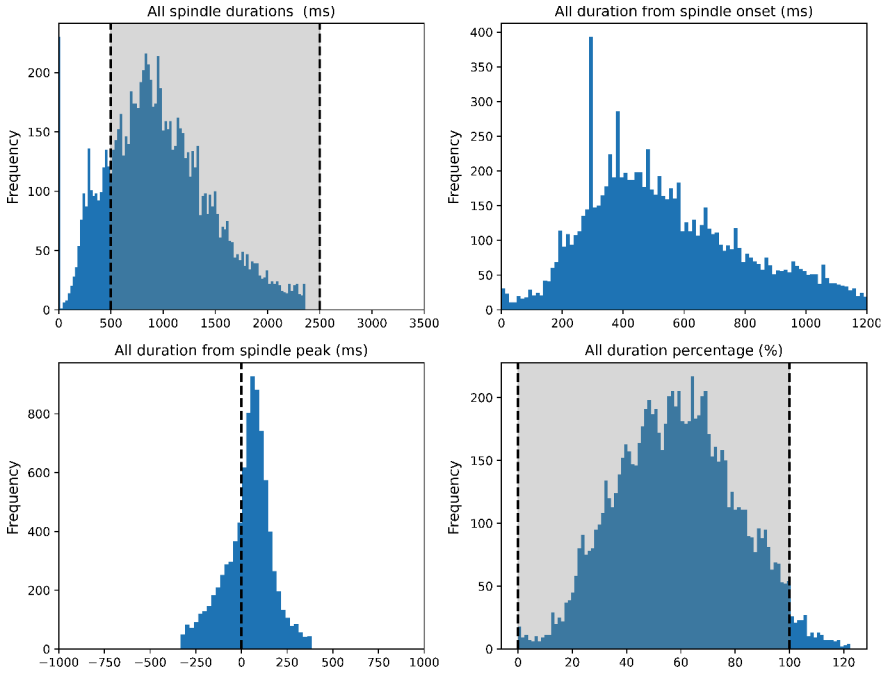

Figure 5.6: Post-hoc characterization of online sleep spindle detection. Spindle onset and offset were identified post-hoc based on deviations in sigma power. A) Spindle duration was calculated as the time difference between the offset and onset. Vertical dashed lines represent the American Academy of Sleep Medicine definition of spindle duration (i.e., 500 ms to 2.5 s). B) For each spindle, the time from spindle onset to stimulation was measured as the interval between spindle onset and the stimulation event. C) Similarly, the duration from the spindle peak was determined by calculating the interval between the stimulation event and the peak of the sigma envelope. The vertical dashed line represent the peak of the spindle envelope. D) The percentage of spindle duration at the time of stimulation provides insight into the phase of the spindle envelope when stimulation occurred. Vertical dashed lines represent the interval for which stimulation occurred within the spindle (97.6% of stimulations in our experimental design).

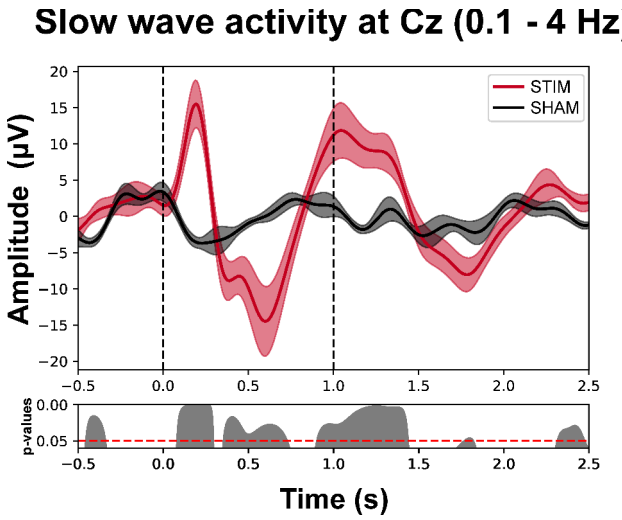

Figure 5.7: Effect of trains of spindle stimulation on slow wave activity (for comparison with the effect on neural responses to non-evoked spindle stimulation in Figure 2, and for comparison with sigma activity evoked by stimulating evoked responses in Figure 4 in the main paper). Dashed vertical lines represent timing of auditory stimulations. Grey areas represent uncorrected p-values and black areas represent corrected p-values.

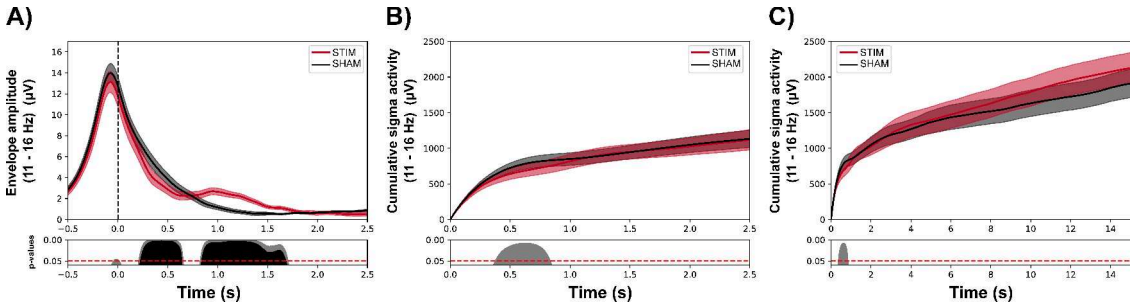

Figure 5.8: Cumulative sigma power (main analysis, i.e., including epochs in which only one stimulation occurred, see also Figure 3 in the main paper, which shows the same information broken down by stimulations that occurred early vs. late in the spindle envelope's evolution). Dashed vertical line represent timing of auditory stimulation. Grey areas represent uncorrected p-values and black areas represent corrected p-values.

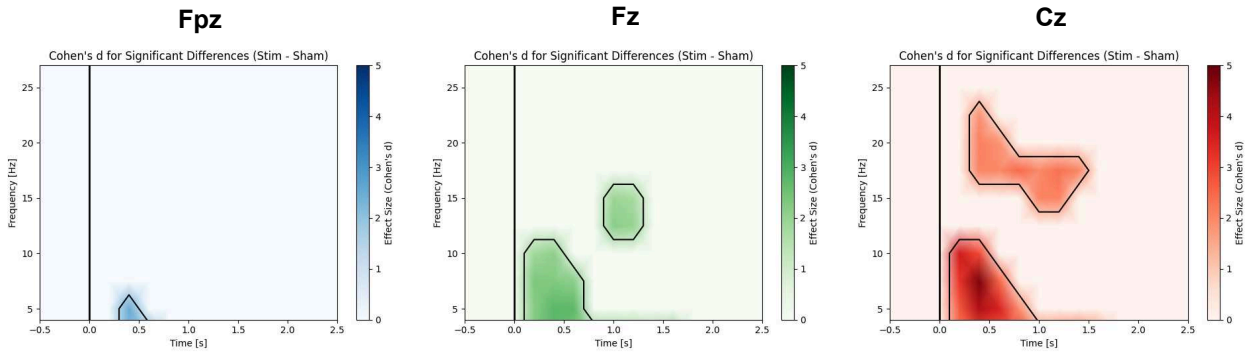

Figure 5.9: Effect sizes for statistically significant clusters in response to closed-loop auditory stimulation of sleep spindles at Fpz, Fz and Cz (for visualization purposes only significant clusters bigger than a single time-frequency bin are represented)

5.8 Acknowledgements

The authors would like to thank colleagues for volunteering as uncompensated participants, as well as the lab of Giovanni Beltrame for contributions to the development of the Portiloop v2 and technical support during early stages of its operation. We also thank members of Julien Doyon's laboratory for participating in beta testing of the Portiloop v2 used in the current work. HRJ was supported by a scholarship from the Quebec Research Funds (Fonds de Recherche de Quebec - Nature et technologies; FRQNT). EBJC is financially supported by grants from the FRQNT, Natural Sciences and Engineering Research Council of Canada (NSERC), and a Concordia University Research Chair in Sleep and Sound.

Chapter 6

Thalamocortical spindle phase modulates the effectiveness of auditory stimulation in sleep

6.1 Abstract

Slow oscillations and sleep spindles are neural events that both occur during non-rapid eye movement sleep and are implicated in sleep-dependent memory consolidation. Their temporal co-occurrence, or 'coupling', is thought to support sleep-dependent memory processes. The roles of these neural events can be explored through non-invasive brain stimulation techniques. Closed-loop auditory stimulation, which precisely times sounds to enhance or disrupt neural events, can induce slow oscillations and spindles, improving memory in some individuals. While spindle-targeted stimulation is now feasible, the effect of slow oscillation-spindle coupling and spindle phase on neurophysiological outcomes remains unexplored. This study investigates how spindle phase influences the neurophysiological effects of closed-loop auditory stimulation timed to slow oscillation up-states. A secondary aim is to characterize predictors of inter-individual differences in stimulation effectiveness. Electroencephalography data collected across multiple nights were analyzed from 16 healthy adults, with stimulation delivered at the slow oscillation up-state or withheld (sham condition). Results show that while slow wave activity is evoked across spindle phases, temporally-coordinated spindle activity emerges only in the peak and rising phases. In contrast, trough stimulation delays spindle activity, and stimulation during the falling phase produces no evoked spindle activity. Across subjects, strength of slow wave and spindle activity was correlated at detection in each frequency band separately, but amplitude at detection did not predict response strength.

These findings refine our understanding of sleep oscillation dynamics and inform future uses of closed-loop stimulation, with a view to advancing fundamental science and potentially restoring sleep and memory functions in clinical applications.

6.2 Introduction

Neural oscillations that appear only in deeper stages of non-rapid eye movement (NREM) sleep (i.e., stages NREM2 and NREM3) are of particular interest for understanding memory. These consist of slow oscillations (SOs) and sleep spindles. SOs are large amplitude, low frequency (∼0.1 - 4 Hz) brain waves that are preferentially generated in frontal and ventral neocortical regions (Neske, 2016). Sleep spindles are transient (0.5 to 2.5 s) oscillatory events with frequencies between ∼11 - 16 Hz that are generated through complex thalamocortical interactions (see Fernandez & Lüthi 2020 for a review). In NREM sleep, SOs and sleep spindles are believed to work in concert with sharp wave ripples: brief, high-frequency oscillations (∼100 - 200 Hz) that occur in the hippocampus during NREM sleep (and quiet wakefulness; Roumis & Frank 2015). Successively higher frequency oscillations are typically nestled within a specific phase of the slower oscillations, a relationship known as phase-amplitude coupling (Staresina et al., 2015). Sleep spindles are most prevalent during SO up-states, and hippocampal ripples are situated in spindles troughs. This configuration is thought to facilitate active memory consolidation, in which newly acquired memories stored temporarily in a hippocampus-dependent fashion are replayed, strengthened, and transferred to the neocortex for integration into existing memory structures and long-term storage (Diekelmann & Born, 2010; Rasch & Born, 2013; Staresina et al., 2015, 2023). Evidence in favour of coupling's importance in memory comes from studies such as Hahn et al. (2020), who demonstrated a positive correlation between SO-spindle coupling and measures of memory formation from childhood to adolescence; and Helfrich et al. (2018), who showed, in older adults, that those who preserved youth-like levels of coupling had better memory functions.

While correlational studies such as these provide evidence of relationships between observed neural events and cognition, the functions of neural oscillations can be more definitively clarified using causal manipulations, like brain stimulation. Closed-loop auditory stimulation uses precisely timed sounds to enhance or disrupt neural events, which induces slow oscillations and spindles, and can improve memory in some individuals (Harrington & Cairney, 2021; Fehér et al., 2021; Choi et al., 2020; Salfi et al., 2020). Recent advancements in real-time deep learning-based algorithms for closed-loop brain stimulation have made it possible to target faster, more elusive oscillations like sleep spindles (Valenchon et al., 2022; Jourde et al., 2025a), and have opened up interesting possibilities for studying the importance and

uniqueness of the temporal coordination of sleep spindles and slow oscillations.

While cross-frequency phase-amplitude coupling is recognized as a general mechanism for memory processing and synaptic plasticity (Bergmann & Born, 2018), many aspects of the specific mechanisms involved and their relationships to different memory processes remain to be clarified. For example, an important open question concerns whether the phase of a spindle coupled to an SO up-state matters to the strength and nature of evoked neurophysiological responses. There is reason to believe it might, on the basis that another form of brain stimulation, transcranial magnetic stimulation (TMS), shows phase-specific effects on corticospinal excitability, suggesting that spindles exert 'asymmetric pulsed inhibition' on other brain circuits (Hassan et al., 2025). The influence of stimulation timing during SO-spindle couples instead is difficult to study in a standard nap or overnight brain stimulation design, because targeting SOs or spindles may yield only a handful of epochs capturing coupling events, which would be insufficient for conducting spindle phase-specific analyses (Hassan et al., 2025). To obtain clear physiological results, several nights' of data are needed. However, multi-night designs introduce complications for studying behavioural effects, as the passage of time and variability introduced by daytime activities make it difficult to isolate stimulation-specific sleep effects.

One approach to address questions about the roles of sleep oscillations and the effect of stimulation timing on them is to break the problem into two parts: studies in which multiple nights' data (in the same subjects) are recorded to characterize the parameters yielding the neural effects of interest (Hassan et al., 2025), and subsequent studies using stimulation optimized through the knowledge thus acquired, to address functional and behavioural questions. The present work is of the former variety. We aim to a) clarify how spindle phase impacts the neurophysiological effects of closed-loop auditory stimulation to slow oscillation up-states in a multi-night, within-subjects design that allows for a deep exploration of phase effects; and b) because brain stimulation may vary in effectiveness across subjects (Salfi et al., 2020; Zrenner & Ziemann, 2024), to characterize inter-individual differences in stimulation effectiveness and their neural antecedents, which will also benefit future attempts to optimize stimulation to the idiosyncrasies of individual brains (Zrenner & Ziemann, 2024).

6.3 Methods

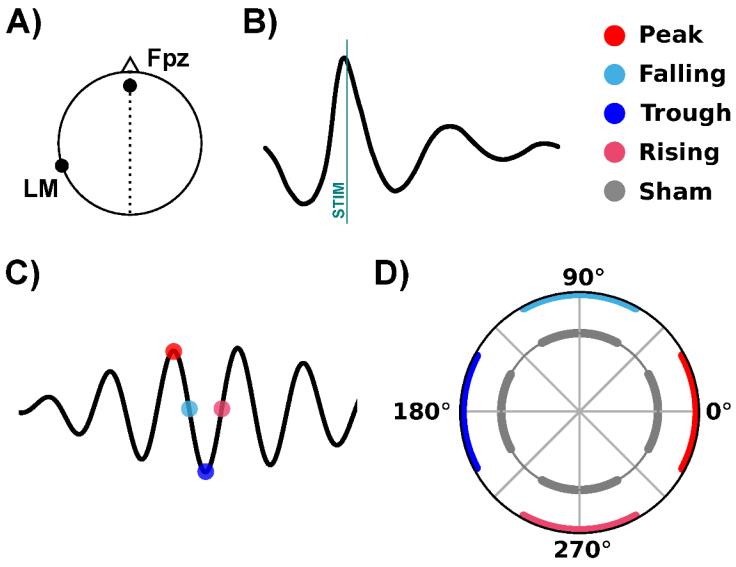

Figure 6.1: Closed-loop auditory stimulation was delivered to slow oscillation up-states, and epochs were later sorted according to the phase of the spindle at detection. A) Electrode montage: ∼Fpz to left mastoid (LM) channel. B) Slow oscillation up-state detection was followed immediately by stimulation delivery (Stim) or withheld (Sham). C) Schematic representation of the four phase conditions used to sort epochs. D) Epoch sorting strategy to investigate the effects of phase specificity of timing of sleep spindle auditory stimulation (averaged across all subjects). Distribution of epochs per condition is represented in the outer circle for the Stim condition (coloured) and in the inner circle for the Sham condition (in grey).

6.3.1 Participants

Subjects were first screened for neurological conditions, and for normal sleep habits via the Munich Chronotype Questionnaire (Roenneberg et al., 2003). All participants reported good neurological health, normal hearing, and were non-smokers. Participants were not taking any sleep- or wakefulness-altering drugs, which can influence sleep characteristics like spindle density (Plante et al., 2015). Throughout the experimental period, participants abstained from consuming alcohol, nicotine, and cannabis, and limited caffeine to their habitual amounts. Sleep logs verified that participants maintained a normal sleeping pattern (6-9 hours) for three days prior to the experiment. Participants were also asked to fill in a sleep diary following each subsequent experimental night. Written informed consent was obtained from participants, and the study protocol was approved by Concordia University's Human Research Ethics Committee. We recruited 23 healthy adults from the local community for this study. Three participants withdrew due to discomfort sleeping with the apparatus or

technical difficulties. Additionally, four participants were excluded for having fewer than 100 clean epochs overall in one of the two coupled conditions (i.e., stimulation condition: 'Stim'; or a sham condition in which detections were marked but stimulation was withheld: 'Sham'). The final sample consisted of 16 participants (10 female; M = 26.29 years, SD = 8.94, age range = 21–55 years). Data used in this study have been used previously to address different research questions, in Jourde & Coffey (2024), Experiment 3.

6.3.2 Study design and participant preparation

Data collection occurred during the COVID-19 pandemic, which necessitated contact-free research protocols. Participants initially met remotely with a research assistant via video conference, during which they provided oral consent to participate. Following this, each participant received a home delivery of study materials, including an Endpoint Connected Hilbert Transformation Box v2 (ecHT; Elemind Technologies, Cambridge, USA) for closed-loop stimulation, a portable battery, a laptop for data collection, EEG materials, and detailed written instructions for the recording procedure. Before the data collection began, a second video chat was conducted with the experimenter to review the protocol in detail, address any questions, and ensure participants understood the proper placement of electrodes.

Participants were instructed to use the equipment for five nights. This multi-night design was intended to capture a sufficient number of slow oscillations (SOs) coupled with sleep spindles (>100), given the relatively low occurrence of coupled SOs (<10 %; Hahn et al. 2020, 2022), and to have a sufficiently high number of coupled events to be able further to separate them into four spindle phases (Hassan et al., 2025). Participants were guided to prepare their skin using alcohol swabs, abrasive strips, and exfoliating paste to ensure good contact and low impedance. They then applied a disposable electrode to their forehead (approximately Fpz, according to the 10–20 International System, Jasper 1958) and a reference electrode to the left mastoid (M1). The ecHT box included an impedance indicator that turned red if the signal quality was poor (impedance >5 kOhms). If this occurred, participants were instructed to reapply the electrodes. Assistance via video conference was available each evening until 10:00 p.m. If participants encountered issues after this time, they were instructed to skip the experimental night, note their concerns, and contact the experimenter the following morning. Participants could also take breaks between recording nights as needed, with a total of 10 days allocated to complete five nights of sleep recordings with the apparatus.

6.3.3 Data acquisition

EEG recordings were acquired from the Fpz-M1 channel at a sampling rate of 500 Hz using the ecHT device. Data were initially inspected for signal quality, and recordings with significant artifacts—commonly due to electrode displacement during in-home use—were excluded (see Supplementary Table 1 for retained nights). Because full polysomnographic data were unavailable in this study, the recordings were not sleep-scored.

6.3.4 Slow oscillation detection and stimulus presentation

The ecHT is a closed-loop auditory stimulation device that continuously monitors a single channel of EEG activity and delivers sound through connected headphones (Schreglmann et al., 2021). The detection of slow oscillation (SO) peaks was enabled by an algorithm developed by D. Lesveque and implemented on the ecHT. This algorithm, validated during pilot testing, achieved performance comparable to offline SO detection methods.

SO peaks were detected when a trough of at least -40 μV was followed by a peak-to-peak amplitude change of at least 75 μV. Sound stimuli, consisting of 40 ms pink noise bursts with 5 ms linear rise and fall ramps, were delivered binaurally at 55 dB SPL via Etymotic ER-3C insert earphones with foam tips. As in previous work, pink noise was used as broadband sound ensures a robust response at the basilar membrane in the inner ear and throughout the auditory neuraxis, and to maintain comparability with earlier results (Ngo et al., 2013b,a). The closed-loop protocol began with 30 minutes of silence to allow participants to fall asleep, since eye blinks sometimes trigger SO stimulation. This period was followed by alternating 5-minute cycles of stimulation and detection without stimulation, separated by 5-second pauses. The design ensured an approximately equal number of Stim and Sham epochs and their even distribution throughout the night (reported in Supplementary Materials Table 1).

6.3.5 EEG processing and analysis

EEG data were analyzed in Python using custom scripts built on freely available packages. We employed NumPy for array manipulation, SciPy's signal module for filtering operations (including notch, bandpass, and band-specific filtering with butter and filtfilt), and Matplotlib for visualizing both filter frequency responses and average brain responses.

Data from all nights were pooled for analysis. The raw EEG signal was filtered into three frequency bands: 1) 70 – 150 Hz to estimate muscle activity, 2) 0.1 – 4 Hz to capture slow wave activity (SWA), and 3) 11 – 16 Hz to measure spindle activity. In all analyses, filters were applied before defining epochs to avoid border effects. Offline spindle detection

was performed using a modified version of the algorithm by (Lacourse et al., 2019), which was adapted to account for differences in broadband noise in the ecHT signal compared to standard EEG systems. One of the original detection criteria, absolute spindle power, was omitted. The quality of spindle detections was confirmed through visual inspection of randomly selected epochs by a trained sleep scorer.

For analyzing stimulation impact in the slow-wave band, we applied a 4th order Butterworth band-pass filter (0.1 to 4 Hz) to the raw data. Similarly, to isolate spindle band activity, we used identical filter parameters but with an 11-16 Hz frequency band. Since phases of both detected and evoked sleep spindles can vary, we used the signal envelope as our metric to estimate spindle power over time (i.e the absolute value of the Hilbert transform of the spindle band signal).

Epochs were defined as being 15 seconds before to 15 seconds after sound onset and categorized based on the presence or absence of spindles at the time of SO detection, according to offline spindle detection. Each epoch was baseline-corrected using the mean amplitude from -2.5 to -0.5 seconds prior to detection. To minimize the influence of movement-induced artifacts, the top 5% of epochs with the highest muscle activity (70 – 150 Hz) were excluded at the participant level. For the Stim and Sham conditions separately, detections were classified according to the instantaneous phase of the spindle at slow oscillation detection. Epochs were included in each condition if the detection occurred within ±0.5 radians (28.7°) from each phase (0°, 90°, 180°, 270°). The centre and distribution of angles in each phase bin is represented graphically in Figure 6.1, C and D. The total number of epochs included for each subject for each condition is reported in Supplementary Materials Table 1. To compare the number of epochs retained in each of the four spindle phase bins, we conducted a 2 (Stimulation conditions) × 4 (Spindle phases) repeated measures ANOVA.

Average evoked responses in both frequency bands of interest (0.1 – 4 Hz for SWA and 11–16 Hz for spindle activity) were computed for each participant by averaging all epochs in each condition. Timeseries were then averaged across participants for statistical comparison of conditions. To visualize inter-subject variability, the timeseries were normalized using z-scoring based on the 5 seconds prior to detection, thereby avoiding incorporation of stimulation effects in the baseline.

The root mean square (RMS) of the 0.1 – 4 Hz signal was computed with a moving average to quantify SWA. Post-stimulation RMS values (0.5 – 1.5 s after onset) were compared between Stim and Sham conditions. The RMS of the 11 – 16 Hz signal was calculated to assess evoked spindle activity. Post-stimulation RMS values (0.75 – 1.5 s after onset) were compared between Stim and Sham conditions. As per our initial goal to explore optimal timing for stimulation, we analyzed how the strength of detected oscillations relates to evoked

neural activity in each condition. These correlations help us understand how detection parameters influence subsequent neural responses.

To investigate the impact of spindle phase at stimulation onset, repeated measures ANOVA were used with two main factors: Condition (i.e. Stim and Sham) and Phase (i.e. Peak, Falling, Trough and Rising). Main effects are reported.

Statistical comparisons of timeseries between conditions were computed across subjects for each timepoint and corrected for False Discovery Rate using a Benjamini-Hochberg correction (alpha = 0.05). Non-parametric statistics were used where assumptions for parametric equivalents were violated (i.e., Wilcoxon signed-rank tests with rank-biserial correlation (r) as an indicator of effect size vs. Student t-test with Cohen's d for effect size).

6.4 Results

6.4.1 Confirmation of SO detection, selection of coupled epochs, and evoked responses

The mean number of nights per subject included in the analysis was 4.7 (SD: 0.8), and the mean percent coupling across all detections was 6.67% (SD: 3.80), in agreement with previous work reporting coupling rates of less than 10% of SOs (Hahn et al., 2020, 2022). The mean number of coupled SOs included in the analyses was 374.1 (SD: 190.2) in the Stimulation condition and 358.9 (SD: 179.4) in the Sham condition. Additional details concerning each participant's number of detected events by condition is available in Supplementary Materials Table 1.

To confirm the success of the SO and of the coupling spindles' detection, we first evaluated the amplitude of each (which is each expressed with reference to its own baseline); see Figure 6.3A. The mean amplitude of slow wave activity averaged across both Stim and Sham conditions at detection was 30.1 μV (SD: 6.3), which was significantly above baseline levels (V=136.00, p<.001, r=1.00). The mean magnitude of spindle band activity at SO detection within the epochs identified as coinciding with a spindle was 5.1 μV (SD: 0.80), which was also significantly above baseline levels (V=136.00, p < .001, r=1.00). Detection and identification success can also be observed in each condition's timeseries as peaks at time 0 (detection) in Figure 6.2B and C (note that the ecHT algorithm detects SO peak slightly after the true peak, but stimulation is nonetheless delivered in the up-state).

6.4.2 Phase-specificity of evoked responses

Prior to evaluating whether spindle phase during coupled SO-spindle events affects the evoked responses, we first compared the number of epochs retained in each of the four spindle phase bins. There was no significant main effect of Stimulation condition ($F(1, 120) = 0.09$, $p = .8$) and the interaction between Stimulation and Phase was not significant, $F(3, 120) = 0.041$, $p = .9$, indicating balanced datasets across stim and sham conditions. However, there was a significant main effect of spindle phase, $F(3, 120) = 28.48$, $p < .001$, indicating significant differences in the numbers of trials were sorted into each phase bin. The highest number of epochs in the Peak condition (mean Stim: 92.3, SD: 46.9; mean Sham: 93.3, SD: 50.6), and lowest number in the Trough condition (mean Stim: 22.5, SD: 9.4; mean Sham: 21.3, SD: 10.31), with the other two conditions falling in an intermediate range, see Supplementary Materials Table 1 for details. These results imply a phase dependency between slow oscillations and spindles, wherein the SO phase most likely to be selected as SO peak by the SO detector is also most likely to be a spindle peak (as would be the case if spindle and SO evocation were dependent upon the same neural process, or perhaps if the detection algorithm were sensitive to superposition of SO and spindle bands, for example due to filter properties). Practically-speaking, the unequal bins could mean that signal-to-noise ratio will be lower in the Trough condition. Nonetheless, group average time series appear clearly in all four phase conditions and both frequency bands (Figure 6.2B and C), suggesting adequate sample sizes for the present research questions. To ensure that the spindle phase conditions adequately separated the four spindle phases (Peak, Falling, Trough, Rising), we averaged epochs in the spindle frequency range over the -0.2 to 0.2 s time range. Visual inspection confirms successful phase alignment Figure 6.2A.

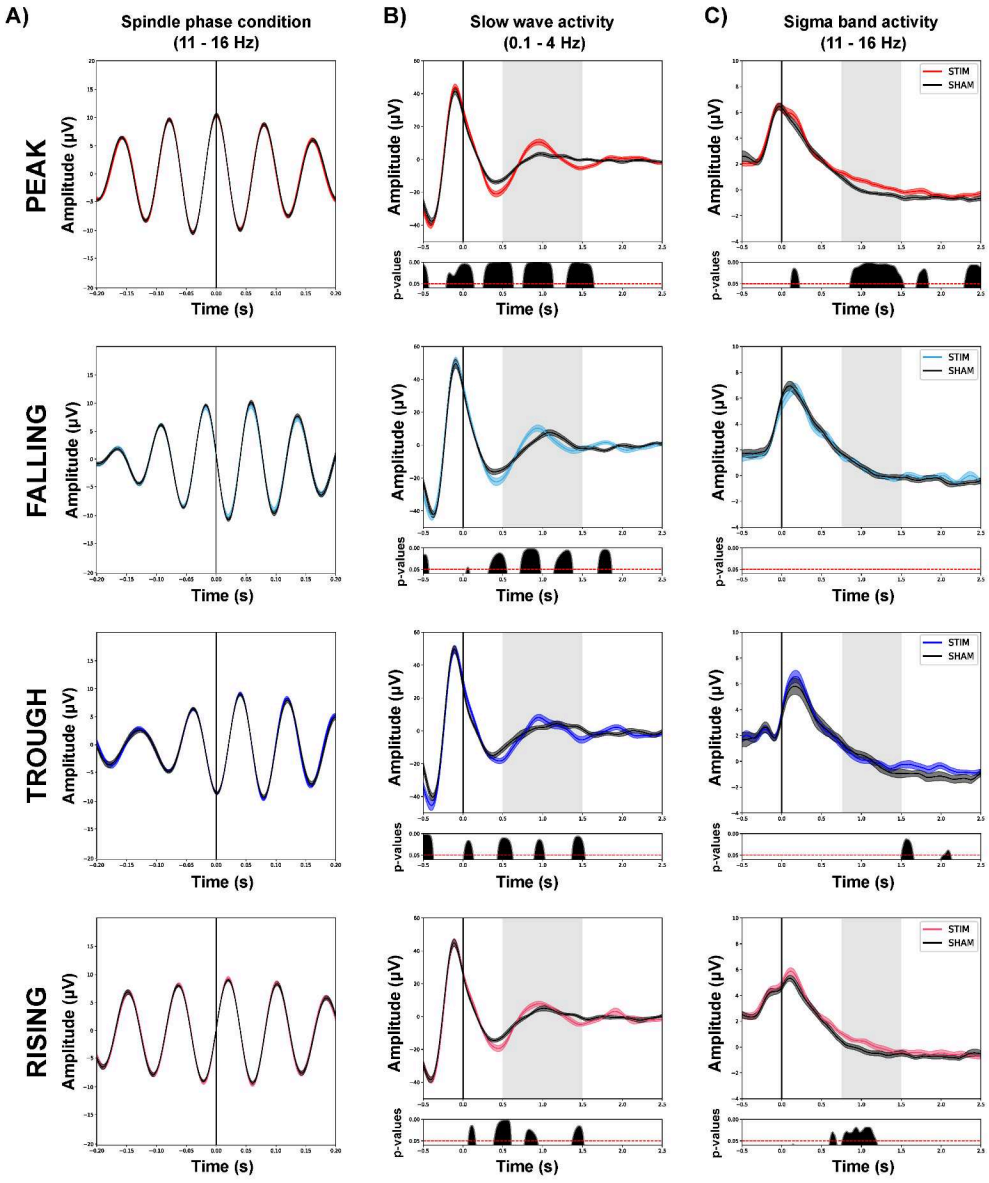

Figure 6.2: Effects of A) spindle phase during slow oscillation up state stimulation on evoked responses in B) slow wave-filtered evoked responses, and C) spindle-band activity. Solid lines indicate group mean and shading represents standard error of the mean. Grey rectangles indicate time windows used to extract mean evoked responses, for subsequent analyses. Statistical differences (Stim vs. Sham) are represented in the bottom panels. Grey areas represent uncorrected p-values and black areas represent corrected p-values; dashed grey line indicates alpha = 0.05.

As observed in Figure 6.2B (see bottom of figures for p-values), stimulation of slow oscillation up-state successfully generated evoked slow wave activity as compared with sham, in all four spindle phases. An analysis of extracted values with the 0.5 to 1.5 s window (Figure 6.3B, top) using a repeated measures ANOVA revealed a significant main effect of stimulation condition ($F(1, 15) = 22.179$, $p < .001$) with evoked amplitude being higher in

the Stim condition. The interaction between spindle phase and stimulation condition was not significant, $F(3, 45) = 1.009$, $p = .397$. This result indicates that the effect of stimulation in the slow frequency band did not differ across the different phases of spindle activity.

As planned comparisons, paired samples t-tests were conducted to compare evoked slow wave activity between Stim and Sham condition for each spindle phase at detection. The results indicated a significant difference between Stim and Sham in the 'Peak' condition ($t(15) = 5.661$, $p < .001$), 'Trough' condition ($t(15) = 2.592$, $p = .010$) and 'Rising' condition ($t(15) = 3.541$, $p = .001$). However, no significant difference was found between the 'Falling' condition ($t(15) = 1.513$, $p = .076$). The non-significance of the falling stage is likely best attributed to higher variability in the Falling condition resulting in lower statistical sensitivity (and perhaps the a priori selection of extraction window, which may miss some of the Stim-Sham differences), rather than a truly different behaviour from the other conditions.

As observed in Figure 6.2C, stimulation of slow oscillation up-state generated spindle activity (as compared to Sham) most clearly in the Peak and Rising conditions. An analysis of RMS spindle band extracted values with the 0.75 to 1.5 s window (Figure 6.3B, bottom) confirmed these observations using a repeated measures ANOVA. Mauchly's test of sphericity was significant ($p < .05$), indicating a violation of the sphericity assumption, and therefore, the Greenhouse-Geisser corrected values were used.

There was a significant main effect of Condition, $F(1, 15) = 5.592$, $p = .032$, with spindle activity being significantly higher in the Stim condition. There was a significant interaction between Phase and Condition, $F(2.143, 32.147) = 4.234$, $p = .021$, suggesting that the effect of stimulation varied across the different phases of sigma activity at stimulation onset. Paired samples t-tests were conducted to compare evoked spindle activity between Stim and Sham condition for each spindle phase at detection. The results indicated a significant difference in the 'Peak' condition ($z(15) = 3.361$, $p < .001$), spindle activity in the Stim condition being significantly greater than in the Sham condition. Similarly, there was a significant difference between Stim and Sham in the 'Rising' condition ($z(15) = 2.430$, $p = .007$). However, no significant differences were found in the 'Falling' ($z(15) = -0.207$, $p = .59$) nor 'Trough' ($z(15) = 0$, $p = .51$) conditions.

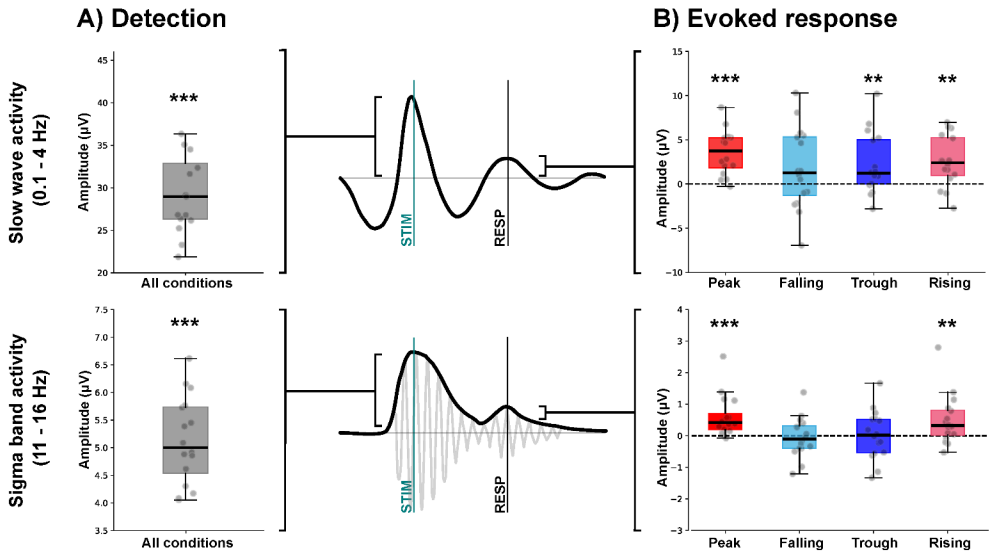

Figure 6.3: Detected and evoked activity. A) The amplitude of slow wave and spindle-band activity at detection, indicating successful real-time detection of slow oscillations and offline detection of sleep spindles (used for defining the coupled conditions). B) Evoked responses in each frequency band across phase conditions (STIM-SHAM). '*', '*', and '***' indicate significance at $p<0.05$, $p<0.01$, and $p<0.001$, respectively (FDR-corrected).

To explore differences between evoked activity in the spindle band across phase stimulation conditions, we compared the timeseries of the Peak and Trough phases visually, which are both the most different of the four phases conceptually (i.e., likely representing different extremes of tissue excitability states), and show the greatest differences from sham in evoked responses (as observed in Figure 6.2C). Figure 6.4 facilitates the comparison of the timing of evoked responses (represented as coloured lines underneath group mean condition vs. sham averages). In Peak condition we observe significant increases in spindle activity starting at about 0.9 s, coherent with previously observations of evoked spindle activity in response to stimulation targeting spindles (independently of phase and the presence of slow oscillations, Jourde et al. 2025a). Conversely, in the Trough condition, sigma activity remains low throughout this period, instead showing an increase only after 1.5 s, suggesting that Peak and Trough stimulation evoke spindle activity with different timing.

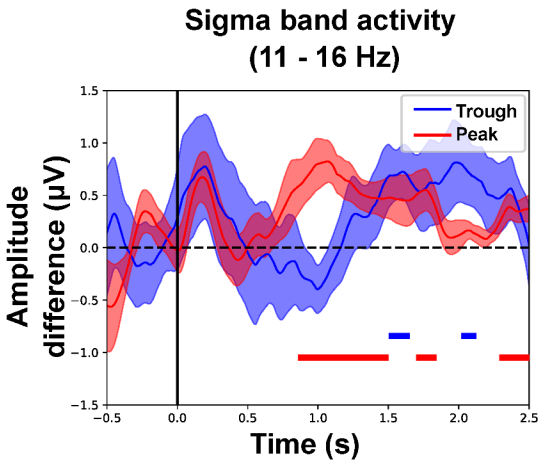

Figure 6.4: Comparison of timing of evoked responses in the spindle band between the two conditions showing the greatest differences in spindle band activity evoked responses (see Figure 6.2C). Solid lines indicate group mean (Stim vs. Sham for each condition) and shading represents standard error of the mean. The timeseries of statistical differences (Stim vs. Sham) are represented in coloured lines underneath the averages for comparison.

6.4.3 Inter-individual variability at detection in predicting evoked response

To explore relationships between mean signal amplitudes for each subject, we computed correlations between pairs of extracted variables in each frequency band and across them. We found a significant positive correlation between slow wave activity and spindle band activity (across all conditions, since no experimental manipulation had yet been applied; Pearson's $r(14) = 0.57$, $p = .02$, with a Fisher's z effect size of 0.65). This result shows that subjects with overall higher amplitude SOs at the time SOs were detected by the CLAS device were also likely to be the same subjects with stronger spindle band activity. As only coupled events are included in the analyses, this is indirect evidence of a dependency between SO and spindle strength.

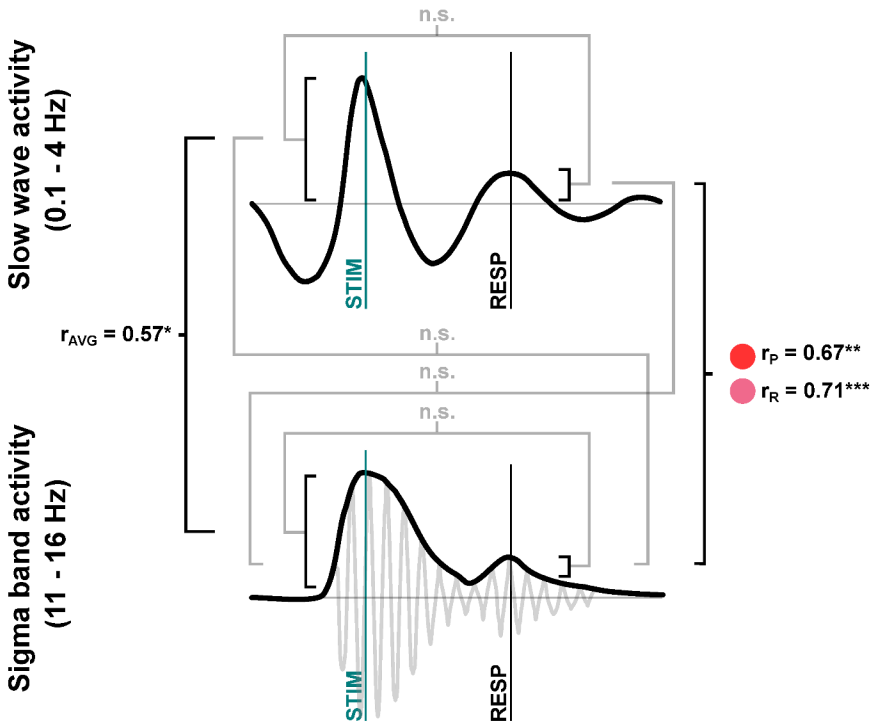

Figure 6.5: Correlations between signal amplitudes. At detection, the amplitude of slow wave activity was positively correlated with the amplitude of spindle band activity (averaged across all conditions). Evoked response amplitudes were correlated in the peak (r_P) and rising (r_R) conditions only. Neither mean slow wave nor spindle amplitude at detection predicted the evoked response amplitude at either frequency band across participants. STIM = amplitude at detection, RESP = amplitude of response. '*', '*', and '***' indicate significance at $p<0.05$, $p<0.01$, and $p<0.001$, respectively.

To evaluate whether evoked responses share a similar cross-frequency strength relationship, we computed correlations between the evoked amplitude (Stim - Sham) in each frequency bin, for each of the four spindle phase conditions. The amplitudes of the evoked responses in both frequency bands were correlated only when stimuli occurred during spindle Peak ($r(14) = 0.67$, $p = .006$, $z = 0.81$) and Rising ($r(14) = 0.71$, $p = 0.003$) phases, but not in Trough ($r(14) = -0.1$, $p = .7$, $z = -0.10$) nor Falling phases ($r(14) = -0.23$, $p = .4$, $z = -0.23$; note that Spearman's correlations are used due to violations of normality).

Finally, to explore whether the strength of a subject's evoked slow oscillations or spindle band activity could be predicted from properties of either their slow oscillations or spindle activity at detection, we computed correlations between detected amplitude of each of the extracted measures of evoked responses, finding no relationships of significance. These results suggest that, at least in this sample of healthy young adults, SO and spindle amplitude during SO-spindle coupled events was not a strong determinant of an individual's susceptibility to stimulation. A schematic representation of correlations between subjects' mean amplitudes

at detection and in response to stimulation is presented in Figure 6.5. For completeness, all Spearman's correlations are included in Supplementary Table 2.

6.5 Discussion

Using slow oscillation closed-loop auditory stimulation in a multi-night design, we assessed the impact of spindle phase on evoked responses. Focusing on two frequency bands of interest for memory consolidation (i.e. slow wave activity from 0.1 to 4 Hz and spindle activity from 11 to 16 Hz) we explored the strength and relationships across conditions. The results demonstrate that while evoked responses in the slow oscillation band remain relatively consistent and insensitive to spindle phase (see Figure 6.2B and Figure 6.3B top), spindle phase does have an effect on the strength and timing of evoked spindle activity. Overall, the strongest spindle response is observed in the Peak condition (see Figure 6.2C and Figure 6.3B bottom), reaching significant levels between about 0.9 and 1.5 s, which is timed similarly to previously reported evoked responses to SO-CLAS (Ngo et al., 2013b) and CLAS of sleep spindle (Jourde et al., 2025a). In the Trough condition, the timing differed, with evoked spindle activity increasing only after 1.5 s (Figure 6.4. Building on this, the current observation of a delayed response is particularly relevant for future work. It suggests a potential means of selectively disrupting evoked SO–spindle coupling through stimulation. More interestingly, when assessing the strength of the evoked SO-spindle coupling, we found that only stimulation delivered during the peak and rising spindle phases yielded significant correlations between slow wave and spindle activity (see Figure 6.5). This provides researchers with an novel target to not only evoke spindle and slow wave activity separately, but to directly evoke coupled oscillations.

We also document the considerable variability in evoked responses across subjects (see Figure 6.3). As hinted in previous work (López-Alonso et al., 2014; Wiethoff et al., 2014), people considerably differ in their responsiveness to brain stimulation. We therefore explored the possibility that people with stronger endogenous oscillations would be those who showed greater evoked responses and found that individual differences in slow wave and spindle strength did not predict stimulation effectiveness within the same frequency band, nor across frequency bands (see Figure 6.5). This result suggests that people with low amplitude endogenous oscillations (e.g., due to age, or clinical reasons) might still benefit from stimulation. Correlation at the time of detection was statistically significant, hinting toward a potential common mechanism generating endogenous activity in both frequency bands (i.e, people with stronger slow oscillations also tend to have stronger spindles).

To take into consideration this variability across participants, and because evoked response amplitude is indicative of the success of the stimulation in reactivating memory-related circuits,

it will be meaningful to explore the precursors of successful stimulation, perhaps tuning detection or stimulation to individuals so as to optimize results (Sobral et al., 2025).

6.6 Conclusion

This study is the first to examine how sleep spindle phase timing influences neural activity during slow oscillation-spindle coupling in human NREM sleep - a hierarchical complex of nested oscillations that is integral to memory consolidation. Our findings suggest that spindle phase matters and supply new ways to causally manipulate the precise timing of SO-spindle coupling which is important for the effectiveness of memory consolidation, and is related to integrity of the nervous system (Helfrich et al., 2018). These phase-dependent effects provide insights into the temporal dynamics of these neural events and their potential manipulation. Future work should explore whether phase-specific effects on neurophysiology translate to behavioural outcomes, particularly in memory consolidation tasks. Additionally, investigating how these findings could be applied to develop more targeted and effective closed-loop stimulation protocols may prove valuable for both basic neuroscience and clinical applications.

Disclosure Statement

Financial disclosure: none. Non-financial disclosure: none.

Data availability

Anonymized, pre-processed EEG data that were used for the main analyses are freely available on Open Science Framework `https://osf.io/tmd25/?view_only=3ed28fa85f5f4968ac2456a31fdbc1c0`. Raw data may be available upon reasonable request, pending ethical approval.

6.7 Supplementary Material

		Detected sleep events (#)			Total coupled SO (#)		Stimulation conditions (#)							
	Night recordings (#)	SO	Spindles	Coupling rate	Stim	Sham	Stim_P	Sham_P	Stim_F	Sham_F	Stim_T	Sham_T	Stim_R	Sham_R
S01	4	8166	6088	8.66%	382	325	81	79	38	44	16	22	62	38
S02	5	9890	6863	4.94%	247	242	58	64	36	32	14	17	33	27
S03	4	7448	6688	6.43%	229	250	55	61	27	21	22	20	29	37
S04	5	12710	7360	5.39%	394	291	112	78	38	27	24	22	64	45
S05	6	12596	15019	11.46%	733	710	169	185	115	108	34	38	98	69
S06	5	10355	11495	8.52%	471	411	116	106	53	61	26	19	78	53
S07	5	7780	6983	6.40%	226	272	64	82	19	24	8	13	34	35
S08	6	11728	3752	2.99%	185	166	39	44	26	19	18	4	20	19
S09	4	9962	5981	11.30%	613	513	165	142	80	68	30	28	59	58
S10	5	23495	6666	2.17%	255	256	55	47	35	39	22	19	40	50
S11	5	13426	6102	3.40%	237	220	52	45	24	25	18	14	37	32
S12	4	8594	7869	10.96%	471	471	114	110	57	45	26	36	65	73
S13	3	10520	8750	14.30%	746	758	183	205	64	61	47	40	130	143
S14	4	13741	6902	4.58%	304	326	80	101	46	52	19	14	43	39
S15	5	23559	6278	3.29%	375	401	93	119	39	36	25	26	61	70
S16	5	13083	6792	1.89%	117	130	41	25	12	16	11	8	25	18
Mean	**4.69**	**12315.81**	**7474.25**	**6.67%**	**374.06**	**358.88**	**92.31**	**93.31**	**44.31**	**42.38**	**22.5**	**21.25**	**54.88**	**50.38**
SD	**0.79**	**4828.06**	**2567.57**	**3.80%**	**190.15**	**179.40**	**46.87**	**50.63**	**25.68**	**23.80**	**9.42**	**10.31**	**29.10**	**30.04**

Figure 6.6: Number of night recordings, detected sleep events, and number of epochs sorted into each condition for each subject. SO = slow oscillation, P = peak, F = falling, T = trough and R = rising.

Spearman's Correlations ▼

Variable		AVR_SWAdetect	AVR_FSA_detect	BinT_SWAevok	BinP_SWAevok	BinR_SWAevok	BinF_SWAevok	BinT_FSAevok	BinP_FSAevok	BinR_FSAevok	BinF_FSAevok
1. AVR_SWAdetect	Spearman's rho	—									
	p-value	—									
2. AVR_FSA_detect	Spearman's rho	0.453	—								
	p-value	0.080	—								
3. BinT_SWAevok	Spearman's rho	0.038	0.079	—							
	p-value	0.891	0.771	—							
4. BinP_SWAevok	Spearman's rho	0.174	0.185	0.191	—						
	p-value	0.519	0.491	0.477	—						
5. BinR_SWAevok	Spearman's rho	−0.035	−0.312	−0.409	0.276	—					
	p-value	0.900	0.239	0.117	0.299	—					
6. BinF_SWAevok	Spearman's rho	0.374	0.332	0.126	0.491	0.471	—				
	p-value	0.155	0.208	0.641	0.056	0.068	—				
7. BinT_FSAevok	Spearman's rho	0.253	−0.374	−0.097	0.103	−0.041	−0.191	—			
	p-value	0.343	0.155	0.721	0.705	0.882	0.477	—			
8. BinP_FSAevok	Spearman's rho	−0.188	−0.141	−0.044	0.671**	0.459	0.397	0.053	—		
	p-value	0.484	0.602	0.874	0.006	0.076	0.129	0.848	—		
9. BinR_FSAevok	Spearman's rho	0.138	−0.153	−0.382	0.159	0.706**	0.274	0.050	0.368	—	
	p-value	0.609	0.571	0.145	0.556	0.003	0.304	0.856	0.162	—	
10. BinF_FSAevok	Spearman's rho	0.350	0.318	−0.097	−0.112	−0.471	−0.226	0.324	−0.471	−0.274	—
	p-value	0.184	0.230	0.721	0.681	0.068	0.398	0.221	0.068	0.304	—

* p < .05, ** p < .01, *** p < .001

Figure 6.7: Correlations (r and p values) between all extracted amplitudes across subjects.

6.8 Acknowledgements

The authors would like to thank Karine Lacourse for advice on spindle detection. We also thank members of our laboratory as well as members of Julien Doyon, Julie Carrier, and Genevieve Albouy's laboratories for participating in beta testing of the ECHT device used in this current work. HRJ was supported by a scholarship from the Quebec Research Funds (Fonds de Recherche de Quebec - Nature et technologies; FRQNT). AU was supported by a summer scholarship from Natural Sciences and Engineering Research Council of Canada (NSERC) and . EBJC was financially supported by grants from the FRQNT, Natural Sciences and Engineering Research Council of Canada (NSERC), and a Concordia University Research Chair in Sleep and Sound.

Chapter 7

Modulating sleep: slow oscillation and spindle stimulation effects on physiology and memory

7.1 Abstract

Sleep plays a role in memory consolidation, with slow oscillations (SO) and sleep spindles (SP) in non-rapid eye movement sleep being central to this process. While the effects of closed-loop auditory stimulation of slow oscillations have been well studied, no prior research has successfully targeted sleep spindles to assess their impact on memory. This study investigates the effects of SO and SP stimulation; and an additional condition in which stimulation was delivered 450 ms after spindle detection, on neurophysiology, and declarative, procedural, and complex memory consolidation. Healthy young adults (N = 102) engaged in tasks assessing simple declarative and procedural learning, and a complex piano task designed to require integrated use of multiple memory systems in a naturalistic fashion. Subjects were randomly assigned to one of the experimental conditions or sham stimulation control group, for a 2 hr nap opportunity, or an equivalent period of wakefulness. Using auditory stimulation, we modulated SOs and, for the first time, directly targeted sleep spindles. Results confirmed successful modulation of sleep neurophysiology. However, behavioural outcomes were complex: regardless of condition, declarative memory declined, motor sequence learning improved, and piano task performance varied between pre- and post-testing. Follow-up analysis showed modest links between evoked spindle activity and some tasks, while evoked SO strength had no clear relationship with performance change. Our findings demonstrate the feasibility an effectiveness of manipulating sleep events via precisely-timed stimulation, yet highlight the

variability of behavioural outcomes.

7.2 Introduction

Sleep is thought to provide the necessary conditions for memory consolidation (Stickgold, 2005), facilitating the transfer of memory traces from temporary storage in the hippocampus to permanent storage in neocortical regions (Rasch et al., 2007). Evidence for sleep's role in memory, is supported by research ranging from place cell recordings in rats to fMRI studies in humans (see Brodt et al. 2023; Diekelmann & Born 2010 for reviews). Two classes of neural oscillations that take place in NREM (non-rapid eye movement) sleep have been particularly implicated in memory processes: slow oscillations (SO; 0.5-1.5 Hz delta waves) and sleep spindles (11-16 Hz sigma waves). These EEG features correlate with behavioural performance in both humans (Rasch & Born, 2013) and animals (Aton et al., 2014, 2013).

According to the active systems consolidation theory (Staresina et al., 2015), the temporal synchrony between SOs and spindles is critical for effective memory consolidation (Born & Wilhelm, 2012). Sleep spindles tend to align preferentially with SO up-states (Cox et al., 2018) and better alignment predicts better consolidation. For example, in a 2015 experiment, Niknazar et al. (2015) demonstrated that enhanced SO–spindle coupling improved verbal recall compared to weaker coupling. Multiple studies across different age groups have since replicated this correlation between the synchrony of SO–spindle coupling and behavioural performance (Hahn et al., 2020; Muehlroth et al., 2019; Mikutta et al., 2019), emphasizing the functional significance of this interaction in memory processes. However, not all models focus on coupling. An alternative perspective emphasizes the frequency and pattern of occurrence of spindles as being critical, particularly for procedural memory consolidation (Boutin et al., 2024; Boutin & Doyon, 2020). In either case, a large number of spindles and slow oscillations occur that are neither part of coupled complexes nor trains, raising questions about whether they still might have functional roles (Schiller et al., 2025). In sum, there are still many gaps in our understanding of the precise roles of sleep-specific neural oscillations in memory consolidation, and how they interact with different memory systems.

Declarative memory involves the conscious recall of information, such as lists of words, whereas procedural memory encompasses skills that can be performed without conscious awareness, once learned. The demands of everyday life generally require the simultaneous or integrated use of various forms of memory, which we term 'complex learning'. Ideally, the outcome of research on sleep and memory would generalize to these complex human experiences. However, to study memory consolidation in laboratory setting, researchers have refined tasks to distinguish clearly between declarative and procedural memory functions – a

reductionist approach that can help us to compare how different types of information are stored. Correlational studies trying to link sleep brain activity to behavioural performance suggest distinct roles in memory processing for slow oscillations and sleep spindles, with SOs preferentially influencing declarative memory (Gais & Born, 2004; Walker, 2009), and spindles impacting procedural memory (Choi et al., 2019; Barakat et al., 2013). However, these associations are not absolute, as there are exceptions: some studies have shown sleep spindles to be important in declarative memory (e.g., Schabus et al. 2004) and slow oscillations to be relevant to procedural memory (e.g., Menicucci et al. 2020). Although each type of task involves some distinct brain regions, brain systems involved play similar functional roles across domains, which depend on common anatomical, physiological, and biochemical substrates - suggesting they might be less separable than assumed by the declarative/procedural memory model (Ullman, 2004; Brown & Robertson, 2007). Tasks considered declarative and procedural both benefit from sleep (Gais & Born, 2004; Schönauer et al., 2014), and the process of consolidation of both subtypes of memory seems to follow a similar process, as sensory information captured during learning transitions from short-term memory into more stable long-term memory formats (Nairne & Neath, 2012). The specific, and potentially different, roles of each sleep oscillation (either separately or temporally synchronized), therefore still remains unclear. Developing tools to experimentally manipulate them is necessary to causally infer the underlying consolidation mechanisms.

In 2013, Ngo et al. demonstrated that slow oscillations can be modulated by targeting their up-states using a technique known as Closed-Loop Auditory Stimulation (CLAS), which resulted in evoked slow wave and spindle band activity, and an improvement in overnight memory consolidation on a declarative memory task (Ngo et al., 2013b). This approach (SO-CLAS) has since been used extensively (for recent reviews, see Harrington & Cairney 2021; Choi et al. 2020). Although all of these studies did observe enhanced slow wave activity following CLAS, only a subset supported the causal link for the relationship between SO activity and memory consolidation by enhancing performance on declarative memory tasks (Ngo et al., 2013b, 2015; Ong et al., 2016; Papalambros et al., 2017). However, discrepancies in behaviour improvements findings in both declarative (Koo-Poeggel et al., 2022; Harrington et al., 2021; Schneider et al., 2020; Henin et al., 2019; Ong et al., 2018) and procedural paradigms (Baxter et al., 2023) suggest a more complex causal relationship.

SO-CLAS research efforts have been primarily focusing on consolidation of simple tasks (e.g. word-pair memorization, simple arithmetic, serial motor reaction time, and motor sequence tasks; Ong et al. 2016; Prehn-Kristensen et al. 2020; Choi et al. 2019). Research of the benefit of CLAS on complex tasks has been limited, but suggests potential influences. For example, Shimizu et al. (2018) found that SO-CLAS improves performance on a navigation

task, showing the feasibility of real-world applications.

A similar CLAS approach on sleep spindles (SP-CLAS) would bring complementary information about their roles. However, CLAS directly targeting spindles has been technically challenging due to their short duration and inter and intra-subject variability (Choi et al., 2018, 2019; Choi & Jun, 2022; Antony & Paller, 2017). Through interdisciplinary collaboration, our lab has developed a device capable of real-time detection and stimulation of sleep spindles, the Portiloop (Valenchon et al., 2022; Sobral et al., 2025). The capacity of SP-CLAS to modulate neural activity has been demonstrated in a multi-night within-subject design (Jourde et al., 2025a). Additionally, research from our lab has challenged the previously established hypothesis regarding the sensory-blocking role of sleep spindles. Our findings demonstrate that auditory information continues to reach the cortex even during spindles and their refractory periods (Jourde & Coffey, 2024). Targeted manipulation of both SO and SP through CLAS, while measuring their effects on procedural, declarative and complex learning may elucidate their specific roles in memory consolidation. Comparing the effects of closed-loop auditory stimulation of both SO and SP in a single study paradigm, may therefore provide information about their contribution to memory consolidation.

In the present study, we aimed to address this issue by investigating the neurophysiological and behavioural outcomes of SO-CLAS and SP-CLAS (using two approaches: immediate and delayed stimulation of spindles) on different memory systems in a between-subjects nap design. Subjects were randomly assigned to one of the experimental conditions (including unstimulated sleep and wake control) for a 2 hr nap opportunity. Evoked brain activity and change in performance on declarative, procedural, and complex tasks were compared across conditions.

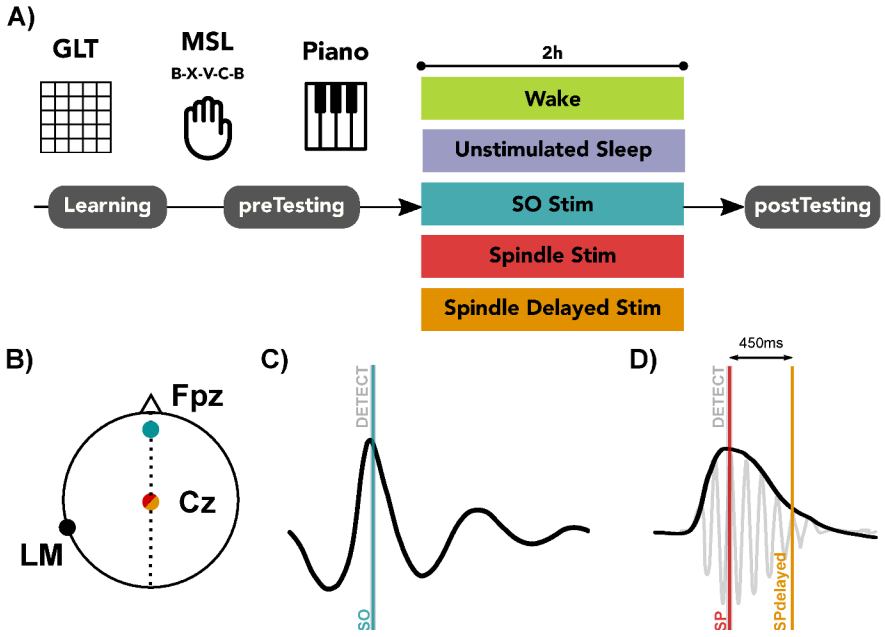

Figure 7.1: Study design. A) Participants learned and were tested on three behavioural tasks (counterbalanced order) before being randomly assigned to a manipulation condition (N = ∼20 per condition). After a 2-hour period, they were tested on the task again and changes in performance were computed. B) Schematic representation of the electrode placements and site of detection for each condition. In the 'SO' condition, brain oscillations were detected at Fpz while in the 'SP' and 'SPd' conditions, brain oscillations were detected at Cz. C) In the 'SO' condition the auditory stimulation (15 ms pink noise) was sent at the SO up-state. D) In the 'SP' condition the auditory stimulation (15 ms pink noise) was sent at spindle detection while in the 'SPd' condition, the stimulation was sent 450 ms later.

7.3 Methods

7.3.1 Participants

One hundred and twenty-six healthy neurotypical right-handed participants between the ages of 18 - 40 were recruited in total for this experiment, with the aim of including approximately 20 subjects per group who each slept at least 30 minutes in NREM2 and NREM3, combined. Pregnancy, BMI $\leq$ 40, and poor sleep habits, were grounds for exclusion due to potential effects on sleep quality (Sahota et al., 2003; Romero-Corral et al., 2010). Individuals with over 2 years or 500 hours of music training were excluded to ensure similar baseline performance on the complex memory (piano) task. All participants self-reported having normal or corrected-to-normal hearing, no history of any diagnosed psychiatric or sleep disorder (Lee & Douglass, 2010), and were not taking medications that target the nervous system. Across all conditions, fourteen participants were excluded for not sleeping enough. Of these, 6 had

been in the 'Sleep' condition, 4 in the 'SO' condition, and 2 in each of the spindle conditions ('SP' and 'SPd'). This distribution does not suggest that sound stimulation was the cause of poor sleep resulting in exclusion. Three subjects were excluded for briefly falling asleep in the 'Wake' condition (> 5 mins) and seven participants were excluded from the analysis due to technical issues. One hundred and two participants (M = 24.6, SD = 5.9) were retained in the main data analyses (72 F, 29 M, 1 non-disclosed; see Supplementary Materials Table S1 for a breakdown of age and sex by experimental condition). Participants received either course credits or financial compensation for their time. The study protocol was approved by the Concordia University Research Ethics Committee, and all participants signed an informed consent form after receiving opportunity to fully understand the purpose and procedure of the study.

7.3.2 Study procedure

The study procedure is illustrated in Figure 7.1. The experimental session consisted of one five hour visit. All participants completed the study at the same time of day (12-5 pm) to eliminate circadian confounds. They were asked to abstain from caffeine and alcohol the night before and the day of the experiment, and to abstain from nicotine, marijuana, and other recreational drugs for a week before the experiment, due to the effects of these substances on sleep architecture and latency (Jaehne et al., 2009; He et al., 2019; Březinová, 1974; Schierenbeck et al., 2008). Participants were instructed to go to sleep one hour later than their usual bedtime to increase sleep pressure and facilitate afternoon napping.

On the day of the experiment, all participants completed a series of sleep questionnaires. Following completion, participants were randomly assigned to one of five conditions: wake ('Wake'), no stimulation/sham ('Sleep'), slow oscillation stimulation ('SO'), spindle stimulation ('SP') or delayed spindle stimulation ('SPd'). In the sleep condition, participants had the opportunity to sleep for up to two hours, and were asked to stay in bed and relax if they were unable to sleep. In the wake condition, participants were asked to read or write/draw for two hours. The use of electronics was not permitted. After the two-hour session, all participants were retested on the same cognitive tasks.

7.3.3 Questionnaires

All participants were asked to complete the Montreal Music History Questionnaire (MMHQ; Coffey et al. 2011) prior to the experiment to confirm eligibility. The MMHQ is used to assess musical experience, including the number of training/practice hours completed, the age at which they began their formal training, as well as some basic demographic information.

On the day of the experiment, participants completed a health questionnaire in addition to several sleep questionnaires including the Morningness-Eveningness Questionnaire (Horne & Östberg, 1976), the Pittsburgh Sleep Quality Index (Buysse et al., 1989) and the Epworth Sleepiness Scale (Johns, 1991).

7.3.4 Cognitive tasks

Psychomotor Vigilance Task

The Psychomotor Vigilance Task (PVT; Evans et al. 2018), was implemented to confirm participant alertness before and after the nap opportunity. The participant is shown a black screen with a red circle in the centre. Once the red circle disappears, participants are instructed to press the space bar of the computer as quickly as possible. This repeats for twenty trials within a five-minute period. Performance on the task was measured by the average reaction time in milliseconds on the fastest 10 % of trials (as used in previous work; Basner et al. 2011).

Grid Location Task

The Grid Location Task (GLT) is a declarative memory task requiring participants to remember the location of images that are sequentially displayed in random positions on a grid (Rasch et al., 2007). In the present implementation, 24 images were displayed in a 5 x 5 grid. Presentation and testing phases were rotated for a minimum of 2 cycles until a 70 percent threshold of correct responses is attained. Performance on the task was measured as the number of images placed within the correct grid location (referred to as **GLT Accuracy**, see Figure 7.4A top for learning curve across participants).

Motor Sequence Learning Task

The Motor Sequence Learning (MSL) task is a procedural learning task that requires participants to use their left hand to repeat a five key sequence on a keyboard as quickly and as accurately as possible (Walker et al., 2002). The specified sequence was B-X-V-C-B in which B represents the index finger, while X represents the pinky finger. The participant was asked to repeat the sequence as quickly and accurately as possible for a 30-second block followed by a 30-second rest period, for a total of 12 active trials (12 minutes).

In literature, performance on the MSL task is reported using a variety of highly-related accuracy and speed metrics. We elected to use the number of correct sequences produced per 30 s block (referred to as **MSL Accuracy**), noting that due to the time constraints on

sequence production, it is strongly correlated with speed-focused metrics such as the average speed of execution of correct sequences ($r = -0.47$, $p = 5.04 \times 10^{-7}$). Being a speed-dependent task, the measure is susceptible to the influence of sleep inertia, and participants require some re-familiarizing with the task before true performance may be assessed. For these reasons and following previous research (Song et al., 2007), the first two trials after the sleep/wake interval were excluded as a warm-up period to avoid a decrease in performance due to sleep inertia and to re-establish task familiarity. Performance data is therefore averaged during the last three trials of the pre-sleep learning period, and the third, fourth and fifth trials from the post-sleep testing period (see Figure 7.4B top).

Piano Task

Musical training, which incorporates visual, spatial, and motor abilities, and involves both declarative and procedural memory, is well-suited for exploring neuroplasticity in complex human learning (Herholz & Zatorre, 2012). Previous research investigating the causal role of sleep oscillations support a sensitivity of this type of learning to sleep (Antony et al., 2012).

The piano-learning task was adapted from a longitudinal design created by Herholz et al. (2015) and consists of a learning session and two testing sessions. This task integrates both declarative and procedural memory representing a more ecologically valid task. The right-handed participants were asked to learn to produce 20 short melodies, using their left hand to increase difficulty and thus allow more room for motor skill improvement. The learning session consists of 6 trials for each of the melodies, in which participants first listened to them and then were asked to produce them on a MIDI keyboard. The melody is played to the participants with a visual representation of the keys needed on a keyboard diagram displayed on the computer monitor. Visual cues, in which the key sequence highlighted during the melody presentation, were offered only on the second and fourth trials, to enable novices to play the melodies. Visual cues were absent in the other trials to discourage reliance upon them and encourage plasticity relating to auditory-motor rather than visual-motor associations. After each trial in the learning phase, participants received feedback on their pitch and rhythmic accuracy in the form of two visual symbolic indicators (i.e., coloured smiley faces). Pitch feedback was binary (all keys correct or not), and rhythm feedback was given in three ranges of accuracy on the basis of pilot testing (good, moderate, poor). Each of the testing sessions (i.e., before and after the nap opportunity) consisted of 2 trials for each melody. Mean performance across all melodies was extracted for the second trial of each testing session as the first one is considered a warm-up trial, allowing the participant to position their hand correctly (see Figure 7.4C and D top). Formal feedback on pitch and rhythm was not provided during testing. Performance on the task was measured using

two metrics: **Pitch accuracy** was calculated as the percentage of correctly played notes in the melody, and **Rhythm accuracy** was computed as a normalized score based on each participant's worst learning performance for each melody, ranging from 0 (no error) to 100 (many errors); this score was then inverted so higher values indicated better performance. For test trials where participants performed worse than during training, normalized rhythm scores below zero were set to 0.

For each task, we used Performance change as our main metric to measure behavioural changes after the 2-hour period of either sleep or wake. Performance change was computed as (Post − Pre)/Pre, where 'Pre' represents performance before the sleep opportunity (or wake period) and 'Post' represents performance afterwards.

7.3.5 Data collection

EEG recordings

Electroencephalography (EEG) is a standard non-invasive method of capturing neural oscillatory activity in the cortex. The electroencephalogram captures changes in electrical potentials between electrodes placed on the scalp (da Silva, 1991). EEG signals were collected using different devices due to the two stimulation conditions requiring different equipment (ecHT (Endpoint Connected Hilbert Transformation (ecHT); Elemind Technologies, Inc., Cambridge, USA) for SO stimulation and Portiloop (Valenchon et al., 2022) for spindle stimulation conditions). All participants were equipped with both measuring devices for homogeneity of experience. The ecHT device acquired EEG data from the Fpz-M1 channel at a sampling rate of 500 Hz. The Portiloop recorded EEG signals at 250 Hz using 5 electrodes placed at midline locations (Fz, FPz, Cz, and Pz) according to the international 10-20 system (Jasper, 1958), and referenced to the left mastoid. The ground electrode was positioned on the left ear lobe. Finally, most participants also wore the Dreem Headband (Dreem.com; Arnal et al. 2020), which was used for automatic sleep staging.

Real-time detection

SOs peaks were automatically detected on Fpz (Cox et al., 2018) using the ecHT device and its online detection algorithm. EEG data was low-pass filtered in the delta band (0.5 - 1.5 Hz) and was analyzed for SO characteristics derived from (Mölle & Born, 2011): time points of positive to negative zero crossings were identified, then the intervals with sufficiently low negative peaks of -40μV, with a duration of the negative peak between 125 and 1500 ms, and an amplitude range 75μV between the peaks were isolated.

Sleep spindles were detected using the Portiloop (Valenchon et al., 2022), which a low-cost deep-learning-based stimulation system with a complex detection algorithm suitable for spindle CLAS. The Portiloop's detection algorithm has been trained to detect sleep spindles in real-time on a large dataset called MASS (O'reilly et al., 2014) using offline detections by Warby et al. (2014) and labels by experts (Lacourse et al., 2020). The current study used this device to deliver precisely-timed sound stimulation during spindles for the two spindle stimulation conditions (i.e., immediately upon spindle detection and with a 450 ms delay).

Auditory stimulation

All stimulation conditions used the same auditory stimuli to maximize comparability: a 15 ms burst of 55 dB SPL pink noise (with 5 ms linear ramps to avoid click generation in the earphones). For participants in the SO conditions, auditory stimulation was delivered as soon as the SO-peak was detected. In the SP condition, stimulation was sent immediately upon spindle detection. In the SPdelayed condition, a delay of 450 ms was introduced between detection and stimulation to target the end-tail of sleep spindles as previous research suggested differential neurophysiological effects according to stimulation timing within the spindle (Jourde et al., 2025a).

7.3.6 EEG data analysis

All data were analyzed in Python using custom scripts built on freely available packages. We used NumPy for array manipulation, SciPy's signal module for filtering operations (including notch, bandpass, and band-specific filtering with butter and filtfilt), and Matplotlib for visualizing both filter frequency responses and average brain responses. In all analyses, filters were applied before defining epochs to prevent border effects. To control for data quality, we applied a 4th order Butterworth band-pass filter (0.5 to 30 Hz) and then applied a custom artifact rejection script to each recording that automatically identified and removed problematic data sections by detecting both absolute signal amplitude and sudden amplitude changes (typically caused by movement).

For analyzing the evoked responses in the slow-wave band, we applied a 4th order Butterworth band-pass filter (0.1 to 4 Hz) to the raw data. For analyzing spindle band activity, we used the same filter parameters but with an 11-16 Hz frequency band. Since phases of both detected and evoked sleep spindles can vary, we used the signal envelope (i.e the absolute value of the Hilbert transform of the spindle band signal) to obtain its magnitude as our metric to estimate spindle power over time.

Epochs definitions

Across all conditions involving detections of sleep events ('Sleep', 'SO', 'SP' and 'SPd') epochs were extracted from - 2.5 seconds before to 2.5 seconds after event detection and baseline-corrected using the mean amplitude from -2.5 to -.5 seconds prior to detection—a window chosen to avoid capturing amplitude changes generated by potential endogenous coupling (Clemens et al., 2007).

For the participants in all conditions except 'SP', for which manual scoring was performed due to lack of equipment availability, sleep staging was extracted from the Dreem headband. Only epochs occurring during NREM2 and NREM3 were included in the analysis.

Average evoked responses in both frequency bands of interest: 0.5–1.5 Hz to capture slow wave activity (SWA) and 11–16 Hz to measure spindle activity (FSA) were computed for each participant by averaging all epochs. Timeseries were then averaged across participants for statistical comparison.

Metrics extraction

Slow wave activity at detection was extracted as the amplitude of each subject's slow wave activity timeseries at time of detection. The evoked slow wave peak-to-peak amplitude was quantified as the difference between amplitude values measured at 550 ms (i.e., mean amplitude in a time window from 500 to 600 ms) and 900 ms post-stimulation (i.e., mean amplitude in a time window from 800 to 1000 ms) to account for latency variability between participants, following the methodology established in (Jourde et al., 2024).

Spindle activity at detection was extracted as the magnitude of each subject's spindle band envelope timeseries at time of detection. The magnitude of the spindle envelope signal from 0.75 to 1.5 s after stimulation onset was computed to assess evoked spindle activity, following previous research using the same stimulation device and auditory stimuli (Jourde et al., 2025a). To account for individual differences, a baseline correction was applied by subtracting each subject's mean magnitude measured during the pre-stimulus period (-2.5 to -0.5 s relative to stimulus onset).

To inform parameter selection in future CLAS studies, we quantified relationships between the magnitude of the detected oscillation and evoked oscillatory activity within and across frequency bands. These correlations provide insight into the relationship between individual differences in neural oscillation strength and subsequent neural responses.

7.3.7 Statistical analysis

To confirm that groups did not differ prior to the experimental manipulation, we conducted a one-way ANOVA on age, a Chi-square test of independence on sex, and a one-way ANOVA on pre-learning PVT reaction time scores as a proxy for general alertness. To assess whether auditory stimulation negatively affected overall sleep quantity, we compared sleep duration (NREM2 and 3 combined) in each stimulation condition to the unstimulated 'Sleep' condition using independent sample Student's t-tests.

To document the electrophysiological effects of auditory stimulation, we compared the evoked responses in each condition in the two frequency bands of interest across subjects in the stimulation condition vs. sham (independent samples t-tests) for each timepoint, correcting for False Discovery Rate using a Benjamini-Hochberg correction (alpha = 0.05) (Figure 7.2).

To inform parameter selection in future closed-loop auditory stimulation paradigms, we computed correlations between evoked and detected activity for each of the three stimulation conditions (Figure 7.3).

Repeated-measures ANOVAs were used to asses changes in behavioural performance over Time (i.e., between the pre-and post- experimental manipulation measurements) and between Conditions.

To explore potential relationship between the strength of evoked brain oscillations and task performance improvements, we examined the correlation between stimulation effectiveness (quantified by evoked oscillation amplitude) and performance changes using correlations, focusing on comparisons that are most informative for the present research questions. Spearman's correlations were used throughout in case of normality violations.

7.4 Results

7.4.1 Homogeneity across groups

We conducted several statistical tests to ensure homogeneity of demographics and alertness across the groups, before experimental manipulation. A one-way ANOVA revealed no significant differences in participants' age across groups ($F(4, 97) = .96$, $p = .44$). Sex distribution was similarly balanced, confirmed by a Chi-square test of independence ($X^2_F(8) = 6.23$, $p = .61$). Participant alertness, as measured by their performance on the PVT before the learning phase, showed no significant differences between the six conditions as indicated by a one-way ANOVA ($F(4, 97) = 1.03$, $p = .39$). Regarding sleep parameters, across all

sleep conditions, participants averaged 71.4 minutes of sleep (SD: 21.8; see Supplementary Table S1 for complete results). To assess whether auditory stimulation affected sleep quality, we compared sleep duration (NREM2 and 3 combined) in each stimulation condition to the unstimulated 'Sleep' condition using independent sample Student's t-tests. No significant differences emerged between any of the stimulated conditions and the control Sleep condition (**SO vs Sleep**: (T(38) = -0.69, p = 0.49, Cohen's d =-0.22); **SP vs Sleep**: (T(40) = 0.73, p = 0.47, Cohen's d =0.23); **SPd vs Sleep**: (T(38) = -1.82, p = 0.08, Cohen's d = -0.58)).

7.4.2 Electrophysiological effects of brain stimulation

Evoked responses

To document the electrophysiological effects of auditory stimulation we compared the evoked responses in each condition in the two frequency bands of interest (i.e., 0.1 - 4 Hz for slow wave activity and 11 - 16 Hz for the spindle activity; see Supplementary Table S2 for complete results). A clear evoked slow oscillation was observed when sound was delivered during SO-up-states, with statistically-significant differences from sham ('Sleep' condition) between 0.5 and 1.5 seconds post stimulation (Figure7.2A top), replicating the results described in (Ngo et al., 2013b, 2015; Ong et al., 2016; Harrington et al., 2021). Similarly, a clear evoked slow response was observed when sound was sent simultaneously with sleep spindle detection ('SP' condition) or 450 ms later ('SP delayed'; Figure7.2A bottom), noting that the difference in the wave form across the SO and two SP stimulation conditions are due to the presence of an SO in the former case (and differences in the recording equipment and montage, see Methods); each waveform is therefore compared with the equivalent detection in the sham condition ('Sleep'). In both conditions the stimulation induced statistically-significant changes in amplitude for the majority of the duration between stimulation and 2 s.

Next, we evaluated the effects of each stimulation type on spindle band activity (11 - 16 Hz). Concerning the 'SO' condition (i.e., auditory stimulation coinciding with the SO up-state), we were also able to replicate the findings described in earlier work of increased spindle activity between 750 ms and 1.5 s post stimulation (e.g., Leminen et al. 2017; Papalambros et al. 2017; Ngo et al. 2019; Ong et al. 2018; Schneider et al. 2020; Baxter et al. 2023; see Figure 7.2B top). Additionally, a transient decrease in spindle band activity was observed relative to sham ∼500 ms post stimulation (although it did not survive multiple comparisons correction).

A clear increase in spindle activity between 750 ms and 1.5 s post stimulation was observed in both the 'SP' and 'SPd' conditions (see Figure 7.2B, bottom). In the 'SP' condition, stimulation appeared to truncate the stimulated spindle ∼500 ms post, corroborating earlier

results (Jourde et al., 2025a).

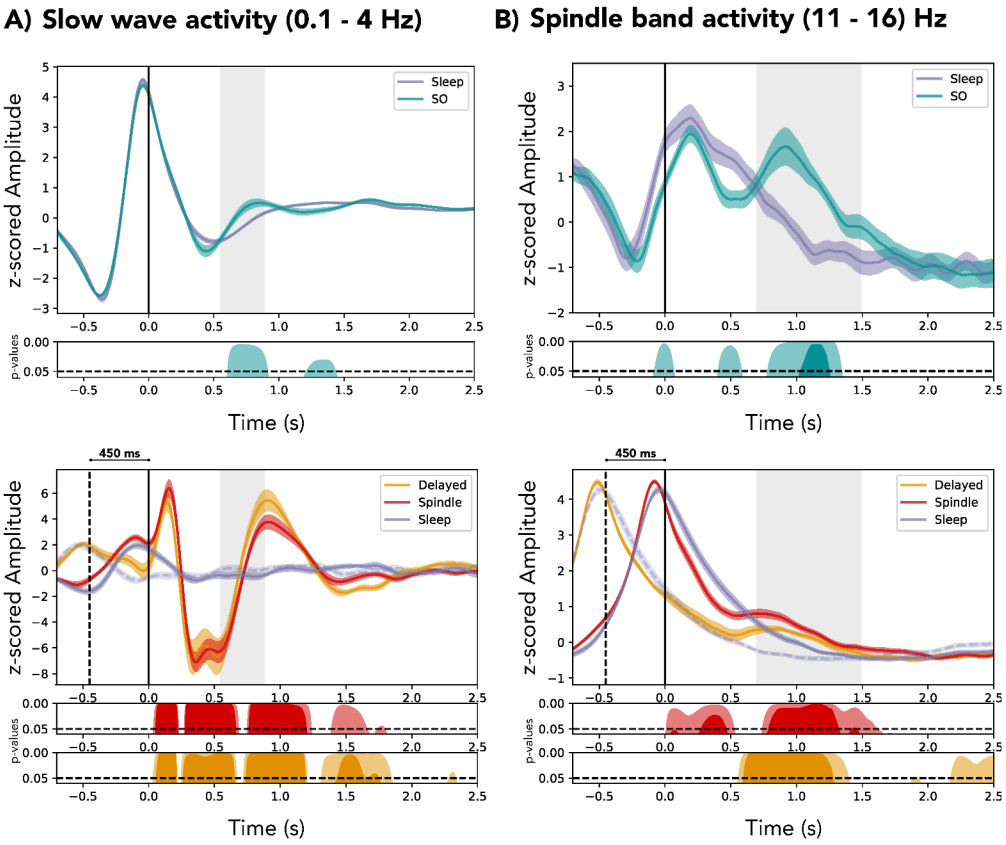

Figure 7.2: Closed-loop auditory simulation of both slow oscillations (detected at Fpz) and sleep spindles (detected at Cz) enhances A) slow wave activity (0.1 - 4 Hz) and B) spindle band activity (11 - 16 Hz). Black vertical lines represent stimulation onset. Dashed vertical lines represent the onset of spindle detection in the 'SPdelayed' condition. Solid lines indicate group mean and shaded lines represent standard error of the mean. Statistical differences compared to unstimulated sleep ('Sleep' condition) are represented in the bottom panels. Solid areas represent corrected p-values and coloured shading represent uncorrected p-values.

Correlations between evoked and detected activity

To inform parameter selection in future closed-loop auditory stimulation paradigms, we investigated the correlations between evoked and detected activity. For each of the three stimulation conditions, we computed correlations between the magnitude of the detected oscillation (either SO or spindle according to the condition) and evoked oscillations in a) the SO and b) the spindle band. We also computed c) the correlation in magnitude between the the evoked oscillations (i.e., SO and spindle activity). The results are presented schematically in Figure 7.3.

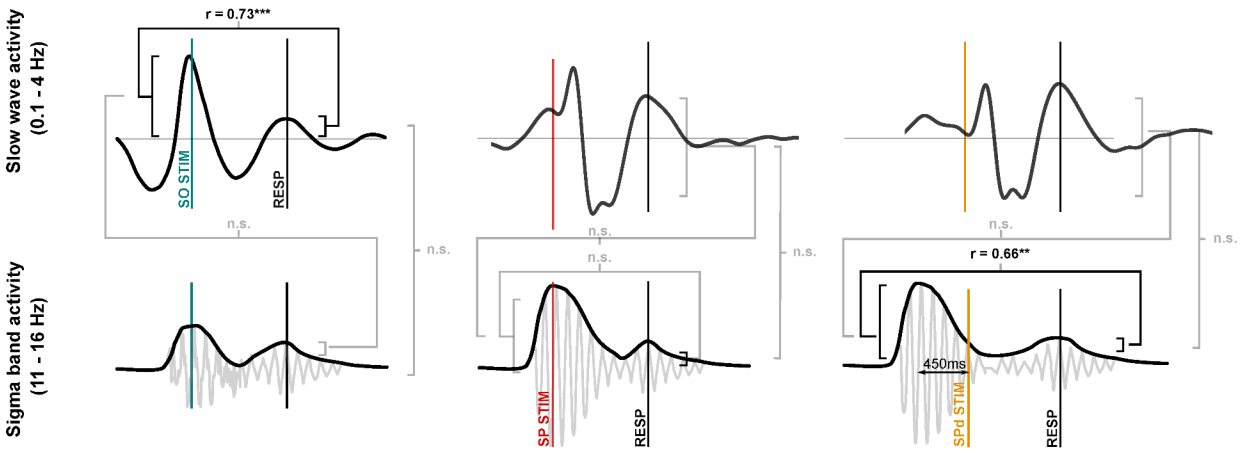

Figure 7.3: Correlations between detected and evoked signal magnitude. The mean magnitude of subjects' SO in the SO-upstate stimulation condition (SO; left) was significantly correlated with the amplitude of their evoked slow oscillation, and the mean magnitude of the detected spindle was correlated with that of that of the evoked spindle in the SPdelayed (SPd) condition. No other correlations were significant. STIM = timing of stimulation, RESP = timing of response measurement.

Stimulating slow-oscillations up-states

For the slow oscillation condition, all detected and evoked values were computed at the Fpz electrode site. There was a significant correlation between amplitude of SO at detection and amplitude of the evoked SO ($r = .73$, $p < .001$), suggesting that participants with overall stronger SOs at detection were those who showed stronger evoked SOs. The amplitude of SO at detection was instead not correlated with the magnitude of the spindle activity ($r = -.07$, $p = .78$), suggesting that participants with larger SOs were not necessarily those who produced larger spindles after stimulation. The magnitude of the two evoked responses was not correlated ($r = .08$ $p = .75$), suggesting that strong SO evocation did not imply strong spindle evocation.

Stimulating sleep spindles

For the two spindle stimulation conditions (i.e. 'SP' and 'SPd'), all detected and evoked values were computed at the at Cz electrode site.

In the 'SP' condition (i.e., stimulation during spindles), none of the correlations tested were significant: detected spindle magnitude did not correlate with the magnitude of evoked slow wave activity ($r = -.02$, $p = .93$) nor evoked spindle activity ($r = .37$, $p = .09$), and the amplitude of evoked slow wave activity was not correlated with that of evoked spindle activity ($r = .27$, $p = .22$). These results indicate that the average magnitude of evoked responses cannot be predicted from a subject's mean spindle activity upon detection, when

stimulating during a spindle.

In the 'SPd' condition (i.e., stimulation 450 ms post spindle detection), the correlation between magnitude of spindle activity at detection and evoked slow wave activity did not reach significance (r = .02, p = .93). However, a significant relationship was found with the magnitude of evoked spindle activity (r = .66, p = .004). We found no correlation between the magnitude of the evoked responses (r = .33, p = .19). These results indicate that the average magnitude of evoked spindle (but not slow wave activity) can be predicted from a subject's mean spindle activity upon detection, when stimulating after a spindle.

7.4.3 Behavioural effects of brain stimulation

Change in performance between conditions

To evaluate the effect of the experimental manipulation on behavioural performance, a repeated measures ANOVA (rmANOVA) was employed for each task investigating the changes in performance over Time (i.e., between the pre-and post- experimental manipulation measurements) and between Conditions.

Grid Location Task

The rmANOVA results revealed a significant main effect of Time, $F(1, 97) = 29.69$, $p < .001$, $\omega^2 = .028$. However, the interaction between Time and Condition was not significant, $F(4, 97) = 0.11$, $p = .979$, $\omega^2 = .00$, indicating that while performance generally decreased during the interval between pre- and post- testing, the experimental conditions did not differentially affect the change in performance on the declarative memory task (GLT) over time (see Figure 7.4A).

Motor Sequence Learning task

The rmANOVA results revealed once again a significant main effect of Time, $F(1, 96) = 5.19$, $p = .025$, $\omega^2 = .007$. However, the interaction between Time and Condition was not significant, $F(4, 96) = 0.71$, $p = .589$, $\omega^2 = .000$ indicating that while all participants improved their performance on the task, the experimental conditions did not differentially affect their change in performance on the procedural task (MSL) over time (see Figure 7.4B).

Piano Learning task Concerning pitch accuracy, the rmANOVA results indicated that the main effect of Time was not significant, $F(1, 96) = 1.52$, $p = .22$, $\omega^2 = 3.79 \times 10^{-4}$. Similarly, the interaction between Time and Condition was also not significant, $F(4, 96) = 1.13$, $p = .347$, $\omega^2 = 3.13 \times 10^{-4}$ suggesting and absence of significative change in performance between the pre and post manipualtions measures in term of pitch accuracy on the Piano

task (see Figure 7.4C).

On the contrary, concerning rhyhtmn accuracy, the results of the rmANOVA showed a significant main effect of Time, $F(1, 96) = 5.19$, $p = .025$, $\omega^2 = .007$, but not in interaction with Condition, $F(4, 96) = 0.71$, $p = .589$, $\omega^2 = .00$. This indicates that while participants across all groups improved their rhythm accuracy performance, this improvement did not differ significantly between experimental conditions (see Figure 7.4D).

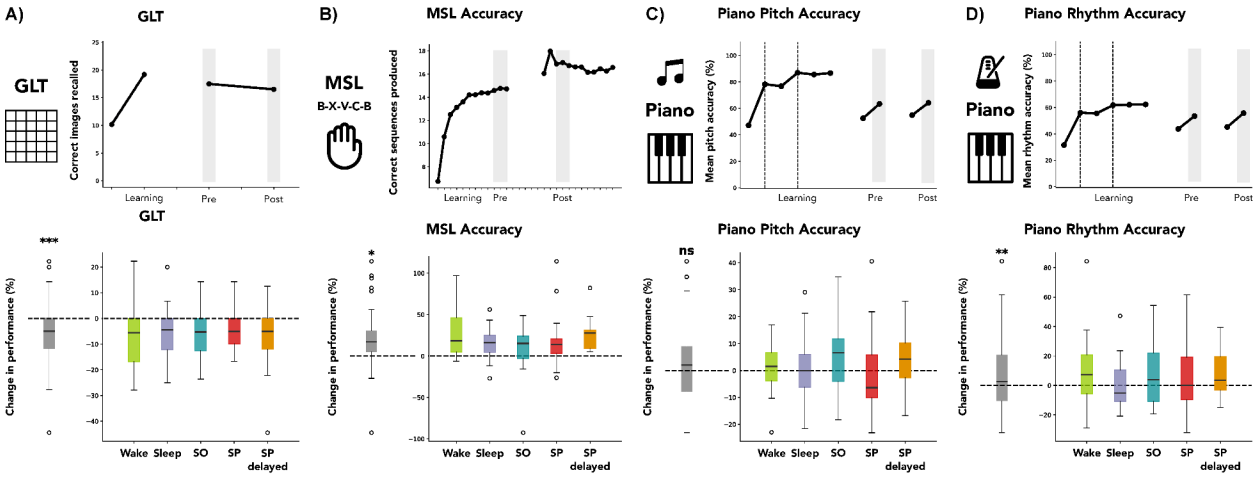

Figure 7.4: Learning curves averaged across all participants (top row) and change in performance by condition for each behavioural task (bottom row), for A) the declarative task (GLT), B) the procedural task (MSL), and the complex task (piano learning), which was measured by C) pitch accuracy and D) rhythm accuracy. While all task metrics except piano pitch accuracy showed a global change over time across conditions, there were no significant interactions between time and condition for any task.

Correlation between evoked responses and change in performance

To explore the causal relationship between the strength of evoked brain oscillations and task performance improvements, we examined the correlation between stimulation effectiveness (quantified by evoked oscillation amplitude) and performance changes. We tested all correlations for each task and each evoked responses in both the slow oscillation and sleep spindles stimulation (including delayed) groups, focusing on comparisons that are most informative for the present research questions. Complete results for all correlations are found in Supplementary Table S3.

Declarative learning and evoked responses

No statistically significant correlations were found in the relationship between change in performance in the declarative task and amplitude of the evoked response in either frequency band of interest (for complete results see Supplementary Table S3).

Procedural learning and evoked responses

Comparison of the change in performance in the accuracy of the procedural task did not yield significant results concerning the correlations between improvement on the task and evoked sleep spindle activity in either conditions (**SP**: r = .27, p = 0.23; **SPd**: r=0.45, p-value=0.08)

Complex learning and evoked responses

Analysis of the Piano task revealed distinct patterns when examining pitch versus rhythm accuracy (for complete results see Supplementary Table S3). For pitch accuracy, we identified a significant negative correlation between evoked spindle activity and performance accuracy in the 'SP' condition (r = -0.50, p = 0.02). Similarly, for rhythm accuracy, evoked spindle activity in the 'SPd' condition showed a significant negative correlation with rhythm performance (r = -0.57, p = 0.02).

A)

	GLT	MSL Accuracy	Piano Pitch	Piano Rhythm
Evoked slow wave activity	n.s.	n.s.	n.s.	n.s.
Evoked spindle activity	n.s.	n.s.	⊖SP	⊖SPd

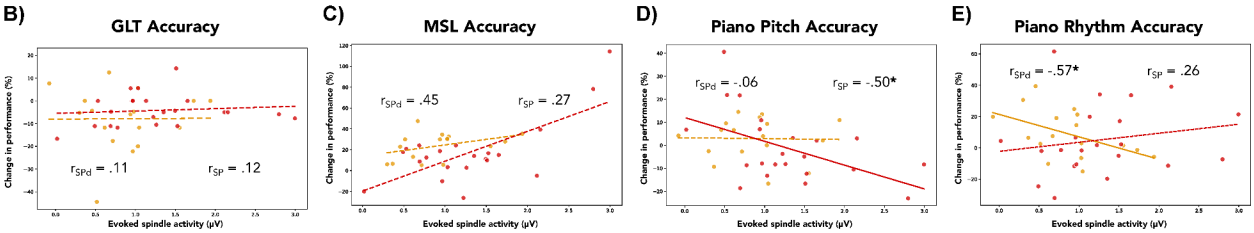

Figure 7.5: Correlations between change in performance on the behavioural tasks and magnitude of evoked responses. A) Summary of statistical significance and direction of correlation for all tasks and evoked responses. B) Change in performance on the declarative task (GLT) was not correlated with evoked spindle activity in either the 'SP' or 'SPd' conditions. C) Although correlations were not significant between the change in performance on the procedural task (MSL) as a function of evoked spindle activity, both conditions ('SP', 'SPd') showed a positive trend. Evoked spindle activity negatively correlated with D) pitch accuracy in SP condition and E) rhythm accuracy in SP-delayed condition. This discrepancy may be suggestive of the importance of stimulation timing for consolidation of complex tasks.

7.5 Discussion

The purpose of this study was to compare the effects of auditory closed-loop stimulation when applied directly upon spindle detection, with a delay following detection, and using the more common slow oscillation-upstate stimulation, to ascertain its effects on physiology as well as declarative, procedural, and complex memory consolidation.

7.5.1 Temporally-specific CLAS induces temporally-specific neurophysiological changes

We first investigated the physiological effects of the three stimulation conditions. We found robust physiological responses in all three stimulation conditions as compared to sham (Figure 7.2), which were broadly similar to one another and to the effects reported to open loop stimulation (i.e., stimulation presented randomly during NREM2 and NREM3 sleep; Jourde et al. (2024); Bellesi et al. (2014); Latreille et al. (2020)). Namely, presenting sounds in sleep that are not loud enough to cause awakening instead evokes a slow oscillation (also referred to as a K-complex; Halász 2016) and increased spindle activity about a second later. Note that it is not possible to compare the SO and spindle stimulation conditions quantitatively in this project because a different recording system and EEG montage was used. The results suggest that all three kinds of stimulation affect the strength and timing of the evoked oscillations, which are of interest for sleep-dependent memory consolidation. If these evoked oscillations are able to reactivate temporarily-stored memories and stimulate their replay, then all three stimulation conditions may provide the necessary circumstances for memory consolidation (noting that the present study does not investigate the informational content of the events). However, timing of stimulation did seem to matter. Stimulation presented immediately upon spindle detection ('SP' condition) appeared to terminate the spindle early (Figure 7.2B, bottom). This shortening of sleep spindle was not observed in the delayed condition ('SPd'), where only an increased spindle activity post stimulation was present. This observation is coherent with our previous work investigating CLAS of spindles, which compared the physiological effects of stimulating the first vs. second half of a spindle. Only earlier stimulation generated this effect (Jourde et al., 2025a). The results across both studies suggest that neural input during the spindle might result in its termination, as proposed in Sela et al. (2016). If the endogenous spindles were involved in information transfer to cortex for long-term storage, this could mean that early stimulation might interrupt this process in the 'SP' condition but not the 'SPd' condition. In future work, to further test this idea, instead of presenting single sounds immediately upon spindle detection, trains of clicks could be used (similarly to Ngo et al. 2015) as a means of repeatedly shortening subsequent evoked spindles, so as to adduce evidence for their role in information transfer through loss-of-function. Disrupting endogenous activity selectively can also be leveraged to causally infer the role of spindles with different characteristics such as their temporal occurrence with other spindles (i.e., if they're present in trains or isolated; Boutin et al. 2024; Boutin & Doyon 2020) or with slow oscillations (i.e., coupled spindles; Baena et al. 2024, 2023; Helfrich et al. 2018; Muehlroth et al. 2019).

7.5.2 Predictors of inter-individual differences in evoked responses

Brain stimulation studies frequently note differences in evoked response amplitudes (López-Alonso et al., 2014; Wiethoff et al., 2014), which might be correlated with effectiveness of memory manipulations or therapeutic interventions (Ridding & Ziemann, 2010). These variations may prove important for understanding how memory systems can be influenced, and to predict who might be most susceptible to different sorts of modulation techniques, for which reason we investigated correlations between detected and evoked signal magnitude in each stimulation condition (summarized in Figure 7.3). Subjects with larger SOs at detection tended to be those who produced larger evoked SOs, and subjects with larger spindles at detection tended to be those who showed larger evoked spindle activity (in the 'SPd' condition but not 'SP'). Interestingly, the opposite was not the case: the average strength of one's SOs or spindles upon detection was not linked to how strong the opposite type of evoked oscillation was. This suggests that while the stimulation target seems to be successfully entrained, this effect does not represent an overall susceptibility of one's brain to response to stimulation. Additionally, the magnitude of evoked SOs and spindles did not correlate with one another across any of the stimulation conditions suggesting that despite temporal co-occurrence suggested by average time series across participants (as observed in Figure 7.2), individuals' susceptibility to produce evoked SO and spindle activity was not linked. This result suggests that auditory stimulation may not consistently generate coupling. In our previous work (Jourde et al., 2025b), we found partly diverging results in a paradigm focusing on stimulating SO-spindle coupled events (note that coupling analysis requires multiple nights' data due to its low prevalence, and was therefore not examined in the present work). In brief, the amplitude of oscillations at detection did not predict the amplitude of the response in either frequency band. However, significant correlations were found between strength of evoked SO and spindle activity, but only when auditory stimulation occurred as specific spindle phases (i.e. rising and peak), suggestive of a common generative mechanism under some circumstances.

Interpretation of the correlational analyses between detected and evoked oscillation strength (and those in Jourde et al. 2025b) must be tempered by the caveat that the populations studied are limited to healthy young adults, who show less variability in SO strength than do other populations such as older adults (who are of interest as they might ultimately be a target for CLAS-based interventions; Helfrich et al. 2018; Muehlroth et al. 2019). Furthermore, the range of SO strength at detection is restricted by the detection algorithm. Slightly weaker-than-threshold SOs were not detected, thereby truncating the range of possible values and lowering the likelihood of finding correlations. It is entirely

possible that, given a broader range of SO or spindle amplitudes at detection that are present in different populations, additional dependencies will be revealed which may be useful to predict or tune effectiveness of auditory manipulations.

Our results nonetheless underscore the importance of timing stimulation to neural events, precisely and selectively, to evoke different neurophysiological responses. They also suggest some independence between the generation and degree of susceptibility of the neural circuits generating the two types of evoked responses, which could be leveraged in future causal investigations of the roles of sleep oscillations. Future work on algorithms may also find ways of optimizing detection to individuals (as demonstrated via online adaptation in Sobral et al. 2025). Another approach might be to adapt detection algorithms or stimulation parameters in real time, based on the effectiveness of each stimulation.

7.5.3 Effects of CLAS on memory consolidation

To study the behavioural effects of these stimulation types, we used three tasks, with wake and undisturbed sleep control groups. The behavioural outcomes proved to be complex. First, we confirmed that the task learning results showed reasonable improvements during the training periods, suggesting that subjects were able to learn and developed a memory trace upon which processes of offline memory consolidation could act, as evidenced by a flattening learning curve and overall high performance level at the end of the training period (Figure 7.4, top row). Next, we investigated the main effect of behavioural change before and after the nap or wake period (Figure 7.4 bottom row; summarized in the grey), and differences between conditions. Three out of four behavioural metrics showed effects of time, but not all were positive. Overall, people got worse on the declarative task (GLT), better at the procedural task (MSL), and better at the more procedural complex task metric (i.e., Piano rhythm accuracy), whereas the more declarative complex task metric (i.e., Piano pitch accuracy) did not change significantly. These results are interesting in themselves, as they suggest that declarative and procedural memory consolidation mechanisms are in fact somewhat dissociable, at least as regards their decay vs. gain due to the passage of time (factors which are likely also affected by the complexity of the task, the level of expertise of the learner, and the volume of training; Ahissar et al. 2009). In fact, sleep-depending memory effects are sometimes observed as 'less forgetting' rather than an actual gain (Ellenbogen et al., 2006).

Unexpectedly, the condition to which the subjects were assigned seemed to have little to do with the degree of change of performance in pre- vs. post testing, as indicated by the lack of any statistical interaction between Time and Condition 7.4 (bottom row). These results mean that not only did the stimulation *not* improve consolidation at least at the group level,

but that undisturbed sleep did not improve consolidation (or reduce forgetting) beyond that expected by the passage of time. The overall increase in procedural performance observed in our study over all conditions is in-keeping with the idea that replay and consolidation is not exclusive to sleep (Fuentemilla, 2025), and contributes to a debate concerning the necessity (rather than facultative effect) of sleep's contribution to memory consolidation (Dastgheib et al., 2022).

Noting considerable variability in both the amplitude of evoked responses and in the behavioural change pre-post sleep, we also explored correlations between the evoked activity in each frequency band and task-related changes at the subject level, for each stimulation condition (summarized in Figure 7.5A). While the strength of evoked slow oscillations was not correlated with change in any of the behavioural metrics, the evoked spindle activity showed a sub-threshold positive relationship with MSL accuracy in both the spindle stimulation conditions but not SO stimulation condition. Conversely, evoked spindle activity was significantly negatively correlated with Piano pitch accuracy in the 'SP' but not 'SPd' condition (uncorrected), and was negatively correlated with Piano rhythm accuracy in the 'SPd' but not 'SP' condition (also at uncorrected critical values). Although we hesitate to interpret the direction of these individual effects in light of current models of memory consolidation due to their weak statistical properties and inconsistency, it seems plausible that the magnitude of evoked response in the spindle band may prove to be an important factor in determining memory outcomes, at least across tasks that have a procedural component.

In sum, none of the stimulation conditions significantly increased memory consolidation nor reduced forgetting over and above the effect of the passage of time, and nor were there clear relationships found between the strength of evoked responses and performance change. While a benefit of SO-CLAS on memory has been replicated, results are found inconsistently across studies. In a recent review, Esfahani et al. (2023) reported that all studies (in healthy young and middle-aged adults) effectively generated evoked neural responses, yet only about 40% showed significant memory improvements (Ngo et al., 2013b, 2015; Ong et al., 2016; Leminen et al., 2017; Papalambros et al., 2017; Diep et al., 2020); effects on memory were inconclusive in a further seven studies (Ngo et al., 2019; Ong et al., 2018; Henin et al., 2019; Schneider et al., 2020; Harrington et al., 2021; Koo-Poeggel et al., 2022; Baxter et al., 2023). These results suggest that either the effect of auditory stimulation is not strong enough to reliably produce memory effects (possibly meaning that more forceful brain stimulation techniques such as transcranial magnetic stimulation is needed), or that CLAS works but is not optimized in commonly used designs including in the present study. Notably, none of the three previously-reported studies using nap rather than night designs (i.e., Ong et al. 2018; Koo-Poeggel et al. 2022; Baxter et al. 2023) yielded positive outcomes, suggesting

that the effectiveness of CLAS may be 'dose-dependent', perhaps requiring a certain number of stimulations to effect meaningful changes in consolidation. CLAS's effects may also be weak due to sub-optimal stimulation strategies. In prior work using simultaneous EEG and source-localized magnetoencephalography, Jourde et al. (2024) showed that the effectiveness of sound stimulation to generate evoked responses was determined by the tissue excitability state in frontal ventral regions (i.e., orbitofrontal cortex), but that up states in these regions coincided with up-states as detected in frontal EEG channels (as is used in most work, see Esfahani et al. 2023) in only 12% of cases. This result suggests that there is a lot of room for improvement for maximizing the effectiveness of CLAS-SO, by either using a different electrode montage or optimizing timing. Similarly, determining the best means of capturing spindles and timing stimulation (for example to hit spindle up-states, see Jourde et al. 2025b, or early vs. late in their temporal evolution; Jourde et al. 2025a), may improve the effectiveness of stimulation and therefore the consistency of cognitive and memory effects. In general, while the neurophysiological outcomes are consistently observed, it will be necessary to develop highly precise, effective, and perhaps personally-optimized causal methods, and to further develop mechanistic models of how stimulation interacts with memory circuits in sleep (Bellesi et al., 2014; Jourde et al., 2024).

7.5.4 Considerations for future work

Some of the particular design choices made in the present study are important to interpret the current results, and when considering the design of future work. A first point is whether our sample size or study design obscured a potential effect of CLAS. The present work was similarly powered with respect to previous work showing significant results in SO-CLAS, the mean number of subjects for which is 20.3 (SD = 8.6; range = 11-37; see Supplementary Figure 1, adapted from Esfahani et al. 2023). Another matter concerns the length of the sleep period. As mentioned previously, overnight designs can be preferable as regards the amount of sleep and number of stimulations possible, (although they also induce circadian confounds and require additional control conditions). In future work, an overnight design would address this issue, and opting for within-subject design might increase statistical sensitivity to subtle performance changes across conditions.

We elected to use three tasks (simple declarative, simple procedural, and a complex task) in the same training session, as a means of being able to compare the effects of stimulation across well-studied representative tasks that target specific memory systems, and to extend the work to a complex task that has some ecological validity. As with any complex task, there may be additional considerations for what exactly is being learned and what is the timecourse

of that learning process, which may be differentially dependent upon sleep processes, if at all.

It is possible that doing three tasks prior to the nap or wake period created some interference (although noting that the tasks were counterbalanced to avoid order-based fatigue or interference effects), or merely decreased the amount of experimental time that could be dedicated to learning each task and thus the quality of the memory representation upon which consolidation could act. We argue that these issues are unlikely to have been an problem in the current work. As regards interference effects, they tend to be weak and seem to only be elicited under very specific experimental conditions designed to maximize interference (Cordi & Rasch, 2021), for example when very similar information is given to disrupt an existing memory trace (Ellenbogen et al., 2006). As our tasks are quite different and generally rely on different neuroanatomy, the conditions for interference are unlikely to have been met; furthermore, the MSL task showed performance improvement, suggesting at least that the history of other tasks did not impede its memory processes. As regards length, the training paradigm used for the GLT and MSL task are relatively standardized in agreement with previous work. Although the specific piano task has not previously been used in the sleep context, its length seems comparable to related work (Antony et al., 2012) and average pitch accuracy was above 80%, suggesting that subjects had a decent representation of the melodies in short-term storage. Finally, performing multiple tasks is ecologically-valid. Thus, even if it could create some memory interference and decrease the clarity of intervention effects, constant learning is the norm in human experience. Future work using complementary designs with multiple or single tasks and both comparing across-tasks within individuals, and within individuals will all be needed to clarify the role of sleep in naturalistic human learning.

Other considerations include the nature of stimulation. While we had intended to boost SO and spindle activity as a means of increasing memory consolidation, it is difficult to know whether the evoked oscillations are equivalent to endogenous memory reactivation, although they seem morphologically similar (Halász, 2016; Jourde et al., 2024). For this reason, disruption may be a more powerful means of first identifying the roles of sleep oscillations (Rouast et al., 2025). The observed early termination of spindles in response to spindle stimulation may thus be harnessed to further investigate spindles' roles via their disruption.

7.6 Conclusion

In the current work, we successfully evoked brain responses using both SO upstate and spindle stimulation, but did not observe clear behavioural changes between experimental conditions as compared to control conditions. The results from prior CLAS studies targeting

slow oscillation upstates have also shown clear neurophysiological responses but mixed memory outcomes. Given results showing that timing and source of endogenous events affects the effectiveness of stimulation in modifying brain responses, we suggest that further methods-focused development will improve the effectiveness of CLAS and thus make it a stronger tool for studying neuroplasticity and memory, with some clinical potential (Fattinger et al., 2019; Papalambros et al., 2019). Our results highlight two conceptual questions about how sleep oscillations contribute to memory consolidation. First, if slow oscillations and spindles are unique to NREM sleep and are considered critical mechanisms for active memory consolidation, why then is memory consolidation not exclusively associated with NREM sleep? Second, how can evoked brain activity during sleep be present without corresponding improvements in memory performance? These questions, along with the relative contributions of spindles and slow oscillations to different sorts of memory, remains stubbornly open. We have nonetheless taken several important steps towards addressing them. Specifically, our results demonstrate successful modulation of slow oscillations and sleep spindles, confirming effectiveness of auditory closed-loop stimulation. The discrepancy in timing and amplitude of evoked activity in response to stimulating different neural events highlights the importance of precise online detection. More importantly, it provides researchers with specific targets that yield diverse outcomes both neurophysiologically and behaviourally. We believe this work establishes novel research options to refine our understanding of sleep, facilitating the causal investigation of sleep events´ functions. In the future, in conjunction with advances in detection algorithms, this will enable investigation of the roles of other memory-relevant neural patterns, including both coupled oscillations (i.e. SO-spindle complex) and grouped oscillations (i.e., spindle trains).

7.7 Supplementary material

Conditions	Age	Sex	NREM2&NREM3 sleep duration
SLEEP	26.8 +/- 7.8	N=20 (F=13, M=7)	73.9 +/- 18.5
SO	23.8 +/- 5.8	N=20 (F=16, M=4)	69.7 +/- 20.2
SPINDLE_DELAYED	24.9 +/- 6.3	N=20 (F=15, M=4)	62.4 +/- 21.4
WAKE	23.3 +/- 3.8	N=20 (F=14, M=6)	0.3 +/- 0.8
SPINDLE	24.5 +/- 4.9	N=22 (F=14, M=8)	78.8 +/- 24.5
ALL	24.6 +/- 5.9	N=102 (F=72, M=29)	
ALL (except Wake)			71.4 +/- 21.8

Figure 7.6: Group descriptions. For each condition, average and stantard deviation for age, sex ratio and time spent sleeping in NREM2 and NREM3 are reported

	SWA evoked	Spindle evoked
SWA detect	**SO**: r = 0.73, p <.001***	**SO**: r = - 0.07, p = 0.78
Spindle detect	**SP**: r = - 0.02, p = 0.93 **SPd**: r = 0.03, p = 0.93	**SP**: r = 0.37, p = 0.09 **SPd**: r = 0.66, p = 0.004**
SWA evoked	———	**SO**: r = 0.08, p = 0.75 **SP**: r = 0.27, p = 0.22 **SPd**: r = 0.33, p = 0.19

Figure 7.7: Correlations between detected and evoked responses in both frequency bands for each stimulation condition.

	GLT	MSL Accuracy	Piano Pitch	Piano Rhythm
Evoked slow wave activity	**SO**: r=-0.05, p-value=0.85 **SP**: r=0.30, p-value=0.17 **SPd**: r=0.10, p-value=0.69	**SO**: r=-0.03, p-value=0.91 **SP**: r=0.29, p-value=0.21 **SPd**: r=0.36, p-value=0.18	**SO**: r=-0.16, p-value=0.51 **SP**: r=-0.21, p-value=0.35 **SPd**: r=0.01, p-value=0.98	**SO**: r=-0.08, p-value=0.75 **SP**: r=0.23, p-value=0.31 **SPd**: r=-0.27, p-value=0.29
Evoked spindle activity	**SO**: r=-0.09, p-value=0.70 **SP**: r=0.12, p-value=0.60 **SPd**: r=-0.11, p-value=0.68	**SO**: r=-0.22, p-value=0.39 **SP**: r=0.27, p-value=0.23 **SPd**: r=0.45, p-value=0.09	**SO**: r=-0.35, p-value=0.13 **SP**: r=-0.50, p-value=0.02 * **SPd**: r=-0.06, p-value=0.82	**SO**: r=-0.16, p-value=0.49 **SP**: r=0.26, p-value=0.25 **SPd**: r=-0.57, p-value=0.02 *

Figure 7.8: Correlations between change in performance on each task and magnitude of evoked response.

Author	Subjects	Mean age	Target	Stimuli	Measures	Design	Sleep	Evoked	Behaviour
Ngo, Martinetz, et al. (2013)	N = 11	24.2 (0.9)	SO up-state	2 clicks	Declarative	Within	Night	↑ SO	↑ Declarative
Ngo, Miedema, et al. (2015)	N = 18	23.8 (0.6)	SO up-state	2 clicks	Declarative	Within	Night	↑ SO	↑ Declarative
Ong, Lo, et al. (2016)	N = 16	22 (1.4)	SO up-state	5 clicks	Declarative	Within	Night	↑ SO	↑ Declarative
Leminen et al. (2017)	N = 15	30.5 (N/A)	SO up-state	1 click	Declarative Procedural	Within	Night	↑ SO ↑ Spindle	↑ Declarative only
Papalambros et al. (2017)	N = 13	75.2 (N/A)	SO up-state	5 clicks	Declarative	Within	Night	↑ SO ↑ Spindle	↑ Declarative
Ngo, Seibold, et al. (2019)	N = 34	25.1 (3.4)	SO up-state	7 clicks	Declarative	Within	Night	↑ SO ↑ Spindle	No change
Ong, Patanaik, et al. (2018)	N = 37	22.5 (2.3)	SO up-state	2 clicks	Declarative	Within	Nap	↑ SO ↑ Spindle	No change
Henin et al. (2019)	N = 31	23.5 (0.6)	SO up-state	1 click	Declarative Navigation	Within	Night	↑ SO ↑ Spindle	No change
Diep et al. (2020)	N = 24	39.9 (4.2)	SO up-state	continuous clicks*	Declarative Procedural	Within	Night	↑ SO	↑ Working memory in high responders
Schneider et al. (2020)	N = 17	55.7 (1.0)	SO up-state	2 clicks	Declarative Procedural	Within	Night	↑ SO ↑ Spindle	No change
Harrington, Ngo, and Cairney (2021)	N = 12	20.0 (2.0)	SO up-state	2 clicks	Declarative	Within	Night	↑ SO	No change
Koo-Poeggel et al. (2022)	N = 16	25.6 (0.6)	SO down-to up-state	2 clicks	Declarative	Within	Nap	↑ SO ↑ Spindle	No change
Baxter et al. (2023)	N = 20	29.0 (5.0)	SO up-state	1 click	Procedural	Within	Nap	↑ SO ↑ Spindle	No change

Figure 7.9: Comprehensive review of SO-CLAS experiments. All these studies used 50ms pink noise. The table has been adapted from Table 1 in Esfahani et al. (2023), retaining only studies involving healthy adult participants while incorporating more recent research findings.

7.8 Acknowledgements

The authors would like to express gratitude to Giovanni Beltrame and his students Nicolas Valenchon, Milo Sobral and Yann Bouteiller for the technical development and support with the Portiloop and training platform all throughout- from piloting to data collection. We thank Alexandre Morinvil for helping develop and support the online platform used for behavioural training and testing (GLT, MSL and Piano tasks).Sarine Tufenkjian The authors would like to thank Ovidiu Lungu, Jean-Marc Lina, and Julien Doyon for providing us with the GLT and MSL scripts that we adapted for this study. We thank laboratory members and colleagues from Julien Doyon, Julie Carrier, and Genevieve Albouy's groups for ecHT device beta testing. We would also like to thank undergraduate students Maya Mergui, Sarine Tufenkjian and Basem Abushamleh for their help with data collection. HRJ was supported by a scholarship from the Quebec Research Funds (Fonds de Recherche de Quebec - Nature et

technologies; FRQNT). EBJC was financially supported by grants from the FRQNT, Natural Sciences and Engineering Research Council of Canada (NSERC), and a Concordia University Research Chair in Sleep and Sound.

Chapter 8

Discussion

The research presented in the preceding chapters advances our understanding of sleep's role in altering auditory processing, and demonstrates how the auditory system can be utilized to modulate brain oscillations, exploring their functional roles in cognition and memory. In the course of this work, we have also advanced novel methodologies for causally manipulating brain activity. This discussion will explore our findings thematically, beginning with an examination of sleep-dependent modulation of auditory processing. We will then analyze the emerging opportunities for and implications of targeted auditory stimulation, and propose a mechanistic model of closed-loop auditory stimulation that integrates our findings with existing literature to explain both neural and behavioural outcomes.

8.1 Sleep-dependent modulation of auditory processing

While most studies on sensation and perception focus on wakefulness, neural activity changes considerably as a function of the system's overall state. Sleep —an altered state of consciousness occurring daily and automatically— presents an ideal context for investigating these perceptual changes and their implications for arousal and cognitive processes. In the work presented here, we chose to focus on auditory processing because of its temporal specificity (in the order of tens of milliseconds), because auditory stimuli can be processed despite the absence of behavioural responses, and for its capacity to interact with brain activity in sleeping subjects. Research in auditory processing often reveals patterns and mechanisms that extend beyond hearing, offering insights into sleep-dependent processing of other sensory modalities (Riedner et al., 2011). These cross-modal connections suggest that certain neural dynamics underlying sensory processing are shared across sensory systems.

In this series of studies, we asked: how, when, and where does sleep modulate auditory processing. By examining this question from multiple perspectives, we deepened our

understanding of sensory processing during sleep, with broader implications for brain stimulation. Initially, we explored the impact of sleep depth on the FFR, an evoked response that indexes the quality of periodicity encoding. By comparing its magnitude across sleep states (see Chapter 2), we showed how cortical but not subcortical sources of the FFR were impacted by sleep depth, with weaker cortical signals in deeper sleep. The results uncover a clear dissociation between cortical and subcortical early pitch processing during sleep. Interestingly, these alterations appeared not directly tied to interactions with specific sleep events (i.e., slow oscillations and sleep spindles) as had been previously thought, but rather reflected broader sleep-depth-dependent changes in information flow and cortical processing. We then further took advantage of the possibilities offered by MEG recordings to explore the neural origins of sleep-dependent components of auditory evoked responses (Chapter 3). Investigating the source of previously reported evoked components that are specific to deeper sleep, our findings are congruent with the idea that the non-lemniscal auditory pathway is involved in slow oscillation generation. Our work also demonstrated how, in response to auditory stimuli, prefrontal regions generate slow waves, which reach broadly distributed brain regions as travelling waves (moving in a generally posterior direction at ∼1.2-7.0 m/sec; Massimini et al. 2004). Together, these studies inform us about how auditory processing of incoming stimuli is modulated by sleep stages, hints at the prominent role of the non-lemniscal pathway, and offers a first insight into a mechanistic explanation of auditory closed-loop stimulation.

Toward assessing feasibility of our final goal of stimulating sleep spindles with sound, we also addressed open questions about their purported protective role against external sensory disruption. Given that spindles originate (in part) in the thalamus, which is also the seat of sensory gating, sleep spindles were thought to block auditory information from reaching cortex (see Section 1.1.3). However, in Chapter 4, we demonstrated with several experiments (1 and 2) that auditory processing is maintained even in the presence of sleep spindles, suggesting that their occurrence is not what is influencing the change in arousability across deepening sleep stages per se. The observation that auditory information is transferred to cortex unimpeded during spindles is complemented by work in Chapter 4 (experiment 3) showing that stimulation to SO upstates generated the expected physiological responses even in the presence of coupled spindles, and is consistent with our work in Chapter 5 showing that CLAS targeting spindles themselves consistently elicited a brain response (observations which would not be compatible with a blocking mechanism).

Collectively, our findings suggest that previously documented changes in auditory processing during sleep likely result from alterations in brain dynamics rather than reduced sensory processing associated with specific sleep oscillations. Our results align with a

conceptualization of sleep's impact on auditory processing being altered by global changes at the level of brain neural communication patterns. In line with the work of Massimini et al. (2005), we believe our experimental findings provide additional evidence supporting the idea that cortical connectivity breaks down during slow-wave sleep. By reframing spindles as by-products of broader neural changes instead of active protective agents, we offer an alternative interpretation that would account for the findings that have been invoked as support for the protective role of sleep spindles. The present work therefore advances our understanding of sleep-dependent modulation of auditory processing, offering new perspectives on the neural mechanisms implicated in sleep maintenance and sensitivity to modulation via sensory stimulation.

8.2 Targeted auditory stimulation: causally probing brain function during sleep

Direct non-invasive manipulation of the brain's endogenous oscillations provides researchers with unprecedented opportunities to establish causal relationships between neural activity and brain functions. This methodological breakthrough represents a valuable evolution from traditional correlational studies, reshaping study designs and widening the field of possibilities. Based on years of cognitive neuroscience literature investigating the roles of different neural oscillations, the potential targets for brain stimulation are numerous. While other stimulation modalities are often used in cognitive neuroscience (such as electrical or magnetic stimulation), our work focused on auditory stimulation for several reasons described in Section 1.2. Auditory stimulation paradigms offers significant practical advantages through their minimal setup requirements and non-invasive nature. This makes it straightforward to implement both in controlled laboratory settings (as demonstrated in Chapters 2, 3 and 7) and in home environments for more ecologically valid recordings (as shown in Chapters 5 and 6).

Traditional polysomnography equipment is cumbersome and can significantly interfere with the very processes being studied; furthermore, in-lab studies are personnel and resource-intensive. We were able to successfully carry out several studies (experiment 3 in Chapter 4, and the experiments in Chapter 5 and 6) using data recorded by subjects themselves in their own homes. By replicating neurophysiological findings in both laboratory and at-home environments, we show that, with adapted tools and protocols, these techniques can be extended beyond the lab into more naturalistic settings. Demonstrating that it is possible to conduct CLAS studies in the home and to record data that are of sufficient quality for

fine-grained analysis of neurophysiological events will facilitate larger, multi-night studies. This research therefore contributes to a broader movement toward naturalistic study designs.

In the context of the novel spindle stimulation condition made possible and explored by our work, we documented the differential outcomes of CLAS of sleep spindles (SP-CLAS). Thanks to our collaborative work with engineers (described in Valenchon et al. 2022; Sobral et al. 2025), we were able to present in this work the first results describing the neurophysiological and behavioural effects of SP-CLAS. First, we provided evidence that evoked activity was dependent on several parameters at detection, such as timing (see Chapters 5 and 6) or amplitude of brain activity at detection (see Chapter 6 and 7). Our exploration of SP-CLAS revealed that timing of stimulation matters. In Chapter 5, we found that stimulating at the beginning versus the end of a spindle led to different outcomes, such as early termination of the spindle or the induction of an additional one. Additionally, we showed that stimulating evoked spindles doesn't work – spindle activity is only induced in response to stimulation of the endogenous spindle, not of subsequent evoked spindles. In Chapter 6, we further observed that the spindle phase at the time of stimulation also influenced spindle generation. We propose that these complementary effects can be harnessed to causally investigate spindles' functional roles by either boosting or disrupting them, hence providing causal evidence, either by gain or loss-of-function. In other words, by making this tool freely available and describing these differential effects, our work provides researchers with a wide range of possibilities for electrophysiological outcomes.

Most of the work conducted to date including ours uses short bursts of pink noise as stimulation. Exploring the effects of using different parameters may help to optimize evoked activity, or create experimentally useful effects such as disrupting deeper sleep by sending louder stimulation upon detection of slow waves (Rouast et al., 2025). In an extension of previous efforts targeting SO-CLAS Nicolas et al. (2022), work is underway to apply SP-CLAS using the Portiloop in targeted memory reactivation designs, in which memories are tagged during training, and reinstated during sleep via an auditory cue. Alternative stimulation methods such as transcranial magnetic stimulation are also being explored as means of altering the neural dynamics of sleep spindles (Hassan et al., 2025).

Shifting focus slightly, it is also worth considering the other effects of CLAS and how they can be used to explore additional functional roles. Even though CLAS was first developed to demonstrate slow oscillations' causal role in memory consolidation, several studies have described other physiological effects. Studies have reported outcomes such as decreased cortisol levels and reduced blood T and B cell counts, suggesting a potential beneficial effect of SO-CLAS on another functional role attributed to endogenous SO immune-supportive functions. (Grimaldi et al., 2019; Besedovsky et al., 2017). A similar approach could be used

to probe additional functional roles of sleep spindles and SO-spindle complexes. Together, these studies illustrate many potential uses of CLAS to explore sleep's clinically-relevant aspects and its potential as a future therapeutic intervention in and outside the realm of memory. As technological advancements expand the range of potential neural targets, close collaboration between engineers and neuroscientists is essential to co-develop increasingly sophisticated and theoretically driven tools for both research and clinical applications.

8.3 Mechanism of closed-loop auditory stimulation

While numerous studies have reported the effects of targeted auditory stimulation on both neural activity and behaviour (see Section 1.3.1), relatively few researchers have investigated its underlying mechanisms, which remain largely unexplored. Our research aimed to address this gap by examining brain activity in response to previously established stimulation protocols. Based on our findings and an earlier model proposed by Bellesi et al. (2014), we proposed an updated model for auditory processing during sleep that highlights the predominance of the non-lemniscal pathway in generating the distinctive sleep-specific brain response.

In the Introduction, we described existing models of auditory processing during wakefulness relying on both the lemniscal pathway which primarily conveys precise stimulus characteristics and the non-lemniscal pathway which processes environmental changes (Kraus et al., 1994; Anderson et al., 2009; Anderson & Linden, 2011) and integrates multimodal stimuli (Komura et al., 2005). A noteworthy anatomical feature is the significant overlap between auditory non-lemniscal pathways and arousal-promoting networks that extend diffuse projections throughout the thalamo-cortical system, including to the locus coeruleus (LC) (Jones, 2003; Hu, 2003; Aston-Jones et al., 2007). The LC is a nucleus located in the pons, which projects throughout the brain including to regions involved in memory processes such as the amygdala and the hippocampus. Bellesi et al. (2014) suggest involvement of the LC, via the non-lemniscal auditory pathway. The capability of LC projections to activate the thalamo-cortical system during sleep are well documented (Halász et al., 2004; Riedner et al., 2011; Jones, 2003). Bellesi et al. propose that auditory inputs during NREM sleep could produce near-simultaneous depolarization of many neurons widely distributed over the cortex through this pathway. This reaction would lead to a fast and efficient synchronization of hundreds of thousands of neurons and be measured as synchronized polarization and depolarization—in other words: a slow wave. In Chapter 3, using directed connectivity measures, we observed that the slow evoked responses (known as K-complexes, which we hypothesize to be at the origin of the effect first described by Ngo et al. 2013b) are actually generated in the same regions as endogenous slow oscillations before travelling to other areas

of the cortex. By demonstrating the common neural origin of these slow evoked responses (i.e. K-complexes) and endogenous activity (i.e. slow oscillations), our work contributes a potential explanation of the behavioural outcomes observed with SO-CLAS. Indeed, if evoked and endogenous oscillations share the same functional role, as suggested by SO-CLAS research, and share neuroanatomical sources, as suggested by our work, their identical nature might be hypothesized. However, it is important to note that other studies rather suggest a reorganization of endogenous SOs being synchronized by CLAS rather than new ones being generated (Piorecky et al., 2021). These seemingly incompatible interpretations might be introduced by methodological differences. For example, SO detection can be influenced by the electrode site and defined threshold. In the case of an evoked response not reaching an offline detection threshold (potentially linked to a more local neural event), observers would conclude that no SO had been induced. Future work should address these issues by probing whether CLAS elicits SO generation within the proposed anatomical source region; or instead organizes the temporal alignment of spatially-distributed events, a question for which MEG would be well-suited.

Another interesting point suggesting ARAS involvement in the mechanism of CLAS comes from animal work highlighting the importance of the LC in both spindle generation and sensory-evoked awakenings (Swift et al., 2018). The LC is the primary source of noradrenaline (NA), a neurotransmitter involved in arousal (Hayat et al., 2020) but also in several cognitive processes, including memory consolidation (Barsegyan et al., 2014; James et al., 2021). Studies have shown that increasing NA levels can enhance memory performance, while blocking noradrenergic receptors can impair it (van Stegeren, 2008). Swift et al. (2018) suggested a link between temporal organization of NA release by the LC and the functional role of sleep spindles. They claim that the periods of silence in NA release, observed during REM and just before sleep spindles, facilitate synaptic plasticity, enabling the integration of new information into existing memory circuits. These observations suggest an inhibitory role of LC activation over spindle generation. A follow-up study by the same team provided additional supporting evidence using optogenetic stimulation of the LC, which induced early termination of sleep spindles (Swift, 2019). This is of particular interest for our work, as a similar early termination of sleep spindles was also observed in rodents (Sela et al., 2016) following auditory stimulation. In our work, we replicated this finding in humans, targeting sleep spindles in a closed-loop fashion (see Chapter 5 and 7; although only observed when sound occurred in the first part of the spindle). We argue that this is additional evidence that auditory information during sleep is processed through the non-lemniscal pathway, involving the LC in the ARAS. The early termination of sleep spindles could be attributed to enhanced LC activity driven by excitatory input from the CN to the ARAS. This artificial disruption of spindles by an

overactive LC would then be counterbalanced by a subsequent LC hyperpolarization, which would limit its inhibitory influence on spindle generation—ultimately leading to a rebound increase in spindle activity.

On the basis of our findings, that a) the lemniscal pathway remains active during sleep (see Chapter 2 and 3), and that b) the non-lemniscal pathway likely contributes to the emergence of sleep-specific evoked responses in both frequency bands (see Chapters 5 and 7), we propose an extension of Bellesi et al.'s model to include the generation of sleep spindles. In our extended model, illustrated in 8.1, auditory information travelling through the non-lemniscal pathway enhances activity in the ARAS, which is relayed to ventral frontal lobe regions—where slow oscillations are generated and from which they propagate. Simultaneously, the ARAS likely projects to the thalamus, via the LC, where its effects are inhibitory. Rebound from sudden inhibition would provide the necessary quiescent period for spindle emergence in the thalamus (accounting for the increase in spindle activity which we observed with some delay after stimulation). In the case that a spindle is ongoing, the inhibitory action from the LC would result in early spindle termination. This theory would therefore posit that both evoked brain events (i.e., slow oscillations and spindles) are being generated through the same processes as endogenous ones, potentially supporting their behavioural relevance. This model is driven by our experimental observations and will require further investigation, including at the cellular-level.

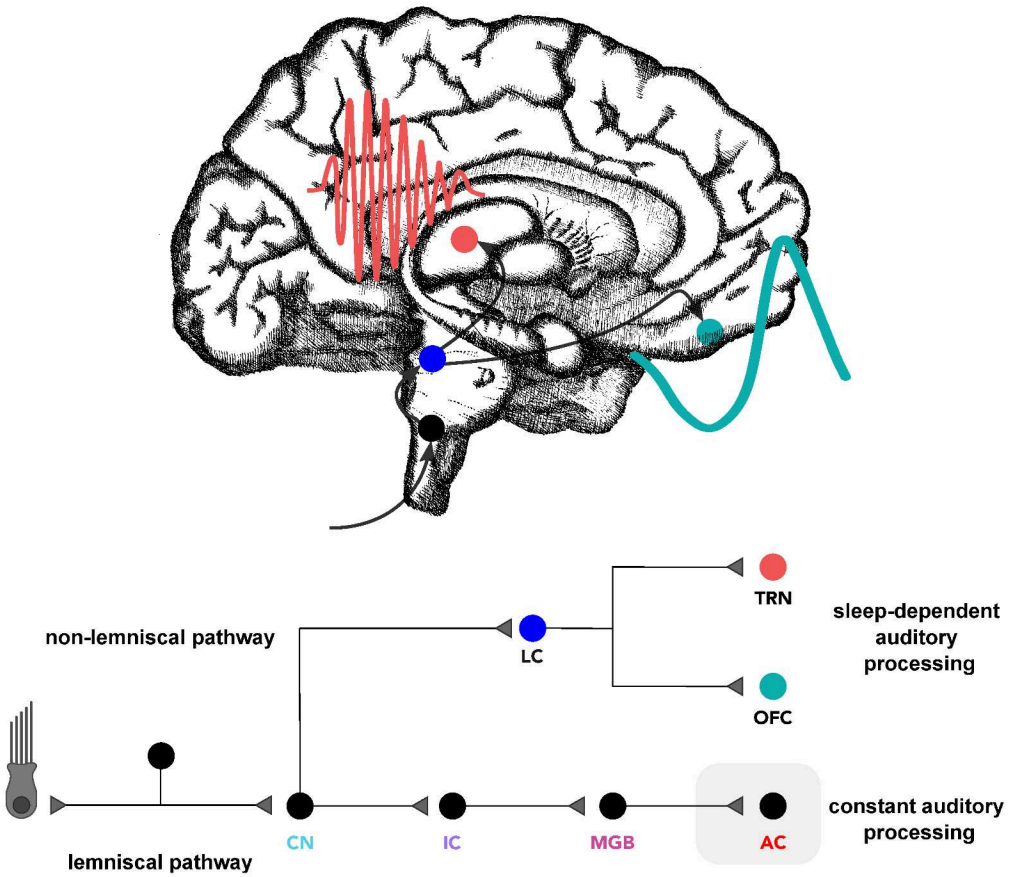

Figure 8.1: Proposed mechanism of sleep-dependent auditory processing involved in CLAS evoked responses. Incoming auditory information is simultaneously processed by the lemniscal (primary) auditory pathway up to the auditory cortex (AC), functioning similarly in wakefulness and sleep, with only limited cortical impact by sleep depth (grey shaded area), and simultaneously by the non-lemniscal pathway. The involvement of the locus coeruleus (LC) within the ascending reticular activating system during sleep is responsible for generating both slow wave activity via projections to the orbitofrontal cortex (OFC) and sleep spindle activity through inhibitory feedback mechanisms in spindle generation circuits.

8.4 Behavioural outcomes of closed-loop auditory stimulation

The most intriguing and therefore compelling aspect of the CLAS technique is its ability to induce behavioural changes that laboratory tasks are sensitive enough to capture. Considering the complexity of most neural processes, this observation suggests a direct link between slow wave activity and memory processes. Since the seminal work by Ngo in 2013, which reported improvement in overnight memory consolidation on a declarative memory task (Ngo et al., 2013b), SO-CLAS has been widely used, and its findings have been replicated multiple times with different tasks (see Harrington & Cairney 2021; Choi et al. 2020).

While the physiological effects of SO-CLAS are almost always observed (although see Perrault et al. 2025) its behavioural outcomes remain more nuanced (see Figure 1.3). This variability appears to stem not only from individual differences in participants' responses but also from the specific memory system being tested, which may be influenced in distinct ways according to their underlying neurocircuitry (see Section 1.3.1). This raises fundamental questions about the precise role of slow oscillations in memory consolidation. Specifically, does their influence extend to all consolidation processes, or is it limited to certain types, such as declarative learning? Clarifying which memory systems are affected by SO-CLAS is essential for understanding its underlying mechanisms. Furthermore, due to their joint role as proposed by the active consolidation system model, the extent to which sleep spindle stimulation replicates the neural and behavioural effects of slow oscillation stimulation was unknown. Addressing these questions therefore required causal manipulations and systematic comparisons of outcomes. In this work, we aimed to fill these gaps by assessing the behavioural outcomes of a novel stimulation condition, SP-CLAS, and compare its outcomes to those of SO-CLAS. This behavioural investigation was made possible by our advancements in the field of online detection of sleep spindles (Valenchon et al., 2022; Sobral et al., 2025).

This approach not only allowed us to compare the impact of stimulation conditions on behavioural paradigms that are tailored to isolate different memory systems (i.e., declarative memory for the GLT and procedural memory for the MSL) but also to inquire into its effect on more naturalistic learning using a complex task (see Chapter 7). We chose musical learning based on literature suggesting it provides a more ecologically valid measure of learning. Research on CLAS benefits for complex tasks remains limited, but suggests that its effects may extend to some more naturalistic behaviours. For instance, Shimizu et al. (2018) demonstrated that SO-CLAS enhanced navigation task performance, indicating potential for practical real-world implementation.

Electrophysiological findings across studies in the present work (see Section 8.2) suggest that evoked activity likely shares generating sources with endogenous oscillations (illustrated in Figure 8.1). For that reason, one would expect an improvement in behavioural performance associated with the enhanced presence of these oscillations, as they are involved in memory consolidation. However, in our experiment, even though our sample size was similar to that in previous studies and some tasks were identical, we did not find a significant effect of stimulation condition on change in performance following stimulation. These results could be at first interpreted as an absence of effect of stimulation but might instead require a bit more perspective.

The fact that no change in performance was observed can be interpreted in different ways. First, it can suggest that no effects were induced by our experimental manipulation. Based on our results, we consider this hypotheses to be unlikely. The presence of consistent evoked neural activity across all experimental conditions clearly demonstrates that our stimulation protocol was effective (although there are several possibilities for further strengthening evoked physiological responses, described in Chapter 7). The absence of clear behavioural effects can also indicate that our metrics were not sensitive enough to measure slight changes caused by stimulation. We believe that our deliberate selection of memory tasks that show sleep benefits in previous work suggest we can reject this interpretation (noting that further work using overnight design might bolster this interpretation). Alternatively, the absence of results could hint that the hypothesized direct relationship between density of sleep events and memory is actually more complex.

In human non-invasive CLAS experimental paradigms, cognitive neuroscientists including ourselves usually measure only the final behavioural outcomes of stimulation, without observing or quantify the intermediate processes that connect the initially evoked neural activity to the ultimate changes in performance. In other words, we're confronting a 'black box' scenario where physiological effects are expected to produce corresponding behavioural outcomes. However, in our study, as in others, we observe the physiological effect without its anticipated behavioural consequence—creating a disconnect between neural changes and measurable performance outcomes which is incompatible with the direct simplistic causal link initially hypothesized.

We posit that providing tools to exert control over brain activity and measure its expected behavioural consequence is only the first step in investigating this process. Is CLAS causing changes in neuroplasticity? Is there evidence of other memory processes, such as replay or activation of memory-related brain structures specifically activated by CLAS? When and how are memory traces reactivated across memory systems and as a results of CLAS targets? We claim that the story will not be complete until we clarify the precise role and mechanism

of the involvement of targeted oscillations. At the cellular level, fine-grained processes can be studied in non-human animal models, for example as in Moreira et al. (2021). At this level, the structural changes implied by memory consolidation and potentially facilitated by CLAS can be characterized. Moving toward understanding how CLAS influences neural circuitry in humans, intracranial recordings (in patients undergoing brain mapping prior to surgery or who have implantations for other forms of brain stimulation) may help us bridge the gap (Scangos et al., 2021; Langbein et al., 2025). In non-invasive human studies, the effect of CLAS on reactivation can be studied using decoding-based techniques, which characterize neural patterns associated with task learning and attempt to detect their spontaneous or cued reoccurrence during sleep (e.g., Schönauer et al. 2017). Due to its superior source localization capacity, MEG would be particularly relevant to explore regionally-specific memory reactivation. This research would enlighten us about CLAS's direct impact on neuroplasticity which, ultimately, changes in behavioural performance are dependent upon.

8.5 Future directions

Our underlying motivation for this work was to improve our understanding of neural oscillations' – and particularly sleep spindles' – role in memory consolidation. To approach these questions in a meaningful fashion, it was necessary to first develop a new stimulation device that was up to the task of precisely targeting spindles (Valenchon et al., 2022), characterize the effects of different stimulation timing parameters on brain activity, develop models of how brain activity can interact with memory processes, and finally start to explore how producing neurophysiological changes influences memory consolidation and behaviour. We believe the work presented in this thesis takes significant steps towards achieving the goal of understanding sleep spindles, but considerable work remains for the future.

First, we need to better understand the active consolidation system mechanism and clarify the specific role of sleep spindles in it. As our behavioural results highlighted, the relationship between evoked spindle activity and change in performance is not straightforward, and requires deeper investigation of the intermediate steps leading to behavioural changes. The ability to modulate their activity (either by boosting or disrupting them) provides insight into their functional role but causal relationships with neuroplasticity or cellular evidence of tangible structural modification is needed. Once we identify exactly how spindles generate the encoding of new memories through neuroplasticity, we can potentially exert control over these processes, using CLAS.

Second, we might need to change how we think about the relationship between spindles and their involvement in memory consolidation. As research progresses into new areas,

initial conceptions of complex phenomena are often oversimplified and potentially, biased. Historically, sleep researchers linked cognitive processes to sleep stages, which were defined arbitrarily based on visual assessment (of 30 s epochs due to the scrolling output of available analogue polysomnography devices). Sleep-stage based analyses assume that brain state is well-characterized by division into a handful of discrete states, that the divisions between these states are functionally relevant, and that the brain stays in each state for tens of seconds at a time. With the development of algorithms to detect neural events, sleep researchers have been able to examine sleep's finer-grained structure. Efforts of late have focused on linking specific cognitive functions to these discrete sleep events, for example clarifying the association between SO or spindle density to declarative or procedural learning. This approach too has limitations as it rests on many assumptions. For example, SOs and spindles are defined somewhat arbitrarily and their successful detection is heavily biased by technical constraints (e.g. sampling rates, electrode montage, and detection criteria). A contrasting approach could be to consider how these discrete EEG-defined brain oscillations index more global changes in brain states. What if these brain oscillations don't have a specific role such as 'transferring the memory from short-term storage to long-term storage' but rather merely represent biomarkers of specific neural states. This perspective would suggest that instead of restricting our frequency bands of interest we should consider the entire brain as a system with variable microstates, such as proposed by recent advances in network theory (Avena-Koenigsberger et al., 2018; Betzel, 2023). What if sleep spindles per se don't have a designated role but rather indicate a specific organization of a network that is particularly efficient for information transfer? Current research looking at changes in brain functional connectivity using MEG or fMRI is already highlighting interesting changes between sleep stages or consciousness states such as reorganization of communication patterns between cortical and subcortical structures (Massimini et al., 2005). In that sense, our Bellesi-extended model of sleep-dependent auditory processing could be the result of an entirely different network organization.

Future research could investigate these changes, using graph theory approaches, in whole-brain connectivity time-locked to sleep events of interest that have been identified by correlational work. This perspective is coherent with the work describing the infra-slow pattern of 0.02 Hz orchestrating several physiological processes throughout the night. This rhythm might represent the frequency of occurrence of these windows of opportunities for memory consolidation that we associated with spindle activity. These windows would constitute microstates of deeper sleep stages and be triggered by deep regions of the brain such as the LC in the ARAS. If we follow that logic, we could imagine that the thalamic involvement in both the ARAS and the auditory pathway is the link between the behavioural

effect of closed-loop auditory stimulation and its memory-enhancing outcomes. Sleep-evoked responses to sensory stimuli involving the ARAS (not limited to the auditory modality) could therefore be considered as defensive mechanisms triggered by the brain to protect the natural occurring alternation of memory consolidation opportunities. By doing so, the brain would be 'artificially' forced to enter a microstate that is beneficial for memory consolidation and that would therefore improve performance on next-day tasks. For sub-arousal-threshold incoming sensory information, the thalamus would be activated, potentially generating more of these windows of opportunity and thereby producing sleep spindles as a by-product. In our current framework, we would measure them at the scalp and conclude that the auditory evoked sleep spindles are responsible for the induced memory consolidation opportunity. Viewing relationships between neurophysiology and memory plasticity from this new conceptual perspective may promote complementary approaches, new research questions, and ultimately, a deeper understanding of how the brain consolidates newly formed memories during sleep.

Chapter 9

Conclusion

Our work advances understanding of the complex relationship between auditory processing and sleep. Using a multi-modal approach combining electroencephalography, magnetoencephalography, and behavioural assessment, we have expanded knowledge on both how sleep affects auditory processing and how auditory stimulation can modulate sleep-dependent cognitive processes. By taking a holistic approach, we have made several contributions to both auditory neuroscience and sleep research. First, we demonstrated that sleep depth differentially affects cortical sources in the primary auditory pathway while sparing subcortical regions. We also challenged the previously accepted hypothesis that auditory input is blocked at the thalamus during sleep spindles, revealing instead a more nuanced mechanism. Our development and validation of deep learning-based tools for real-time spindle modulation represents a significant methodological advancement, enabling more precise targeting of specific sleep oscillations. The comparative analysis of slow oscillation and sleep spindle closed-loop auditory stimulation across diverse cognitive tasks—from simple laboratory paradigms to complex musical learning—provides insight into how non-invasive brain stimulation affects different memory systems. These findings enhance our understanding of the cognitive role of sleep spindles and their responsiveness to auditory stimulation, while also addressing broader questions about sleep's function in human memory consolidation. The open science tools and frameworks developed throughout this research will enable future work linking sleep neurophysiology with the neuroplasticity of learning.

Bibliography

Achermann, P., Finelli, L. A., & Borbély, A. A. (2001). Unihemispheric enhancement of delta power in human frontal sleep eeg by prolonged wakefulness. *Brain research*, 913(2), 220–223.

Ackermann, S. & Rasch, B. (2014). Differential effects of non-rem and rem sleep on memory consolidation? *Current neurology and neuroscience reports*, 14, 1–10.

Aczel, B., Palfi, B., Szollosi, A., Kovacs, M., Szaszi, B., Szecsi, P., Zrubka, M., Gronau, Q. F., van den Bergh, D., & Wagenmakers, E.-J. (2018). Quantifying support for the null hypothesis in psychology: An empirical investigation. *Advances in Methods and Practices in Psychological Science*, 1(3), 357–366.

Ahissar, M., Nahum, M., Nelken, I., & Hochstein, S. (2009). Reverse hierarchies and sensory learning. *Philosophical Transactions of the Royal Society B: Biological Sciences*, 364(1515), 285–299.

Ahlfors, S. P., Han, J., Belliveau, J. W., & Hämäläinen, M. S. (2010). Sensitivity of meg and eeg to source orientation. *Brain topography*, 23, 227–232.

Albouy, G., King, B. R., Maquet, P., & Doyon, J. (2013). Hippocampus and striatum: Dynamics and interaction during acquisition and sleep-related motor sequence memory consolidation. *Hippocampus*, 23(11), 985–1004.

Albouy, P., Benjamin, L., Morillon, B., & Zatorre, R. J. (2020). Distinct sensitivity to spectrotemporal modulation supports brain asymmetry for speech and melody. *Science*, 367(6481), 1043–1047.

Amadeo, M. & Shagass, C. (1973). Brief latency click-evoked potentials during waking and sleep in man. *Psychophysiology*, 10(3), 244–250.

Amzica, F. & Steriade, M. (1997). Cellular substrates and laminar profile of sleep k-complex. *Neuroscience*, 82(3), 671–686.

Anderson, L. A., Christianson, G. B., & Linden, J. F. (2009). Stimulus-specific adaptation occurs in the auditory thalamus. *Journal of Neuroscience*, 29(22), 7359–7363.

Anderson, L. A. & Linden, J. F. (2011). Physiological differences between histologically defined subdivisions in the mouse auditory thalamus. *Hearing research*, 274(1-2), 48–60.

Andrillon, T. & Kouider, S. (2020). The vigilant sleeper: neural mechanisms of sensory (de) coupling during sleep. *Current Opinion in Physiology*, 15, 47–59.

Andrillon, T., Poulsen, A. T., Hansen, L. K., Léger, D., & Kouider, S. (2016). Neural markers of responsiveness to the environment in human sleep. *Journal of Neuroscience*, 36(24), 6583–6596.

Antony, J. W., Gobel, E. W., O'hare, J. K., Reber, P. J., & Paller, K. A. (2012). Cued memory reactivation during sleep influences skill learning. *Nature neuroscience*, 15(8), 1114–1116.

Antony, J. W., Ngo, H.-V. V., Bergmann, T. O., & Rasch, B. (2022). Real-time, closed-loop, or open-loop stimulation? navigating a terminological jungle. *Journal of Sleep Research*, (pp. e13755).

Antony, J. W. & Paller, K. A. (2017). Using oscillating sounds to manipulate sleep spindles. *Sleep*, 40(3), zsw068.

Antony, J. W., Piloto, L., Wang, M., Pacheco, P., Norman, K. A., & Paller, K. A. (2018). Sleep spindle refractoriness segregates periods of memory reactivation. *Current Biology*, 28(11), 1736–1743.

Antony, J. W., Schönauer, M., Staresina, B. P., & Cairney, S. A. (2019). Sleep spindles and memory reprocessing. *Trends in neurosciences*, 42(1), 1–3.

Arnal, P. J., Thorey, V., Debellemaniere, E., Ballard, M. E., Bou Hernandez, A., Guillot, A., Jourde, H., Harris, M., Guillard, M., Van Beers, P., et al. (2020). The dreem headband compared to polysomnography for electroencephalographic signal acquisition and sleep staging. *Sleep*, 43(11), zsaa097.

Aston-Jones, G., Gonzalez, M., & Doran, S. (2007). Role of the locus coeruleus-norepinephrine system in arousal and circadian regulation of the sleep–wake cycle. *Brain norepinephrine: Neurobiology and therapeutics*, (pp. 157–195).

Aton, S. J., Broussard, C., Dumoulin, M., Seibt, J., Watson, A., Coleman, T., & Frank, M. G. (2013). Visual experience and subsequent sleep induce sequential plastic changes in putative inhibitory and excitatory cortical neurons. *Proceedings of the National Academy of Sciences*, 110(8), 3101–3106.

Aton, S. J., Suresh, A., Broussard, C., & Frank, M. G. (2014). Sleep promotes cortical response potentiation following visual experience. *Sleep*, 37(7), 1163–1170.

Attal, Y. & Schwartz, D. (2013). Assessment of subcortical source localization using deep brain activity imaging model with minimum norm operators: a meg study. *Plos one*, 8(3), e59856.

Avena-Koenigsberger, A., Misic, B., & Sporns, O. (2018). Communication dynamics in complex brain networks. *Nature reviews neuroscience*, 19(1), 17–33.

Axmacher, N., Elger, C. E., & Fell, J. (2008). Ripples in the medial temporal lobe are relevant for human memory consolidation. *Brain*, 131(7), 1806–1817.

Badia, P., Wesensten, N., Lammers, W., Culpepper, J., & Harsh, J. (1990). Responsiveness to olfactory stimuli presented in sleep. *Physiology & behavior*, 48(1), 87–90.

Baena, D., Fang, Z., Gibbings, A., Smith, D., Ray, L. B., Doyon, J., Owen, A. M., & Fogel, S. M. (2023). Functional differences in cerebral activation between slow wave-coupled and uncoupled sleep spindles. *Frontiers in Neuroscience*, 16, 1090045.

Baena, D., Gabitov, E., Ray, L. B., Doyon, J., & Fogel, S. M. (2024). Motor learning promotes regionally-specific spindle-slow wave coupled cerebral memory reactivation. *Communications Biology*, 7(1), 1492.

Baillet, S. (2017). Magnetoencephalography for brain electrophysiology and imaging. *Nature neuroscience*, 20(3), 327–339.

Baillet, S., Mosher, J. C., & Leahy, R. M. (2001). Electromagnetic brain mapping. *IEEE Signal processing magazine*, 18(6), 14–30.

Baker, D. H., Vilidaite, G., Lygo, F. A., Smith, A. K., Flack, T. R., Gouws, A. D., & Andrews, T. J. (2021). Power contours: Optimising sample size and precision in experimental psychology and human neuroscience. *Psychological methods*, 26(3), 295.

Barakat, M., Carrier, J., Debas, K., Lungu, O., Fogel, S., Vandewalle, G., Hoge, R. D., Bellec, P., Karni, A., Ungerleider, L. G., et al. (2013). Sleep spindles predict neural and behavioral changes in motor sequence consolidation. *Human brain mapping*, 34(11), 2918–2928.

Barakat, M., Doyon, J., Debas, K., Vandewalle, G., Morin, A., Poirier, G., Martin, N., Lafortune, M., Karni, A., Ungerleider, L., et al. (2011). Fast and slow spindle involvement in the consolidation of a new motor sequence. *Behavioural brain research*, 217(1), 117–121.

Barnes, T. D., Kubota, Y., Hu, D., Jin, D. Z., & Graybiel, A. M. (2005). Activity of striatal neurons reflects dynamic encoding and recoding of procedural memories. *Nature*, 437(7062), 1158–1161.

Barsegyan, A., McGaugh, J. L., & Roozendaal, B. (2014). Noradrenergic activation of the basolateral amygdala modulates the consolidation of object-in-context recognition memory. *Frontiers in behavioral neuroscience*, 8, 160.

Bashore, T. R. & Van der Molen, M. W. (1991). Discovery of the p300: a tribute. *Biological psychology*, 32(2-3), 155–171.

Basner, M. & McGuire, S. (2018). Who environmental noise guidelines for the european region: a systematic review on environmental noise and effects on sleep. *International journal of environmental research and public health*, 15(3), 519.

Basner, M., Mollicone, D., & Dinges, D. F. (2011). Validity and sensitivity of a brief psychomotor vigilance test (pvt-b) to total and partial sleep deprivation. *Acta astronautica*, 69(11-12), 949–959.

Bastien, C. & Campbell, K. (1992). The evoked k-complex: all-or-none phenomenon? *Sleep*, 15(3), 236–245.

Bastien, C. & Campbell, K. (1994). Effects of rate of tone-pip stimulation on the evoked k-complex. *Journal of sleep research*, 3(2), 65–72.

Bastien, C. H., Crowley, K. E., & Colrain, I. M. (2002). Evoked potential components unique to non-rem sleep: relationship to evoked k-complexes and vertex sharp waves. *International Journal of Psychophysiology*, 46(3), 257–274.

Bates, D., Mächler, M., Bolker, B., & Walker, S. (2015). Fitting linear mixed-effects models using lme4. *Journal of Statistical Software*, 67(1), 1–48.

Baxter, B. S., Mylonas, D., Kwok, K. S., Talbot, C. E., Patel, R., Zhu, L., Vangel, M., Stickgold, R., & Manoach, D. S. (2023). The effects of closed-loop auditory stimulation on sleep oscillatory dynamics in relation to motor procedural memory consolidation. *Sleep*, 46(10), zsad206.

Bellesi, M., Riedner, B. A., Garcia-Molina, G. N., Cirelli, C., & Tononi, G. (2014). Enhancement of sleep slow waves: underlying mechanisms and practical consequences. *Frontiers in systems neuroscience*, 8, 208.

Bénar, C.-G., Velmurugan, J., Lopez-Madrona, V. J., Pizzo, F., & Badier, J.-M. (2021). Detection and localization of deep sources in magnetoencephalography: A review. *Current Opinion in Biomedical Engineering*, 18, 100285.

Bergmann, T. O. & Born, J. (2018). Phase-Amplitude Coupling: A General Mechanism for Memory Processing and Synaptic Plasticity?

Besedovsky, L., Ngo, H.-V. V., Dimitrov, S., Gassenmaier, C., Lehmann, R., & Born, J. (2017). Auditory closed-loop stimulation of eeg slow oscillations strengthens sleep and signs of its immune-supportive function. *Nature communications*, 8(1), 1–8.

Betzel, R. F. (2023). Community detection in network neuroscience. In *Connectome Analysis* (pp. 149–171). Elsevier.

Blanco, W., Pereira, C. M., Cota, V. R., Souza, A. C., Rennó-Costa, C., Santos, S., Dias, G., Guerreiro, A. M., Tort, A. B., Neto, A. D., et al. (2015). Synaptic homeostasis and restructuring across the sleep-wake cycle. *PLoS computational biology*, 11(5), e1004241.

Blume, C., Del Giudice, R., Wislowska, M., Heib, D. P., & Schabus, M. (2018). Standing sentinel during human sleep: continued evaluation of environmental stimuli in the absence of consciousness. *Neuroimage*, 178, 638–648.

Bódizs, R., Kis, T., Lázár, A. S., Havrán, L., Rigó, P., Clemens, Z., & Halász, P. (2005). Prediction of general mental ability based on neural oscillation measures of sleep. *Journal of sleep research*, 14(3), 285–292.

Born, J., Rasch, B., & Gais, S. (2006). Sleep to remember. *The Neuroscientist*, 12(5), 410–424.

Born, J. & Wilhelm, I. (2012). System consolidation of memory during sleep. *Psychological research*, 76, 192–203.

Boutin, A. & Doyon, J. (2020). A sleep spindle framework for motor memory consolidation. *Philosophical Transactions of the Royal Society B*, 375(1799), 20190232.

Boutin, A., Gabitov, E., Pinsard, B., Boré, A., Carrier, J., & Doyon, J. (2024). Temporal cluster-based organization of sleep spindles underlies motor memory consolidation. *Proceedings of the Royal Society B*, 291(2014), 20231408.

Březinová, V. (1974). Effect of caffeine on sleep: Eeg study in late middle age people. *British Journal of Clinical Pharmacology*, 1(3), 203.

Briere, M., Forest, G., Lussier, I., & Godbout, R. (2000). Implicit verbal recall correlates positively with eeg sleep spindle activity. *Sleep*, 23(Suppl 2), A219.

Brodt, S., Inostroza, M., Niethard, N., & Born, J. (2023). Sleep—a brain-state serving systems memory consolidation. *Neuron*, 111(7), 1050–1075.

Brown, R. M. & Robertson, E. M. (2007). Off-line processing: reciprocal interactions between declarative and procedural memories. *Journal of Neuroscience*, 27(39), 10468–10475.

Brysbaert, M. & Stevens, M. (2018). Power analysis and effect size in mixed effects models: A tutorial. *Journal of cognition*, 1(1).

Buysse, D. J., Reynolds III, C. F., Monk, T. H., Berman, S. R., & Kupfer, D. J. (1989). The pittsburgh sleep quality index: a new instrument for psychiatric practice and research. *Psychiatry research*, 28(2), 193–213.

Buzsáki, G. & Tingley, D. (2018). Space and time: the hippocampus as a sequence generator. *Trends in cognitive sciences*, 22(10), 853–869.

Cabeza, R. & Nyberg, L. (2000). Neural bases of learning and memory: functional neuroimaging evidence. *Current opinion in neurology*, 13(4), 415–421.

Campbell, K. (2010). Event-related potentials as a measure of sleep disturbance: a tutorial review. *Noise and Health*, 12(47), 137–153.

Campos-Beltrán, D. & Marshall, L. (2021). Changes in sleep eeg with aging in humans and rodents. *Pflügers Archiv-European Journal of Physiology*, 473(5), 841–851.

Capezuti, E., Pain, K., Alamag, E., Chen, X., Philibert, V., & Krieger, A. C. (2022). Systematic review: auditory stimulation and sleep. *Journal of Clinical Sleep Medicine*, 18(6), 1697–1709.

Carrier, J., Viens, I., Poirier, G., Robillard, R., Lafortune, M., Vandewalle, G., Martin, N., Barakat, M., Paquet, J., & Filipini, D. (2011). Sleep slow wave changes during the middle years of life. *European Journal of Neuroscience*, 33(4), 758–766.

Censor, N., Dayan, E., & Cohen, L. G. (2014). Cortico-subcortical neuronal circuitry associated with reconsolidation of human procedural memories. *Cortex*, 58, 281–288.

Choi, J., Han, S., Won, K., & Jun, S. C. (2018). The neurophysiological effect of acoustic stimulation with real-time sleep spindle detection. In *2018 40th Annual International Conference of the IEEE Engineering in Medicine and Biology Society (EMBC)* (pp. 470–473).: IEEE.

Choi, J. & Jun, S. C. (2022). Spindle-targeted acoustic stimulation may stabilize an ongoing nap. *Journal of Sleep Research*, 31(6), e13583.

Choi, J., Kwon, M., & Jun, S. C. (2020). A systematic review of closed-loop feedback techniques in sleep studies—related issues and future directions. *Sensors*, 20(10), 2770.

Choi, J., Won, K., & Jun, S. C. (2019). Acoustic stimulation following sleep spindle activity may enhance procedural memory consolidation during a nap. *Ieee Access*, 7, 56297–56307.

Clawson, B. C., Durkin, J., Aton, S. J., et al. (2016). Form and function of sleep spindles across the lifespan. *Neural plasticity*, 2016.

Clemens, Z., Fabó, D., & Halász, P. (2005). Overnight verbal memory retention correlates with the number of sleep spindles. *Neuroscience*, 132(2), 529–535.

Clemens, Z., Mölle, M., Erőss, L., Barsi, P., Halász, P., & Born, J. (2007). Temporal coupling of parahippocampal ripples, sleep spindles and slow oscillations in humans. *Brain*, 130(11), 2868–2878.

Coenen, A. (2024). Sensory gating and gaining in sleep: the balance between the protection of sleep and the safeness of life (a review). *Journal of Sleep Research*, (pp. e14152).

Coffey, E., Herholz, S., Scala, S., & Zatorre, R. (2011). Montreal music history questionnaire: a tool for the assessment of music-related experience in music cognition research. In *The Neurosciences and Music IV: Learning and Memory, Conference. Edinburgh, UK.*

Coffey, E. B. (2016). *Periodic sound encoding in the human auditory system: variability and plasticity*. McGill University (Canada).

Coffey, E. B., Arseneau-Bruneau, I., Zhang, X., Baillet, S., & Zatorre, R. J. (2021). Oscillatory entrainment of the frequency-following response in auditory cortical and subcortical structures. *Journal of Neuroscience*, 41(18), 4073–4087.

Coffey, E. B., Chepesiuk, A. M., Herholz, S. C., Baillet, S., & Zatorre, R. J. (2017a). Neural correlates of early sound encoding and their relationship to speech-in-noise perception. *Frontiers in neuroscience*, 11, 479.

Coffey, E. B., Colagrosso, E. M., Lehmann, A., Schönwiesner, M., & Zatorre, R. J. (2016a). Individual differences in the frequency-following response: relation to pitch perception. *PloS one*, 11(3), e0152374.

Coffey, E. B., Herholz, S. C., Chepesiuk, A. M., Baillet, S., & Zatorre, R. J. (2016b). Cortical contributions to the auditory frequency-following response revealed by meg. *Nature communications*, 7(1), 11070.

Coffey, E. B., Musacchia, G., & Zatorre, R. J. (2017b). Cortical correlates of the auditory frequency-following and onset responses: Eeg and fmri evidence. *Journal of Neuroscience*, 37(4), 830–838.

Coffey, E. B., Nicol, T., White-Schwoch, T., Chandrasekaran, B., Krizman, J., Skoe, E., Zatorre, R. J., & Kraus, N. (2019). Evolving perspectives on the sources of the frequency-following response. *Nature communications*, 10(1), 1–10.

Colrain, I. M. (2005). The k-complex: a 7-decade history. *Sleep*, 28(2), 255–273.

Colrain, I. M. & Campbell, K. B. (2007). The use of evoked potentials in sleep research. *Sleep medicine reviews*, 11(4), 277–293.

Colrain, I. M., Crowley, K. E., Nicholas, C. L., Afifi, L., Baker, F. C., Padilla, M., Turlington, S. R., & Trinder, J. (2010). Sleep evoked delta frequency responses show a linear decline in amplitude across the adult lifespan. *Neurobiology of aging*, 31(5), 874–883.

Cordi, M. J. & Rasch, B. (2021). How robust are sleep-mediated memory benefits? *Current Opinion in Neurobiology*, 67, 1–7.

Cote, K. A., Epps, T. M., & Campbell, K. B. (2000). The role of the spindle in human information processing of high-intensity stimuli during sleep. *Journal of sleep research*, 9(1), 19–26.

Cox, R., Mylonas, D. S., Manoach, D. S., & Stickgold, R. (2018). Large-scale structure and individual fingerprints of locally coupled sleep oscillations. *Sleep*, 41(12), zsy175.

Cox, R., Schapiro, A. C., Manoach, D. S., & Stickgold, R. (2017). Individual differences in frequency and topography of slow and fast sleep spindles. *Frontiers in human neuroscience*, 11, 433.

Crabtree, J. W. (2018). Functional diversity of thalamic reticular subnetworks. *Frontiers in systems neuroscience*, 12, 41.

Crowley, K., Trinder, J., Kim, Y., Carrington, M., & Colrain, I. M. (2002). The effects of normal aging on sleep spindle and k-complex production. *Clinical neurophysiology*, 113(10), 1615–1622.

Csernai, M., Borbély, S., Kocsis, K., Burka, D., Fekete, Z., Balogh, V., Káli, S., Emri, Z., & Barthó, P. (2019). Dynamics of sleep oscillations is coupled to brain temperature on multiple scales. *The Journal of physiology*, 597(15), 4069–4086.

Czisch, M., Wehrle, R., Kaufmann, C., Wetter, T. C., Holsboer, F., Pollmächer, T., & Auer, D. P. (2004). Functional mri during sleep: Bold signal decreases and their electrophysiological correlates. *European Journal of Neuroscience*, 20(2), 566–574.

Czisch, M., Wetter, T. C., Kaufmann, C., Pollmächer, T., Holsboer, F., & Auer, D. P. (2002). Altered processing of acoustic stimuli during sleep: reduced auditory activation and visual deactivation detected by a combined fmri/eeg study. *Neuroimage*, 16(1), 251–258.

da Silva, F. L. (1991). Neural mechanisms underlying brain waves: from neural membranes to networks. *Electroencephalography and clinical neurophysiology*, 79(2), 81–93.

Dang-Vu, T. T., Bonjean, M., Schabus, M., Boly, M., Darsaud, A., Desseilles, M., Degueldre, C., Balteau, E., Phillips, C., Luxen, A., et al. (2011). Interplay between spontaneous and induced brain activity during human non-rapid eye movement sleep. *Proceedings of the National Academy of Sciences*, 108(37), 15438–15443.

Dang-Vu, T. T., McKinney, S. M., Buxton, O. M., Solet, J. M., & Ellenbogen, J. M. (2010). Spontaneous brain rhythms predict sleep stability in the face of noise. *Current biology*, 20(15), R626–R627.

Dastgheib, M., Kulanayagam, A., & Dringenberg, H. C. (2022). Is the role of sleep in memory consolidation overrated? *Neuroscience & Biobehavioral Reviews*, 140, 104799.

Datta, S. (2010). Cellular and chemical neuroscience of mammalian sleep. *Sleep medicine*, 11(5), 431–440.

Daunizeau, J., Mattout, J., Clonda, D., Goulard, B., Benali, H., & Lina, J.-M. (2006). Bayesian spatio-temporal approach for eeg source reconstruction: conciliating ecd and distributed models. *IEEE Transactions on Biomedical Engineering*, 53(3), 503–516.

De Zeeuw, C. I. & Ten Brinke, M. M. (2015). Motor learning and the cerebellum. *Cold Spring Harbor perspectives in biology*, 7(9), a021683.

Debellemanière, E., Pinaud, C., Schneider, J., Arnal, P. J., Casson, A. J., Chennaoui, M., Galtier, M., Navarrete, M., & Lewis, P. A. (2022). Optimising sounds for the driving of sleep oscillations by closed-loop auditory stimulation. *Journal of Sleep Research*, 31(6), e13676.

Dehnavi, F., Koo-Poeggel, P. C., Ghorbani, M., & Marshall, L. (2021). Spontaneous slow oscillation—slow spindle features predict induced overnight memory retention. *Sleep*, 44(10), zsab127.

Denis, D., Mylonas, D., Poskanzer, C., Bursal, V., Payne, J. D., & Stickgold, R. (2021). Sleep spindles preferentially consolidate weakly encoded memories. *Journal of Neuroscience*, 41(18), 4088–4099.

Destrieux, C., Fischl, B., Dale, A., & Halgren, E. (2010). Automatic parcellation of human cortical gyri and sulci using standard anatomical nomenclature. *Neuroimage*, 53(1), 1–15.

Diekelmann, S. & Born, J. (2010). The memory function of sleep. *Nature Reviews Neuroscience*, 11(2), 114–126.

Diep, C., Ftouni, S., Manousakis, J. E., Nicholas, C. L., Drummond, S. P., & Anderson, C. (2020). Acoustic slow wave sleep enhancement via a novel, automated device improves executive function in middle-aged men. *Sleep*, 43(1), zsz197.

Donoghue, T., Haller, M., Peterson, E. J., Varma, P., Sebastian, P., Gao, R., Noto, T., Lara, A. H., Wallis, J. D., Knight, R. T., et al. (2020). Parameterizing neural power spectra into periodic and aperiodic components. *Nature neuroscience*, 23(12), 1655–1665.

Doyon, J., Korman, M., Morin, A., Dostie, V., Tahar, A. H., Benali, H., Karni, A., Ungerleider, L. G., & Carrier, J. (2009). Contribution of night and day sleep vs. simple passage of time to the consolidation of motor sequence and visuomotor adaptation learning. *Experimental brain research*, 195, 15–26.

Doyon, J., Ungerleider, L. G., Squire, L., & Schacter, D. (2002). Functional anatomy of motor skill learning. *Neuropsychology of memory*, 3, 225–238.

Eggermont, J. J. & Ponton, C. W. (2002). The neurophysiology of auditory perception: from single units to evoked potentials. *Audiology and Neurotology*, 7(2), 71–99.

Eichenbaum, H. (2000). A cortical–hippocampal system for declarative memory. *Nature reviews neuroscience*, 1(1), 41–50.

Eimer, M. (1996). The n2pc component as an indicator of attentional selectivity. *Electroencephalography and clinical neurophysiology*, 99(3), 225–234.

Ellenbogen, J. M., Hulbert, J. C., Stickgold, R., Dinges, D. F., & Thompson-Schill, S. L. (2006). Interfering with theories of sleep and memory: sleep, declarative memory, and associative interference. *Current Biology*, 16(13), 1290–1294.

Elton, M., Winter, O., Heslenfeld, D., Loewy, D., Campbell, K., & Kok, A. (1997). Event-related potentials to tones in the absence and presence of sleep spindles. *Journal of sleep research*, 6(2), 78–83.

Esfahani, M. J., Farboud, S., Ngo, H.-V. V., Schneider, J., Weber, F. D., Talamini, L. M., & Dresler, M. (2023). Closed-loop auditory stimulation of sleep slow oscillations: basic principles and best practices. *Neuroscience & Biobehavioral Reviews*, 153, 105379.

Esser, S. K., Hill, S., & Tononi, G. (2009). Breakdown of effective connectivity during slow wave sleep: investigating the mechanism underlying a cortical gate using large-scale modeling. *Journal of neurophysiology*, 102(4), 2096–2111.

Evans, J. & Silver, R. (2022). The suprachiasmatic nucleus and the circadian timekeeping system of the body. In *Neuroscience in the 21st century: from basic to clinical* (pp. 2577–2625). Springer.

Evans, M. S., Harborne, D., & Smith, A. P. (2018). Developing an objective indicator of fatigue: An alternative mobile version of the psychomotor vigilance task (m-pvt). In *International Symposium on Human Mental Workload: Models and Applications* (pp. 49–71).: Springer.

Fattinger, S., Heinzle, B. B., Ramantani, G., Abela, L., Schmitt, B., & Huber, R. (2019). Closed-loop acoustic stimulation during sleep in children with epilepsy: a hypothesis-driven novel approach to interact with spike-wave activity and pilot data assessing feasibility. *Frontiers in Human Neuroscience*, 13, 166.

Fehér, K. D., Wunderlin, M., Maier, J. G., Hertenstein, E., Schneider, C. L., Mikutta, C., Züst, M. A., Klöppel, S., & Nissen, C. (2021). Shaping the slow waves of sleep: A systematic and integrative review of sleep slow wave modulation in humans using non-invasive brain stimulation. *Sleep medicine reviews*, 58, 101438.

Fernandez, L. M. & Lüthi, A. (2020). Sleep spindles: mechanisms and functions. *Physiological reviews*, 100(2), 805–868.

Fischl, B. (2012). Freesurfer. *Neuroimage*, 62(2), 774–781.

Fischl, B., Salat, D. H., Busa, E., Albert, M., Dieterich, M., Haselgrove, C., Van Der Kouwe, A., Killiany, R., Kennedy, D., Klaveness, S., et al. (2002). Whole brain segmentation: automated labeling of neuroanatomical structures in the human brain. *Neuron*, 33(3), 341–355.

Fogel, S., Nader, R., Cote, K., & Smith, C. (2007a). Sleep spindles and learning potential. *Behavioral neuroscience*, 121(1), 1.

Fogel, S. M., Ray, L. B., Binnie, L., & Owen, A. M. (2015). How to become an expert: a new perspective on the role of sleep in the mastery of procedural skills. *Neurobiology of Learning and Memory*, 125, 236–248.

Fogel, S. M., Smith, C. T., & Cote, K. A. (2007b). Dissociable learning-dependent changes in rem and non-rem sleep in declarative and procedural memory systems. *Behavioural brain research*, 180(1), 48–61.

Fuentemilla, L. (2025). Memory consolidation accelerates. *Nature Neuroscience*, (pp. 1–2).

Funahashi, S. & Kubota, K. (1994). Working memory and prefrontal cortex. *Neuroscience research*, 21(1), 1–11.

Gais, S. & Born, J. (2004). Declarative memory consolidation: mechanisms acting during human sleep. *Learning & memory*, 11(6), 679–685.

Gais, S., Mölle, M., Helms, K., & Born, J. (2002). Learning-dependent increases in sleep spindle density. *Journal of Neuroscience*, 22(15), 6830–6834.

Galbraith, G. C., Olfman, D. M., & Huffman, T. M. (2003). Selective attention affects human brain stem frequency-following response. *Neuroreport*, 14(5), 735–738.

Gaudreault, P.-O., Gosselin, N., Lafortune, M., Deslauriers-Gauthier, S., Martin, N., Bouchard, M., Dubé, J., Lina, J.-M., Doyon, J., & Carrier, J. (2018). The association between white matter and sleep spindles differs in young and older individuals. *Sleep*, 41(9), zsy113.

Gehring, W., Liu, Y., Orr, J., Carp, J., Luck, S., & Kappenman, E. (2012). Oxford handbook of event-related potential components.

Girardeau, G. & Lopes-Dos-Santos, V. (2021). Brain neural patterns and the memory function of sleep. *Science*, 374(6567), 560–564.

Gonzalez, C. E., Mak-McCully, R. A., Rosen, B. Q., Cash, S. S., Chauvel, P. Y., Bastuji, H., Rey, M., & Halgren, E. (2018). Theta bursts precede, and spindles follow, cortical and thalamic downstates in human nrem sleep. *Journal of Neuroscience*, 38(46), 9989–10001.

Goosens, K. A. & Maren, S. (2001). Contextual and auditory fear conditioning are mediated by the lateral, basal, and central amygdaloid nuclei in rats. *Learning & memory*, 8(3), 148–155.

Gorina-Careta, N., Kurkela, J. L., Hämäläinen, J., Astikainen, P., & Escera, C. (2021). Neural generators of the frequency-following response elicited to stimuli of low and high frequency: a magnetoencephalographic (meg) study. *Neuroimage*, 231, 117866.

Goto, A. (2022). Synaptic plasticity during systems memory consolidation. *Neuroscience research*, 183, 1–6.

Grimaldi, D., Papalambros, N. A., Reid, K. J., Abbott, S. M., Malkani, R. G., Gendy, M., Iwanaszko, M., Braun, R. I., Sanchez, D. J., Paller, K. A., et al. (2019). Strengthening sleep–autonomic interaction via acoustic enhancement of slow oscillations. *Sleep*, 42(5), zsz036.

Grimaldi, D., Papalambros, N. A., Zee, P. C., & Malkani, R. G. (2020). Neurostimulation techniques to enhance sleep and improve cognition in aging. *Neurobiology of disease*, 141, 104865.

Grissom, R. J. & Kim, J. J. (2012). *Effect sizes for research: Univariate and multivariate applications*. Routledge.

Gross, J., Baillet, S., Barnes, G. R., Henson, R. N., Hillebrand, A., Jensen, O., Jerbi, K., Litvak, V., Maess, B., Oostenveld, R., et al. (2013). Good practice for conducting and reporting meg research. *Neuroimage*, 65, 349–363.

Guerra, A., López-Alonso, V., Cheeran, B., & Suppa, A. (2020). Solutions for managing variability in non-invasive brain stimulation studies. *Neuroscience letters*, 719, 133332.

Hahn, M. A., Bothe, K., Heib, D., Schabus, M., Helfrich, R. F., & Hoedlmoser, K. (2022). Slow oscillation–spindle coupling strength predicts real-life gross-motor learning in adolescents and adults. *Elife*, 11.

Hahn, M. A., Heib, D., Schabus, M., Hoedlmoser, K., & Helfrich, R. F. (2020). Slow oscillation-spindle coupling predicts enhanced memory formation from childhood to adolescence. *Elife*, 9, e53730.

Halász, P. (2016). The k-complex as a special reactive sleep slow wave–a theoretical update. *Sleep medicine reviews*, 29, 34–40.

Halász, P., Terzano, M., Parrino, L., & Bódizs, R. (2004). The nature of arousal in sleep. *Journal of sleep research*, 13(1), 1–23.

Hale, J. R., White, T. P., Mayhew, S. D., Wilson, R. S., Rollings, D. T., Khalsa, S., Arvanitis, T. N., & Bagshaw, A. P. (2016). Altered thalamocortical and intra-thalamic functional connectivity during light sleep compared with wake. *Neuroimage*, 125, 657–667.

Hämäläinen, M. (2009). *MNE Software User's Guide v2. 7*. Technical report, MGH/HMS/MIT Athinoula A.

Harrington, M. O. & Cairney, S. A. (2021). Sounding it out: Auditory stimulation and overnight memory processing. *Current Sleep Medicine Reports*, 7(3), 112–119.

Harrington, M. O., Ngo, H.-V. V., & Cairney, S. A. (2021). No benefit of auditory closed-loop stimulation on memory for semantically-incongruent associations. *Neurobiology of learning and memory*, 183, 107482.

Hartmann, T. & Weisz, N. (2019). Auditory cortical generators of the frequency following response are modulated by intermodal attention. *bioRxiv*, (pp. 633834).

Hassan, U., Feld, G. B., & Bergmann, T. O. (2022). Automated real-time eeg sleep spindle detection for brain-state-dependent brain stimulation. *Journal of sleep research*, 31(6), e13733.

Hassan, U., Okyere, P., Masouleh, M. A., Zrenner, C., Ziemann, U., & Bergmann, T. O. (2025). Pulsed inhibition of corticospinal excitability by the thalamocortical sleep spindle. *Brain Stimulation*.

Hastings, M. H., Maywood, E. S., & Brancaccio, M. (2018). Generation of circadian rhythms in the suprachiasmatic nucleus. *Nature Reviews Neuroscience*, 19(8), 453–469.

Hauglund, N. L., Pavan, C., & Nedergaard, M. (2020). Cleaning the sleeping brain–the potential restorative function of the glymphatic system. *Current Opinion in Physiology*, 15, 1–6.

Hayat, H., Marmelshtein, A., Krom, A. J., Sela, Y., Tankus, A., Strauss, I., Fahoum, F., Fried, I., & Nir, Y. (2022). Reduced neural feedback signaling despite robust neuron and gamma auditory responses during human sleep. *Nature neuroscience*, 25(7), 935–943.

Hayat, H., Regev, N., Matosevich, N., Sales, A., Paredes-Rodriguez, E., Krom, A. J., Bergman, L., Li, Y., Lavigne, M., Kremer, E. J., et al. (2020). Locus coeruleus norepinephrine activity mediates sensory-evoked awakenings from sleep. *Science advances*, 6(15), eaaz4232.

He, S., Hasler, B. P., & Chakravorty, S. (2019). Alcohol and sleep-related problems. *Current opinion in psychology*, 30, 117–122.

Helfrich, R. F., Mander, B. A., Jagust, W. J., Knight, R. T., & Walker, M. P. (2018). Old brains come uncoupled in sleep: slow wave-spindle synchrony, brain atrophy, and forgetting. *Neuron*, 97(1), 221–230.

Henin, S., Borges, H., Shankar, A., Sarac, C., Melloni, L., Friedman, D., Flinker, A., Parra, L. C., Buzsaki, G., Devinsky, O., et al. (2019). Closed-loop acoustic stimulation enhances sleep oscillations but not memory performance. *eneuro*, 6(6).

Hennevin, E., Huetz, C., & Edeline, J.-M. (2007). Neural representations during sleep: from sensory processing to memory traces. *Neurobiology of learning and memory*, 87(3), 416–440.

Herholz, S. C., Coffey, E. B., Pantev, C., & Zatorre, R. J. (2015). Dissociation of neural networks for predisposition and for training-related plasticity in auditory-motor learning. *Cerebral Cortex*, 26(7), 3125–3134.

Herholz, S. C. & Zatorre, R. J. (2012). Musical training as a framework for brain plasticity: behavior, function, and structure. *Neuron*, 76(3), 486–502.

Hillebrand, A., Tewarie, P., Van Dellen, E., Yu, M., Carbo, E. W., Douw, L., Gouw, A. A., Van Straaten, E. C., & Stam, C. J. (2016). Direction of information flow in large-scale resting-state networks is frequency-dependent. *Proceedings of the National Academy of Sciences*, 113(14), 3867–3872.

Himmer, L., Bürger, Z., Fresz, L., Maschke, J., Wagner, L., Brodt, S., Braun, C., Schönauer, M., & Gais, S. (2021). Localizing spontaneous memory reprocessing during human sleep. *bioRxiv*.

Holst, S. C. & Landolt, H.-P. (2015). Sleep homeostasis, metabolism, and adenosine. *Current Sleep Medicine Reports*, 1, 27–37.

Holz, J., Piosczyk, H., Feige, B., Spiegelhalder, K., Baglioni, C., Riemann, D., & Nissen, C. (2012). Eeg sigma and slow-wave activity during nrem sleep correlate with overnight declarative and procedural memory consolidation. *Journal of sleep research*, 21(6), 612–619.

Homan, R. W., Herman, J., & Purdy, P. (1987). Cerebral location of international 10–20 system electrode placement. *Electroencephalography and clinical neurophysiology*, 66(4), 376–382.

Horne, J. A. & Östberg, O. (1976). A self-assessment questionnaire to determine morningness-eveningness in human circadian rhythms. *International journal of chronobiology*.

Hu, B. (2003). Functional organization of lemniscal and nonlemniscal auditory thalamus. *Experimental Brain Research*, 153, 543–549.

Huber, R., Felice Ghilardi, M., Massimini, M., & Tononi, G. (2004). Local sleep and learning. *Nature*, 430(6995), 78–81.

Iber, C. (2007). The aasm manual for the scoring of sleep and associated events: Rules. *Terminology and Technical Specification*.

Jaar, O., Pilon, M., Carrier, J., Montplaisir, J., & Zadra, A. (2010). Analysis of slow-wave activity and slow-wave oscillations prior to somnambulism. *Sleep*, 33(11), 1511–1516.

Jaehne, A., Loessl, B., Bárkai, Z., Riemann, D., & Hornyak, M. (2009). Effects of nicotine on sleep during consumption, withdrawal and replacement therapy. *Sleep medicine reviews*, 13(5), 363–377.

James, T., Kula, B., Choi, S., Khan, S. S., Bekar, L. K., & Smith, N. A. (2021). Locus coeruleus in memory formation and alzheimer's disease. *European Journal of Neuroscience*, 54(8), 6948–6959.

Jaramillo, J., Mejias, J. F., & Wang, X.-J. (2019). Engagement of pulvino-cortical feedforward and feedback pathways in cognitive computations. *Neuron*, 101(2), 321–336.

Jasper, H. H. (1958). Ten-twenty electrode system of the international federation. *Electroencephalogr Clin Neurophysiol*, 10, 371–375.

Jobst, B. M., Hindriks, R., Laufs, H., Tagliazucchi, E., Hahn, G., Ponce-Alvarez, A., Stevner, A. B., Kringelbach, M. L., & Deco, G. (2017). Increased stability and breakdown of brain effective connectivity during slow-wave sleep: mechanistic insights from whole-brain computational modelling. *Scientific reports*, 7(1), 4634.

Johns, M. W. (1991). A new method for measuring daytime sleepiness: the epworth sleepiness scale. *sleep*, 14(6), 540–545.

Johnson, L., Hanson, K., & Bickford, R. (1976). Effect of flurazepam on sleep spindles and k-complexes. *Electroencephalography and clinical neurophysiology*, 40(1), 67–77.

Jones, B. E. (2003). Arousal systems. *Front Biosci*, 8(5), 438–51.

Jourde, H. R. & Coffey, E. B. (2024). Auditory processing up to cortex is maintained during sleep spindles. *PNAS nexus*, 3(11), pgae479.

Jourde, H. R., Merlo, R., Brooks, M., Rowe, M., & Coffey, E. B. (2022). The neurophysiology of closed-loop auditory stimulation in sleep: a meg study. *bioRxiv*, (pp. 2022–12).

Jourde, H. R., Merlo, R., Brooks, M., Rowe, M., & Coffey, E. B. (2024). The neurophysiology of closed-loop auditory stimulation in sleep: A magnetoencephalography study. *European Journal of Neuroscience*, 59(4), 613–640.

Jourde, H. R., Sobral, M., Beltrame, G., & Coffey, E. B. (2025a). Neurophysiological effects of targeting sleep spindles with closed-loop auditory stimulation. *Sleep advances*, In press.

Jourde, H. R., Ujevco, A., & Coffey, E. B. (2025b). Phase-specific effects of sleep spindle auditory stimulation. *Brain Stimulation*, Submitted.

Jung, M. W., Baeg, E. H., Kim, M. J., Kim, Y. B., & Kim, J. J. (2008). Plasticity and memory in the prefrontal cortex. *Reviews in the Neurosciences*, 19(1), 29–46.

Kaas, J. H., Hackett, T. A., & Tramo, M. J. (1999). Auditory processing in primate cerebral cortex. *Current opinion in neurobiology*, 9(2), 164–170.

Kaestner, E. J., Wixted, J. T., & Mednick, S. C. (2013). Pharmacologically increasing sleep spindles enhances recognition for negative and high-arousal memories. *Journal of cognitive neuroscience*, 25(10), 1597–1610.

Kállai, I., Harsh, J., & Voss, U. (2003). Attention to external stimuli during wakefulness and sleep: Evoked 40-hz response and n350. *Psychophysiology*, 40(6), 955–966.

Kelley, D. H., Bohr, T., Hjorth, P. G., Holst, S. C., Hrabětová, S., Kiviniemi, V., Lilius, T., Lundgaard, I., Mardal, K.-A., Martens, E. A., et al. (2022). The glymphatic system: Current understanding and modeling. *Iscience*, (pp. 104987).

Kelter, R. (2020). Bayesian alternatives to null hypothesis significance testing in biomedical research: a non-technical introduction to bayesian inference with jasp. *BMC medical research methodology*, 20, 1–12.

Kim, A., Latchoumane, C., Lee, S., Kim, G. B., Cheong, E., Augustine, G. J., & Shin, H.-S. (2012). Optogenetically induced sleep spindle rhythms alter sleep architectures in mice. *Proceedings of the National Academy of Sciences*, 109(50), 20673–20678.

Kim, J., Gulati, T., & Ganguly, K. (2019). Competing roles of slow oscillations and delta waves in memory consolidation versus forgetting. *Cell*, 179(2), 514–526.

King, B. R., Hoedlmoser, K., Hirschauer, F., Dolfen, N., & Albouy, G. (2017). Sleeping on the motor engram: The multifaceted nature of sleep-related motor memory consolidation. *Neuroscience & Biobehavioral Reviews*, 80, 1–22.

Kirschstein, T. & Köhling, R. (2009). What is the source of the eeg? *Clinical EEG and neuroscience*, 40(3), 146–149.

Kjaerby, C., Andersen, M., Hauglund, N., Untiet, V., Dall, C., Sigurdsson, B., Ding, F., Feng, J., Li, Y., Weikop, P., et al. (2022). Memory-enhancing properties of sleep depend on the oscillatory amplitude of norepinephrine. *Nature Neuroscience*, 25(8), 1059–1070.

Klinzing, J. G., Mölle, M., Weber, F., Supp, G., Hipp, J. F., Engel, A. K., & Born, J. (2016). Spindle activity phase-locked to sleep slow oscillations. *Neuroimage*, 134, 607–616.

Klinzing, J. G., Niethard, N., & Born, J. (2019). Mechanisms of systems memory consolidation during sleep. *Nature neuroscience*, 22(10), 1598–1610.

Koch, C. (1987). The action of the corticofugal pathway on sensory thalamic nuclei: a hypothesis. *Neuroscience*, 23(2), 399–406.

Komura, Y., Tamura, R., Uwano, T., Nishijo, H., & Ono, T. (2005). Auditory thalamus integrates visual inputs into behavioral gains. *Nature neuroscience*, 8(9), 1203–1209.

Koo-Poeggel, P., Neuwerk, S., Petersen, E., Grasshoff, J., Mölle, M., Martinetz, T., & Marshall, L. (2022). Closed-loop acoustic stimulation during an afternoon nap to modulate subsequent encoding. *Journal of Sleep Research*, 31(6), e13734.

Koroma, M., Lacaux, C., Andrillon, T., Legendre, G., Léger, D., & Kouider, S. (2020). Sleepers selectively suppress informative inputs during rapid eye movements. *Current Biology*, 30(12), 2411–2417.

Kraus, N. (2011). Musical training gives edge in auditory processing. *The Hearing Journal*, 64(2), 10–12.

Kraus, N., McGee, T., Littman, T., Nicol, T., & King, C. (1994). Nonprimary auditory thalamic representation of acoustic change. *Journal of neurophysiology*, 72(3), 1270–1277.

Krizman, J. & Kraus, N. (2019). Analyzing the ffr: A tutorial for decoding the richness of auditory function. *Hearing research*, 382, 107779.

Krol, A., Wimmer, R. D., Halassa, M. M., & Feng, G. (2018). Thalamic reticular dysfunction as a circuit endophenotype in neurodevelopmental disorders. *Neuron*, 98(2), 282–295.

Kucewicz, M. T., Cimbalnik, J., Matsumoto, J. Y., Brinkmann, B. H., Bower, M. R., Vasoli, V., Sulc, V., Meyer, F., Marsh, W., Stead, S., et al. (2014). High frequency oscillations are associated with cognitive processing in human recognition memory. *Brain*, 137(8), 2231–2244.

Kumar, A. A. (2021). Semantic memory: A review of methods, models, and current challenges. *Psychonomic Bulletin & Review*, 28(1), 40–80.

Kutas, M. & Hillyard, S. A. (1980). Reading senseless sentences: Brain potentials reflect semantic incongruity. *Science*, 207(4427), 203–205.

Lachaux, J.-P., Axmacher, N., Mormann, F., Halgren, E., & Crone, N. E. (2012). High-frequency neural activity and human cognition: past, present and possible future of intracranial eeg research. *Progress in neurobiology*, 98(3), 279–301.

Lacourse, K., Delfrate, J., Beaudry, J., Peppard, P., & Warby, S. C. (2019). A sleep spindle detection algorithm that emulates human expert spindle scoring. *Journal of neuroscience methods*, 316, 3–11.

Lacourse, K., Yetton, B., Mednick, S., & Warby, S. C. (2020). Massive online data annotation, crowdsourcing to generate high quality sleep spindle annotations from eeg data. *Scientific data*, 7(1), 190.

Langbein, J., Boddeti, U., Xie, W., & Ksendzovsky, A. (2025). Intracranial closed-loop neuromodulation as an intervention for neuropsychiatric disorders: an overview. *Frontiers in Psychiatry*, 16, 1479240.

Latchoumane, C.-F. V., Ngo, H.-V. V., Born, J., & Shin, H.-S. (2017). Thalamic spindles promote memory formation during sleep through triple phase-locking of cortical, thalamic, and hippocampal rhythms. *Neuron*, 95(2), 424–435.

Latreille, V., von Ellenrieder, N., Peter-Derex, L., Dubeau, F., Gotman, J., & Frauscher, B. (2020). The human k-complex: insights from combined scalp-intracranial eeg recordings. *Neuroimage*, 213, 116748.

Laurino, M., Menicucci, D., Piarulli, A., Mastorci, F., Bedini, R., Allegrini, P., & Gemignani, A. (2014). Disentangling different functional roles of evoked k-complex components: mapping the sleeping brain while quenching sensory processing. *Neuroimage*, 86, 433–445.

Laventure, S., Fogel, S., Lungu, O., Albouy, G., Sévigny-Dupont, P., Vien, C., Sayour, C., Carrier, J., Benali, H., & Doyon, J. (2016). Nrem2 and sleep spindles are instrumental to the consolidation of motor sequence memories. *PLoS biology*, 14(3), e1002429.

Lecci, S., Fernandez, L. M., Weber, F. D., Cardis, R., Chatton, J.-Y., Born, J., & Lüthi, A. (2017). Coordinated infraslow neural and cardiac oscillations mark fragility and offline periods in mammalian sleep. *Science Advances*, 3(2), e1602026.

Lee, C. C. (2015). Exploring functions for the non-lemniscal auditory thalamus. *Frontiers in Neural Circuits*, 9, 69.

Lee, E. K. & Douglass, A. B. (2010). Sleep in psychiatric disorders: where are we now? *The Canadian Journal of Psychiatry*, 55(7), 403–412.

Lee, M. D. & Wagenmakers, E.-J. (2014). *Bayesian cognitive modeling: A practical course*. Cambridge university press.

Legendre, G., Andrillon, T., Koroma, M., & Kouider, S. (2019). Sleepers track informative speech in a multitalker environment. *Nature Human Behaviour*, 3(3), 274–283.

Leminen, M. M., Virkkala, J., Saure, E., Paajanen, T., Zee, P. C., Santostasi, G., Hublin, C., Müller, K., Porkka-Heiskanen, T., Huotilainen, M., et al. (2017). Enhanced memory consolidation via automatic sound stimulation during non-rem sleep. *Sleep*, 40(3), zsx003.

Lenth, R. V. (2022). *emmeans: Estimated Marginal Means, aka Least-Squares Means*. R package version 1.8.2.

Lerousseau, J. P., Trébuchon, A., Morillon, B., & Schön, D. (2021). Frequency selectivity of persistent cortical oscillatory responses to auditory rhythmic stimulation. *Journal of Neuroscience*, 41(38), 7991–8006.

Li, J., Vitiello, M. V., & Gooneratne, N. S. (2022). Sleep in normal aging. *Sleep medicine clinics*, 17(2), 161–171.

Lijffijt, M., Lane, S. D., Meier, S. L., Boutros, N. N., Burroughs, S., Steinberg, J. L., Gerard Moeller, F., & Swann, A. C. (2009). P50, n100, and p200 sensory gating: relationships with behavioral inhibition, attention, and working memory. *Psychophysiology*, 46(5), 1059–1068.

Lobier, M., Siebenhühner, F., Palva, S., & Palva, J. M. (2014). Phase transfer entropy: a novel phase-based measure for directed connectivity in networks coupled by oscillatory interactions. *Neuroimage*, 85, 853–872.

Logg, J. M. & Dorison, C. A. (2021). Pre-registration: Weighing costs and benefits for researchers. *Organizational Behavior and Human Decision Processes*, 167, 18–27.

Loomis, A. L., Harvey, E. N., & Hobart III, G. A. (1938). Distribution of disturbance-patterns in the human electroencephalogram, with special reference to sleep. *Journal of Neurophysiology*, 1(5), 413–430.

López-Alonso, V., Cheeran, B., Río-Rodríguez, D., & Fernández-del Olmo, M. (2014). Inter-individual variability in response to non-invasive brain stimulation paradigms. *Brain stimulation*, 7(3), 372–380.

López-Madrona, V. J., Medina Villalon, S., Badier, J.-M., Trébuchon, A., Jayabal, V., Bartolomei, F., Carron, R., Barborica, A., Vulliémoz, S., Alario, F.-X., et al. (2022). Magnetoencephalography can reveal deep brain network activities linked to memory processes. *Human Brain Mapping*, 43(15), 4733–4749.

Lustenberger, C., Boyle, M. R., Alagapan, S., Mellin, J. M., Vaughn, B. V., & Fröhlich, F. (2016). Feedback-controlled transcranial alternating current stimulation reveals a functional role of sleep spindles in motor memory consolidation. *Current Biology*, 26(16), 2127–2136.

Lustenberger, C., Wehrle, F., Tüshaus, L., Achermann, P., & Huber, R. (2015). The multidimensional aspects of sleep spindles and their relationship to word-pair memory consolidation. *Sleep*, 38(7), 1093–1103.

Lüthi, A. (2014). Sleep spindles: where they come from, what they do. *The Neuroscientist*, 20(3), 243–256.

Mai, G., Schoof, T., & Howell, P. (2019). Modulation of phase-locked neural responses to speech during different arousal states is age-dependent. *NeuroImage*, 189, 734–744.

Makov, S., Sharon, O., Ding, N., Ben-Shachar, M., Nir, Y., & Golumbic, E. Z. (2017). Sleep disrupts high-level speech parsing despite significant basic auditory processing. *Journal of Neuroscience*, 37(32), 7772–7781.

Mander, B. A., Rao, V., Lu, B., Saletin, J. M., Ancoli-Israel, S., Jagust, W. J., & Walker, M. P. (2014). Impaired prefrontal sleep spindle regulation of hippocampal-dependent learning in older adults. *Cerebral cortex*, 24(12), 3301–3309.

Manns, J. R. & Eichenbaum, H. (2006). Evolution of declarative memory. *Hippocampus*, 16(9), 795–808.

Manoach, D. S., Pan, J. Q., Purcell, S. M., & Stickgold, R. (2016). Reduced sleep spindles in schizophrenia: a treatable endophenotype that links risk genes to impaired cognition? *Biological psychiatry*, 80(8), 599–608.

Manoach, D. S. & Stickgold, R. (2019). Abnormal sleep spindles, memory consolidation, and schizophrenia. *Annual review of clinical psychology*, 15(1), 451–479.

Marsh, J. E. & Campbell, T. A. (2016). Processing complex sounds passing through the rostral brainstem: The new early filter model. *Frontiers in Neuroscience*, 10, 136.

Marsman, M. & Wagenmakers, E.-J. (2017). Bayesian benefits with jasp. *European Journal of Developmental Psychology*, 14(5), 545–555.

Massimini, M., Ferrarelli, F., Huber, R., Esser, S. K., Singh, H., & Tononi, G. (2005). Breakdown of cortical effective connectivity during sleep. *Science*, 309(5744), 2228–2232.

Massimini, M., Ferrarelli, F., Murphy, M., Huber, R., Riedner, B., Casarotto, S., & Tononi, G. (2010). Cortical reactivity and effective connectivity during rem sleep in humans. *Cognitive neuroscience*, 1(3), 176–183.

Massimini, M., Huber, R., Ferrarelli, F., Hill, S., & Tononi, G. (2004). The sleep slow oscillation as a traveling wave. *Journal of Neuroscience*, 24(31), 6862–6870.

McCormick, D. A. & Bal, T. (1994). Sensory gating mechanisms of the thalamus. *Current opinion in neurobiology*, 4(4), 550–556.

McCoy, J. G. & Strecker, R. E. (2011). The cognitive cost of sleep lost. *Neurobiology of learning and memory*, 96(4), 564–582.

Meeren, H., Van Walsum, A. V. C., Van Luijtelaar, E., & Coenen, A. (2001). Auditory evoked potentials from auditory cortex, medial geniculate nucleus, and inferior colliculus during sleep–wake states and spike-wave discharges in the wag/rij rat. *Brain research*, 898(2), 321–331.

Menicucci, D., Piarulli, A., Laurino, M., Zaccaro, A., Agrimi, J., & Gemignani, A. (2020). Sleep slow oscillations favour local cortical plasticity underlying the consolidation of reinforced procedural learning in human sleep. *Journal of Sleep Research*, 29(5), e13117.

Michon, K. J., Khammash, D., Simmonite, M., Hamlin, A. M., & Polk, T. A. (2022). Person-specific and precision neuroimaging: Current methods and future directions. *Neuroimage*, (pp. 119589).

Mikutta, C., Feige, B., Maier, J. G., Hertenstein, E., Holz, J., Riemann, D., & Nissen, C. (2019). Phase-amplitude coupling of sleep slow oscillatory and spindle activity correlates with overnight memory consolidation. *Journal of sleep research*, 28(6), e12835.

Milner, B., Squire, L. R., & Kandel, E. R. (1998). Cognitive neuroscience and the study of memory. *Neuron*, 20(3), 445–468.

Molinari, M., Leggio, M. G., Solida, A., Ciorra, R., Misciagna, S., Silveri, M. C., & Petrosini, L. (1997). Cerebellum and procedural learning: evidence from focal cerebellar lesions. *Brain: a journal of neurology*, 120(10), 1753–1762.

Mölle, M., Bergmann, T. O., Marshall, L., & Born, J. (2011). Fast and slow spindles during the sleep slow oscillation: disparate coalescence and engagement in memory processing. *Sleep*, 34(10), 1411–1421.

Mölle, M. & Born, J. (2011). Slow oscillations orchestrating fast oscillations and memory consolidation. *Progress in brain research*, 193, 93–110.

Mölle, M., Yeshenko, O., Marshall, L., Sara, S. J., & Born, J. (2006). Hippocampal sharp wave-ripples linked to slow oscillations in rat slow-wave sleep. *Journal of neurophysiology*.

Morales-Cobas, G., Ferreira, M. I., & Velluti, R. A. (1995). Firing of inferior colliculus neurons in response to low-frequency sound stimulation during sleep and waking. *Journal of Sleep Research*, 4(4), 242–251.

Moreira, C. G., Baumann, C. R., Scandella, M., Nemirovsky, S. I., Leach, S., Huber, R., & Noain, D. (2021). Closed-loop auditory stimulation method to modulate sleep slow waves and motor learning performance in rats. *Elife*, 10, e68043.

Morgan, K. K., Hathaway, E., Carson, M., Fernandez-Corazza, M., Shusterman, R., Luu, P., & Tucker, D. M. (2021). Focal limbic sources create the large slow oscillations of the eeg in human deep sleep. *Sleep Medicine*, 85, 291–302.

Morin, A., Doyon, J., Dostie, V., Barakat, M., Tahar, A. H., Korman, M., Benali, H., Karni, A., Ungerleider, L. G., & Carrier, J. (2008). Motor sequence learning increases sleep spindles and fast frequencies in post-training sleep. *Sleep*, 31(8), 1149–1156.

Muehlroth, B. E., Sander, M. C., Fandakova, Y., Grandy, T. H., Rasch, B., Shing, Y. L., & Werkle-Bergner, M. (2019). Precise slow oscillation–spindle coupling promotes memory consolidation in younger and older adults. *Scientific reports*, 9(1), 1940.

Murphy, E. & Starr, A. (1971). Evoked responses to electrical stimulation of the auditory pathway during the wake/sleep cycle. *Brain Research*, 35(2), 491–500.

Musacchia, G., Sams, M., Skoe, E., & Kraus, N. (2007). Musicians have enhanced subcortical auditory and audiovisual processing of speech and music. *Proceedings of the National Academy of Sciences*, 104(40), 15894–15898.

Musacchia, G., Strait, D., & Kraus, N. (2008). Relationships between behavior, brainstem and cortical encoding of seen and heard speech in musicians and non-musicians. *Hearing research*, 241(1-2), 34–42.

Nader, R. & Smith, C. (2001). The relationship between stage 2 sleep spindles and intelligence. In *Sleep*, volume 24 (pp. A160–A160).: AMER ACAD SLEEP MEDICINE 6301 BANDEL RD, STE 101, ROCHESTER, MN 55901 USA.

Nairne, J. S. & Neath, I. (2012). Sensory and working memory. *Handbook of Psychology, Second Edition*, 4.

Nasr, K., Haslacher, D., Dayan, E., Censor, N., Cohen, L. G., & Soekadar, S. R. (2022). Breaking the boundaries of interacting with the human brain using adaptive closed-loop stimulation. *Progress in Neurobiology*, (pp. 102311).

Navarrete, M., Schneider, J., Ngo, H.-V. V., Valderrama, M., Casson, A. J., & Lewis, P. A. (2020). Examining the optimal timing for closed-loop auditory stimulation of slow-wave sleep in young and older adults. *Sleep*, 43(6), zsz315.

Neske, G. T. (2016). The slow oscillation in cortical and thalamic networks: mechanisms and functions. *Frontiers in neural circuits*, 9, 88.

Neves, G., Cooke, S. F., & Bliss, T. V. (2008). Synaptic plasticity, memory and the hippocampus: a neural network approach to causality. *Nature reviews neuroscience*, 9(1), 65–75.

Ngo, H.-V. V., Claussen, J. C., Born, J., & Mölle, M. (2013a). Induction of slow oscillations by rhythmic acoustic stimulation. *Journal of sleep research*, 22(1), 22–31.

Ngo, H.-V. V., Martinetz, T., Born, J., & Mölle, M. (2013b). Auditory closed-loop stimulation of the sleep slow oscillation enhances memory. *Neuron*, 78(3), 545–553.

Ngo, H.-V. V., Miedema, A., Faude, I., Martinetz, T., Mölle, M., & Born, J. (2015). Driving sleep slow oscillations by auditory closed-loop stimulation—a self-limiting process. *Journal of Neuroscience*, 35(17), 6630–6638.

Ngo, H.-V. V., Seibold, M., Boche, D. C., Mölle, M., & Born, J. (2019). Insights on auditory closed-loop stimulation targeting sleep spindles in slow oscillation up-states. *Journal of Neuroscience Methods*, 316, 117–124.

Ni, K.-M., Hou, X.-J., Yang, C.-H., Dong, P., Li, Y., Zhang, Y., Jiang, P., Berg, D. K., Duan, S., & Li, X.-M. (2016). Selectively driving cholinergic fibers optically in the thalamic reticular nucleus promotes sleep. *elife*, 5, e10382.

Nicolas, J., King, B. R., Levesque, D., Lazzouni, L., Coffey, E., Swinnen, S., Doyon, J., Carrier, J., & Albouy, G. (2022). Sigma oscillations protect or reinstate motor memory depending on their temporal coordination with slow waves. *Elife*, 11, e73930.

Niiyama, Y., Fujiwara, R., Satoh, N., & Hishikawa, Y. (1994). Endogenous components of event-related potential appearing during nrem stage 1 and rem sleep in man. *International Journal of Psychophysiology*, 17(2), 165–174.

Niknazar, M., Krishnan, G. P., Bazhenov, M., & Mednick, S. C. (2015). Coupling of thalamocortical sleep oscillations are important for memory consolidation in humans. *PloS one*, 10(12), e0144720.

Niso, G., Rogers, C., Moreau, J. T., Chen, L.-Y., Madjar, C., Das, S., Bock, E., Tadel, F., Evans, A. C., Jolicoeur, P., et al. (2016). Omega: the open meg archive. *Neuroimage*, 124, 1182–1187.

Occhionero, M., Tonetti, L., Fabbri, M., Boreggiani, M., Martoni, M., Giovagnoli, S., & Natale, V. (2020). Prospective memory, sleep, and age. *Brain Sciences*, 10(7), 422.

Ogilvie, R. D., Simons, I. A., Kuderian, R. H., MacDonald, T., & Rustenburg, J. (1991). Behavioral, event-related potential, and eeg/fft changes at sleep onset. *Psychophysiology*, 28(1), 54–64.

Ong, J. L., Lo, J. C., Chee, N. I., Santostasi, G., Paller, K. A., Zee, P. C., & Chee, M. W. (2016). Effects of phase-locked acoustic stimulation during a nap on eeg spectra and declarative memory consolidation. *Sleep medicine*, 20, 88–97.

Ong, J. L., Patanaik, A., Chee, N. I., Lee, X. K., Poh, J.-H., & Chee, M. W. (2018). Auditory stimulation of sleep slow oscillations modulates subsequent memory encoding through altered hippocampal function. *Sleep*, 41(5), zsy031.

O'reilly, C., Gosselin, N., Carrier, J., & Nielsen, T. (2014). Montreal archive of sleep studies: an open-access resource for instrument benchmarking and exploratory research. *Journal of sleep research*, 23(6), 628–635.

Pace-Schott, E. F. & Spencer, R. (2014). Sleep-dependent memory consolidation in healthy aging and mild cognitive impairment. *Sleep, neuronal plasticity and brain function*, (pp. 307–330).

Paller, K. A., Creery, J. D., & Schechtman, E. (2021). Memory and sleep: how sleep cognition can change the waking mind for the better. *Annual review of psychology*, 72(1), 123–150.

Papalambros, N. A., Santostasi, G., Malkani, R. G., Braun, R., Weintraub, S., Paller, K. A., & Zee, P. C. (2017). Acoustic enhancement of sleep slow oscillations and concomitant memory improvement in older adults. *Frontiers in human neuroscience*, 11, 247563.

Papalambros, N. A., Weintraub, S., Chen, T., Grimaldi, D., Santostasi, G., Paller, K. A., Zee, P. C., & Malkani, R. G. (2019). Acoustic enhancement of sleep slow oscillations in mild cognitive impairment. *Annals of clinical and translational neurology*, 6(7), 1191–1201.

Parbery-Clark, A., Strait, D. L., Hittner, E., & Kraus, N. (2013). Musical training enhances neural processing of binaural sounds. *Journal of Neuroscience*, 33(42), 16741–16747.

Parkkonen, L., Fujiki, N., & Mäkelä, J. P. (2009). Sources of auditory brainstem responses revisited: contribution by magnetoencephalography. *Human brain mapping*, 30(6), 1772–1782.

Payne, J. D., Stickgold, R., Swanberg, K., & Kensinger, E. A. (2008). Sleep preferentially enhances memory for emotional components of scenes. *Psychological science*, 19(8), 781–788.

Perrault, A. A., Ong, J. L. A., Phillips, E. M., Cross, N. E., Teo, T. B., Dicom, A. R., Chee, N. I., Patanaik, A., Chee, M. W., & Dang-Vu, T. T. (2025). Closed-loop auditory stimulation (clas) does not improve sleep or declarative memory in chronic insomnia. *medRxiv*, (pp. 2025–03).

Perrin, F., Garcia-Larrea, L., Mauguière, F., & Bastuji, H. (1999). A differential brain response to the subject's own name persists during sleep. *Clinical neurophysiology*, 110(12), 2153–2164.

Phelps, E. A. (2004). Human emotion and memory: interactions of the amygdala and hippocampal complex. *Current opinion in neurobiology*, 14(2), 198–202.

Piantoni, G., Poil, S.-S., Linkenkaer-Hansen, K., Verweij, I. M., Ramautar, J. R., Van Someren, E. J., & Van Der Werf, Y. D. (2013). Individual differences in white matter diffusion affect sleep oscillations. *Journal of Neuroscience*, 33(1), 227–233.

Piastra, M. C., Nüßing, A., Vorwerk, J., Clerc, M., Engwer, C., & Wolters, C. H. (2021). A comprehensive study on electroencephalography and magnetoencephalography sensitivity to cortical and subcortical sources. *Human Brain Mapping*, 42(4), 978–992.

Picchioni, D., Pixa, M. L., Fukunaga, M., Carr, W. S., Horovitz, S. G., Braun, A. R., & Duyn, J. H. (2014). Decreased connectivity between the thalamus and the neocortex during human nonrapid eye movement sleep. *Sleep*, 37(2), 387–397.

Pinheiro, J. & Bates, D. (2006). *Mixed-effects models in S and S-PLUS*. Springer science & business media.

Piorecky, M., Koudelka, V., Piorecka, V., Strobl, J., Dudysova, D., & Koprivova, J. (2021). Real-time excitation of slow oscillations during deep sleep using acoustic stimulation. *Sensors*, 21(15), 5169.

Pizzo, F., Roehri, N., Medina Villalon, S., Trébuchon, A., Chen, S., Lagarde, S., Carron, R., Gavaret, M., Giusiano, B., McGonigal, A., et al. (2019). Deep brain activities can be detected with magnetoencephalography. *Nature communications*, 10(1), 971.

Plakke, B. & Romanski, L. M. (2014). Auditory connections and functions of prefrontal cortex. *Frontiers in neuroscience*, 8, 199.

Plante, D., Goldstein, M., Cook, J., Smith, R., Riedner, B., Rumble, M., Jelenchick, L., Roth, A., Tononi, G., Benca, R., et al. (2015). Effects of oral temazepam on sleep spindles during non-rapid eye movement sleep: a high-density eeg investigation. *European Neuropsychopharmacology*, 25(10), 1600–1610.

Poe, G. R., Foote, S., Eschenko, O., Johansen, J. P., Bouret, S., Aston-Jones, G., Harley, C. W., Manahan-Vaughan, D., Weinshenker, D., Valentino, R., et al. (2020). Locus coeruleus: a new look at the blue spot. *Nature Reviews Neuroscience*, 21(11), 644–659.

Prehn-Kristensen, A., Ngo, H.-V. V., Lentfer, L., Berghäuser, J., Brandes, L., Schulze, L., Göder, R., Mölle, M., & Baving, L. (2020). Acoustic closed-loop stimulation during sleep improves consolidation of reward-related memory information in healthy children but not in children with attention-deficit hyperactivity disorder. *Sleep*, 43(8), zsaa017.

Pu, Y., Cheyne, D. O., Cornwell, B. R., & Johnson, B. W. (2018). Non-invasive investigation of human hippocampal rhythms using magnetoencephalography: a review. *Frontiers in neuroscience*, 12, 273.

Purcell, S., Manoach, D., Demanuele, C., Cade, B., Mariani, S., Cox, R., Panagiotaropoulou, G., Saxena, R., Pan, J., Smoller, J., et al. (2017). Characterizing sleep spindles in 11,630 individuals from the national sleep research resource. *Nature communications*, 8(1), 15930.

Ramot, M. & Martin, A. (2022). Closed-loop neuromodulation for studying spontaneous activity and causality. *Trends in cognitive sciences*.

Rasch, B. & Born, J. (2013). About sleep's role in memory. *Physiological reviews*.

Rasch, B., Büchel, C., Gais, S., & Born, J. (2007). Odor cues during slow-wave sleep prompt declarative memory consolidation. *Science*, 315(5817), 1426–1429.

Rasch, B., Pommer, J., Diekelmann, S., & Born, J. (2009). Pharmacological rem sleep suppression paradoxically improves rather than impairs skill memory. *Nature neuroscience*, 12(4), 396–397.

Rauschecker, J. P. & Scott, S. K. (2009). Maps and streams in the auditory cortex: nonhuman primates illuminate human speech processing. *Nature neuroscience*, 12(6), 718–724.

Ridding, M. C. & Ziemann, U. (2010). Determinants of the induction of cortical plasticity by non-invasive brain stimulation in healthy subjects. *The Journal of physiology*, 588(13), 2291–2304.

Riedner, B. A., Hulse, B. K., Murphy, M. J., Ferrarelli, F., & Tononi, G. (2011). Temporal dynamics of cortical sources underlying spontaneous and peripherally evoked slow waves. *Progress in brain research*, 193, 201–218.

Roenneberg, T., Wirz-Justice, A., & Merrow, M. (2003). Life between clocks: daily temporal patterns of human chronotypes. *Journal of biological rhythms*, 18(1), 80–90.

Romanella, S. M., Roe, D., Paciorek, R., Cappon, D., Ruffini, G., Menardi, A., Rossi, A., Rossi, S., & Santarnecchi, E. (2020). Sleep, noninvasive brain stimulation, and the aging brain: challenges and opportunities. *Ageing research reviews*, 61, 101067.

Romero-Corral, A., Caples, S. M., Lopez-Jimenez, F., & Somers, V. K. (2010). Interactions between obesity and obstructive sleep apnea: implications for treatment. *Chest*, 137(3), 711–719.

Rosanova, M. & Ulrich, D. (2005). Pattern-specific associative long-term potentiation induced by a sleep spindle-related spike train. *Journal of Neuroscience*, 25(41), 9398–9405.

Rosinvil, T., Bouvier, J., Dubé, J., Lafrenière, A., Bouchard, M., Cyr-Cronier, J., Gosselin, N., Carrier, J., & Lina, J.-M. (2021). Are age and sex effects on sleep slow waves only a matter of electroencephalogram amplitude? *Sleep*, 44(3), zsaa186.

Rouast, N. M., Kumral, D., Gais, S., & Schonauer, M. (2025). Random auditory stimulation disturbs traveling slow waves and declarative memory. *bioRxiv*, (pp. 2025–02).

Roumis, D. K. & Frank, L. M. (2015). Hippocampal sharp-wave ripples in waking and sleeping states. *Current opinion in neurobiology*, 35, 6–12.

Roux, L., Hu, B., Eichler, R., Stark, E., & Buzsáki, G. (2017). Sharp wave ripples during learning stabilize the hippocampal spatial map. *Nature neuroscience*, 20(6), 845–853.

Ruch, S., Schmidig, F. J., Knüsel, L., & Henke, K. (2022). Closed-loop modulation of local slow oscillations in human nrem sleep. *NeuroImage*, 264, 119682.

Ruzich, E., Crespo-García, M., Dalal, S. S., & Schneiderman, J. F. (2019). Characterizing hippocampal dynamics with meg: A systematic review and evidence-based guidelines. *Human brain mapping*, 40(4), 1353–1375.

Sahota, P. K., Jain, S. S., & Dhand, R. (2003). Sleep disorders in pregnancy. *Current opinion in pulmonary medicine*, 9(6), 477–483.

Salfi, F., D'Atri, A., Tempesta, D., De Gennaro, L., & Ferrara, M. (2020). Boosting slow oscillations during sleep to improve memory function in elderly people: a review of the literature. *Brain sciences*, 10(5), 300.

Sanchez-Vives, M. V. (2020). Origin and dynamics of cortical slow oscillations. *Current Opinion in Physiology*, 15, 217–223.

Sato, Y., Fukuoka, Y., Minamitani, H., & Honda, K. (2007). Sensory stimulation triggers spindles during sleep stage 2. *Sleep*, 30(4), 511–518.

Scangos, K. W., Khambhati, A. N., Daly, P. M., Makhoul, G. S., Sugrue, L. P., Zamanian, H., Liu, T. X., Rao, V. R., Sellers, K. K., Dawes, H. E., et al. (2021). Closed-loop neuromodulation in an individual with treatment-resistant depression. *Nature medicine*, 27(10), 1696–1700.

Schabus, M., Dang-Vu, T. T., Heib, D. P. J., Boly, M., Desseilles, M., Vandewalle, G., Schmidt, C., Albouy, G., Darsaud, A., Gais, S., et al. (2012). The fate of incoming stimuli during nrem sleep is determined by spindles and the phase of the slow oscillation. *Frontiers in neurology*, 3, 40.

Schabus, M., Gruber, G., Parapatics, S., Sauter, C., Klösch, G., Anderer, P., Klimesch, W., Saletu, B., & Zeitlhofer, J. (2004). Sleep spindles and their significance for declarative memory consolidation. *Sleep*, 27(8), 1479–1485.

Schabus, M., Hödlmoser, K., Gruber, G., Sauter, C., Anderer, P., Klösch, G., Parapatics, S., Saletu, B., Klimesch, W., & Zeitlhofer, J. (2006). Sleep spindle-related activity in the human eeg and its relation to general cognitive and learning abilities. *European Journal of Neuroscience*, 23(7), 1738–1746.

Schabus, M., Hoedlmoser, K., Pecherstorfer, T., Anderer, P., Gruber, G., Parapatics, S., Sauter, C., Kloesch, G., Klimesch, W., Saletu, B., et al. (2008). Interindividual sleep spindle differences and their relation to learning-related enhancements. *Brain research*, 1191, 127–135.

Schierenbeck, T., Riemann, D., Berger, M., & Hornyak, M. (2008). Effect of illicit recreational drugs upon sleep: cocaine, ecstasy and marijuana. *Sleep medicine reviews*, 12(5), 381–389.

Schiller, K., von Ellenrieder, N., Mansilla, D., Abdallah, C., Jaber, K., Garcia-Asensi, A., Thomas, J., Minato, E., Gotman, J., & Frauscher, B. (2025). Widespread decoupling of spindles and slow waves in temporal lobe epilepsy. *Epilepsia*.

Schmidt, C., Peigneux, P., Muto, V., Schenkel, M., Knoblauch, V., Münch, M., Dominique, J.-F., Wirz-Justice, A., & Cajochen, C. (2006). Encoding difficulty promotes postlearning changes in sleep spindle activity during napping. *Journal of Neuroscience*, 26(35), 8976–8982.

Schneider, J., Lewis, P. A., Koester, D., Born, J., & Ngo, H.-V. V. (2020). Susceptibility to auditory closed-loop stimulation of sleep slow oscillations changes with age. *Sleep*, 43(12), zsaa111.

Schönauer, M., Alizadeh, S., Jamalabadi, H., Abraham, A., Pawlizki, A., & Gais, S. (2017). Decoding material-specific memory reprocessing during sleep in humans. *Nature Communications*, 8(1), 15404.

Schönauer, M., Geisler, T., & Gais, S. (2014). Strengthening procedural memories by reactivation in sleep. *Journal of cognitive neuroscience*, 26(1), 143–153.

Schreglmann, S. R., Wang, D., Peach, R. L., Li, J., Zhang, X., Latorre, A., Rhodes, E., Panella, E., Cassara, A. M., Boyden, E. S., et al. (2021). Non-invasive suppression of essential tremor via phase-locked disruption of its temporal coherence. *Nature communications*, 12(1), 1–15.

Schulz, H. (2008). Rethinking sleep analysis: comment on the aasm manual for the scoring of sleep and associated events. *Journal of Clinical Sleep Medicine*, 4(2), 99–103.

Sela, Y., Vyazovskiy, V. V., Cirelli, C., Tononi, G., & Nir, Y. (2016). Responses in rat core auditory cortex are preserved during sleep spindle oscillations. *Sleep*, 39(5), 1069–1082.

Shimizu, R. E., Connolly, P. M., Cellini, N., Armstrong, D. M., Hernandez, L. T., Estrada, R., Aguilar, M., Weisend, M. P., Mednick, S. C., & Simons, S. B. (2018). Closed-loop targeted memory reactivation during sleep improves spatial navigation. *Frontiers in human neuroscience*, 12, 28.

Simon, K. C., Nadel, L., & Payne, J. D. (2022). The functions of sleep: A cognitive neuroscience perspective.

Skoe, E. & Kraus, N. (2010). Auditory brainstem response to complex sounds: a tutorial. *Ear and hearing*, 31(3), 302.

Smith, P. L. & Little, D. R. (2018). Small is beautiful: In defense of the small-n design. *Psychonomic bulletin & review*, 25(6), 2083–2101.

Sobral, M., Jourde, H. R., Bajestani, E. M., Coffey, E. B., & Beltrame, G. (2025). Advancing closed-loop brain stimulation: Continual learning for subject-specific sleep spindle detection. *Journal of Neural Engineering*, Submitted.

Song, S., Howard, J. H., & Howard, D. V. (2007). Sleep does not benefit probabilistic motor sequence learning. *Journal of Neuroscience*, 27(46), 12475–12483.

Squire, L. R. (1992). Declarative and nondeclarative memory: Multiple brain systems supporting learning and memory. *Journal of cognitive neuroscience*, 4(3), 232–243.

Squire, L. R. & Zola, S. M. (1996). Structure and function of declarative and nondeclarative memory systems. *Proceedings of the National Academy of Sciences*, 93(24), 13515–13522.

Staresina, B. P., Bergmann, T. O., Bonnefond, M., Van Der Meij, R., Jensen, O., Deuker, L., Elger, C. E., Axmacher, N., & Fell, J. (2015). Hierarchical nesting of slow oscillations, spindles and ripples in the human hippocampus during sleep. *Nature neuroscience*, 18(11), 1679–1686.

Staresina, B. P., Niediek, J., Borger, V., Surges, R., & Mormann, F. (2023). How coupled slow oscillations, spindles and ripples coordinate neuronal processing and communication during human sleep. *Nature Neuroscience*, (pp. 1–9).

Stepanski, E. J. (2002). The effect of sleep fragmentation on daytime function. *Sleep*, 25(3), 268–276.

Steriade, M., Nunez, A., & Amzica, F. (1993). A novel slow (¡ 1 hz) oscillation of neocortical neurons in vivo: depolarizing and hyperpolarizing components. *Journal of neuroscience*, 13(8), 3252–3265.

Stickgold, R. (2005). Sleep-dependent memory consolidation. *Nature*, 437(7063), 1272–1278.

Stickgold, R. (2013). Parsing the role of sleep in memory processing. *Current opinion in neurobiology*, 23(5), 847–853.

Stickgold, R. & Walker, M. P. (2005). Memory consolidation and reconsolidation: what is the role of sleep? *Trends in neurosciences*, 28(8), 408–415.

Stickgold, R. & Walker, M. P. (2007). Sleep-dependent memory consolidation and reconsolidation. *Sleep medicine*, 8(4), 331–343.

Stickgold, R. & Walker, M. P. (2013). Sleep-dependent memory triage: evolving generalization through selective processing. *Nature neuroscience*, 16(2), 139–145.

Stroganova, T. A., Kozunov, V. V., Posikera, I. N., Galuta, I. A., Gratchev, V. V., & Orekhova, E. V. (2013). Abnormal pre-attentive arousal in young children with autism spectrum disorder contributes to their atypical auditory behavior: an erp study. *PloS one*, 8(7), e69100.

Stropahl, M., Bauer, A.-K. R., Debener, S., & Bleichner, M. G. (2018). Source-modeling auditory processes of eeg data using eeglab and brainstorm. *Frontiers in neuroscience*, 12, 309.

Swift, K. (2019). *Locus Coeruleus Optogenetic Stimulation and the Estrous Cycle Manipulate Sleep Characteristics and Memory Consolidation*. PhD thesis.

Swift, K. M., Gross, B. A., Frazer, M. A., Bauer, D. S., Clark, K. J., Vazey, E. M., Aston-Jones, G., Li, Y., Pickering, A. E., Sara, S. J., et al. (2018). Abnormal locus coeruleus sleep activity alters sleep signatures of memory consolidation and impairs place cell stability and spatial memory. *Current Biology*, 28(22), 3599–3609.

Tadel, F., Baillet, S., Mosher, J. C., Pantazis, D., & Leahy, R. M. (2011). Brainstorm: a user-friendly application for meg/eeg analysis. *Computational intelligence and neuroscience*, 2011.

Tamaki, M., Matsuoka, T., Nittono, H., & Hori, T. (2008). Fast sleep spindle (13–15 hz) activity correlates with sleep-dependent improvement in visuomotor performance. *Sleep*, 31(2), 204–211.

Tamminen, J., Payne, J. D., Stickgold, R., Wamsley, E. J., & Gaskell, M. G. (2010). Sleep spindle activity is associated with the integration of new memories and existing knowledge. *Journal of Neuroscience*, 30(43), 14356–14360.

Tamminen, J., Ralph, M. A. L., & Lewis, P. A. (2013). The role of sleep spindles and slow-wave activity in integrating new information in semantic memory. *Journal of Neuroscience*, 33(39), 15376–15381.

Tanaka, J. W. & Curran, T. (2001). A neural basis for expert object recognition. *Psychological science*, 12(1), 43–47.

Tesche, C., Uusitalo, M., Ilmoniemi, R., Huotilainen, M., Kajola, M., & Salonen, O. (1995). Signal-space projections of meg data characterize both distributed and well-localized neuronal sources. *Electroencephalography and clinical neurophysiology*, 95(3), 189–200.

Thigpen, N. N., Kappenman, E. S., & Keil, A. (2017). Assessing the internal consistency of the event-related potential: An example analysis. *Psychophysiology*, 54(1), 123–138.

Thissen, D., Steinberg, L., & Kuang, D. (2002). Quick and easy implementation of the benjamini-hochberg procedure for controlling the false positive rate in multiple comparisons. *Journal of educational and behavioral statistics*, 27(1), 77–83.

Tichko, P. & Skoe, E. (2017). Frequency-dependent fine structure in the frequency-following response: The byproduct of multiple generators. *Hearing research*, 348, 1–15.

Timofeev, I. & Chauvette, S. (2017). Sleep slow oscillation and plasticity. *Current opinion in neurobiology*, 44, 116–126.

Tononi, G. & Cirelli, C. (2006). Sleep function and synaptic homeostasis. *Sleep medicine reviews*, 10(1), 49–62.

Tucker, M. A. & Fishbein, W. (2009). The impact of sleep duration and subject intelligence on declarative and motor memory performance: how much is enough? *Journal of sleep research*, 18(3), 304–312.

Tulving, E. et al. (1972). Episodic and semantic memory. *Organization of memory*, 1(381-403), 1.

Ujszászi, J. & Halász, P. (1988). Long latency evoked potential components in human slow wave sleep. *Electroencephalography and clinical Neurophysiology*, 69(6), 516–522.

Ullman, M. T. (2004). Contributions of memory circuits to language: The declarative/procedural model. *Cognition*, 92(1-2), 231–270.

Valenchon, N., Bouteiller, Y., Jourde, H. R., L'Heureux, X., Sobral, M., Coffey, E. B., & Beltrame, G. (2022). The portiloop: A deep learning-based open science tool for closed-loop brain stimulation. *PloS one*, 17(8), e0270696.

Van den Bulcke, L., Peeters, A.-M., Heremans, E., Davidoff, H., Borzée, P., De Vos, M., Emsell, L., Van den Stock, J., De Roo, M., Tournoy, J., et al. (2023). Acoustic stimulation as a promising technique to enhance slow-wave sleep in alzheimer's disease: results of a pilot study. *Journal of Clinical Sleep Medicine*, (pp. jcsm–10778).

van Kronenberg, P., Milinski, L., Kruschke, Z., & de Hoz, L. (2022). Sound disrupts sleep-associated brain oscillations in rodents in a meaning-dependent manner. *Scientific Reports*, 12(1), 6051.

van Stegeren, A. H. (2008). The role of the noradrenergic system in emotional memory. *Acta psychologica*, 127(3), 532–541.

Vantomme, G., Osorio-Forero, A., Lüthi, A., & Fernandez, L. M. (2019). Regulation of local sleep by the thalamic reticular nucleus. *Frontiers in neuroscience*, 13, 576.

Velluti, R. (1997). Interactions between sleep and sensory physiology. *Journal of sleep research*, 6(2), 61–77.

Vyazovskiy, V. V. & Harris, K. D. (2013). Sleep and the single neuron: the role of global slow oscillations in individual cell rest. *Nature Reviews Neuroscience*, 14(6), 443–451.

Wagenmakers, E.-J., Morey, R. D., & Lee, M. D. (2016). Bayesian benefits for the pragmatic researcher. *Current Directions in Psychological Science*, 25(3), 169–176.

Walker, M. P. (2009). The role of sleep in cognition and emotion. *Annals of the New York Academy of Sciences*, 1156(1), 168–197.

Walker, M. P., Brakefield, T., Morgan, A., Hobson, J. A., & Stickgold, R. (2002). Practice with sleep makes perfect: sleep-dependent motor skill learning. *Neuron*, 35(1), 205–211.

Walker, M. P. & Stickgold, R. (2004). Sleep-dependent learning and memory consolidation. *Neuron*, 44(1), 121–133.

Wamsley, E. J., Tucker, M. A., Shinn, A. K., Ono, K. E., McKinley, S. K., Ely, A. V., Goff, D. C., Stickgold, R., & Manoach, D. S. (2012). Reduced sleep spindles and spindle coherence in schizophrenia: mechanisms of impaired memory consolidation? *Biological psychiatry*, 71(2), 154–161.

Wang, Y., Lu, L., Zou, G., Zheng, L., Qin, L., Zou, Q., & Gao, J.-H. (2022). Disrupted neural tracking of sound localization during non-rapid eye movement sleep. *NeuroImage*, 260, 119490.

Warby, S. C., Wendt, S. L., Welinder, P., Munk, E. G., Carrillo, O., Sorensen, H. B., Jennum, P., Peppard, P. E., Perona, P., & Mignot, E. (2014). Sleep-spindle detection: crowdsourcing and evaluating performance of experts, non-experts and automated methods. *Nature methods*, 11(4), 385–392.

Ward, L. M. (2013). The thalamus: gateway to the mind. *Wiley Interdisciplinary Reviews: Cognitive Science*, 4(6), 609–622.

Wei, Y., Krishnan, G. P., & Bazhenov, M. (2016). Synaptic mechanisms of memory consolidation during sleep slow oscillations. *Journal of Neuroscience*, 36(15), 4231–4247.

Weiner, O. M., O'Byrne, J., Cross, N. E., Giraud, J., Tarelli, L., Yue, V., Homer, L., Walker, K., Carbone, R., & Dang-Vu, T. T. (2023). Slow oscillation-spindle cross-frequency coupling predicts overnight declarative memory consolidation in older adults. *European Journal of Neuroscience*.

Wetzels, R., Raaijmakers, J. G., Jakab, E., & Wagenmakers, E.-J. (2009). How to quantify support for and against the null hypothesis: A flexible winbugs implementation of a default bayesian t test. *Psychonomic bulletin & review*, 16(4), 752–760.

Wiethoff, S., Hamada, M., & Rothwell, J. C. (2014). Variability in response to transcranial direct current stimulation of the motor cortex. *Brain stimulation*, 7(3), 468–475.

Wijdicks, E. F. (2019). The ascending reticular activating system. *Neurocritical Care*, 31(2), 419–422.

Wilf, M., Ramot, M., Furman-Haran, E., Arzi, A., Levkovitz, Y., & Malach, R. (2016). Diminished auditory responses during nrem sleep correlate with the hierarchy of language processing. *PloS one*, 11(6), e0157143.

Wilhelm, I., Diekelmann, S., Molzow, I., Ayoub, A., Mölle, M., & Born, J. (2011). Sleep selectively enhances memory expected to be of future relevance. *Journal of Neuroscience*, 31(5), 1563–1569.

Wilson, M. A. & McNaughton, B. L. (1994). Reactivation of hippocampal ensemble memories during sleep. *Science*, 265(5172), 676–679.

Wimmer, R. D., Astori, S., Bond, C. T., Rovó, Z., Chatton, J.-Y., Adelman, J. P., Franken, P., & Lüthi, A. (2012). Sustaining sleep spindles through enhanced sk2-channel activity consolidates sleep and elevates arousal threshold. *Journal of Neuroscience*, 32(40), 13917–13928.

Wunderlin, M., Züst, M. A., Hertenstein, E., Fehér, K. D., Schneider, C. L., Klöppel, S., & Nissen, C. (2021). Modulating overnight memory consolidation by acoustic stimulation during slow-wave sleep: A systematic review and meta-analysis. *Sleep*, 44(7), zsaa296.

Wüst, L. N., Antonenko, D., Malinowski, R., Khakimova, L., Grittner, U., Obermayer, K., Ladenbauer, J., & Flöel, A. (2021). Interrelations between delta waves, spindles and slow oscillations in human nrem sleep and their functional role in memory. *bioRxiv*, (pp. 2021–09).

Yang, W. (2021). A new type of right-leg-drive circuit ecg amplifier using new operational amplifier. In *Journal of Physics: Conference Series*, volume 1846 (pp. 012034).: IOP Publishing.

Yeo, S. S., Chang, P. H., & Jang, S. H. (2013). The ascending reticular activating system from pontine reticular formation to the thalamus in the human brain. *Frontiers in human neuroscience*, 7, 416.

Yüzgeç, Ö., Prsa, M., Zimmermann, R., & Huber, D. (2018). Pupil size coupling to cortical states protects the stability of deep sleep via parasympathetic modulation. *Current Biology*, 28(3), 392–400.

Yvert, B., Fischer, C., Bertrand, O., & Pernier, J. (2005). Localization of human supratemporal auditory areas from intracerebral auditory evoked potentials using distributed source models. *Neuroimage*, 28(1), 140–153.

Ziemann, U. & Siebner, H. R. (2015). Inter-subject and inter-session variability of plasticity induction by non-invasive brain stimulation: boon or bane? *Brain Stimulation: Basic, Translational, and Clinical Research in Neuromodulation*, 8(3), 662–663.

Zrenner, C. & Ziemann, U. (2024). Closed-loop brain stimulation. *Biological Psychiatry*, 95(6), 545–552.

Chapter A
The Portiloop: a deep learning-based open science tool for closed-loop brain stimulation

A.1 Abstract

Closed-loop brain stimulation refers to capturing neurophysiological measures such as electroencephalography (EEG), quickly identifying neural events of interest, and producing auditory, magnetic or electrical stimulation so as to interact with brain processes precisely. It is a promising new method for fundamental neuroscience and perhaps for clinical applications such as restoring degraded memory function; however, existing tools are expensive, cumbersome, and offer limited experimental flexibility. In this article, we propose the Portiloop, a deep learning-based, portable and low-cost closed-loop stimulation system able to target specific brain oscillations. We first document open-hardware implementations that can be constructed from commercially available components. We also provide a fast, lightweight neural network model and an exploration algorithm that automatically optimizes the model hyperparameters to the desired brain oscillation. Finally, we validate the technology on a challenging test case of real-time sleep spindle detection, with results comparable to off-line expert performance on the Massive Online Data Annotation spindle dataset (MODA; group consensus). Software and plans are available to the community as an open science initiative to encourage further development and advance closed-loop neuroscience research [https://github.com/Portiloop].

A.2 Link to paper

The paper was published in PLoS One in August 2022. It is available following this link:
https://doi.org/10.1371/journal.pone.0270696

Chapter B
Advancing closed-loop brain stimulation: continual learning for subject-specific sleep spindle detection

B.1 Abstract

Personalized closed-loop brain stimulation, in which algorithms used to detect neural events adapt to a user's unique neural characteristics, may be crucial to enable optimized and consistent stimulation quality for both fundamental research and clinical applications. Precise stimulation of sleep spindles—transient patterns of brain activity that occur during non rapid eye movement sleep that are involved in memory consolidation-presents an exciting frontier for studying memory functions; however, this endeavor is challenged by the spindles' fleeting nature, inter-individual variability, and the necessity of real-time detection. *Methods:* This paper introduces an approach to tackle these challenges, centered around a novel continual learning framework. Using a pre-trained model capable of both online classification of sleep stages and spindle detection, we implement an algorithm that refines spindle detection, tailoring it to the individual throughout one or more nights without manual intervention. *Results:* Our methodology achieves accurate, subject-specific targeting of sleep spindles and enables advanced closed-loop stimulation studies. *Conclusion:* While fine-tuning alone offers minimal benefits for single nights, our approach combining weight averaging demonstrates significant improvement over multiple nights, effectively mitigating catastrophic forgetting. *Significance:* This advancement represents a crucial step towards personalized closed-loop brain stimulation, potentially leading to a deeper understanding of sleep spindle functions and their role in memory consolidation. It holds the promise of deepening our understanding of sleep spindles' role in memory consolidation for cognitive neuroscience research and therapeutic applications.

B.2 Link to paper

The paper was submitted for publication. It is not yet available online.

Chapter C
Exploring deep magnetoencephalography via thalamocortical sleep spindles

C.1 Abstract

Magnetoencephalography (MEG) enables the study of widespread brain networks with high temporal resolution, but the degree to which deep sources like the thalamus can be resolved remains unclear. Functional connectivity methods may enhance differentiation, yet few studies have extended them beyond the cortex. We investigated thalamocortical sleep spindles as a test case, leveraging their well-characterized circuitry. MEG and electroencephalography (EEG) were recorded in 19 participants during a 2-hour nap. Spindle and non-spindle periods were identified, and connectivity was assessed using coherence and imaginary coherence within a spindle-related network. Graph theory was also applied to identify network hubs. As expected, functional connectivity increased during spindles within a distributed thalamocortical-hippocampal network. Cortical connectivity patterns allowed differentiation among small thalamic nuclei, but metric choice and contrast use influenced topography and distance effects. Graph theory revealed distinct cortical, thalamic, and hippocampal contributions to fast (13–16 Hz) and slow (10–13 Hz) sigma-band connectivity. These findings demonstrate that MEG functional connectivity can resolve deep brain networks, and demonstrate how it can be used to study the functional roles of subcortical regions non-invasively in healthy humans. By clarifying methodological influences, we aim to guide future research design and interpretation.

C.2 Link to paper

The paper was submitted for publication. It is not yet available online.

Chapter D
Beyond the lab: feasibility of cognitive neuroscience data collection during a speleological expedition

D.1 Abstract

In human cognitive neuroscience and neuropsychology studies, laboratory-based research tasks have been important to establish principles of brain function and its relationship to behaviour; however, they differ greatly from real-life experiences. Several elements of real-life situations that impact human performance, such as stressors, are difficult or impossible to replicate in the laboratory. Expeditions offer unique possibilities for studying human cognition in complex environments that can transfer to other situations with similar features. For example, as caves share several of the physical and psychological challenges of safety-critical environments such as spaceflight, underground expeditions have been developed as an analogue for astronaut training purposes, suggesting that they might also be suitable for studying aspects of behaviour and cognition that cannot be fully examined under laboratory conditions. While a large range of topics and tools have been proposed for application in such environments, few have been used in the field. Methods and procedures for maximizing the robustness and scientific value of expedition research designs must first be developed and validated. We tested the feasibility of collecting human physiological, cognitive, and subjective experience data concerning brain state, sleep, cognitive workload, and fatigue, during a speleological expedition in a remote region. We document our approaches and challenges experienced, and provide recommendations and suggestions to aid future work. The data support the idea that cave expeditions are relevant naturalistic paradigms that offer unique possibilities for cognitive neuroscience to complement laboratory work and help improve human performance and safety in operational environments.

D.2 Link to paper

The paper was published in Journal of Environmental Psychology in November 2024. It is available following this link:

https://doi.org/10.1016/j.jenvp.2024.102443